frontiers | Research Topics

Emerging anti-cancer compounds and immunomodulators for pancreatic cancer treatment

Edited by
Stephen Safe, Jennifer M. Bailey-Lundberg and Kathleen E. DelGiorno

Published in
Frontiers in Oncology

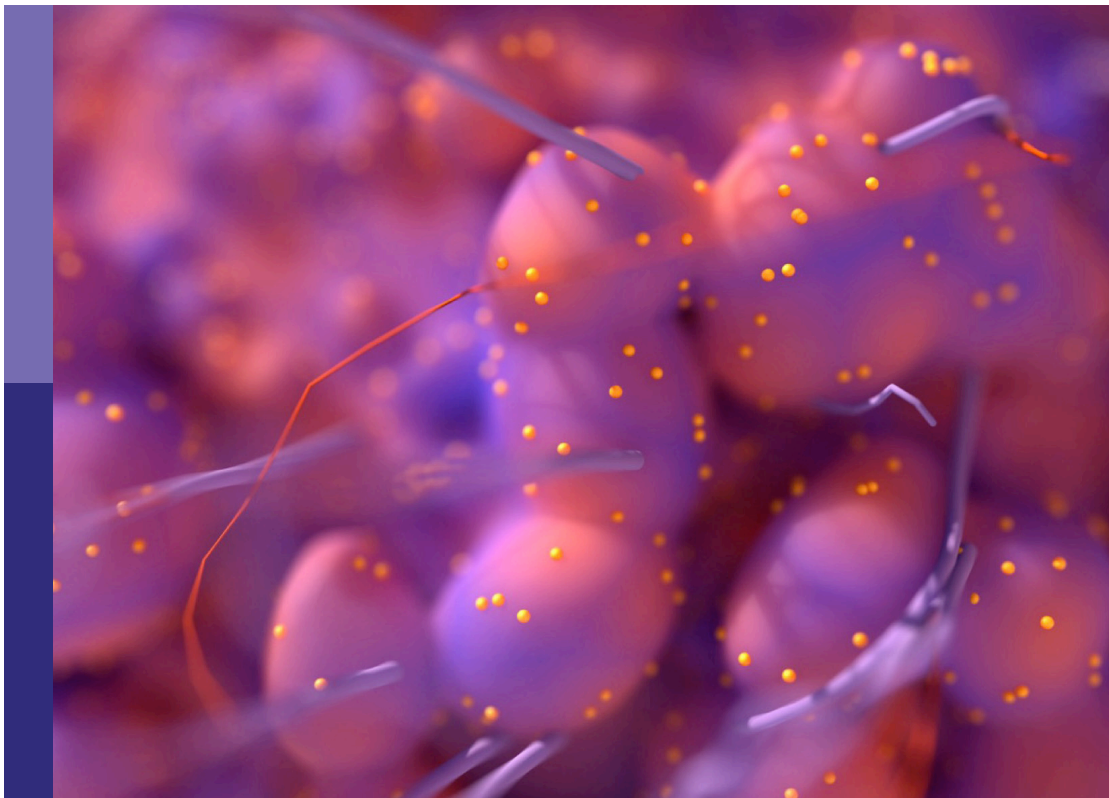

ISSN 1664-8714
ISBN 978-2-8325-4848-6
DOI 10.3389/978-2-8325-4848-6

About Frontiers

Frontiers is more than just an open access publisher of scholarly articles: it is a pioneering approach to the world of academia, radically improving the way scholarly research is managed. The grand vision of Frontiers is a world where all people have an equal opportunity to seek, share and generate knowledge. Frontiers provides immediate and permanent online open access to all its publications, but this alone is not enough to realize our grand goals.

Frontiers journal series

The Frontiers journal series is a multi-tier and interdisciplinary set of open-access, online journals, promising a paradigm shift from the current review, selection and dissemination processes in academic publishing. All Frontiers journals are driven by researchers for researchers; therefore, they constitute a service to the scholarly community. At the same time, the *Frontiers journal series* operates on a revolutionary invention, the tiered publishing system, initially addressing specific communities of scholars, and gradually climbing up to broader public understanding, thus serving the interests of the lay society, too.

Dedication to quality

Each Frontiers article is a landmark of the highest quality, thanks to genuinely collaborative interactions between authors and review editors, who include some of the world's best academicians. Research must be certified by peers before entering a stream of knowledge that may eventually reach the public - and shape society; therefore, Frontiers only applies the most rigorous and unbiased reviews. Frontiers revolutionizes research publishing by freely delivering the most outstanding research, evaluated with no bias from both the academic and social point of view. By applying the most advanced information technologies, Frontiers is catapulting scholarly publishing into a new generation.

What are Frontiers Research Topics?

Frontiers Research Topics are very popular trademarks of the *Frontiers journals series*: they are collections of at least ten articles, all centered on a particular subject. With their unique mix of varied contributions from Original Research to Review Articles, Frontiers Research Topics unify the most influential researchers, the latest key findings and historical advances in a hot research area.

Find out more on how to host your own Frontiers Research Topic or contribute to one as an author by contacting the Frontiers editorial office: frontiersin.org/about/contact

Emerging anti-cancer compounds and immunomodulators for pancreatic cancer treatment

Topic editors

Stephen Safe — Texas A and M University, United States

Jennifer M. Bailey-Lundberg — University of Texas Health Science Center at Houston, United States

Kathleen E. DelGiorno — Vanderbilt University, United States

Citation

Safe, S., Bailey-Lundberg, J. M., DelGiorno, K. E., eds. (2024). *Emerging anti-cancer compounds and immunomodulators for pancreatic cancer treatment*. Lausanne: Frontiers Media SA. doi: 10.3389/978-2-8325-4848-6

Table of contents

frontiers | Frontiers in Oncology

TYPE Editorial
PUBLISHED 19 April 2024
DOI 10.3389/fonc.2024.1411836

OPEN ACCESS

EDITED AND REVIEWED BY
Massimo Broggini,
Mario Negri Institute for Pharmacological Research (IRCCS), Italy

*CORRESPONDENCE
Jennifer M. Bailey-Lundberg
Jennifer.M.Bailey@uth.tmc.edu

RECEIVED 03 April 2024
ACCEPTED 09 April 2024
PUBLISHED 19 April 2024

CITATION
DelGiorno KE, Safe S and Bailey-Lundberg JM (2024) Editorial: Emerging anti-cancer compounds and immunomodulators for pancreatic cancer treatment.
Front. Oncol. 14:1411836.
doi: 10.3389/fonc.2024.1411836

Editorial: Emerging anti-cancer compounds and immunomodulators for pancreatic cancer treatment

Kathleen E. DelGiorno[1], Stephen Safe[2] and Jennifer M. Bailey-Lundberg[3]*

[1]Department of Cell and Developmental Biology, Vanderbilt University, Nashville, TN, United States, [2]Department of Veterinary Physiology and Pharmacology, Texas A&M University, College Station, TX, United States, [3]Department of Anesthesiology, Critical Care, and Pain Medicine, McGovern Medical School, The University of Texas Health Science Center at Houston, Houston, TX, United States

KEYWORDS

pancreatic adenocarcinoma, immunotherapy combined therapy, artificial intelligence, therapeutics, chemotherapy - oncology

Editorial on the Research Topic
Emerging anti-cancer compounds and immunomodulators for pancreatic cancer treatment

Several recent studies have shown that cancers arising in the gastrointestinal tract are on the rise, especially in younger adults. Of those gastrointestinal cancers, pancreatic adenocarcinoma, a subtype of pancreatic cancer, remains one of the deadliest (1). Pancreatic adenocarcinoma is expected to surpass colorectal cancer-related deaths by the year 2030 to become the second leading cause of cancer-related deaths in the United States (2). Despite advances in radiation therapy, immune-oncology, surgery, and new therapeutics, the 5-year survival rate for all stages is 12%. Several factors contribute to the poor prognosis for these patients including a hostile, hypoxic and immune suppressed tumor microenvironment, limited approaches for early detection, minimal surgical resection options for most patients who are diagnosed with locally advanced or metastatic pancreatic cancer, and other complications including malignant ascites, as reviewed by Han and Borazanci. In a systematic review published by Su et al., a significant association between early incidence of venous thromboembolism and poorer overall survival in patients with pancreatic cancer indicates another clinical consideration in understanding overall survival rates for this malignancy.

There are several emerging therapeutic strategies for treating pancreatic cancer. In a review by Tindall et al., therapeutic strategies targeting the TGF-β family are considered with an emphasis on the stage of disease. Targeting TGF-β has gained traction for pancreatic cancer as pathway activation can promote immune suppression and extracellular matrix production, two critical components of the pancreatic cancer microenvironment that inhibit the function of chemo and immunotherapeutic agents. Studies by Wang et al. have discovered a new agent called C150 that inhibits epithelial to mesenchymal transition (EMT) through enhancement of proteosome assembly and subsequent degradation of transcription factors important for epithelial to mesenchymal

transition. Experiments were conducted in an orthotopic model of pancreatic cancer and treatment with C150 (150 mg/kg 3x weekly) significantly increased survival of mice showing strong preclinical consideration.

IL-6 overexpression has been associated with poor prognosis in patients with pancreatic cancer. Leukemia inhibitory factor (LIF) is a cytokine that belongs to the IL-6 family. LIF mediates intracellular signaling by binding to a heterodimeric receptor complex including LIF receptor and Gp130. A recent study by Di Giorgo et al. showed BAR502, a non-bile acid steroidal ligand for two LIF receptors, Farnesoid-X-Receptor (FXR) and G Protein Bile Acid Activated Receptor (GPBAR1), reduced binding of LIF to the LIF receptor complex and reduced proliferation of MIA PaCa-2 pancreatic cancer cells.

An emerging consideration for therapeutic targeting is Claudin18.2, a tight junction protein highly expressed in pancreatic cancer primary tumors and in metastatic lesions. There are several clinical trials targeting Claudin18.2, as reviewed in Xu et al., and a number of emerging strategies to target Claudin18.2 including monoclonal antibodies, antibody-drug conjugates, bispecific antibodies, and a CAR-T cell drug targeting Claudin18.2, also currently being evaluated in clinical trials.

Development of more effective treatment of metastatic pancreatic cancer is critically needed for patients diagnosed with unresectable pancreatic adenocarcinoma. In a recent study published by Lu et al., third-line treatment for patients with metastatic pancreatic cancer prolonged the survival time of patients. In this study, survival was evaluated in 72 patients, 36 of whom received chemotherapy alone, 16 who received chemotherapy combined with targeted therapy or immunotherapy, 14 who received chemotherapy-free anti-tumor agents, and 6 who received palliative care. While the data show improved survival with chemotherapy, the study also revealed that third-line treatment with targeted therapy or immunotherapy did not improve survival benefits to chemotherapy alone and was associated with more adverse side effects. In a somewhat related study published by Cheng et al., patients who were diagnosed with stage III/IV pancreatic cancer were assigned into groups based on treatment with programmed cell death protein 1 (PD-1) blockade plus gemcitabine and nab-paclitaxel or chemotherapy alone. The patients treated with PD-1/chemotherapy had a progression free survival of 8 months as compared to 3.5 months in the chemotherapy alone cohort and the median overall survival was 15 months in the PD-1/chemotherapy arm as compared to 8 months in the chemotherapy alone arm. This study is timely as immunotherapeutic strategies targeting PD-1 in combination with other strategies have not previously shown survival comparison in patients with pancreatic cancer.

Future clinical trials will need to evaluate overall response to therapy to assist in treating this aggressive gastrointestinal malignancy. Additionally, expanded efforts in early detection are promising to aid in the diagnosis of patients with resectable early-stage cancer, who qualify for surgical resection, which has a more promising outlook for survival. Artificial Intelligence (AI) uses machines to reproduce human cognition and learning. AI methods are under evaluation for assisting with early screening, diagnosis, surgical treatment, risk prediction and management of post operative complications for patients with pancreatic cancer (reviewed in Zhao et al.). In the field of early detection and the diagnosis of intraductal papillary mucinous neoplasia or pancreatic adenocarcinoma, deep learning models have emerged with superior performance and high diagnostic accuracy. Additionally, in this review, the use of deep learning models and algorithms enabled risk prediction models for postoperative complications with strong area under the curve measures, indicating AI through the amalgamation of imaging modalities, tree models and AI-driven random forest and neural network algorithms can aid in the postoperative care of patients. Combined use of AI, immune-oncology and radiation, ablation, and new therapeutic approaches are all promising for the future care and management of pancreatic cancer.

Author contributions

KD: Writing – review & editing. SS: Writing – review & editing. JB-L: Writing – original draft.

Conflict of interest

The authors declare that the research was conducted in the absence of any commercial or financial relationships that could be construed as a potential conflict of interest.

The author(s) declared that they were an editorial board member of Frontiers, at the time of submission. This had no impact on the peer review process and the final decision.

Publisher's note

References

1. Arnold M, Abnet CC, Neale RE, Vignat J, Giovannucci EL, McGlynn KA, et al. Global burden of 5 major types of gastrointestinal cancer. *Gastroenterology*. (2020) 159:335–349.e15. doi: 10.1053/j.gastro.2020.02.068.

2. Siegel RL, Miller KD, Wagle NS, Jemal A. Cancer statistics, 2023. *CA: A Cancer J Clin*. (2023) 73:17–48. doi: 10.3322/caac.21763

frontiers | Frontiers in Oncology

TYPE Original Research
PUBLISHED 05 October 2022
DOI 10.3389/fonc.2022.870473

OPEN ACCESS

EDITED BY
O. Micheau,
Université de Bourgogne, France

REVIEWED BY
Pádraig D'Arcy,
Linköping University, Sweden
Claudio Brancolini,
Facoltà di Medicina e Chirurgia,
Università di Udine, Italy

*CORRESPONDENCE
Qi Chen
qchen@kumc.edu

SPECIALTY SECTION
This article was submitted to Cancer Molecular Targets and Therapeutics, a section of the journal Frontiers in Oncology

RECEIVED 06 February 2022
ACCEPTED 13 September 2022
PUBLISHED 05 October 2022

CITATION
Wang T, Chen P, Weir S, Baltezor M, Schoenen FJ and Chen Q (2022) Novel compound C150 inhibits pancreatic cancer through induction of ER stress and proteosome assembly.
Front. Oncol. 12:870473.
doi: 10.3389/fonc.2022.870473

Novel compound C150 inhibits pancreatic cancer through induction of ER stress and proteosome assembly

Tao Wang[1], Ping Chen[1], Scott Weir[2], Michael Baltezor[3], Frank J. Schoenen[4,5] and Qi Chen[1]*

[1]Department of Pharmacology, Toxicology and Therapeutics, University of Kansas Medical Center, Kansas, KS, United States, [2]Department of Cancer Biology, University of Kansas Medical Center, Kansas, KS, United States, [3]Biotechnology Innovation and Optimization Center, University of Kansas, Lawrence, KS, United States, [4]Higuchi Biosciences Center, University of Kansas, Lawrence, KS, United States, [5]Medicinal Chemistry Core Laboratory, Lead Development and Optimization Shared Resource, University of Kansas Cancer Center, Lawrence, KS, United States

Pancreatic cancer is a devastating disease with a dismal prognosis and poor treatment outcomes. Searching for new agents for pancreatic cancer treatment is of great significance. We previously identified a novel activity of compound C150 to inhibit pancreatic cancer epithelial-to-mesenchymal transition (EMT). Here, we further revealed its mechanism of action. C150 induced ER stress in pancreatic cancer cells and subsequently increased proteasome activity by enhancing proteasome assembly, which subsequently enhanced the degradation of critical EMT transcription factors (EMT-TFs). In addition, as cellular responses to ER stress, autophagy was elevated, and general protein synthesis was inhibited in pancreatic cancer cells. Besides EMT inhibition, the C150-induced ER stress resulted in G2/M cell cycle arrest, which halted cell proliferation and led to cellular senescence. In an orthotopic syngeneic mouse model, an oral dose of C150 at 150 mg/kg 3× weekly significantly increased survival of mice bearing pancreatic tumors, and reduced tumor growth and ascites occurrence. These results suggested that compound C150 holds promises in comprehensively inhibiting pancreatic cancer progression.

KEYWORDS

pancreatic cancer, ER stress, cell senescence, proteasome, autophagy

Introduction

Pancreatic cancer is among the most malignant types of cancers and will soon become the third leading cause of cancer-related death in the United States (1). The current estimated overall 5-year survival rate is only 10% (1). Despite our increasing understanding of the genetic and molecular makeups of the disease over the past few decades, the prognosis of pancreatic cancer remains very poor. Current first-line chemotherapy options include gemcitabine plus nab-paclitaxel and the regimen of FOLFIRINOX (oxaliplatin, irinotecan, fluorouracil, and leucovorin). These therapies improved the median survival by a few months compared to gemcitabine mono treatment, but they added significant toxicities to patients (2, 3).

The homeostasis between protein loading and protein folding in the endoplasmic reticulum (ER) is essential for cell survival. Cellular insults that perturb the homeostasis lead to misfolded protein accumulation and ER stress (4). In response to ER stress, cells activate the unfolded protein response (UPR) pathways to restore homeostasis in the ER, as a survival mechanism (5). The UPR is controlled by three ER membrane-bound proteins, protein kinase RNA-like ER kinase (PERK), inositol-requiring protein 1α (IRE1α), and activating transcription factor 6 (ATF-6) (5). Activation of PERK, IRE1α, and ATF-6 activates their direct downstream transcription factors, ATF-4, XBP1-s, and spliced-ATF-6, respectively, leading to increased gene expressions of chaperone proteins to enhance protein folding capacity in the ER (6, 7). In addition, PERK activation results in the attenuation of mRNA translation through eIF2α phosphorylation, therefore reducing new protein load to the ER (8). Finally, ER stress also activates the ER-associated degradation (ERAD) pathway to facilitate misfolded protein removal through the ubiquitin–proteasome system and autophagy (9, 10). By increasing the level of protein folding chaperones, reducing protein synthesis, and enhancing protein removal through ERAD, the UPR signaling functions as a pro-survival mechanism to restore ER homeostasis (10). However, severe or prolonged ER stress that goes beyond the UPR rescue capacity would lead to cell proliferation arrest, cell death, and/or senescence (11–13).

As the major protein degradation system in the cell, proteasome levels and activities are often elevated upon ER stress, to facilitate the clearance of misfolded or damaged proteins (14). The two major forms of proteasomes in the mammalian cells are 20s proteasome and 26s proteasome, both of which are multi-subunit protein complexes. The 20s proteasome is made up of two sets of α subunits (α_{1-7}) and two sets of β subunits (β_{1-7}) with a stoichiometry of $\alpha_{1-7}\beta_{1-7}\beta_{1-7}\alpha_{1-7}$, while the 26s proteasome is composed of a 20s proteasome flanked at one or both ends by a 19s regulatory particle (19s RP) that is made up of 19 different subunits (15). Therefore, the assembly of a full 26s proteasome requires the steps of 20s proteasome assembly, 19s RP assembly, and the docking of 19sRP to the 20s proteasome (16). The 26s proteasomes serve as the main complex for cellular protein degradation in an ATP- and ubiquitin-dependent manner (17), while the 20s are also capable of degrading a portion of cellular proteins independent of ATP and ubiquitin (18, 19).

Because of the essential role of ER balance in cell survival, disrupting ER balance has been proposed as a potential therapeutic approach in cancer treatment (20, 21). We have previously reported that a quinoline compound (namely, C150) enhanced the proteasome-mediated degradation of Snail protein in pancreatic cancer cells, causing EMT inhibition and reduced cancer cell invasion (22). In this study, we further revealed that C150 induced profound ER stress in pancreatic cancer cells and led to the increase of proteasome assembly, cellular autophagy, and attenuation of general mRNA translation. C150 treatment arrested pancreatic cancer cells in the G2/M phase, induced cellular senescence, and increased cellular sensitivity to gemcitabine treatment. C150 treatment significantly increased survival and reduced tumor growth in a syngeneic pancreatic cancer mouse model.

Materials and methods

Cell culture and reagents

Human pancreatic cancer cells PANC-1 and MIA PaCa2 were obtained from the American Type Culture Collection (ATCC). Murine pancreatic cancer Pan02 cells were generously donated by Dr. Shrikant Anant from the University of Kansas Medical Center. Cells were cultured in DMEM (10-013-CV, Corning Life Sciences) with 10% FBS (F0926, Sigma-Aldrich) and 100 units/ml penicillin/streptomycin (30-001-CI, Corning Life Sciences) in a 37°C cell incubator with humidified 5% CO_2. All cells were cultured within 20 passages in our laboratory. Compound C150 was purchased from ChemBridge Chemical Library (ChemBridge, San Diego, CA) and stocked in dimethyl sulfoxide (DMSO). All C150 treatments were diluted in cell culture medium with a final DMSO concentration lower than 0.1% (v/v%). Control cells were treated with the same concentrations of DMSO with respect to drug-treated groups (<0.1% v/v%).

Proteasome activity assay

PANC-1 cells were seeded and grown in 100-mm petri dishes at 1×10^6 cells/dish. The next day, medium was replaced with fresh medium containing C150 or DMSO, and cells were treated for 24 h. After treatment, cells were lysed in

proteasome activity lysis buffer (50 mM HEPES, 10 mM $NaCl_2$, 1.5 mM $MgCl_2$, 1 mM EDTA, 2 mM ATP, and 1% Triton X-100) on ice for 1 h. The supernatants of the cell lysates were collected by centrifugation at 16,000 × *g* for 15 min and kept on ice. The Pierce BCA protein assay (23225, Thermo Scientific) was performed to determine protein concentrations in the cell lysates. In a black-wall 96-well plate, 150 µl of fluorescent proteasome substrate solution Suc-LLVY-AMC (BML-P802-0005, Enzo Life Science, Farmingdale, NY) and 50 µl of cell lysates were added per well to a final substrate concentration of 100 µM. The proteasome inhibitor epoxomicin (4 µM) was added in the negative control group. The plate was then placed in a fluorescent plate reader with 37°C incubation and read under the kinetic mode at 360/460 nm every 20 min for 80 min. Fluorescent readings were then normalized to the protein amounts in the cell lysates of each sample.

Western blots

Cells were lysed in Pierce RIPA buffer (89901, Thermo Scientific) supplemented with protease and phosphatase inhibitor cocktails (P8340, P5726, and P0044, Sigma-Aldrich). Protein concentrations of the lysates were determined using the Pierce BCA protein assay (23225, Thermo Scientific). The cell lysates were then mixed with 2× Laemmli SDS loading buffer (161-0737, Bio-Rad), run in 8% or 10% SDS-PAGE gel, and transferred onto 0.2-µm PVDF membranes (ISEQ00010, MilliporeSigma). Membranes were blocked in 5% blocking grade milk in 0.1% TBST solution (0.1% Tween-20 in 1× TBS) for 2 h at room temperature, then incubated with primary antibody at 4°C overnight in 5% BSA/0.1% TBST solution. Mouse monoclonal antibodies against 20s subunits β-1 (sc-374405), β-2 (sc-58410), β-5 (sc-393931), α-5 (sc-137240), α-6 (sc-271187), and 19s subunits PSMC-2 (sc-166972), PSMC-3 (sc-100462), and PSMC-4 (sc-166115) were purchased from Santa Cruz Biotechnology (Dallas, TX). Rabbit monoclonal antibodies against Bip (3177T), ATF-4 (11815S), ATF-6 (65880T), XBP-1s (40435S), LC-3 (3868S), phospho-eIF2α (3398T), Vinculin (4650S), and GAPDH (2118S) were purchased from Cell Signaling Technology (Danvers, MA). Mouse monoclonal anti-puromycin (PMY-2A4) and anti-eIF2α (PCRP-EIF2S1-1E2) antibodies were purchased from Developmental Studies Hybridoma Banks (the University of Iowa, Iowa City, IA). Following primary antibody incubation, membranes were washed three times in 0.1% TBST solution and then incubated with HRP-linked anti-rabbit (7074S) or anti-mouse (7076S) secondary antibodies (Cell Signaling Technology, Danvers, MA) in 5% milk for 2 h at room temperature. Blotting bands were then detected by using Pierce ECL plus reagents (32132, Thermo Scientific).

Native gel analysis for assembled proteasome

PANC-1 cells were seeded and treated the same way as in the proteasome activity assay. After treatments, cells were lysed in proteasome activity assay lysis buffer on ice for 1 h. The supernatants of the cell lysates were collected by centrifugation at 16,000 × *g* for 15 min and kept on ice. After determining the protein concentrations in the lysates with Pierce BCA protein assay, the samples were then mixed with 2× non-denaturing loading buffer (161-0738, Bio-Rad). A total of 30 µg of protein from each sample was loaded and separated in 4% Tris-Borate native gel at 100 V for 3.5 h in running buffer (89 mM Tris, 89 mM boric acid, 2 mM EDTA, 5 mM $MgCl_2$, and 1 mM ATP). The 4% Tris-Borate native gels were made as follows (10 ml): 7.5 ml of H_2O + 1.333 ml of 30% polyacrylamide (1610158, Bio-Rad) + 50 µl of $MgCl_2$ (1 M) + 100 µl of ATP (0.1 M) + 1 ml of 10× Tris-Boric-EDTA buffer (161-0733, Bio-Rad) + 100 µl of 10% APS + 10 µl TEMED. After electrophoresis, gels were soaked in 1× Tris-Glycine buffer with 0.1% SDS for 30 min. Proteins in gels were then transferred onto 0.2 µm PVDF membranes at 100 V for 3.5 h at 4°C in transferring buffer (1× Tris-Glycine buffer with 20% methanol). Subsequently, membranes were stained with Ponceau S to reveal protein bands, then washed in 0.1% TBST solution and blocked in 5% blocking grade milk for 2 h at room temperature before incubating with anti-20s β-5 antibody and anti-19s PSMC-3 antibody for overnight at 4°C. The membrane was then washed in 0.1% TBST buffer and incubated with HDR-conjugated anti-mouse secondary antibody (7076S, Cell Signaling Technology, Danvers, MA). Protein bands were detected with Pierce ECL plus reagents (32132, Thermo Scientific).

RT-qPCR

Total RNA was extracted from cells using TRIZOL reagents (AM9738, Invitrogen) according to the manufacturer's protocol. The synthesis of cDNA was carried out with 1 µg of total RNA using the OneScript cDNA Synthesis Kit (G234, Applied Biological Materials, Richmond, BC, Canada). cDNA was then diluted five times in nuclease-free H_2O for RT-qPCR reaction. RT-qPCR was performed using the Bio-Rad iQ iCycler detection system with One-Step BrightGreen reagents (MasterMix-S, Applied Biological Materials, Richmond, BC, Canada) according to the manufacturer's protocol. Each reaction was carried out in 10 µl volume with 5 µl of 2× BrightGreen qPCR MasterMix, 0.6 µl of forward and reverse primer mix (10 µM), 2 µl of diluted cDNA, and 2.4 µl of nuclease-free H_2O. All qPCR reactions were run under the following cycling conditions according to the protocol from the

kit: enzyme activation at 95°C for 10 min, followed by 40 cycles of denaturation (95°C for 15 s) and annealing/extension (60°C for 60 s). The melting curve was detected at 55°C–95°C with 0.5°C increments. Three independent experiments were carried out, and reactions were run in triplicate for each sample. Gene expression was quantified using the $2^{\Delta\Delta\text{-Ct}}$ method with GAPDH as the internal control gene. Primers for detected genes are listed in Table 1.

Cell cycle analysis

PANC-1 cells were seeded and grown in 60-mm petri dishes at 5×10^5 cells/dish. The next day, the medium was changed into fresh medium with C150 or DMSO. At 24 h or 48 h, cells were collected by trypsinization, washed with 1× PBS twice, and fixed in 70% ethanol at −20°C overnight. Cells were then washed with 1× PBS and stained in PI staining solution (20 μg/ml propidium iodide in 1× PBS solution with 0.1 mg/ml RNase A and 0.1% Triton X-100) at 37°C for 15 min protected from light. Cells were kept in the staining solution overnight at 4°C protected from light before being analyzed for cell cycle distribution with flow cytometry (BD LSR II, BD Biosciences).

Cell growth curve by MTT assay

Cells were seeded in 96-well plates at 5,000 cells/well and incubated in the cell culture incubator overnight. The next day, the medium was changed into fresh medium containing C150 at the indicated concentrations. Cells were further incubated for 0, 24, 48, 72, and 96 h, then MTT (3-(4,5-dimethylthiazol-2-yl)-2,5-diphenyltetrazolium bromide) was added to each well to a final concentration of 0.5 mg/ml, and the plates were further incubated for 4 h. The medium was then removed and 150 μl of DMSO was added to each well. Absorbance was measured at 570 nm using a microplate reader (BioTek, Winooski, Vermont).

Gemcitabine combination treatment

PANC-1 cells were seeded in 96-well plates at 5,000 cells/well and incubated overnight, and then changed into fresh medium with treating drug combinations in a matrix design as shown in Figure 3D. Cells were treated for 72 h and viability was detected by MTT assay. The combination index was calculated according to Chou-Talalay's method using CompuSyn software (23).

Immunofluorescent staining for LC-3 puncta

PANC-1 cells were seeded and grown in eight-chamber microscope cell culture slides (PEZGS0816, MilliporeSigma) at 6×10^4 cells per chamber. The next day, the medium was replaced with fresh medium containing C150 or DMSO, and the cells were treated for 24 h. After treatment, cells were washed

TABLE 1 Gene primer sequences for RT-qPCR.

Gene name	Forward (5' -> 3')	Reverse (5' -> 3')
PSMG-1 (PAC-1)	TCC TTT CCT GAG AGC CCT AAA A	TGT TCT AGC AAT GGA CAA CAC G
PSMG-2 (PAC-2)	ACC GAT TGT CTT GTG CCA ATG	AGG CAA TGA ATA CAC TTC AGC AT
PSMG-3 (PAC-3)	GAA GAC ACG CCG TTG GTG ATA	GAA GGA CTT TTG TGG TGA GCA
PSMG-4 (PAC-4)	GTC CAC TTC CAC GTC ATG C	GGG AGG TAG ACA CGG GGA T
POMP	ACT TGG ATC TGA GCT AAA GGA CA	GGG GAT GAC TAG GCA AAA GTT C
PAAF-1	GGA GGT CTT GGT GTG TCT TCT	CAA CGA TGG CTG TAT CCA GGA
PSMD-10	GGG TGT GTG TCT AAC CTA ATG G	GGC CAG AAT ACT CTC CTT CAA CT
PSMD-5	GCG CTG CTG AGA GAG GTA G	AGT CTT TTC CCT ATG GTT CTC GT
PSMD-9	AGG AGG AGA TAG AAG CGC AGA	GTG CGG ACT TGG TAC AGG T
IL6	CCCCTCAGCAATGTTGTTTGT	CTCCGGGACTGCTAACTGG
IL7	CCCTCGTGGAGGTAAAGTGC	CCTTCCCGATAGACGACACTC
IL-13	CCTCATGGCGCTTTTGTTGAC	TCTGGTTCTGGGTGATGTTGA
IL-15	TTTCAGTGCAGGGCTTCCTAA	GGGTGAACATCACTTTCCGTAT
CCL5	CCAGCAGTCGTCTTTGTCAC	CTCTGGGTTGGCACACACTT
CXCL10	GTGGCATTCAAGGAGTACCTC	TGATGGCCTTCGATTCTGGATT
PAI-1	CCACCTCCGTGAAGGAATGAC	GGTAGTGTGGCATAAACAGCA
TNF-a	CCTCTCTCTAATCAGCCCTCTG	GAGGACCTGGGAGTAGATGAG
MCP1	CAGCCAGATGCAATCAATGCC	TGGAATCCTGAACCCACTTCT
GAPDH	CCA GGT GGT CTC CTC TGA CTT CAA CA	AGG GTC TCT CTC TTC CTC TTG TGC TC

twice with 1× PBS and fixed in ice-cold 100% methanol at −20°C for 15 min. Cells were then washed three times with 1× PBS and blocked in 5% normal goat serum (5425S, Cell Signaling Technology, Danvers, MA) in 1× PBS with 0.3% Triton X-100 for 1 h at room temperature. Cells were then incubated with anti-LC-3 antibody (3868S, Cell Signaling Technology, Danvers, MA) at 4°C overnight in antibody incubation buffer (1× PBS with 0.3% Triton X-100 and 1% BSA). After three washes with 1× PBS, cells were incubated with Alexa-488 conjugated secondary antibody (4412S, Cell Signaling Technology, Danvers, MA) for 2 h at room temperature and protected from light. After three washes with 1× PBS, the slide was then coverslipped with the anti-fade mounting solution with DAPI (8961S, Cell Signaling Technology, Danvers, MA) and cured in the dark overnight at room temperature to stain the nuclei before being imaged with fluorescence microscopy at 600× magnification.

β-galactosidase staining for cellular senescence

The senescence β-galactosidase staining kit (9860S, Cell Signaling Technology, Danvers, MA) was utilized according to the manufacturer's protocol. Briefly, PANC-1 cells were seeded and grown in 24-well plates at 5×10^4 cells per well. The next day, the old medium in the plates was replaced with fresh medium containing C150 or DMSO, and cells were treated for 24 and 48 h. After treatment, cells in the plates were washed with 1× PBS twice and fixed in 0.5 ml fixative solution for 15 min at room temperature. Following cell fixation, 0.5 ml staining solution with X-gal (1 mg/ml) at pH 6.0 was added to each well. The plates were then sealed with parafilm, wrapped in aluminum foil, and incubated in a 37°C dry oven for 24 h. After removal of the staining solution, cells were washed three times with 1× PBS and covered in 0.5 ml 70% glycerol. At least five random fields per well were imaged using a light microscope under the bright field at 200× magnification. Positively stained cells and the total cells in each image were counted using the multi-point manual counting tool in ImageJ software.

Syngeneic mouse model of pancreatic cancer

All animal experiments followed an Animal Care and Use Protocol (2018-2443) approved by the Institutional Animal Care and Use Committee at the University of Kansas Medical Center. Female C57BL/6 mice (6–8 weeks old) were purchased from the Jackson Laboratory (Bar Harbor, ME). For tumor cell implantation, mice were put under anesthesia by isoflurane inhalation (5% isoflurane for induction of anesthesia and 2% for maintenance). A subcostal laparotomy was performed to expose the pancreas. A total of 4×10^5 Pan02 mouse pancreatic cancer cells suspended in 50 µl of 1× PBS were injected into the tail of the pancreas. The wound was then sealed with wound clips. Twenty-one days after tumor cell inoculation, two random mice were sacrificed to confirm tumor formation. Subsequently, mice were randomly grouped into two groups (vehicle: $n = 9$, treatment: $n = 8$). Treatments were then commenced with 150 mg/kg of C150 or vehicle (5% Tween-80 + 95% H_2O) by oral gavage. Mice were treated three times a week for 2 weeks and monitored twice daily for signs of moribund state. The moribund state was determined using body score (<2), or any signs of extreme lethargy, lack of responsiveness to manual stimulus, immobility, or hypothermia. When these signs were observed, the mice were euthanized and counted as death events. Necropsy was then immediately performed, and tumors were weighed and collected. If ascites were present, ascites volume was measured. All survived mice at the endpoint (35 days after tumor inoculation) were euthanized and tumors and ascites were collected upon necropsy.

Statistics

All data were presented as mean ± SD unless otherwise stated. The Student's *t*-test was performed for two-group comparisons. One-way ANOVA with the Tukey *post-hoc* test was performed for multi-group comparisons. A p-value < 0.05 is considered statistically significant.

Results

C150 increased proteasome activity in PANC-1 cells by increasing proteasome assembly

We have previously reported that C150 enhanced the proteasomal degradation of the pro-EMT transcription factor Snail in PANC-1 cells (22). In addition, we found that β-catenin, TP53, and Sox2 protein levels were also reduced by C150 treatment (Figure 1A). All of these transcription factors are proteasome substrates (24–26). Therefore, we postulated that C150 increased proteasome activity in the cell. To examine the cellular proteasome activity upon C150 treatment, PANC-1 cells were first treated with C150 (1 µM and 2 µM) for 24 h. The cell lysates were collected under non-denaturing conditions and incubated with a proteasome substrate, Suc-LLVY-AMC, which generates fluorescence upon proteasomal degradation. The results showed that lysates from C150-treated cells exhibited a significantly higher proteasome activity compared to the DMSO-treated group (Ctrl) in a concentration-dependent manner to C150 (Figure 1B). This increase was completely attenuated by a specific proteasome inhibitor epoxomicin

10.3389/fonc.2022.870473

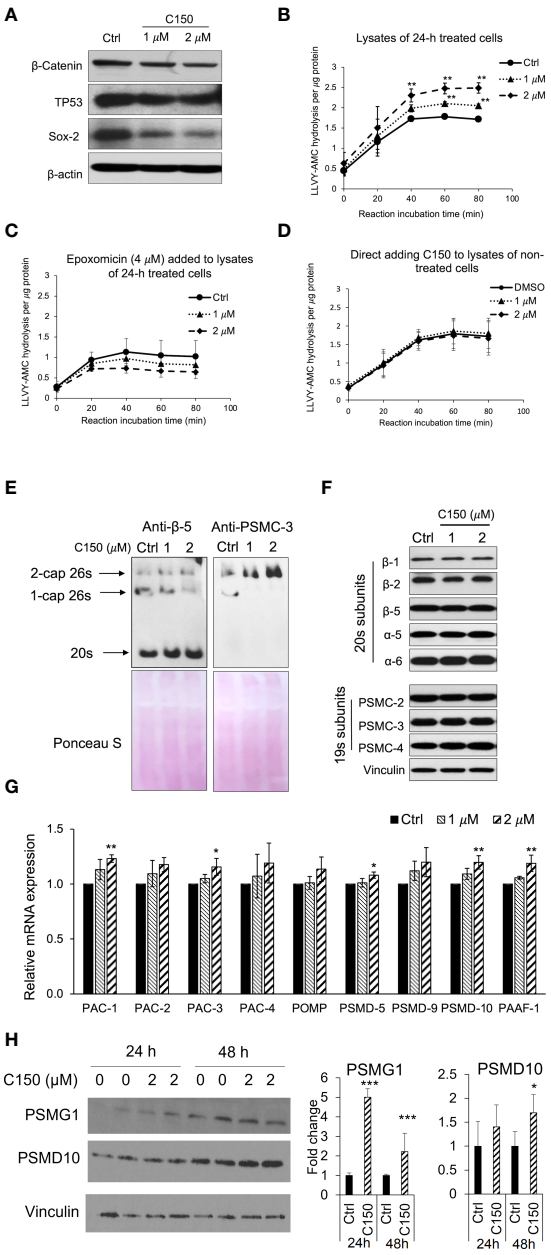

FIGURE 1
C150 enhanced proteasome activity by increasing 20s proteasome and 26s proteasome assembly. **(A)** C150 decreased β-catenin, TP53, and Sox-2 protein level. PANC-1 cells were treated with DMSO (Ctrl) or C150 (1 μM and 2 μM) for 24 h. Total cell lysate was analyzed. β-Actin was blotted as loading control. **(B, C)** Proteasome activity in PANC-1 cells treated with C150. PANC-1 cells were treated with C150 (1 μM and 2 μM) or DMSO (Ctrl) for 24 h. Cell lysates were collected and incubated with proteasome substrate Suc-LLVY-AMC at 37°C, in the absence **(B)** and presence **(C)** of epoxomicin (4 μM), and the kinetics of fluorescence signal was detected every 20 min for 80 min at 360/460 nm. Fluorescence signal intensity was quantified to the protein amounts in each reaction. **(D)** Proteasome activity in PANC-1 cell lysate incubated with C150. DMSO (Ctrl) or C150 (1 μM and 2 μM) was directly added into lysates of non-treated PANC-1 cells and incubated at room temperature for 30 min before mixing with Suc-LLVY-AMC substrate. **(E)** Native gel blots for assembled 20s and 26s proteasome. Anti b-5 antibody was used to show the 20s and anti-PSMC-3 was used to show the 26s proteasomes. Lower panels show Ponceau S staining. **(F)** Western blots of proteasome subunits. PANC-1 cells were treated with C150 (1 μM and 2 μM) or DMSO (Ctrl) for 24 h. Total cell lysates were used. Vinculin was a loading control. **(G)** RT-qPCR for mRNA expressions of proteasome assembly chaperones. PANC-1 cells were treated with C150 (1 μM and 2 μM) or DMSO (Ctrl) for 24 h. Results were quantified and normalized to Ctrl group using the $2^{-\Delta\Delta Ct}$ method with GAPDH as a housekeeping gene. **(H)** Western blots of PSMG-1 (*PAC-1* gene product) and PSMD-10 proteins. The left panel is a representative image of the Western blots. The right panel shows fold changes of relative bands intensity normalized to Vinculin. All data are presented as mean ± SD of three independent experiments. *$p < 0.05$, **$p < 0.01$, ***$p < 0.001$ (vs. Ctrl) by either Student's *t*-tests between two groups, or one-way ANOVA with Tukey HSD tests among multiple groups.

(Figure 1C). To examine whether C150 directly increased the activity of proteasome, non-treated PANC-1 cell lysates were incubated with C150 and the proteasome substrate. The direct incubation of C150 in non-treated cell lysates did not affect proteasome activity (Figure 1D). These data suggested that C150-mediated increase in proteasome activity was dependent on a cellular process that requires the integrity of the cell but was not through direct interaction with proteasomes.

We then investigated the total levels of the assembled 20s and 26s proteasome in the PANC-1 cells treated with C150. Anti-β-5 subunit antibody was used to show the 20s proteasomes. Because the 26s proteasome is composed of a 20s proteasome flanked by one or two 19s caps at its ends, an anti-PSMC-3 subunit for 19s RP was also used to show the 1-cap or 2-cap 26s proteasomes. Native gel protein electrophoresis and Western blots showed that the assembled 20s proteasomes and 2-cap 26s proteasomes were both elevated upon C150 treatment (Figure 1E). To determine if the increased 20s and 26s proteasome levels were the results of the increased expressions of their subunits, we detected a panel of 20s and 19s subunits by Western blot. All the examined subunits remained unchanged by C150 treatment (Figure 1F). Because the abundance of proteasomes in the cell is also regulated by their chaperone-dependent assembly (14, 27), we then examined the expressions of nine proteasome assembly chaperones by RT-qPCR. We found that 24-h C150 treatment (1 μM and 2 μM) significantly increased the expressions of the chaperones PAC-1, PAC-3, PSMD-5, PSMD-10, and PAAF-1, with the other four chaperones showing a trend of increase (Figure 1G). We then detected the protein expression of PSMG-1 (PAC-1 gene product) and PSMD-10 as representatives of the increased chaperones. The protein levels of PSMG-1 were increased upon 2 μM C150 treatment at 24 and 48 h (Figure 1H), and the protein levels of PSMD-10 were significantly increased at 48 h of treatment (Figure 1H). Taken together, the data suggested that C150 enhanced proteasome activity in PANC-1 cells by increasing proteasome assembly.

C150 induced ER stress, increased autophagy, and attenuated protein synthesis in PANC-1 cells

An increase in proteasome levels can be induced by ER stress (28, 29). We next investigated whether C150 treatment induced ER stress in PANC-1 cells. At 24-h treatment, C150 (1 μM and 2 μM) resulted in a profound upregulation of ER stress markers, Bip, ATF-4, and XBP-1s (Figure 2A). During ER stress response, autophagy is often initiated to further assist the removal of misfolded and damaged proteins (30). Our data showed that C150 treatment significantly increased LC-I and LC-3II, and the LC-3II level was further enhanced by the additional treatment of chloroquine at 20 μM for 4 h (Figure 2B), suggesting an increased autophagy flux by C150 treatment. The increased autophagy was further confirmed by immunostaining of LC-3 puncta in the cells (Figure 2C). There was a robust increase in the phosphorylation of the translation initiation factor eIF2α upon C150 treatment (Figure 2D). The phosphorylation of eIF2α is known to downregulate global translation, but to stimulate translation of some mRNAs such as those involved in stress responses (31). Our data in the increased expression of chaperone proteins PSMG-1 and PSMD-10 (Figure 1H) were consistent with this. Expecting a possible reduction of global protein synthesis (32), we then performed a puromycin incorporation assay (33) to detect protein neosynthesis (33). Puromycin can effectively incorporate into newly synthesized peptides and later be detected using Western blotting (33, 34). PANC-1 cells were treated with C150 (1 μM and 2 μM) for 24 and 48 h, and then pulse-treated with 2 μM puromycin for 20 min. Newly synthesized proteins were detected by Western blots in survived cells using an anti-puromycin antibody. Significant decreases in the levels of incorporated puromycin were detected with the treatments at either 24 or 48 h (Figure 2E), consistent with the eIF2α phosphorylation.

C150 caused G2/M cell cycle arrest, induced cell senescence, and synergized with gemcitabine in PANC-1 cells

It was reported that ER stress was able to induce cell cycle arrest (11, 35). Upon C150 treatment (1 μM and 2 μM) for 24 h and 48 h in PANC-1 cells, there was a robust increase in the cell population in the G2/M phase as demonstrated by PI cell cycle analysis (Figure 3A), suggesting a G2/M cell cycle arrest under C150 treatment. Cell growth curves showed a significantly reduced proliferation rate by C150 treatment (Figure 3B). Sustained cell cycle arrest commonly results in apoptosis and/or cell senescence (36). Our previous data have shown that C150 treatment did not induce apoptosis (22). Notably, data here showed that C150 treatments at 24 and 48 h effectively induced senescence in PANC-1 cells as indicated by the increased β-galactosidase (SA-β-galactosidase) staining at pH 6.0 (Figure 3C). Western blots showed that two of the known markers of cellular senescence PAI-1 and TNF-α were significantly upregulated in PANC-1 cells treated with C150 (Figure 3D) at 24 and 48 h, consistent with the observed senescent phenotype. Induction of senescence was reported to sensitize pancreatic cancer cells to chemotherapeutic agents (37). We found that the combination treatment of C150 with gemcitabine more effectively reduced PANC-1 cell viabilities compared to single-agent treatment (Figure 3E). Strong synergistic effects were shown when C150 was added to gemcitabine, with Chou-Talalay's combination index (CI) (23) being far less than 1 (Figure 3E).

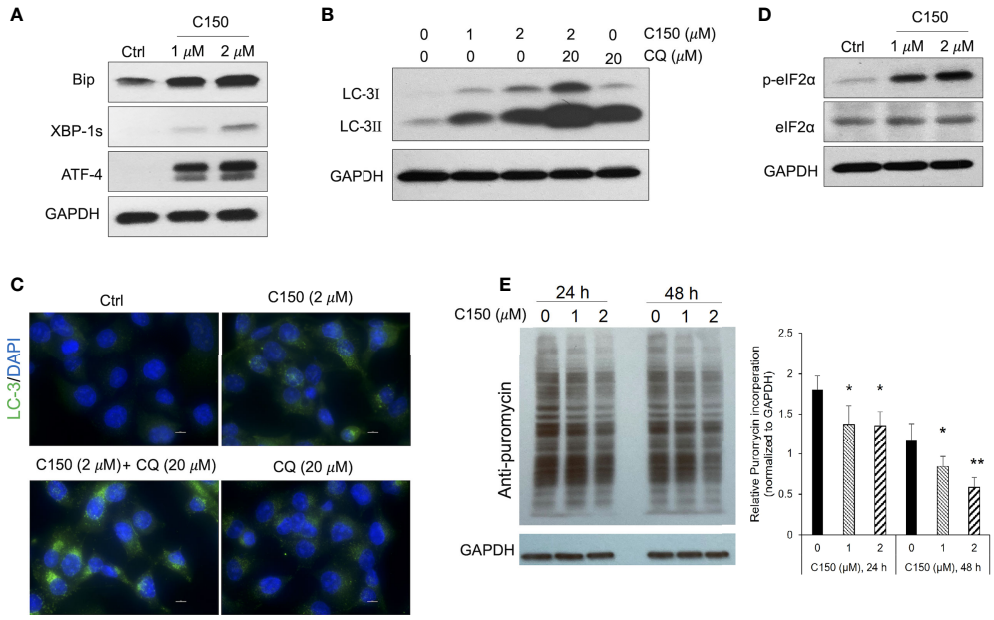

FIGURE 2
C150 induced ER stress, resulted in autophagy and attenuation of protein translation in PANC-1 cells. PANC-1 cells were treated with DMSO (Ctrl) or C150 (1 μM and 2 μM) for 24 h. **(A)** Western blots of ER stress makers. GAPDH was blotted as loading control. **(B)** Western blots of the autophagy marker LC-3. CQ, chloroquine (20 μM, 4 h treatment). **(C)** Immunofluorescence staining for LC-3 puncta. Cells were fixed and stained against LC-3 (green) and DAPI (blue). Scale bar, 10 μm. **(D)** Western blots of eIF2α and p-eIF2α. **(E)** Puromycin incorporation showing protein synthesis inhibition. PANC-1 cells were treated with 2 μM puromycin for 20 min after 24 or 48 h of treatment with C150. Total cell lysates were analyzed and blotted with anti-puromycin antibody. GAPDH was blotted as loading control. The left panel is a representative image of the Western blots. The right panel shows total band intensity normalized to GAPDH. Data are presented as mean ± SD of three independent experiments. *$p < 0.05$, **$p < 0.01$ (vs. Ctrl) by one-way ANOVA with Tukey HSD tests.

C150 reduced tumor growth and increased survival in a syngeneic pancreatic cancer mouse model

A syngeneic pancreatic cancer mouse model was used to evaluate the activities of C150 *in vivo*. Compared with xenografts in immune-compromised mice, the syngeneic model preserves the intact immune functions, which plays an important role in cancer progression and responses to treatment. Pan02 mouse pancreatic cancer cells were orthotopically injected into the pancreas of C57BL/6 mice. Three weeks (21 days) after cell implantation, mice were treated with C150 (150 mg/kg) or vehicle by oral gavage three times a week for 2 weeks. Data showed that C150 treatments significantly improved the survival rate of mice at 35 days after tumor inoculation (80% survival rate in C150-treated group versus 10% in the vehicle-treated group) (Figure 4A). The tumor weight at necropsy was significantly reduced by C150 treatment ($n = 8$) compared to vehicle-treated controls ($n = 9$) (Figure 4B). Moreover, 89% (8/9) of mice in the vehicle-treated group developed ascites, whereas only 50% (4/8) in the C150 group had ascites (Figure 4C). In the mice that had ascites, the average volume was lower in C150-treated mice (Figure 4D). The expression levels of ER markers were examined in tumor tissues. Consistent with our *in vitro* data, the ER stress markers Bip, cleaved-ATF-6, ATF-4, and XBP-1s were elevated in C150-treated tumors compared to vehicle-treated controls (Supplementary Figure 1). A panel of cellular senescence markers were detected for their expression in the tumor samples using RT-qPCR. Data showed a significant increase in the mRNA levels of *PAI-1, MCP-1, IL6, CCL5*, and *TNF-α* in tumors treated with C150 (Figure 4E). Lamin B1, whose level decreases during cellular senescence (38), was also found to be decreased in C150-treated tumors (Figure 4F).

Because ascites developed in the tumor-bearing mice, we decided bodyweight was not a good indication of toxicity in this scenario. Instead, we examined the histology of liver and kidney at necropsy. There was no difference found in both organs between the control group and the C150-treated group (Figure 4G).

Discussion

Interrupting ER homeostasis has been shown as an effective way to inhibit tumor progress because of the vital role the ER plays in cellular protein homeostasis and cell survival (39, 40).

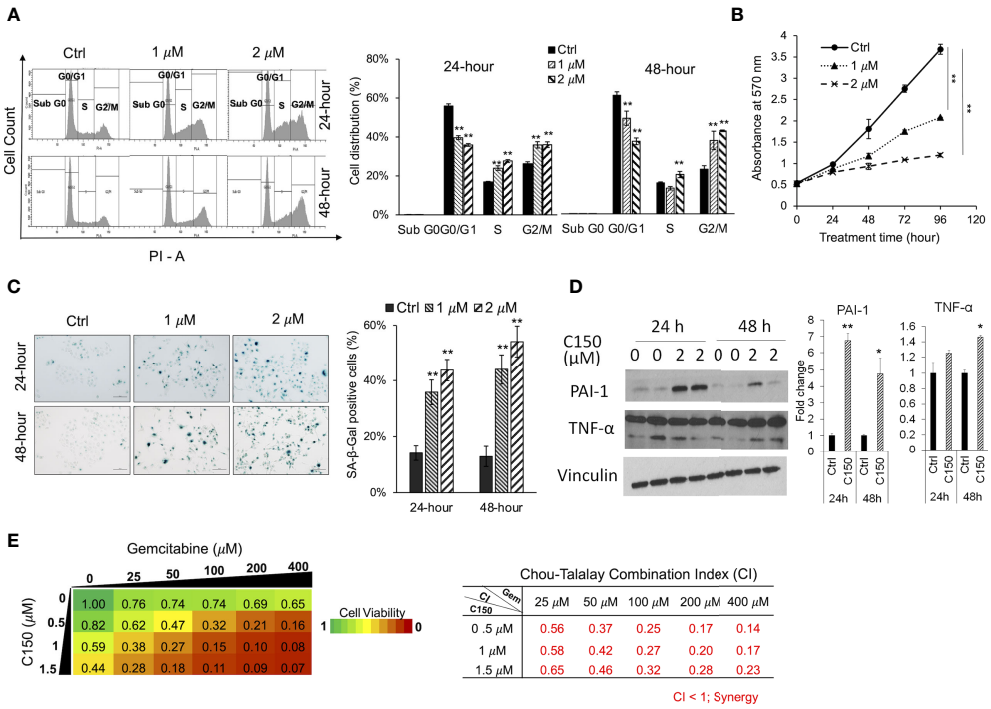

FIGURE 3
C150 caused G2/M cell cycle arrest, cellular senescence, and synergized with gemcitabine in PANC-1 cells. **(A)** Cell cycle analysis. PANC-1 cells were treated with DMSO (Ctrl) or C150 (1 μM and 2 μM) for 24 and 48 h. Cells were stained with propidium iodide (PI) and analyzed for cell cycle distributions with flow cytometry. Bar graph shows the quantification of the percentage of cells in each cell cycle. Data presented as mean ± SD of three independent experiments. **(B)** Cell growth curve. PANC-1 cells were seed at 5,000 cells per well in 96-well plates in triplicates and treated for 0, 24, 48, 72, and 96 h. Viable cells were detected by MTT assay. Data presented as mean ± SD of three experiments. **(C)** SA-β-galactosidase staining at pH 6.0 for cell senescence. Senescent cells were identified by the green-blue staining under bright field light microscopy at 200× magnification. Scale bar, 100 μm. Bar graph shows the percentage of senescent cells per imaging field with five random fields in each sample. Data presented as mean ± SD of two independent experiments each done in triplicate. **(D)** Western blots of two cell senescence markers PAI-1 and TNF-α. Band intensities were normalized to Vinculin and then compared to the untreated control. Bar graphs show fold changes versus control. Data presented as mean ± SD of two independent experiments each done in duplicate. **(E)** Heatmap of cell viabilities and combination index of C150 and gemcitabine in PANC-1 cells. PANC-1 cells were treated with C150 and gemcitabine at the indicated concentrations for 72 h. Cell viability was detected using MTT assay. Data presented as mean viability from three independent experiments each done in duplicate. The drug combination index was calculated according to the Chou-Talalay's method. Mean CI values from three experiments were presented. *$p < 0.05$, **$p < 0.01$ (vs. Ctrl) by one-way ANOVA with Tukey HSD test.

Due to high proliferation demand and hypoxic microenvironment, cancer cells are under higher endogenous ER stress, resulting in a higher endogenous activation level of UPR signaling (41). As such, pancreatic tumor tissues have higher Bip and ATF-6 expression levels than the normal pancreatic tissues (42). The high basal activation of UPR renders pancreatic cancer cells more vulnerable to the disturbance in ER homeostasis. Disrupting UPR signaling by either inhibiting or further activating it would both impede the cellular capacity to rescue ER stress, leading to catastrophic effects in the cancer cells (39, 43, 44). In agreement with this notion, our study found that C150 induced profound ER stress and further aggravated UPR signals in pancreatic cancer cells, which subsequently impeded cell proliferation, triggered cell cycle arrest, and led to pancreatic cancer cell senescence.

Findings in our study showed that C150 treatment significantly increased proteasome activity by enhancing proteasome assembly. The increased proteasome activity under ER stress is a pro-survival response of pancreatic cancer cells to restore ER proteomic homeostasis (45). However, C150-mediated increase in proteasome activity accelerated the degradation of several critical transcription factors in EMT/CSC/cell death pathways, such as Snail (22), β-catenin, Sox2, and TP53, as detected in this study. It is possible that many other important proteins in cancer cell growth/proliferation, invasion, and stemness are also influenced. The degradation of Snail and the other regulatory proteins consequently led to the inhibition of EMT and cell invasion in pancreatic cancer cells, as we previously reported (22). These results indicated that the increased proteasome activity under C150-induced ER stress

10.3389/fonc.2022.870473

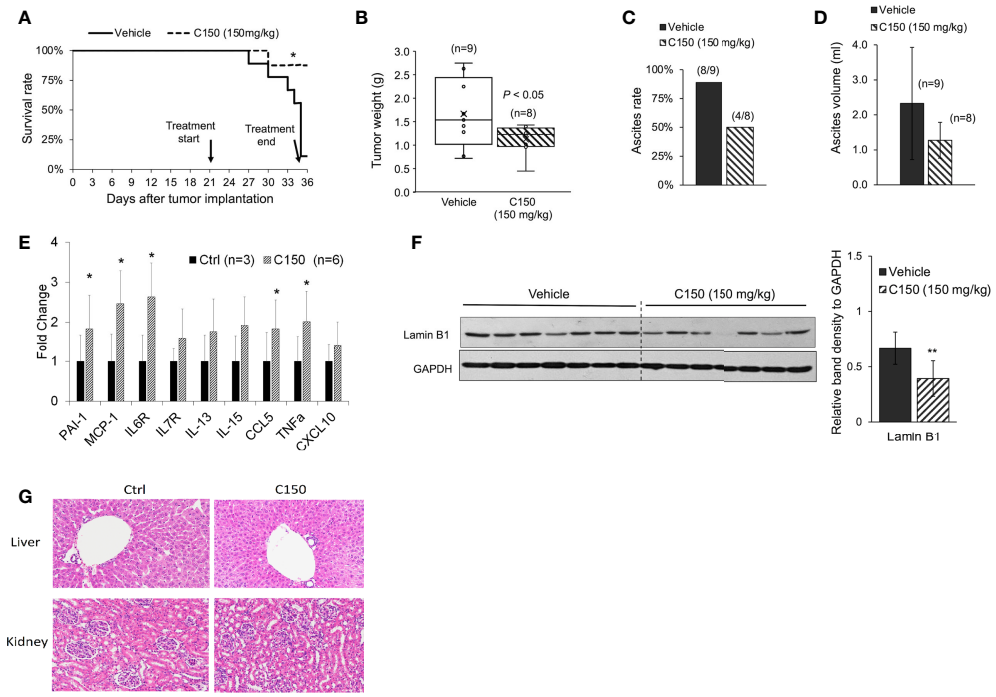

FIGURE 4
C150 treatment increased survival rate and reduced tumor growth in a syngeneic mouse model. **(A)** Kaplan–Meier survival curve of tumor-bearing mice. *$p < 0.05$ (vs. vehicle) by log-rank test. **(B)** Tumor weight at necropsy ($n = 9$ for vehicle, $n = 8$ for C150). $p < 0.05$ by Student's t-test. **(C)** Ascites occurrence rate. **(D)** Average volume of ascites presented as mean ± SD ($n = 9$ for vehicle, $n = 8$ for C150). **(E)** RT-qPCR for mRNA expressions of senescence markers. Tumor samples from three mice in the control group and six mice in the treated group were evaluated. Results were quantified and normalized to the Ctrl group using $2^{-\Delta\Delta Ct}$ method with GAPDH as a housekeeping gene. **(F)** Western blotting of Lamin B1 in mouse tumor tissues. Tumors from seven individual mice in each group were analyzed. GAPDH was blotted as loading control. Bar graph shows the quantification of band density relative to GAPDH. Data presented as mean ± SD. **$p < 0.01$ (vs. Vehicle) by Student's t-test. **(G)** H&E staining of liver and kidney tissues. Five animals from each group were examined. Representative images were shown.

may have a broad effect on degrading proteins important to pancreatic oncogenesis, resulting in comprehensive inhibition of pancreatic cancer progression through multiple pathways.

Cellular senescence is effectively evaded in pancreatic cancer due to the highly frequent loss-of-function mutations of CDKN2A and p53 (46, 47). Re-introduction of senescence has been reported as an effective approach to inhibit pancreatic cancer growth (48, 49). In our study, C150 successfully induced senescence regardless of the mutations of CDKN2A and p53 in PANC-1 cells (50). Senescence was also detected in Pan02 orthotopic mouse xenografts treated with C150, as shown by the decreased level of Lamin B1 (Figure 4E). Tumor growth was significantly inhibited, and survival of mice was improved. Moreover, C150-induced senescence greatly sensitized PANC-1 cells to gemcitabine treatment (Figures 3D, E). Therefore, C150 holds great promises in combination treatment with gemcitabine in pancreatic cancer. This synergy may be extended to other drugs, too. Further investigations are worthwhile to validate the synergistic effects in animal studies.

Data availability statement

The original contributions presented in the study are included in the article/Supplementary Material. Further inquiries can be directed to the corresponding author.

Ethics statement

The animal study was reviewed and approved by The University of Kansas Medical Center Institutional Animal Care and Use Committee.

Author contributions

QC conceptualized and oversaw the studies and provided resources. QC and TW designed the experiments. TW performed the experiments, collected the data, interpreted the data and wrote the manuscript. PC assisted with data collection,

analysis, and discussion. SW, FS, and MB participated in discussion. QC, TW, and PC have seen and can confirm the authenticity of the raw data. All authors contributed to the article and approved the submitted version.

Funding

The present study was supported by a Lied Basic Science Pilot Project Award through the Frontiers Pilot and Collaborative Funding Program provided by the NIH/NCATS (PI: Chen), and partially by a bridging grant from the University of Kansas Research Institute (Kansas, USA), and a grant provided by the GR's Foundation, Mosby Lincoln Foundation, Donlan Foundation (Kansas, USA), and the University of Kansas Cancer Center support grant (P30 CA168524, PI: Jensen).

Acknowledgments

The authors would like to thank Dr. Shrikant Anant at the University of Kansas Cancer Center for providing the Pan02 cells for the animal study.

Conflict of interest

The authors declare that the research was conducted in the absence of any commercial or financial relationships that could be construed as a potential conflict of interest.

Publisher's note

Supplementary material

The Supplementary Material for this article can be found online at: https://www.frontiersin.org/articles/10.3389/fonc.2022.870473/full#supplementary-material

References

1. Siegel RL, Miller KD, Fuchs HE, Jemal A. Cancer statistics, 2021. *CA: A Cancer J Clin* (2021) 71:7–33. doi: 10.3322/caac.21654

2. Von Hoff DD, Ervin T, Arena FP, Chiorean EG, Infante J, Moore M, et al. Increased survival in pancreatic cancer with nab-paclitaxel plus gemcitabine. *New Engl J Med* (2013) 369:1691–703. doi: 10.1056/NEJMoa1304369

3. Conroy T, Desseigne F, Ychou M, Bouche O, Guimbaud R, Becouarn Y, et al. FOLFIRINOX versus gemcitabine for metastatic pancreatic cancer. *N Engl J Med* (2011) 364:1817–25. doi: 10.1056/NEJMoa1011923

4. Schröder M, Kaufman RJ. ER stress and the unfolded protein response. *Mutat Res* (2005) 569:29–63. doi: 10.1016/j.mrfmmm.2004.06.056

5. Hetz C. The unfolded protein response: controlling cell fate decisions under ER stress and beyond. *Nat Rev Mol Cell Biol* (2012) 13:89–102. doi: 10.1038/nrm3270

6. Zhao L, Ackerman SL. Endoplasmic reticulum stress in health and disease. *Curr Opin Cell Biol* (2006) 18:444–52. doi: 10.1016/j.ceb.2006.06.005

7. Kaufman RJ. Molecular chaperones and the heat shock response. Sponsored by cold spring harbor laboratory, 6-10 may 1998. *Biochim Biophys Acta* (1999) 1423:R13–27. doi: 10.1016/s0304-419x(98)00029-8

8. Wek RC, Cavener DR. Translational control and the unfolded protein response. *Antioxid Redox Signal* (2007) 9:2357–71. doi: 10.1089/ars.2007.1764

9. Travers KJ, Patil CK, Wodicka L, Lockhart DJ, Weissman JS, Walter P. Functional and genomic analyses reveal an essential coordination between the unfolded protein response and ER-associated degradation. *Cell* (2000) 101:249–58. doi: 10.1016/S0092-8674(00)80835-1

10. Ron D, Walter P. Signal integration in the endoplasmic reticulum unfolded protein response. *Nat Rev Mol Cell Biol* (2007) 8:519–29. doi: 10.1038/nrm2199

11. Brewer JW, Diehl JA. PERK mediates cell-cycle exit during the mammalian unfolded protein response. *Proc Natl Acad Sci* (2000) 97:12625. doi: 10.1073/pnas.220247197

12. Shore GC, Papa FR, Oakes SA. Signaling cell death from the endoplasmic reticulum stress response. *Curr Opin Cell Biol* (2011) 23:143–9. doi: 10.1016/j.ceb.2010.11.003

13. Pluquet O, Pourtier A, Abbadie C. The unfolded protein response and cellular senescence. a review in the theme: Cellular mechanisms of endoplasmic reticulum stress signaling in health and disease. *Am J Physiol-Cell Physiol* (2014) 308:C415–25. doi: 10.1152/ajpcell.00334.2014

14. Rousseau A, Bertolotti A. Regulation of proteasome assembly and activity in health and disease. *Nat Rev Mol Cell Biol* (2018) 19:697–712. doi: 10.1038/s41580-018-0040-z

15. Tanaka K. The proteasome: overview of structure and functions. *Proc Jpn Acad Ser B Phys Biol Sci* (2009) 85:12–36. doi: 10.2183/pjab.85.12

16. Murata S, Yashiroda H, Tanaka K. Molecular mechanisms of proteasome assembly. *Nat Rev Mol Cell Biol* (2009) 10:104–15. doi: 10.1038/nrm2630

17. Collins GA, Goldberg AL. The logic of the 26S proteasome. *Cell* (2017) 169:792–806. doi: 10.1016/j.cell.2017.04.023

18. Baugh JM, Viktorova EG, Pilipenko EV. Proteasomes can degrade a significant proportion of cellular proteins independent of ubiquitination. *J Mol Biol* (2009) 386:814–27. doi: 10.1016/j.jmb.2008.12.081

19. Kumar Deshmukh F, Yaffe D, Olshina MA, Ben-Nissan G, Sharon M. The contribution of the 20S proteasome to proteostasis. *Biomolecules* (2019) 9:190. doi: 10.3390/biom9050190

20. Verfaillie T, Garg AD, Agostinis P. Targeting ER stress induced apoptosis and inflammation in cancer. *Cancer Lett* (2013) 332:249–64. doi: 10.1016/j.canlet.2010.07.016

21. Schonthal AH. Targeting endoplasmic reticulum stress for cancer therapy. *Front Biosci* (2012) 4:412–31. doi: 10.2741/s276

22. Wang T, Chen P, Dong R, Weir S, Baltezor M, Schoenen FJ, et al. Novel compound C150 inhibits pancreatic cancer cell epithelial-to-Mesenchymal transition and tumor growth in mice. *Front Oncol* (2021) 11:773350. doi: 10.3389/fonc.2021.773350

23. Chou TC. Drug combination studies and their synergy quantification using the chou-talalay method. *Cancer Res* (2010) 70:440–6. doi: 10.1158/0008-5472.CAN-09-1947

24. Aberle H, Bauer A, Stappert J, Kispert A, Kemler R. Beta-catenin is a target for the ubiquitin-proteasome pathway. *EMBO J* (1997) 16:3797–804. doi: 10.1093/emboj/16.13.3797

25. Love IM, Shi D, Grossman SR. p53 ubiquitination and proteasomal degradation. *Methods Mol Biol* (2013) 962:63–73. doi: 10.1007/978-1-62703-236-0_5

26. Fang L, Zhang L, Wei W, Jin X, Wang P, Tong Y, et al. A methylation-phosphorylation switch determines Sox2 stability and function in ESC

maintenance or differentiation. *Mol Cell* (2014) 55:537–51. doi: 10.1016/j.molcel.2014.06.018

27. Bedford L, Paine S, Sheppard PW, Mayer RJ, Roelofs J. Assembly, structure, and function of the 26S proteasome. *Trends Cell Biol* (2010) 20:391–401. doi: 10.1016/j.tcb.2010.03.007

28. Lee W, Kim Y, Park J, Shim S, Lee J, S.-h. Hong H-H, et al. iRhom1 regulates proteasome activity *via* PAC1/2 under ER stress. *Sci Rep* (2015) 5:11559. doi: 10.1038/srep11559

29. Rousseau A, Bertolotti A. An evolutionarily conserved pathway controls proteasome homeostasis. *Nature* (2016) 536:184–9. doi: 10.1038/nature18943

30. Deegan S, Saveljeva S, Gorman AM, Samali A. Stress-induced self-cannibalism: on the regulation of autophagy by endoplasmic reticulum stress. *Cell Mol Life Sci* (2013) 70:2425–41. doi: 10.1007/s00018-012-1173-4

31. Boye E, Grallert B. eIF2alpha phosphorylation and the regulation of translation. *Curr Genet* (2020) 66:293–7. doi: 10.1007/s00294-019-01026-1

32. Walter P, Ron D. The unfolded protein response: From stress pathway to homeostatic regulation. *Science* (2011) 334:1081. doi: 10.1126/science.1209038

33. Schmidt EK, Clavarino G, Ceppi M, Pierre P. SUnSET, a nonradioactive method to monitor protein synthesis. *Nat Methods* (2009) 6:275–7. doi: 10.1038/nmeth.1314

34. Goodman CA, Hornberger TA. Measuring protein synthesis with SUnSET: a valid alternative to traditional techniques? *Exerc Sport Sci Rev* (2013) 41:107–15. doi: 10.1097/JES.0b013e3182798a95

35. Bourougaa K, Naski N, Boularan C, Mlynarczyk C, Candeias MM, Marullo S, et al. Endoplasmic reticulum stress induces G2 cell-cycle arrest *via* mRNA translation of the p53 isoform p53/47. *Mol Cell* (2010) 38:78–88. doi: 10.1016/j.molcel.2010.01.041

36. Gire V, Dulic V. Senescence from G2 arrest, revisited. *Cell Cycle* (2015) 14:297–304. doi: 10.1080/15384101.2014.1000134

37. Ruscetti M, J.P.t. Morris R, Mezzadra, Russell J, Leibold J, Romesser PB, et al. Senescence-induced vascular remodeling creates therapeutic vulnerabilities in pancreas cancer. *Cell* (2020) 181:424–441.e21. doi: 10.1016/j.cell.2020.03.008

38. Freund A, Laberge R-M, Demaria M, Campisi J. Lamin B1 loss is a senescence-associated biomarker. *Mol Biol Cell* (2012) 23:2066–75. doi: 10.1091/mbc.e11-10-0884

39. Mujumdar N, Banerjee S, Chen Z, Sangwan V, Chugh R, Dudeja V, et al. Triptolide activates unfolded protein response leading to chronic ER stress in pancreatic cancer cells. *Am J Physiol-Gastroint Liver Physiol* (2014) 306:G1011–20. doi: 10.1152/ajpgi.00466.2013

40. Schönthal AH. Pharmacological targeting of endoplasmic reticulum stress signaling in cancer. *Biochem Pharmacol* (2013) 85:653–66. doi: 10.1016/j.bcp.2012.09.012

41. Oakes SA. Endoplasmic reticulum stress signaling in cancer cells. *Am J Pathol* (2020) 190:934–46. doi: 10.1016/j.ajpath.2020.01.010

42. Niu Z, Wang M, Zhou L, Yao L, Liao Q, Zhao Y. Elevated GRP78 expression is associated with poor prognosis in patients with pancreatic cancer. *Sci Rep* (2015) 5:16067. doi: 10.1038/srep16067

43. Chien W, Ding L-W, Sun Q-Y, Torres-Fernandez LA, Tan SZ, Xiao J, et al. Selective inhibition of unfolded protein response induces apoptosis in pancreatic cancer cells. *Oncotarget* (2014) 5:4881–94. doi: 10.18632/oncotarget.2051

44. Dauer P, Gupta VK, McGinn O, Nomura A, Sharma NS, Arora N, et al. Inhibition of Sp1 prevents ER homeostasis and causes cell death by lysosomal membrane permeabilization in pancreatic cancer. *Sci Rep* (2017) 7:1564. doi: 10.1038/s41598-017-01696-2

45. Hwang J, Qi L. Quality control in the endoplasmic reticulum: Crosstalk between ERAD and UPR pathways. *Trends Biochem Sci* (2018) 43:593–605. doi: 10.1016/j.tibs.2018.06.005

46. Morton JP, Timpson P, Karim SA, Ridgway RA, Athineos D, Doyle B, et al. Mutant p53 drives metastasis and overcomes growth arrest/senescence in pancreatic cancer. *Proc Natl Acad Sci* (2010) 107:246. doi: 10.1073/pnas.0908428107

47. Ag Moir J, White SA, Mann J. Arrested development and the great escape – the role of cellular senescence in pancreatic cancer. *Int J Biochem Cell Biol* (2014) 57:142–8. doi: 10.1016/j.biocel.2014.10.018

48. Yuan Y, Wang Q, Paulk J, Kubicek S, Kemp MM, Adams DJ, et al. A small-molecule probe of the histone methyltransferase G9a induces cellular senescence in pancreatic adenocarcinoma. *ACS Chem Biol* (2012) 7:1152–7. doi: 10.1021/cb300139y

49. Neault M, Frédérick A, Mallette, Richard S. miR-137 modulates a tumor suppressor network-inducing senescence in pancreatic cancer cells. *Cell Rep* (2016) 14:1966–78. doi: 10.1016/j.celrep.2016.01.068

50. Gradiz R, Silva HC, Carvalho L, Botelho MF, Mota-Pinto A. MIA PaCa-2 and PANC-1 – pancreas ductal adenocarcinoma cell lines with neuroendocrine differentiation and somatostatin receptors. *Sci Rep* (2016) 6:21648. doi: 10.1038/srep21648

frontiers | Frontiers in Oncology

TYPE Original Research
PUBLISHED 14 March 2023
DOI 10.3389/fonc.2023.1140730

OPEN ACCESS

EDITED BY
Stephen Safe,
Texas A&M University, United States

REVIEWED BY
Li Zhang,
University of Minnesota Twin Cities, United States
Jianjun Liu,
Dalian Medical University, China

*CORRESPONDENCE
Stefano Fiorucci
stefano.fiorucci@unipg.it

SPECIALTY SECTION
This article was submitted to Cancer Molecular Targets and Therapeutics, a section of the journal Frontiers in Oncology

RECEIVED 09 January 2023
ACCEPTED 20 February 2023
PUBLISHED 14 March 2023

CITATION
Di Giorgio C, Bellini R, Lupia A, Massa C, Bordoni M, Marchianò S, Rosselli R, Sepe V, Rapacciuolo P, Moraca F, Morretta E, Ricci P, Urbani G, Monti MC, Biagioli M, Distrutti E, Catalanotti B, Zampella A and Fiorucci S (2023) Discovery of BAR502, as potent steroidal antagonist of leukemia inhibitory factor receptor for the treatment of pancreatic adenocarcinoma. *Front. Oncol.* 13:1140730. doi: 10.3389/fonc.2023.1140730

Discovery of BAR502, as potent steroidal antagonist of leukemia inhibitory factor receptor for the treatment of pancreatic adenocarcinoma

Cristina Di Giorgio[1], Rachele Bellini[1], Antonio Lupia[2,3], Carmen Massa[1], Martina Bordoni[1], Silvia Marchianò[1], Rosalinda Rosselli[2], Valentina Sepe[2], Pasquale Rapacciuolo[2], Federica Moraca[2,3], Elva Morretta[4], Patrizia Ricci[1], Ginevra Urbani[1], Maria Chiara Monti[4], Michele Biagioli[1], Eleonora Distrutti[5], Bruno Catalanotti[2], Angela Zampella[2] and Stefano Fiorucci[1]*

[1]Department of Medicine and Surgery, University of Perugia, Perugia, Italy, [2]Department of Pharmacy, University of Naples Federico II, Naples, Italy, [3]Net4Science srl, University "Magna Græcia", Catanzaro, Italy, [4]Department of Pharmacy, University of Salerno, Salerno, Italy, [5]Department of Gastroenterology, Azienda Ospedaliera di Perugia, Perugia, Italy

Introduction: The leukemia inhibitory factor (LIF), is a cytokine belonging to IL-6 family, whose overexpression correlate with poor prognosis in cancer patients, including pancreatic ductal adenocarcinoma (PDAC). LIF signaling is mediate by its binding to the heterodimeric LIF receptor (LIFR) complex formed by the LIFR receptor and Gp130, leading to JAK1/STAT3 activation. Bile acids are steroid that modulates the expression/activity of membrane and nuclear receptors, including the Farnesoid-X-Receptor (FXR) and G Protein Bile Acid Activated Receptor (GPBAR1).

Methods: Herein we have investigated whether ligands to FXR and GPBAR1 modulate LIF/LIFR pathway in PDAC cells and whether these receptors are expressed in human neoplastic tissues.

Results: The transcriptome analysis of a cohort of PDCA patients revealed that expression of LIF and LIFR is increased in the neoplastic tissue in comparison to paired non-neoplastic tissues. By *in vitro* assay we found that both primary and secondary bile acids exert a weak antagonistic effect on LIF/LIFR signaling. In contrast, BAR502 a non-bile acid steroidal dual FXR and GPBAR1 ligand, potently inhibits binding of LIF to LIFR with an IC_{50} of 3.8 μM.

Discussion: BAR502 reverses the pattern LIF-induced in a FXR and GPBAR1 independent manner, suggesting a potential role for BAR502 in the treatment of LIFR overexpressing-PDAC.

KEYWORDS

PDAC, LIF, LIFR, bile acids, steroid, proliferation, EMT

Introduction

Pancreatic ductal adenocarcinoma (PDAC) represents the ≈ 85% of pancreatic cancer (PC) but is projected to become the second leading cause of cancer death in industrialized countries by 2030 (1, 2). Due to a late diagnosis (3), ≈90% of PDAC are detected at an advanced stage beyond the criteria for curative surgery (4). PDAC risk factors include high alcohol consumption, smoking, a sedentary life style and chronic high caloric intake, obesity, diabetes, hypertriglyceridemia, biliary stones and acute recurrent and chronic pancreatitis (5). The PDAC has also a strong genetic background and associates with several somatic mutations in oncogenes and tumour suppressor genes, including: KRAS, TP53, CDKN2A/p16, and SMAD4 (6). Most commonly, PDAC patients develop resistance to chemotherapy, making the identification of mechanistic molecular pathways and putative biomarkers an urgent need (7).

Next generation sequencing studies of PDAC have identified several markers linked to patient's survival. Transcriptome studies have identified the Leukaemia Inhibitory Factor (LIF) as a potential biomarker of poor prognosis in PDAC patients. LIF is a pleiotropic member of interleukin (IL)-6 cytokine family (8), that regulates cell differentiation, proliferation and survival in embryo and adult cells and is involved in cancer growth and progression (9). LIF signalling is mediated *via* binding to an heterodimeric LIF receptor (LIFR) complex, formed by LIFR and the glycoprotein (gp) 130. This complex is also targeted by other potential oncogenic factors including oncostatin M, cardiotropin 1 (CT1) and neutrophil ciliary factor (CNTF) and the cardiotropin-like cytokine factor (CLCF1) whose expression and activity has been detected in several tumors (10). Upon binding to its ligands, LIFR undergoes a series of conformational rearrangements that promote the phosphorylation of the Jak-Tyk, two proteins that are constitutively associated to cytoplasmic domain of the gp130/LIFR complex (11), activating the downstream signalling pathways which include JAK1/STAT3, MAPK and AKT. The LIF/LIFR axis and JAK/STAT3 signalling pathway is over-regulated in several type of solid tumours, including PDAC (12), gastric cancer (GC) (13), hepatocellular carcinoma (HCC) (14), colon-rectal cancer (CRC) (15) and breast cancer (16), and promotes cancer cell proliferation, epithelial-to-mesenchymal transition (EMT) (17) and regulates aberrantly the self-renewal of cancer cell-initiating tumors (18), as well as promoting radio (19) and chemo-resistance (15). Several studies support the suppression of LIFR signalling as potential target in inhibiting cell growth and tumour progression (9), and we have shown recently, that LIFR-mediated antagonism supports the anti-oncogenic effect of mifepristone in pancreatic cancer and chemoresistance (20). Furthermore, while LIFR antagonists are not approved for clinical use (21), several anti-LIFR molecules are investigated in phase II and III clinical trials in various oncologic settings (22).

Bile acids are steroid derivatives of cholesterol, synthetized in the liver and metabolized by microbiota hydrolase in the intestine (e.g from Bacteroidetes, Clostridium and Enterococcus) (23) and reabsorbed through the enterohepatic circulation (24). Despite, secondary bile acids (lithocholic and cholic acid, LCA and DCA) are traditionally considered as potential causative factors for development of gastrointestinal cancers (25), more recent studies have reported that bile acids exert robust anti-tumor effects (26). The effects that various bile acid species exert on cancer growth and progression are dependent on their concentrations and cellular environment as well as differential expression of their main receptors, the Farnesoid-X-Receptor (FXR) (27–29) and the bile acid activated G protein coupled receptor (GPBAR1) (30, 31). Generally, while high concentrations of bile acids promote cells injury and cell proliferation, lower concentrations, corresponding to their plasmatic or tissue concentrations, exert anticancer activity in a large subset of gastrointestinal malignancies (32). It has been previously reported that UDCA (0.25-1 mM) promotes apoptosis of gastric cancer cell lines such as SNU601 and SNU638 cells (33) and MKN45 cells, while DCA (200 μM) induces MUC2 expression and inhibits tumour invasion and migration in colon cancer cells (CRC) (34). In several *in vitro* models of CRC, UDCA (0.2 mM) (35) and DCA (36) induce apoptosis and inhibit cell proliferation. In the same manner, TUDCA (50 μg/ml) suppresses NF-kB signalling and ameliorates colitis-associated tumorigenesis (37) and LCA (150-400 μM) (38), DCA (500 μM) and CDCA (500 μM) inhibit cell growth and induce programmed cell death (39). It is worth noting that UDCA reduced intracellular ROS levels and Prx2 expression, as well as suppresses EMT process and interferes with "self-renewal" ability of cancer stem cells (CSC), in pancreatic cancer cell lines such as HPAC and Capan1 cells (40).

Building on the background that steroidal-like agents such as mifepristone and EC359 exert LIFR antagonist effects, we have evaluated the molecular docking of an in-house library based on both natural and synthetic bile acids on hLIFR, and found that LCA and CDCA act as weak LIFR antagonists. Additionally, we have shown BAR502 (41, 42), a semisynthetic bile alcohol steroidal agonist of FXR and GPBAR1, as a potential hLIFR antagonist acting as a tumour suppressor and reverting proliferation and EMT process in a LIFR-dependent manner.

Materials and methods

GSE196009 data sets

The GSE196009 repository (https://www.ncbi.nlm.nih.gov/geo/query/acc.cgi?acc=GSE196009) accessed on 1 August 2022 includes gene expression profiles (RNA-seq analysis, Illumina HiSeq 2000) of fresh or frozen PDAC tissues and adjacent normal pancreatic tissues from 12 Japanese patients.

Alpha screen

Recombinant human LIFR (His Tag) and biotinylated recombinant human LIF were purchased from Sino Biologicals (Sino Biological Europe GmbH, Dusseldorf, Germany) and R&D Systems (Abingdon, UK), respectively, and both were reconstituted as required by the manufacturer. Inhibition of LIFR/LIF binding by LCA, CDCA, PDL103 and BAR502 was measured by Alpha Screen

(Amplified Luminescent Proximity Homogeneous Assay). The assay was carried out in white, low-volume, 384-well AlphaPlates (PerkinElmer, Waltham, MA, USA) using a final volume of 25 µL and an assay buffer containing 25 mM Hepes (pH 7.4), 100 mM NaCl, and 0.005% Kathon. The concentration of DMSO in each well was maintained at 5%. LIFR (His Tag, final concentration 4.5 nM) was incubated with LCA, CDCA, PDL103, a dual FXR/GPBAR1 antagonist, and BAR502 or a vehicle for 45 min under continuous shaking. Then, LIF was added (biotinylated, final concentration 9 nM), and the samples were incubated for 15 min prior to adding His-Tag acceptor beads (final concentration 20 ng/µL) for 30 min. Then, streptavidin donor beads were added (final concentration 20 ng/µL), and the plate was incubated in the dark for 2 h and then read in an EnSpire Alpha multimode plate reader (PerkinElmer, Waltham, MA, USA).

Transactivation assay

To perform STAT3 transactivation, HepG2 (HB, 8065 from ATCC), an immortalized human epatocarcinoma cell line was used, as described previously (20). On day 0, HepG2 were seeded at 7.5 × 104 cells/well in a 24-well plate and maintained at 37°C and 5% CO2 in E-MEM supplemented with 10% FBS, 1% glutamine, and 1% penicillin/streptomycin. On day 1, cells were transiently transfected with the reporter plasmid pGL4.47[luc2P/SIE/Hygro] (200 ng) (CAT#: E4041 Promega, Madison, WI, USA), a vector encoding the hLIFR (CAT# RC226327) (100 ng) and CD130 (IL6ST) (100 ng) (CAT#: RC215123, OriGene Technologies, Inc. Rockville, MD, USA), and finally a vector encoding the human RENILLA luciferase gene (pGL4.70) (100 ng) (Promega, Madison, WI, USA). On day 2, cells were exposed to the cytokine LIF (10 ng/mL) alone or in combination with BAR502 (from 0.1 to 20 µM). To investigate the GPBAR1 activation, HEK-293T cells were transiently transfected with 200 ng of human pGL4.29 (Promega), a reporter vector containing a cAMP response element (CRE) that drives the transcription of the luciferase reporter gene luc2P, with 100 ng of pCMVSPORT6-human GPBAR1 and with 100 ng of pGL4.70 as described previously (42, 43). For FXR mediated transactivation, HepG2 cells were plated at 7.5 × 104 cells/well in a 24 well plate. Cells were transfected with 200 ng of the reporter vector p(hsp27)-TK-LUC containing a FXR response element (IR1) cloned from the promoter of heat shock protein 27 (hsp27), 100 ng of pSG5-FXR, 100 ng of pSG5-RXR, and 100 ng of pGL4.70 (Promega), a vector encoding the human Renilla gene. To perform STAT3 transactivation, HepG2 were seeded at 7.5× 104 cells/well in a 24-well plate. On the day-1, cells were transiently transfected with 200 ng of the reporter plasmid pGL4.47[luc2P/SIE/Hygro] (CAT#: E4041 Promega, Madison, WI, USA), 100 ng of a vector encoding the hLIFR (CAT# RC226327) and 100 ng of CD130 (IL6ST) (CAT#: RC215123, OriGene Technologies, Inc. Rockville, MD USA), and finally with 100 ng of a vector encoding the human RENILLA luciferase gene (pGL4.70) (Promega, Madison, WI, USA). At 24 h post-transfection, HepG2 and HEK293T were stimulated 18 h with Taurolithocholic Acid (TLCA,10 µM) or Chenodeoxycholic acid (CDCA, 10 µM) or Leukemia Inhibitory factor (LIF, 10 ng/ml) as positive controls and compound PDL103 at increasing concentrations (from 0.1 µM to 100 µM) in combination with the relative positive controls. Then, after 24 h, the cells were lysed in 100 µL of lysis buffer (25 mM Tris-phosphate, pH 7.8; 2 mM dithiothreitol (DTT); 10% glycerol; 1% Triton X-100). Then, 10 µL cellular lysates were assayed for luciferase and RENILLA activities using the Dual-Luciferase Reporter assay system (Promega, Madison, WI, USA). Luminescence was measured using a Glomax 20/20 luminometer (Promega, Madison, WI, USA). LUCIFERASE activities (RLU) were normalized with RENILLA activities (RRU).

Computational studies

Protein and ligand preparations

The three-dimensional (3D) crystallographic structures of the human LIFR, hLIFR (Uniprot ID Code: P42702, PDB X-Ray 3E0G [REF DOI: 10.1186/1756-9966-28-83) was retrieved from the RCSB Protein Data Bank (www.rcsb.org). The downloaded structure was subjected to Maestro's *Protein Preparation Wizard* (PPW) tool (Schrödinger Release 2021-1) to assign bond orders, add hydrogen atoms, adjust disulphide bonds, add caps to chains break, and assign residues protonation state at pH 7.4. The in-house library of natural and synthetic bile acids (Bile acids) was prepared using LigPrep (LigPrep. Schrödinger, release 2021–1, LigPrep; Schrödinger, LLC: New York, NY, USA, 2021) and Epik (Schrödinger; Release 2021-1: Epik, S., LLC, New York, NY, USA, 2021) modules to generate and optimize the 3D structures of the ligands at the protonation states of pH 7.4.

Docking procedures

The optimized structure of hLIFR was used for the accurate QM-Polarized Ligands Docking (QPLD) (Glide, S., LLC, New York, NY, USA, 2021; Jaguar, S., LLC, New York, NY, USA, 2021) and Induced Fit Docking (IFD) (Glide, S., LLC, New York, NY, USA, 2021; Prime, S., LLC, New York, NY, USA, 2021) docking protocols, following the same procedures described in our previous work (Di Giorgio et al.). Briefly, the centroid of the hLIFR binding site was used to generate the grid box coordinate in default size (10.0 Å). Ten docking poses were saved for each ligand of the in-house library after the QPLD process, and the most representatives were submitted to the IFD procedure using the extended sampling protocol. A maximum of 80 poses was generated, and the energy window for the ligand conformational sampling was 2.5 kcal/mol.

Molecular dynamics simulations

The best scored IFD docking pose of BAR502 was subjected to 100 ns of MDs. The CUDA version of the AMBER18 package (44) was used to MD simulation, using the Amber ff14SB force field (45, 46) to treat the protein. Ligand charges were, instead, calculated using the restrained electrostatic potential (RESP) fitting procedure (40). The Gaussian16 package (47): was used to calculate the ligand ESP using the 6-31G* bile acids is set at the Hartree-Fock level of

theory. Antechamber (48): coupled with the general amber force field (GAFF2) parameters (49), allowed RESP charges and the ligand force field parameters. The system was solvated in a 10 Å layer of the octahedral box using TIP3P (50): water molecules parameters. The SHAKE algorithm was used to constraint bonds involving hydrogen atoms with two fs integration time steps. Next, the system was minimized and thermally equilibrated as described in our latest work (20). The MD trajectory was visualized by using Visual Molecular Dynamics (VMD) graphics ver. 1.9.3 (51), while clustering and analysis procedures were performed through the CPPTRAJ module (52). For the most representative cluster population, intermolecular interaction energy was analysed *via* the Molecular Mechanics/Generalized Born Surface Area (MM/GBSA) equation (53). All images were rendered using Maestro GUI Suite 2021-1 (Schrödinger Release 2021-1) and Adobe Illustrator (Adobe Systems, San Jose, CA, USA).

Cell lines

Human pancreatic cell lines MIA-PaCa-2 and PANC-1 were from ATCC (Manassas, VA; USA). The cells were grown in DMEM (Sigma-Merk LIFe Science S.r.l. Milan, Italy) medium supplemented with 10% Fetal Bovine Serum (FBS), 1% L-Glutamine, 1% Penicillin/Streptomycin, in a humidified 5% CO_2 atmosphere, 37°C. U-937 a cell line exhibiting monocyte morphology were purchased from Sigma Aldrich (Sigma-Merk LIFe Science S.r.l. Milan, Italy). U937 and MKN45 were grown in RPMI complete medium, supplemented with 10% FBS, 1% L-Glutamine, 1% Penicillin/Streptomycin. A human hepatocarcinoma cell line, HEPG2 (ATCC) was grown at 37°C in E-MEM complete medium containing 10% FBS, 1% L-glutamine and 1% penicillin/streptomycin. Cells are free from Mycoplasma contamination as confirmed by Mycoplasma PCR Detection test (Sigma-Merk LIFe Science S.r.l. Milan, Italy) and were regularly passaged to maintain exponential growth and used from early passages (<10 passages after thawing). In all experiments, cells were serum starved for 24 h before exposure to tested agent.

Real-time PCR

The RNA was extracted from cell lines using and Direct-zol™ RNA MiniPrep w/Zymo-Spin™ IIC Columns (Zymo Research, Irvine, CA, USA)., according to the manufacturer's protocol as described previously (20). After purification from genomic DNA by DNase-I treatment (ThermoFisher Scientific, Waltham, MA USA), 2 µg of RNA from each sample was reverse-transcribed using Kit FastGene Scriptase Basic (Nippon Genetics, Mariaweilerstraße, Düren, Germania) in a 20 µL reaction volume. Finally, 50 ng cDNA were amp LIFied in a 20 µL solution containing 200 nM of each primer and 10 µL of SYBR Select Master Mix (ThermoFisher Scientific). All reactions were performed in triplicate, and the thermal cycling conditions were as follows: 3 min at 95°C, followed by 40 cycles of 95°C for 15 s, 56°C for 20 s and 72°C for 30 s, using a Step One Plus machine (Applied Biosystem). The relative mRNA expression was calculated accordingly to the $2^{-\Delta Ct}$ method. Primers used in this study were designed using the PRIMER3 (http://frodo.wi.mit.edu/primer3/) software using the NCBI databile acids e. RT-PCR primers used in this study for human sample and human cell lines were as follow [forward (for) and reverse (rev)]:

LIFR (for GCTCGTAAAATTAGTGACCCACA; rev GCACATTCCAAGGGCATATC),

LIF (for CCCTGTCGCTCTCTAAGCAC; rev GGGAT GGACAGATGGACAAC),

GPBAR1 (for ACTGCAGCTCCCAGGCTAT; rev GA CAGAGAGGAAGGCAGCA),

FXR (for GCAGCCTGAAGAGTGGTACTCTC; rev CATTCAGCCAACATTCCCATCTC),

SNAIL1 (for ACCCACACTGGCGAGAAG; rev TGA CATCTGAGTGGGTCTGG),

VIMENTIN (for TCAGAGAGAGGAAGCCGAAA; rev ATTCCACTTTGCGTTCAAGG),

CXCR4 (for AACGTCAGTGAGGCAGATGA; revTGGAGTGTGACAGCTTGGAG).

Immunofluorescence

Immunofluorescence (IF) staining was carried out using MIA PaCa-2 cells. Cells cytospins were fixed in methanol for 20 min and then washed 3 times with phosphate buffered saline (PBS 1X), permeabilized and then incubated with Blocking buffer (PBS 1X with 10% horse serum and 1% BSA) for 1h at room temperature. Primary antibodies, anti- GPBAR1 (NBP2-23669), (Novus Biologicals) and anti-FXR (ORB156973) (Biorbyt) were dissolved in Blocking Buffer and incubated overnight at 4°. On the following day cells were washed three times with PBS 1X containing 0,1% Tween 20 (PBST), and then incubated with the secondary antibody, Goat anti-rabbit IgG (H + L) Alexa Fluor 488 (ab150077) (Abcam) for GPBAR1 and Goat anti-rabbit IgG (H + L) Alexa Fluor 568 (A11011) for FXR (Invitrogen), diluted in Blocking Buffer for 1h at room temperature in the dark. After 3 washes with PBST, nucleus was counterstained with DAPI 1X for 1 min in the dark and the reaction was stopped by a final wash in PBS 1X for 5 min. Then, slides were mounted with ProLong Glass Antifade Mountant (P36980) (Invitrogen, Thermofisher scientific Waltham, Massachusetts, USA), sealed with nail polish and observed at fluorescence microscope (Olympus BX60, Rome, Italy).

Cell proliferation assay

The cell viability assay was done using the CellTiter 96 Aqueous One Solution Cell Proliferation Assay (Promega, Milano, Italy), a colorimetric method for accessing the number of viable cells in proliferation as described previously (13). MIA-PaCa 2 cells were seeded in DMEM complete medium at 36 $*10^3$ cells/100 uL well into 96-well tissue culture plate. After 24 h, cells were serum starved for 24 h and then were primed with the LIFR major ligand, LIF (10 ng/ml) alone or in combination with BAR502 (5,10 and 20 µM) or

only with vehicle. In another experimental setting, MIA-PaCa 2 cells were triggered with PDL103 (10 μM) alone, LIF (10 ng/ml) alone or plus PDL103 or BAR502 (10 μM) or both. In a different setting cell were exposed to an antagonist of the Farnesoid X receptor (FXR), 3-(naphthalen-2-yl)-5-(piperidin-4-yl)-1,2,4-oxadiazole (GP7) (10 μM) (54), LIF (10 ng/ml) alone or in combination with GP7 or BAR502 or both. Then cell proliferation assessed as mentioned above. Absorbance was measured using a 96 well reader spectrophotometer (490 nm). In these experiments each experimental setting was replicated ten folds. For analysis the background readings with the medium alone, were subtracted from the samples read-outs.

Flow cytometry

MIA-PaCa2 cells were seeded in 6-well tissue culture plate (cell density 700 × 103/well) and cultured as specified above. Cells were serum-starved for 8 h and then incubated with LIF (10 ng/mL) alone or plus BAR502 (10, 20 μM) or a vehicle for 24 h. The intracellular flow cytometry staining for Ki-67 was performed using the following reagents: Ki-67 Monoclonal Antibody (SolA15), Alexa Fluor™ 488, (eBioscience™, San Diego, California, USA) and 7-AAD to characterize the cell cycle phases G0-G1 and S-G2-M. Before intracellular IC-FACS, staining cells were fixed for 30 min in the dark using IC Fixation buffer (eBioscience™) and then permeabilized using Permeabilization buffer (10X) (eBioscience™). The staining for Annexin V was performed using the Annexin V Antibody (A13199, Thermofisher Scientific, Waltham, MA, USA) to evaluate the apoptosis rate. Briefly, 5 μL of Annexin V Antibody was added to each 100 μL of cell suspension, and cells were incubated the at room temperature for 15 min. Flow cytometry analyses were carried out using a 3-laser standard configuration ATTUNE NxT (LIFe Technologies, Carlsbad, CA, USA). Data were analyzed using FlowJo software (TreeStar) and the gates set using a fluorescence minus-one (FMO) control strategy. FMO controls are samples that include all conjugated Abs present in the test samples except for one. The channel in which the conjugated Ab is missing is the one for which the fluorescence minus one provides a gating control.

Western blot analysis

MIA-PaCa 2 cells were seeded in 6-well tissue culture plate (cell density 1.5 * 10^6/well) in DMEM complete medium. After serum starving, cells were incubated with LIF (10 ng/mL) alone or plus BAR502 (10 μM) for 10 min. Total lysates were prepared by homogenization of MIA-PaCa2 cells in RIPA buffer containing phosphatase and protease inhibitors. Protein extracts were electrophoresed on 12% acrylamide Tris-Glycine gel (Invitrogen), blotted to nitrocellulose membrane, and then incubated overnight with primary Abs against GAPDH (bs2188R 1:1000; Bioss antibodies), STAT3 (sc-8019 1:500; Santa Cruz Biotechnology), Vimentin (ab92547 1:1000;Abcam), phosho-Stat3 (GTX118000 1:1000; Genetex). Primary Abs were detected with the HRP-labeled secondary Abs. Proteins were visualized by Immobilon Western Chemiluminescent Reagent (MilliporeSigma) and iBright Imaging Systems (Invitrogen). Quantitative densitometry analysis was performed using ImageJ software. The degree of STAT3 phosphorylation was calculated as the ratio between the densitometry readings of Vimentin/GAPDH and p-STAT3/STAT3.

Wound healing assay

MIA PaCa-2 cells were seeded in DMEM complete medium at 800x10^3 cells/well into 24-well plate and used at 70-80% confluence rate. The assay was performed as previously described (20), particularly on the day 1, the cell monolayers were gently scraped vertically with a new 0.2 mL pipette tip across the centre of the well. After scratching, the well was gently washed twice with PBS (Euroclone, Milan, Italy) to remove the detached cells and cell debris and finally fresh medium containing LIF (10 ng/mL) alone or in combination with BAR502 (10 μM) or EC359 (25 nM) was added into each well. Immediately after scratch creation, the 24-plate was placed under a phase-contrast microscope and the first image of the scratch acquired (T0) with using a OPTIKAM Pro Cool 5 – 4083.CL5 camera. Cells were grown for additional 48 h and images taken at 24h (T1) and 48 h (T2). The gap distance between scarps borders was quantified by assessing that area between the two margins of the scratches. All experiments were performed in triplicate.

Chemistry

(E)-2,6-dichlorobenzaldehyde oxime (2). A solution of hydroxylamine hydrochloride (1.5 eq) and NaOH (1.5 eq) in water was added to a solution of 2,6-dichlorobenzaldehyde (1) in ethanol. The mixture was left to stir for 5h. After starting material consumption, ethanol was evaporated, and the residue was extracted with ethyl acetate (x 3). The reunited organics were washed with brine, dried over anhydrous Na_2SO_4, and concentrated to afford the oxime as a white solid (98%) which was used for the next step without further purification. ^{1}H NMR (400 MHz, $CDCl_3$) δ 8.37 (s, 1H), 7.45 (d, J = 0.6 Hz, 2H), 7.28 (dd, J = 8.8, 7.8 Hz, 1H); ^{13}C NMR (100 MHz, $CDCl_3$) δ 144.24, 132.82, 130.12, 129.99, 128.32; HRMS (ESI) m/z [M+H^+] calcd for $C_7H_5Cl_2NO$ 189.9748, found 189.9744.

(Z)-2,6-dichloro-N-hydroxybenzimidoyl chloride (3). To a solution of compound 2 in dry DMF, N-chlorosuccinimide (1.2 eq) was slowly added at 0°C. The mixture was stirred overnight and partitioned with distilled water and diethyl ether. The organic phase was dried over anhydrous Na_2SO_4 and concentrated to afford the chloro oxime (95%) as a colourless oil, used for the next step without purification. ^{1}H NMR (400 MHz, $CDCl_3$) δ 7.44 – 7.32 (m, 3H). ^{13}C NMR (100 MHz, $CDCl_3$) δ 143.92, 132.02, 131.73, 130.49, 128.27; HRMS (ESI) m/z [M+H^+] calcd for $C_7H_4Cl_3NO$ 223.9358, found 223.9352.

(3-(2,6-dichlorophenyl)isoxazol-5-yl)methanol (4). To a solution of compound 3 in t-BuOH/H_2O 1:1 were added in

sequence propargylic alcohol (3 eq), $CuSO_4{\cdot}5H_2O$ (0.02 eq), sodium ascorbate (0.1 eq) and $NaHCO_3$ (4 eq). The mixture's appearance rapidly shifted from clear to opaque yellow upon the addition of the bile acids e. After 3h, the reaction was quenched by adding sat. NH_4Cl solution and then extracted with ethyl acetate (x3). The reunited organics were washed with brine, dried over anhydrous Na_2SO_4, and concentrated to afford the isoxazole as a colourless oil (quantitative yield) which was used for the next step without further purification. ^{1}H NMR (400 MHz, $CDCl_3$) δ 7.52 (dd, *J* = 8.0, 0.7 Hz, 2H), 7.41 (dd, *J* = 8.8, 7.3 Hz, 1H), 6.61 (s, 1H), 4.79 (s, 2H). ^{13}C NMR (100 MHz, $CDCl_3$) δ 169.35, 158.33, 133.88, 130.31, 128.38, 128.07, 100.54, 57.56; HRMS (ESI) m/z [M+H$^+$] calcd for $C_{10}H_7Cl_2NO_2$ 243.9854, found 243.9850.

(3-(2,6-dichlorophenyl)isoxazol-5-yl)methyl methanesulfonate (5). To a solution of compound 4 in dry THF were added triethylamine (4 eq) and mesyl chloride (3 eq) at -20°C. The reaction was stirred for 2h and then quenched by adding 1M HCl solution. The mixture was extracted with ethyl acetate (x3). The reunited organics were washed with brine, dried over anhydrous Na_2SO_4, and concentrated to afford the mesylate as an off-white solid (92%). ^{1}H NMR (400 MHz, $CDCl_3$) δ 7.52 (dd, *J* = 8.1, 0.7 Hz, 2H), 7.41 (dd, *J* = 8.8, 7.3 Hz, 1H), 6.59 (s, 1H), 5.52 (s, 2H), 3.15 (s, 3H). ^{13}C NMR (100 MHz, $CDCl_3$) δ 165.48, 158.18, 133.43, 130.31, 128.38, 127.81, 100.75, 61.12, 37.62; HRMS (ESI) m/z [M+Na$^+$] calcd for $C_{11}H_9Cl_2NO_4S$ 343.9527, found 343.9523.

Methyl 4'-((3-(2,6-dichlorophenyl)isoxazol-5-yl)methoxy)-[1,1'-biphenyl]-4-carboxylate (6). Compound 5 was dissolved in dry DMF and methyl 4'-hydroxy-4-biphenylcarboxylate (1.2 eq) and K_2CO_3 (2 eq) were added. The reaction was stirred at 100°C for 8h, then distilled water was added and the mixture was extracted with ethyl acetate (x3). The reunited organics were washed with brine, dried over anhydrous Na_2SO_4, and concentrated. The crude product was purified by flash column chromatography (silica gel, ethyl acetate/petroleum ether 15:85) to yield compound 1 (66%) as a white solid. An analytical sample was analysed by HPLC purification on a Nucleodur 100-5 column (5 µm; 10 mm i.d. x 250 mm) eluting with n-hexane/ethyl acetate 85:15 v/v (flow rate 3 mL/min, t_R = 19.5 min). ^{1}H NMR (400 MHz, $CDCl_3$) δ 8.09 (m, 2H), 7.61 (m, 4H), 7.42 (dd, *J* = 8.0, 1.0 Hz, 2H), 7.34 (dd, *J* = 9.0, 7.1 Hz, 1H), 7.10 (m, 2H), 6.48 (s, 1H), 5.31 (s, 2H), 3.94 (s, 3H). ^{13}C NMR (100 MHz, $CDCl_3$) δ 168.20, 167.16, 159.09, 158.13, 145.03, 135.69 (x2), 133.90, 131.32, 130.29 (x2), 128.72 (x2), 128.68, 128.41 (x2), 128.24, 126.75 (x2), 115.52 (x2), 105.18, 61.83, 52.26; HRMS (ESI) m/z [M+H$^+$] calcd for $C_{24}H_{17}Cl_2NO_4$ 454.0535, found 454.0531.

(4'-((3-(2,6-dichlorophenyl)isoxazol-5-yl)methoxy)-[1,1'-biphenyl]-4-yl)methanol (PDL103). To a solution of compound 6 in dry THF were added dry MeOH (3 eq) and 1M $LiBH_4$ (3 eq) in THF at 0°C. The reaction was left stirring overnight. The mixture was quenched by adding 1M NaOH solution (3 eq) at 0°C and then was extracted with ethyl acetate (x 3). The reunited organics were washed with brine, dried over anhydrous Na_2SO_4, and concentrated to afford PDL103 (82%). An analytic sample was obtained by HPLC on a Phenomenex Luna C18 (5 µm; 250 mm x 4.6 mm) column in gradient ($t_{0\ min}$= 60% B – $t_{3\ min}$= 60% B – $t_{25\ min}$= 95% B – $t_{30\ min}$= 95% B, solvent B = MeOH + 0.1% TFA, flow rate 1 mL/min, t_R = 22 min). ^{1}H NMR (400 MHz, $CDCl_3$) δ 7.56 (m, 4H), 7.43 (m, 4H), 7.33 (dd, *J* = 9.0, 7.1 Hz, 1H), 7.07 (d, *J* = 8.8 Hz, 2H), 6.47 (s, 1H), 5.30 (s, 2H), 4.74 (s, 2H). ^{13}C NMR (100 MHz, CDCl3) δ 168.38, 159.08, 157.54, 140.11, 139.66, 135.69 (x2), 134.83, 131.30, 128.45 (x2), 128.40 (x2), 128.27, 127.67 (x2), 127.13 (x2), 115.44 (x2), 105.12, 65.29, 61.89; HRMS (ESI) m/z [M+H$^+$] calcd for $C_{23}H_{17}Cl_2NO_3$ 426.0585, found 426.0580.

AmpliSeq transcriptome

MIA PaCa-2 cells were cultured in 6-well tissue culture plate (cell density 1.5 * 10^6/well) in DMEM complete medium. After serum starving, cells were exposed with LIF (10 ng/mL) alone or plus BAR502 (10 µM) or left untreated for 24h. High-quality RNA was extracted from MIA PaCa-2 cells using the PureLink™ RNA Mini Kit (Thermo Fisher Scientific), according to the manufacturer's instructions. RNA quality and quantity were assessed with the Qubit® RNA HS Assay Kit and a Qubit 3.0 fluorometer followed by agarose gel electrophoresis. Libraries were generated using the Ion AmpliSeq™ Transcriptome Human Gene Expression Core Panel and Chef-Ready Kit (Thermo Fisher Scientific), according to the manufacturer's instructions. Briefly, 10 ng of RNA was reverse transcribed with SuperScript™ Vilo™ cDNA Synthesis Kit (Thermo Fisher Scientific, Waltham, MA) before library preparation on the Ion Chef™ instrument (Thermo Fisher Scientific, Waltham, MA). The resulting cDNA was amplified to prepare barcoded libraries using the Ion Code™ PCR Plate, and the Ion AmpliSeq™ Transcriptome Human Gene Expression Core Panel (Thermo Fisher Scientific, Waltham, MA), Chef-Ready Kit, according to the manufacturer's instructions. Barcoded libraries were combined to a final concentration of 100 pM, and used to prepare Template-Positive Ion Sphere™ (Thermo Fisher Scientific, Waltham, MA) Particles to load on Ion 540™ Chips, using the Ion 540™ Kit-Chef (Thermo Fisher Scientific, Waltham, MA). Sequencing was performed on an Ion S5™ Sequencer with Torrent Suite™ Software v6 (Thermo Fisher Scientific). The analyses were performed with a range of fold <–2 and >+2 and a p value < 0.05, using Transcriptome Analysis Console Software (version 4.0.2), certified for AmpliSeq analysis (Thermo-Fisher). The transcriptomic data have been deposited as dataset on Mendeley data repository (ab92547 1:1000;Abcam).

Statistical analysis

Statistical analysis was carried out using the one-tailed unpaired Student's t test comparisons (* p < 0.05) using the Prism 8.0 software (GraphPad San Diego, CA, USA).

Results

LIF/LIFR and bile acid receptor expression in PDAC

We have first investigated the expression of LIF and LIFR and the expression of FXR (NR1H4) and GPBAR1 in human PDAC.

10.3389/fonc.2023.1140730

For this purpose, we have used a human repository of PDAC tissues, that includes cancer tissues along with the adjacent normal tissue excided from 12 Japanese patients (Repository GSE196009 series) (Figure 1). As described previously (20), LIF and LIFR show an opposite modulation in the cancer tissues, thus while LIF expression is higher in PDAC in comparison with the adjacent normal tissue (Figure 1A), the expression of LIFR is subject to opposite modulation (Figure 1B). Similarly, the expression of FXR (NR1H4) was downregulated in cancer tissues compared to the non-neoplastic tissues (Figure 1C). Instead, GPBAR1 was not detectable in both cancer and adjacent normal tissues (Figure 1D).

Since there are robust evidence that the LIF/LIFR pathway exerts a pro-oncogenic role in PDAC cell lines (13, 20, 55), and because FXR expression is increased in human PDAC tissues, we have focused our attention on the role that natural and synthetic steroids exert in modulating pancreatic cancer cell lines. For these purposes, we have first carried out a series of docking calculations on hLIFR using a small library of natural steroids (Figure 2), including LCA and CDCA (56), and the semisynthetic bile alcohol steroidal agonist BAR502 (57).

The efficacy of LCA, CDCA and BAR502 as LIFR antagonists in a cell-free system was then measured using a well-consolidated platform based on Alpha Screen assay. The results of these studies reported in Figure 2D demonstrated that LCA and CDCA elicited a slight, thought significant, inhibitory effect on LIF/LIFR complex formation. In contrast, BAR502 could be considered as a potent LIFR antagonist that inhibits LIF/LIFR interaction with IC_{50} of 3.59 μM (Figure 2F), this result was confirmed by STAT3 transactivation assay performed in HepG2 cells, with an IC_{50} of 2.73 μM (Figure 2G).

Because BAR502 was significantly more potent than natural bile acids and is currently advanced into clinical trials (58), we have used this agent in the following experiments.

BAR502 binds within loops 2 and 3 and disrupts LIF binding site

The binding between BAR502 and LIFR was investigated through a two-steps docking procedure followed by molecular dynamic (MD) simulation. Specifically, we have first used the QM-Polarized Ligand Docking (QPLD) protocol, whose best poses (-5.207 kcal/mol) were submitted to a second, more accurate Induced Fit Docking (IFD) analysis, that includes also the receptor flexibility. Given the high flexibility of the L1, L2 and L3 loops of the hLIFR binding site, the best pose obtained by IFD (-5.826 kcal/mol) was further refined using 100 ns of MD. From the analysis of the MD trajectory of BAR502, and of the ligand root means square deviation (L-RMSD) plot, it was found that after about 20 ns (Supplementary Figure Sx1, A), the ligand binding conformation was stabilized in a pocket defined by loops L2 and L3, with the 3-OH group anchored *via* H-bonding to the guanidine group of Arg333 (Figure 3A). The clustering analysis results showed that the MD trajectory of BAR502 produced two very similar binding conformations, accounting for 56% and 26% of the hypothetical binding poses, respectively (Supplementary Figure Sx1B, C). In both clusters, BAR502 bound to loops L2 and L3 (Supplementary Figure SX2), engaging hydrogen bond (H-bond) with the 3-OH to Arg333 and, discontinuously, to the backbone of Gly312. The 7-OH group established discontinuous H-bonds with the carbonyl backbone of Thr338. In the most populated cluster, the hydroxyl function at C23 H-bonds with Lys332, while in the second cluster, it was bound to the carbonyl group of the backbone of Tyr342. The B-C-D ring systems engaged hydrophobic interactions with residues from both L2 (Trp302, Val311 and Ala315), and L3 (Arg333 chain, Thr388 and Leu331) and the β-sheet (Tyr318). Moreover, the 6-ethyl group of BAR502 was firmly in contact with the Cβ of Asn339, helping to maintain the A and B rings in a "box" formed by Arg333, Asn339, Val311 and Ala315 (Supporting Figure Sx2). Overall, the MD of BAR502 highlights a significant alteration of

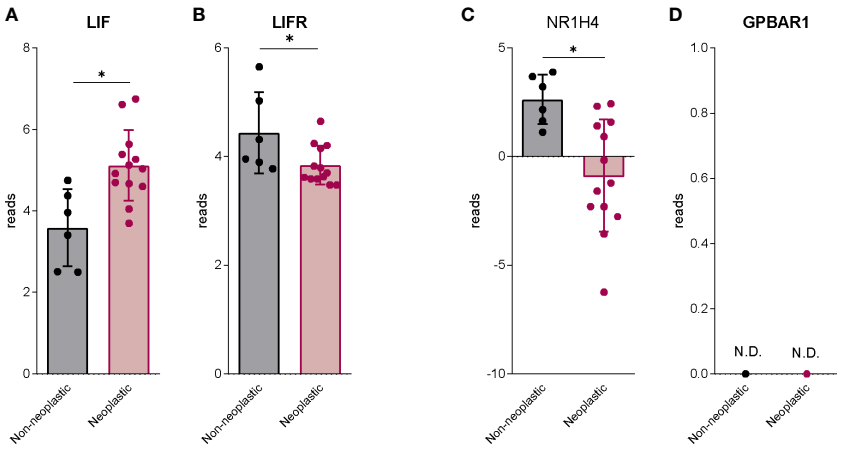

FIGURE 1
The bile acids receptors expression is downregulated in human PDAC. RNA-seq analysis of non-neoplastic and neoplastic mucosa of PDAC from GSE196009 repository. Each dot represents a patient. Data shown represent the gene profile expression of **(A)** LIF, **(B)** LIFR, Nuclear Receptor Subfamily 1 Group H Member 4 **(C)** NR1H4, The G protein-coupled bile acid receptor 1 **(D)** GPBAR1. Results are the mean ± SEM of 6 (Non-neoplastic) and 13 (Neoplastic) samples per group. *p < 0.05.

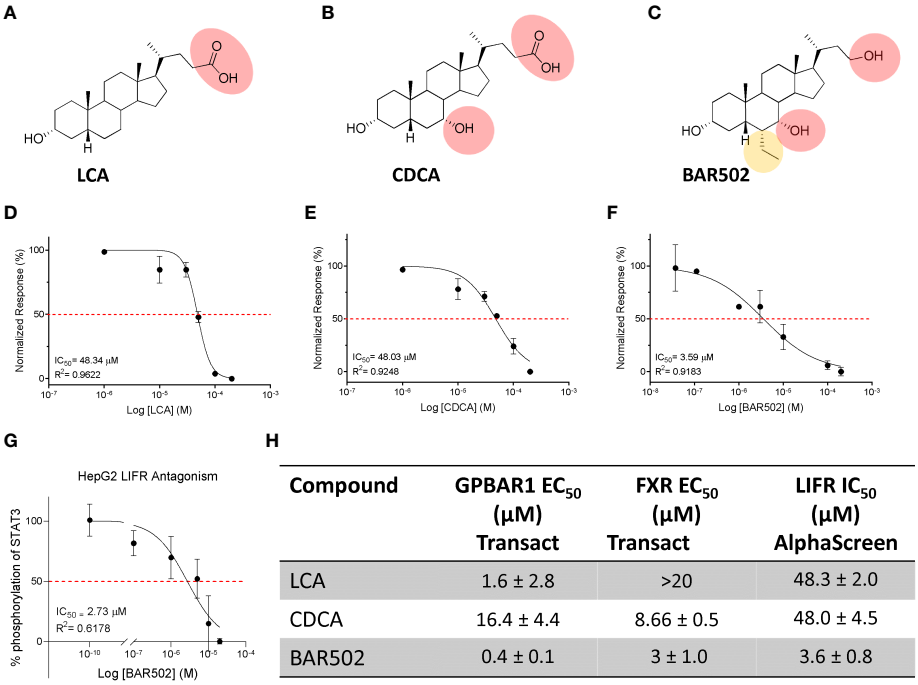

Compound	GPBAR1 EC_{50} (μM) Transact	FXR EC_{50} (μM) Transact	LIFR IC_{50} (μM) AlphaScreen
LCA	1.6 ± 2.8	>20	48.3 ± 2.0
CDCA	16.4 ± 4.4	8.66 ± 0.5	48.0 ± 4.5
BAR502	0.4 ± 0.1	3 ± 1.0	3.6 ± 0.8

FIGURE 2
Natural and synthetic bile acids antagonize LIFR. The figure shows two-dimensional structure of **(A)** LCA **(B)** CDCA **(C)** BAR502. Natural and synthetic bile acids inhibition activity of LIFR/LIF binding accessed by a cell-free AlphaScreen assay, particularly in **(D)** LCA **(E)** CDCA and **(F)** BAR502 IC_{50} are shown. **(G)** STAT3 transactivation on HepG2 cells. The table **(H)** summarizes EC50 on FXR and GPBAR1 and IC_{50} on LIFR of Natural and synthetic bile acids.

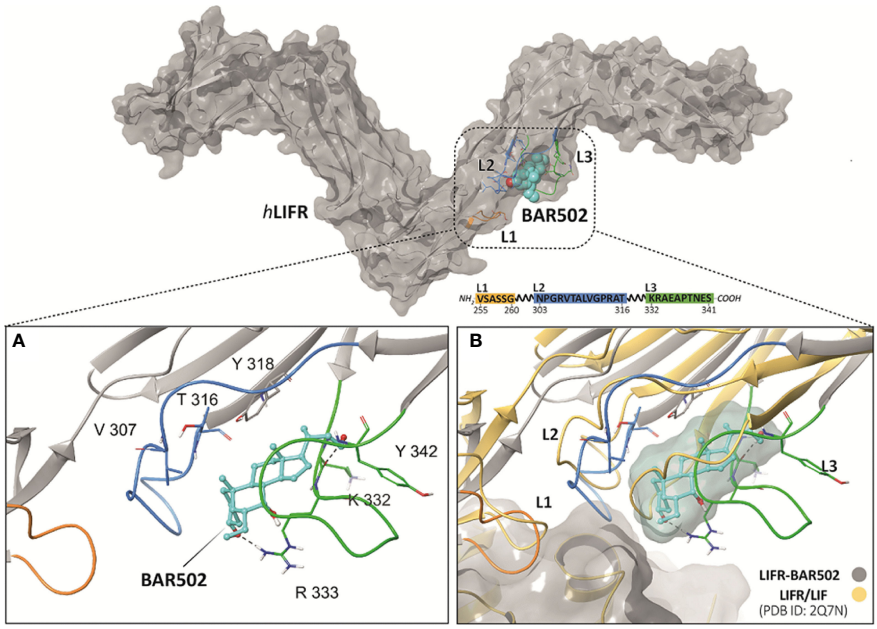

FIGURE 3
(A) View of the hLIFR-BAR502 representative cluster obtained after 100 ns of MD and **(B)** superimposed respect to the LIF-LIFR complex (PDB: 2Q7N). The pocket is defined by three loops, namely L1 (255-VSASSG-260), L2 (303-NPGRVTALVGPRAT-316), and L3 (332-KRAEAPTNES-341) (rectangular), which was already characterized as binding sites for EC359 and Mifepristone. L1, L2 and L3 are highlighted in yellow, blue, and green, respectively. BAR502 (cyan) and the relevant residues are labelled and coloured.

the L2 and L3 loops conformation, thus causing the distortion of the LIF binding site (Figure 3B).

LIFR antagonism exerts by BAR502 limits MIA PaCa-2 cells proliferation and migration

To functionally characterize the effect of BAR502 as LIFR antagonist, we have then performed *in vitro* assays using a human macrophage cell line, U937 cells, and liver, HEPG2, PDAC and gastric cancer, MKN45 cell lines (59). As shown in Figures 4A, B, PANC-1 exhibits highest levels of expression of LIF and LIFR compared to MKN45 cells. However, since our previous studies (20) have shown that MIA PaCA-2 cells are highly responsible to LIF, we have used this cell line for the following experiments.

In contrast to LIF/LIFR, the expression (mRNA and Immunofluorescence analysis) of GPBAR1 was almost undetectable in PDCA cell lines, as compared to U937 cells (Figures 4C, E), while PDAC cell lines express the nuclear receptor FXR (Figures 4C, D, F), though the expression was significantly lower than that detected in HEPG2 cells.

We have then investigated whether LIF acts as an autocrine factor to perpetuate PDAC cells growth and proliferation (60) and these effects were modulated by BAR502. For this purpose, MIA PaCa-2 cells, grown in a serum free medium, were exposed to 10 ng/mL LIF alone or in combination with increasing concentrations of BAR502 (5, 10, 20 μM) for 24 h. As shown in Figure 5A, BAR502 reversed the LIF-proliferative effect in a concentration-dependent manner.

The action of BAR502 on cell replication was also investigated by Ki-67/7-AAD IC-FACS staining (Figures 5B-F). More specifically, the analysis of Ki-67$^+$ cells (Figures 5B, C) revealed that not only exposure to LIF increased the number of Ki-67 positive cells in a statistically-dependent manner, but shifted the fluorescence pick to the right, compared to cells left untreated (Figure 5B). This pattern was reversed by LIFR inhibition with BAR502 (Figure 5B). In addition, BAR502 (10-20 μM) modulates the cell cycle progression (Figures 5C-F) and the apoptosis cell rates, as assessed by Annexin V staining (Figures 5G, H). Together these results demonstrated that LIF increases the S-G2-M transition and that this effect was significantly reversed by BAR502 that also increased the percentage of Annexin V$^+$ cells ($p<0.05$) (Figure 5H).

Since the LIF/LIFR axis promotes EMT in various cell systems (13), we have then investigated whether BAR502 also reverses EMT features in MIA PaCa-2 cells and found that BAR502 (10-20 μM) reversed the induction of vimentin expression, RNA (Figure 6A) and protein (Figures 6B, C) caused by LIF. Furthermore, BAR502 significantly attenuated STAT3 phosphorylation caused by LIF (Figures 6B-D). The inhibition of LIFR exerted by BAR502 also reversed the mRNA expression of the pro-inflammatory factor CXCR4, whose expression was increased by LIF (Figure 6E). Since CXCR4 overexpression is a strong prognostic marker of lymph node involvement and metastasis development in PDAC, this finding might have a translational readout (61).

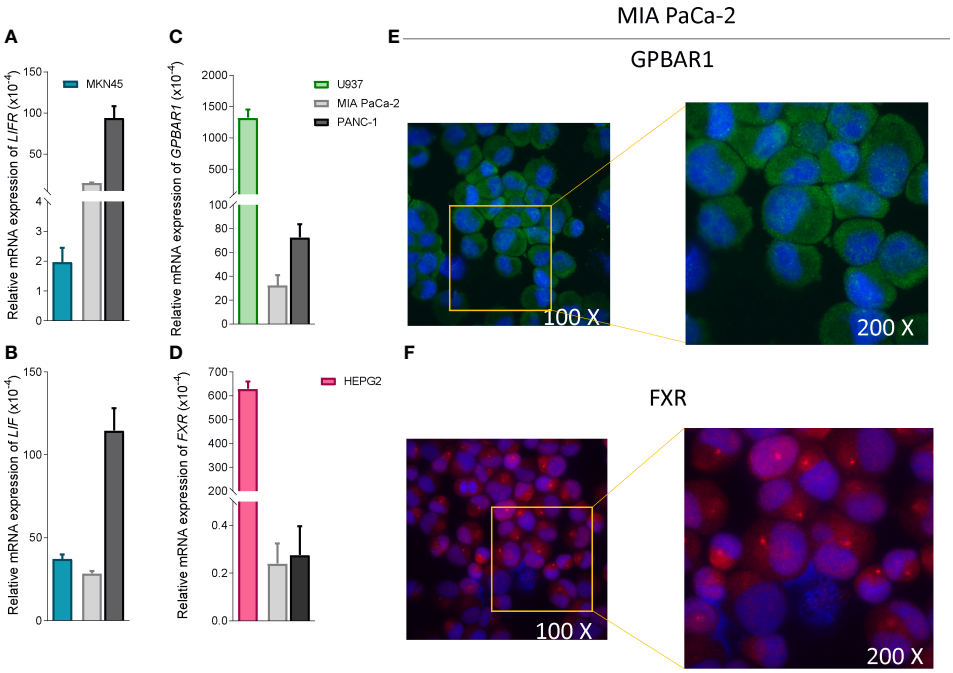

FIGURE 4
PDAC cells expressed low levels of bile acids receptors. Relative mRNA expression of **(A)** LIFR **(B)** LIF compared to MKN45 **(C)** GPBAR1 compared to U937 and **(D)** FXR compared to HEPG2. Each value is normalized to GAPDH and is expressed relative to those of positive controls, which are arbitrarily set to 1. Results are the mean ± SEM of three samples for group. Immunofluorescence analysis of **(E)** Gpbar1 and **(F)** Fxr in MIA PaCa-2 cells (Magnification 100x on left and 200x on right).

10.3389/fonc.2023.1140730

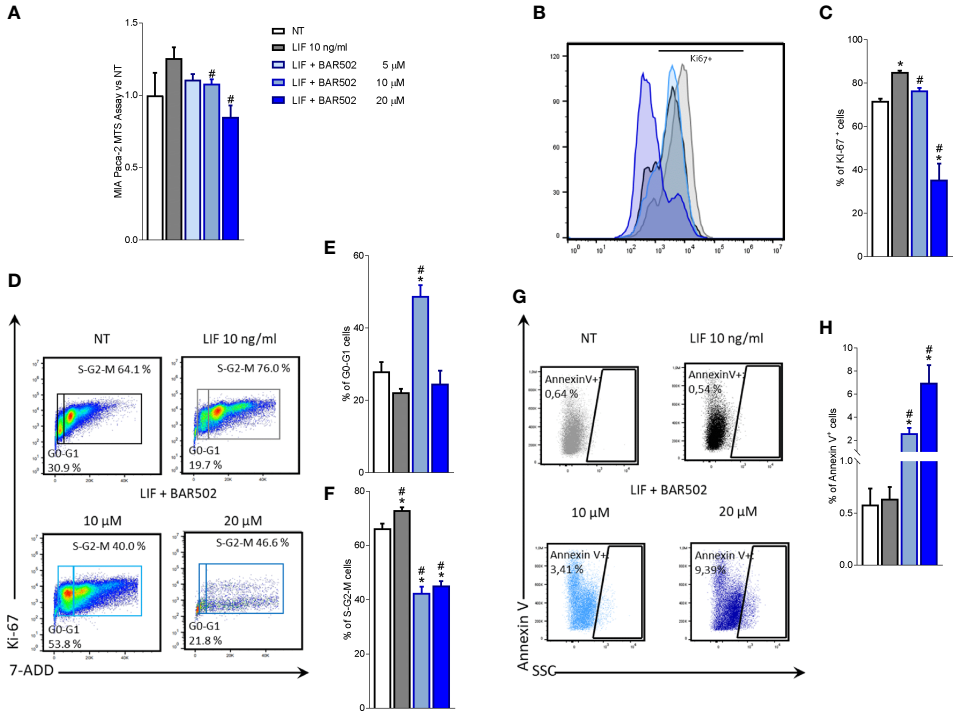

FIGURE 5
LIFR inhibition reverses PDAC cell proliferation promoted by LIF. MIA PaCa-2 cells were serum-starved and primed with LIF (10 ng/mL) alone or in combination with increasing concentrations of BAR502 (5, 10,20 µM). Data shown are **(A)** MTS assay performed on MIA PaCa-2. Each value is expressed relative to the non-treated (NT) value, which is arbitrarily set to 1. Results are the mean ± SEM of 10 samples per group. Cell cycle phase analysis was performed by Ki-67/7-AAD staining through IC-FACS. **(B)** Representative IC-FACS shows Ki-67 positive MIA PaCa-2 cells and **(C)** frequencies of Ki-67 positive cells. **(D)** Representative IC-FACS shows cell cycle fraction in each experimental group. Data shown are frequencies of cells in the **(E)** G0-G1 phase and **(F)** S-G2-M phase. **(G)** Representative IC-FACS shows Annexin V+ cells. **(H)** Data shown are frequencies of Annexin V+ single cells. Results are the mean ± SEM of five samples for group (* represents statistical significance versus NT, and # versus LIF, $p < 0.05$).

Since the above mentioned data demonstrated that BAR502 prevents the acquisition of a migratory phenotype, we have measured the motility of MIA PaCA-2 cells using a wound healing assay (Figure 6F). To this end, MIA PaCa-2 cells were growth in a complete serum starved DMEM medium and after the production of a scratch (Day 0), cells were exposed to 10 ng/mL LIF, alone or in combination with BAR502 (10 µM). The gain in the capacity of cells to differentiate into a migratory phenotype was calculated as the area between the two scratch edges at prespecified time points: 0 h, 24h and 48 h. As illustrated in Figures 6F, G, LIF induced cell migration and promoted the wound closure with a reduction of the scratch area by ≈ 16%. These findings were reversed by treatment with BAR502 that significantly decreased MIA PaCa-2 detachment and migration, with a reduction of ≈40% compared to LIF ($p<0.05$) (Figure 6G).

Altogether these findings suggest that LIFR antagonism in PDAC cell lines reduced cell proliferation and migration by reducing STAT3 phosphorylation.

BAR502 anti-cancer activity is due to LIFR inhibition

To tight the biological effect of BAR502 to the LIF/LIFR antagonism, we have synthesized a dual FXR and GPBAR1 antagonist (Figure 7A). To this end we have generated a small library of 3,5-disubstituted isoxazole derivatives as potential dual FXR and GPBAR1 antagonists and tested them in a transactivation assay on FXR and GPBAR1 (data not published). From this library, PDL103 was proven to be a relatively potent novel dual FXR/GPBAR1 antagonist (IC_{50} = 10 µM and 19 µM, respectively) (Figures 7B, C). PDL103 was also tested in Alpha screen on LIF/LIFR. However, the result shown in Figure 7D, demonstrated that this compound was inactive towards LIF/LIFR complex. Because PDL103 is a dual FXR and GPBAR1 antagonist but is neutral toward LIF/LIFR, this agent represents an useful tool to rule out the involvement of the two receptors in the observed antagonism exerted by BAR502 on the LIF pathway. Indeed, as shown in Figures 7E-G, co-treating MIA PaCa-2 cells with this agent failed to reverse the effect of BAR502 on LIF/LIFR induced proliferation (Panel E and F) and EMT (Panel G).

RNAseq analysis of the effects of BAR502 on MIA PaCa-2 cells

To further characterize the transcriptional profile modulated by exposure to LIF and BAR502, a AmpliSeq Transcriptome analysis (RNAseq) was conducted on MIA PaCa-2 cells left untreated or challenged with LIF alone or in combination with BAR502 (10 µM).

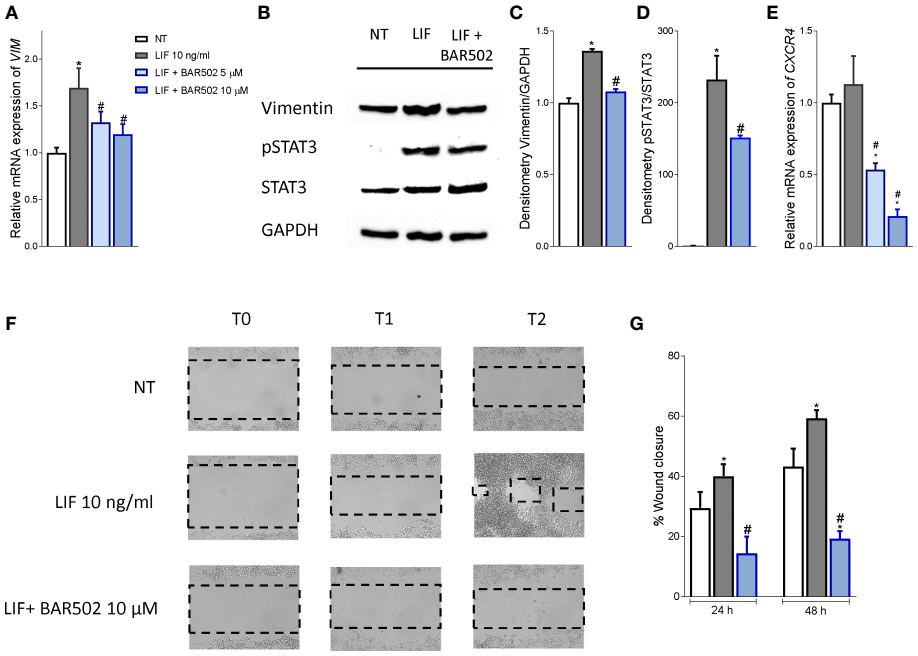

FIGURE 6
BAR502 inhibits *in vitro* migration in STAT3-dependent signalling. MIA PaCa-2 cells were serum-starved for 24 hours and exposed to LIF (10 ng/mL) alone or in combination with increasing concentrations of BAR502 (5, 10 µM) for 24 hours. Data displayed are: **(A)** Relative mRNA expression of the EMT markers, VIM. Each value is normalized to GAPDH and is expressed relative to those of positive controls, which are arbitrarily set to 1. **(B)** Representative Western blot analysis of Vimentin, phospho-STAT3 and STAT3 proteins in MIA-PaCa-2 cells exposed to LIF (10 ng/ml) alone or plus BAR502 (10 µM) for 20 minutes. **(C)** Densitometric analysis demonstrating Vimentin/GAPDH and **(D)** phospho-STAT3/STAT3 ratio. **(E)** Relative mRNA expression of the prognostic marker, CXCR4. Each value is normalized to GAPDH and is expressed relative to those of positive controls, which are arbitrarily set to 1. **(F, G)** Scratch wound healing assay. MIA PaCa-2 cell monolayers were scraped in a straight line using a p200 pipette tip; then, they were left untreated or primed with LIF 10 ng/mL alone or in combination with BAR502 10 µM. The wound generated was captured at 0, 24 and 48 h of incubation with the compounds above described. The images show cell migration at the three times point indicated. **(G)** Images of obtained points were analysed, measuring scraped area and its closure *vs* the first time point at 0 (h) Results are the mean ± SEM of five samples per group (* represents statistical significance versus NT, and # versus LIF, $p < 0.05$).

The Principal Component Analysis (PCA) of the resulting transcriptome (Figure 8A) highlighted major dissimilarities between MIA PaCa-2 left untreated or treated with LIF and LIF/BAR502. Figure 8B displayed the Venn Diagram analysis of differentially expressed transcripts. As shown in Figure 8B, the analysis identified 2.043 transcripts differentially regulated across the three experimental groups: 168 transcripts were differentially modulated by LIF *versus* control cells (Subset A); 1.906 transcripts were differentially modulated by exposure to LIF/BAR502 in comparison to LIF alone (Subset B), while the AB subset includes only 31 transcripts that were modulated by LIF and LIF/BAR502 in comparison to control (NT) cells. The Scatter Plot (Figure 8C) of the 1.906 transcripts demonstrated that 884 transcripts were up-regulated and 1022 were down-regulated (Figure 8C). Then, the *per pathways* analysis of these differentially expressed transcript sets was performed using the TAC software (Affymetrix) to inspect the molecular pathways modulated by the exposure of MA PaCa-2 cells to LIF and BAR502. As illustrated in Figure 8D, the higher number of downregulated genes belong to the cell cycle (35 genes), G1 to S cell cycle control (21 genes), mitotic G1 phase and G1/S transition (19 genes), mitotic S-G2/M phases (15), DNA replication (17 genes), PI3K-Akt signalling pathway (19 genes). In contrast, the highest up-regulated genes fell in to the p53 transcriptional gene network (18 genes) and Apoptosis (11 genes) (Figure 8D). Within the genes that belonged to these pathways, the most downregulated gene by BAR502 was the *Kinesin Family Member 20A* (KIF20A) with a Fold Change (FC) of -17,49. KIF20A is a motor kinesin protein involved in mitosis process (62). The overexpression of KIF20A occurs in several tumours, including gastric cancer (GC) (63), lung cancer (64), cervical cancer (65), glioma (66) and also PDAC (67). In addition to KIF20A, BAR502 potently downregulated the expression of the *Ribonucleotide reductase subunit M2* (RRM2), (FC: -14,34) (68) and *TNF Receptor Superfamily Member 1B* (TNFRSF1B or TNFR2) (FC: -11,72) (69) and *DNA topoisomerase II alpha* (TOP2A) (FC: -9,61), an important regulator of DNA replication and cell cycle progression and up-regulated in PDAC (70). On the other hand, exposure to BAR502 increased the expression of a number of genes, including the *Solute carrier family 7 member 11* (SLC7A11) (FC: 35,54), a cysteine transporter involved in the inhibition of the ferroptosis programmed cell death (71), that was the most upregulated gene, and the *Cyclin D2* (CCND2) (FC: 16,13) (72) and *Sestrin 2* (SESN2) (FC: 15,84) (73),, whose expression are robustly reduced in PDAC cells (74).

Discussion

LIF is the most pleiotropic member of the IL-6 family of cytokines and controls multiple biological functions, including the

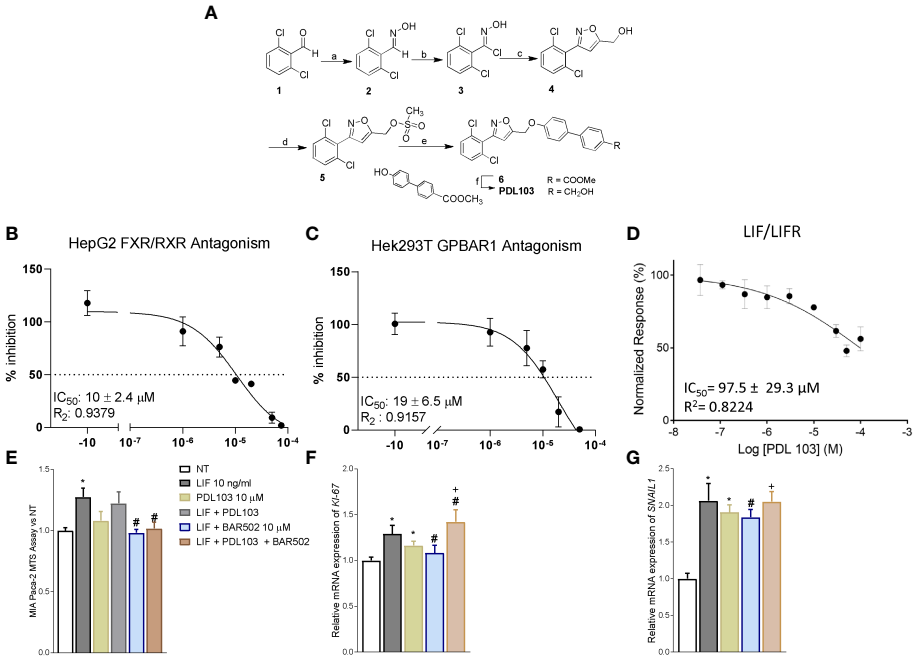

FIGURE 7
The effect of BAR502 is mediated through selectively LIFR inhibition. **(A)** Scheme 1. Reagents and conditions: a) $NH_2OH{\cdot}HCl$, NaOH, EtOH, Δ, 98%; b) N-clorosuccinimide, dry DMF, 0°C, 95%; c) propargylic alcohol, $NaHCO_3$, $CuSO_4{\cdot}5H_2O$, sodium ascorbate, t-BuOH/H_2O 1:1, quantitative yield; d) methanesulfonyl chloride, TEA, dry THF, 92%; e) methyl 4′-hydroxy-4-biphenylcarboxylate, K_2CO_3, dry DMF, 0°C, 66%; f) $LiBH_4$, MeOH, dry THF, 0°C, 82%. The synthetic strategy was as following: the commercially available 2,6-dichlorobenzaldehyde (1) was treated with hydroxylamine hydrochloride to form the oxime (2) which was in turn chlorinated with NCS to afford the chloro oxime (3). The 3,5-disubstituted isoxazole 4 was easily obtained as only regioisomer *via* [3 + 2]-cycloaddition between the 2,6-dichloro-N-hydroxybenzimidoyl chloride (3) and propargyl alcohol in presence of $NaHCO_3$, catalytic $CuSO_4{\cdot}5H_2O$ and sodium ascorbate with quantitative yield. The intermediate 4 was then reacted with mesyl chloride and triethylamine to afford the mesyl ester (5) which was in turn coupled to methyl 4′-hydroxy-4-biphenylcarboxylate to afford the methyl esters 6. Finally, reduction with $LiBH_4$ gave PDL103. **(B, C)** Antagonistic effects of PDL103 on FXR and GPBAR1 transactivation induced by CDCA and LCA, respectively, in HepG2 cells. **(D)** PDL103 inhibition activity of LIFR/LIF binding accessed by a cell-free AlphaScreen assay. **(E)** MTS assay performed on MIA PaCa-2. Each value is expressed relative to the non-treated (NT) value, which is arbitrarily set to 1. Results are the mean ± SEM of 10 samples per group. Relative mRNA expression of the proliferative marker (* represents statistical significance versus NT; # versus LIF; + versus PDL103) **(F)** KI-67 and **(G)** the EMT marker SNAIL1. Each value is normalized to GAPDH and is expressed relative to those of positive controls, which are arbitrarily set to 1. Results are the mean ± SEM of 5 samples per group.

stem cell ability to "self-renew", the embryonic implantation and placental formation and cell proliferation and differentiation (10). LIF exploits its function by binding to an heterodimeric membrane receptor complex assembled by the LIFR and glycoprotein 130 (gp130) (12). LIFR lacks an intrinsic tyrosine kinase activity, but either LIFR and gp130 are constitutively associated with of cytoplasmic tyrosine kinases belonging to the Jak family (55). Consequently, binding of LIF to LIFR induces the assembly of the heterodimeric complex LIFR:gp130 and promotes a Jak-Tyk phosphorylation and propagation of downstream signalling (75).

The LIF/LIFR axis plays a central role in tumour growth and progression, regulating key aspects of cancer biology including cancer cell growth, proliferation, migration and chemotherapy resistance (76). Consistent with this view, an aberrant production of LIF and/or an increase in the circulating levels of LIF correlate with tumour chemoresistance in several solid cancers (60).

LIF acts as a growth factor in PDAC cells (12) and high levels of LIF expression occur in human PDAC and correlate with a shorter overall survival (12). LIF/LIFR signalling promotes tumorigenesis and metastasis by the upregulation of LIF/LIFR-JAK-STAT3 signalling *via* autocrine and paracrine mechanisms (77). We have previously demonstrated that inhibition of the LIF/LIFR axis reversed the increased proliferation rate and propensity to develop a EMT phenotype in MIA PaCa-2 and PANC-1 cells. More specifically we have reported that the small steroidal molecule LIFR inhibitor, EC359, reduced the mRNA expression of VIM and Snail1, validating the potential role of LIFR as therapeutic target in PDAC (20).

Prompted by these findings and by the fact that steroids such as mifepristone, an antiprogesterone agent, effectively counteracted the effects of LIF on PDAC cells, we have embarked in a screening project of an in-house library of natural and synthetic bile acids. This screening allowed us to show that LCA, CDCA and BAR502 exert LIFR antagonism. By Alpha screen assay, we have then confirmed that BAR502 is a potent LIFR inhibitor with an IC_{50} of 3.59 µM. Traditionally, bile acids have been linked to development of gastrointestinal and liver cancers, but the putative mechanisms have remained elusive. In contrast, a number of recent investigations, as detailed in the introduction, have shown the opposite, suggesting that bile acids might exert anti-tumour effects in solid cancers (26), but these effects are strictly dependent on their concentrations, cellular microenvironment and expression of key receptors such as FXR and GPBAR1 (30). In general, it appears that low concentrations of bile acids exert anti-cancer effects, while in super-physiological concentrations, bile acids promote cell proliferation, migration and

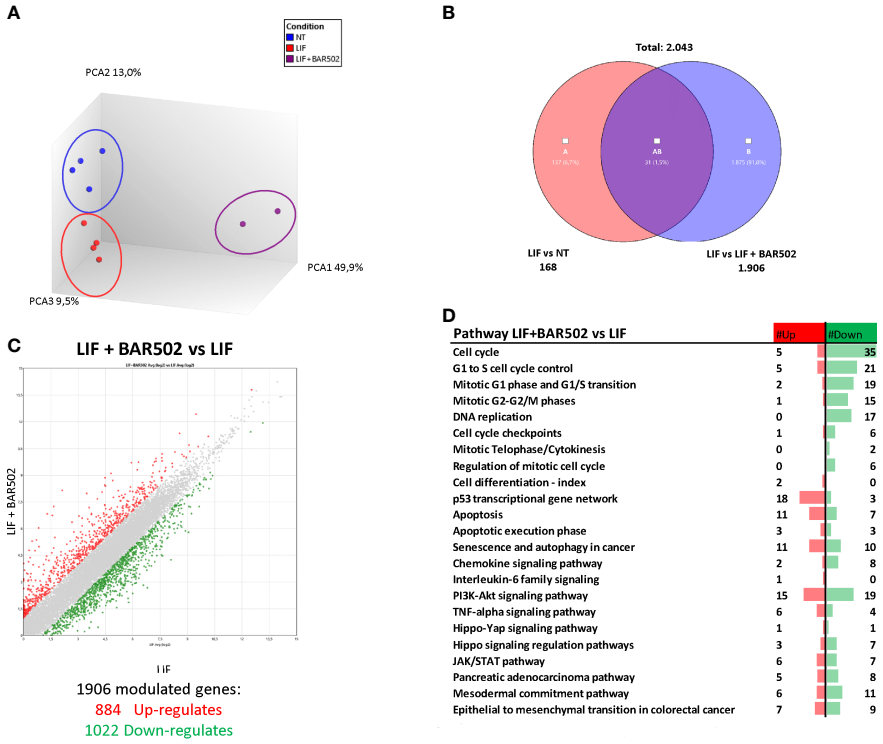

FIGURE 8
RNA-seq analysis of BAR502 effects on MIA PaCa-2 cells exposed to LIF alone or in combination with BAR502. MIA PaCa-2 cells were serum-starved for 24 hours and exposed to LIF (10 ng/mL) alone or in combination with increasing concentrations of BAR502 (10 μM) for 24 hours. **(A)** Heterogeneity characterization of the three experimental groups as shown by principal component analysis (PCA) plot. **(B)** Venn diagram of differentially expressed genes showing the overlapping region between the three experimental groups. **(C)** Scatter plots of transcripts differentially expressed between different experimental groups (fold change <−2 or >+2, p value < 0.05). Red dots represent significantly upregulated genes, and green dots represent significantly downregulated genes. **(D)** Table showing pathway modulated by LIF plus BAR502 versus LIF.

invasion. This phenomenon is due to their amphipathic structure and the activation of off-target mechanisms not observed at physiological concentrations.

By computational analysis we have clarifies the structural requirement for the binding to LIFR. Our results indicated that natural bile acids and BAR502 bind to the same pocket within loops L2 and L3 of LIFR. Because these two loops are involved in LIF binding to hLIFR, we speculated that antagonism of BAR502 against LIFR is due to the ability of this agent to prevent LIF/LIFR binding. Moreover, molecular dynamic analysis of the BAR502 in conjunction with LIFR showed a stable binding mode of BAR502 over the time of the simulation. The binding was stabilized by H-bonds of the ligand 3-, 7- and 23-OH, and by hydrophobic contacts with both L2, L3 and β-sheet residues with the steroidal agent. Importantly we found that the 6-ethyl group contributed to further stabilize the binding mode through the contact with the Cβ of Asn339, entrapping the A and B rings in a box formed by Arg333, Asn339, Val311 and Ala315 (Figure 3A). The computational results highlighted that the binding of BAR502 within loops L2 and L3 might impact with the position of L2 and L3 widening the distance between the two loops (Figure 3B), likely affecting the 3D structure of the whole LIF binding site.

To further characterize functionally the relevance of LIFR inhibition caused by BAR502, we have assessed whether BAR502 counteracts the effects exerted by LIF in MIA PaCa-2 cells. The results of these experiments were consistent with the cell-free assay and demonstrated that BAR502 effectively counteracted the pro-oncogenic effects caused by LIF in a concentration-dependent manner and in a FXR/GPBAR1 independent manner, reducing cell vitality, the number ki-67+ cells and increasing the frequencies of cells in the resting G0-G1 cell cycle phase, blocking S-G2-M transition and increasing the frequencies of AnnexinV^{+} apoptotic cells. Similarly, BAR502 reversed EMT features, diminished the regulation of Vimentin, CXCR4 and the gain of the migratory phenotype, and STAT3 phosphorylation induced by LIF, further suggesting a potential utility in counteracting the pro-oncogenic activity of LIF/LIFR pathway.

In order to better dissect the molecular mechanisms that mediates anti LIF/LIFR effects of BAR502, we have carried out a RNAseq analysis on MIA PaCa-2 cells exposed to LIF. The results of these studies demonstrated that antagonism of LIF/LIFR exerted by BAR502 was supported by regulation of the expression of large group of genes, including 35 genes involved in the Cell cycle modulation, 21 genes involved in G1 to S cell cycle control, 19 genes in G1-S phase transition, 17 genes involved in DNA replication, 15 genes involved in the G2/M shift, 18 in p53 transcriptional gene network and 11 in apoptosis. The most downregulated of these genes was KIF20A, a motor kinesin

protein involved in mitosis process and in the trafficking of organelles and vesicles. Positive expression of KIF20A correlates with a poor prognosis and tumour growth and progression in early-stage of several types of cancer including breast (78), colorectal (79) and cervical cancers (65) but also PDAC (67) and glioma (80). Overexpression of KIF20A enhances resistance to chemotherapy (79) while KIF20A inhibition reduces cell proliferation, migration and invasion of pancreatic cancer cells in PDAC (67). In addition to KIF20A, BAR502 reduced the expression of LIF-induced RRM2 in MIA PaCA-2 cells. Expression RRM2 correlates with a poor prognosis in several tumours including lung cancer (81) and PDAC (82). Also, RRM2 is a validated biomarker of sensitivity of PDAC to chemotherapy, and it is demonstrated that the high levels of RRM2 predict poor prognosis and resistance to gemcitabine in PDAC patients (66, 83).

Another gene that was downregulated by BAR502 in LIF-challenged MIA PaCa-2 cells was TNFR2, one of two membrane receptors that binds tumour necrosis factor-alpha (TNFα) (84). TNFR2 is expressed by immunomodulatory cells such as myeloid-derived suppressor cells (MDSCs) (85) and regulatory T cells (Tregs) (86), and plays a central role in their homeostasis by regulating their expansion, enhancing their phenotypic stability and immune-suppressive abilities (87). High expression of TNFR2 is a characteristic of tumour-associated Treg that promotes cancer growth by hindering the anti-tumour immune responses (85, 88, 89). TNFR2 regulates the transcription of PDL1 *via* the p65 NF-κB pathway, suggesting that BAR502 by downregulating the expression of TNFR2, might restore immune surveillance of pancreatic cancer cells in PDAC (69).

BAR502 also modulated the expression of a groups of genes whose expression is usually suppressed in neoplastic tissues in comparison to non-neoplastic counterparts (Figure 9). Exposure to BAR502 robustly increased the expression of SSN2, a highly conserved stress-induced protein. SSN2 is secreted by macrophages, T lymphocytes and epithelial cells, in a wide variety of stress conditions such as oxidative stress, hypoxia or DNA damage, and inhibits the accumulation of reactive oxygen species (ROS) through the activation of the nuclear factor-erythrocyte 2-related factor (Nrf2) signalling. SSN2 plays a tumour suppressive role by the inhibition of tumour growth and the activation of autophagy process, regulating the mTOR/AMPK signalling pathway (90).

In summary, by molecular modelling and pharmacological experiments, we have shown that BAR502 binds LIFR and acts as LIF/LIFR inhibitor. BAR502, a semisynthetic bile alcohol steroidal agonist (42), functions as a potent LIFR antagonist, directly binding within the loops L2 and L3 of the Ig-like domain of LIFR, and preventing its activation and signalling. BAR502 decreases PDAC cell proliferation and slows down cell cycle progression, arresting

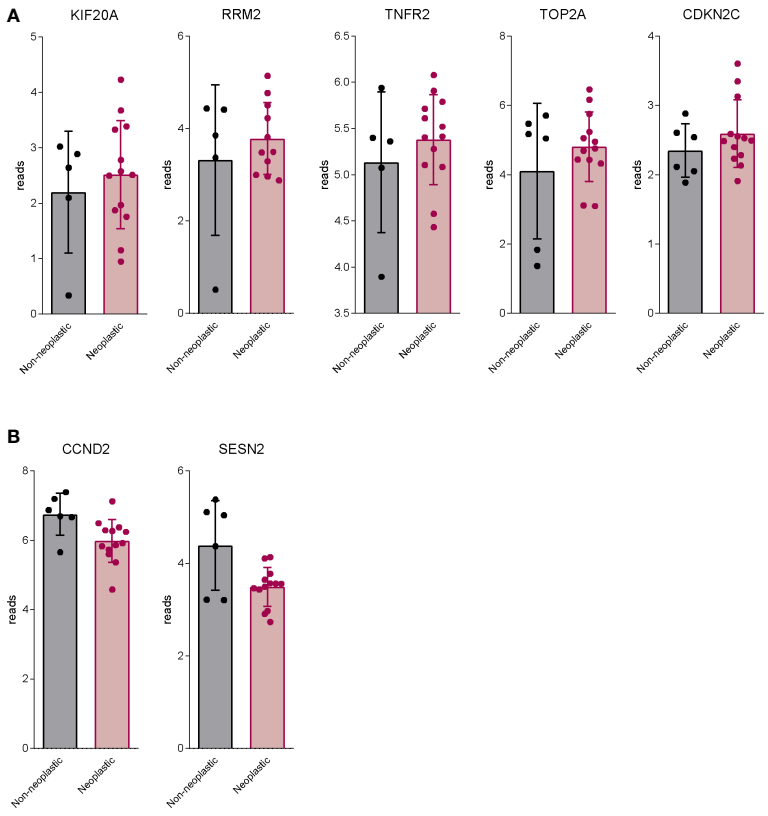

FIGURE 9
BAR502 modulated genes generally regulated aberrantly in PDAC. RNA-seq analysis of non-neoplastic and neoplastic mucosa of PDAC from GSE196009 repository. Each dot represents a patient. Data shown represent the gene profile expression of **(A)** genes upregulated in human PDAC, which are downregulated by BAR502 exposure in MIA PaCa-2 cells. **(B)** genes down-regulated in human PDAC, which are upregulated by BAR502 exposure in MIA PaCa-2 cells.

PDAC cells in the G0–G1 phases and retarding the transition toward S-G2-M phase. BAR502 promotes the apoptosis of PDCA cells and reverses the migratory phenotype induced by LIF.

The present study has several limitations. The most relevant of which is that the role of LIF/LIFR system has been tested in *in vitro* models and therefore the real anti-cancer potential of BAR502 in PDAC should be further investigated in clinically relevant settings.

In conclusion, in the present study we have described a dual GPBAR1/FXR agonist as a potential antagonist of LIFR and suggested that BAR502 could be used to regulate the LIF/LIFR pathway in relevant clinical settings such as LIF overexpressing-PDAC.

Data availability statement

The datasets presented in this study can be found in online repositories. The names of the repository/repositories and accession number(s) can be found in the article/Supplementary Material.

Author contributions

SF, AZ and BC contributed to conception and design of the study. AZ and SF provided research funding. CG, SM, MBi, AL, FM, MM and MBo performed the data analysis. CG, MBi, AL, FM, MM, VS, MBo and PRa performed the statistical analysis. SF, CG, AL, BC, VS, EM, PRi and ED wrote the manuscript. CG, SM, RR, MBo, RB, CM, GU, RR, AL, EM and MM contributed to the experiments. All authors contributed to manuscript revision and read and approved the submitted version. All authors contributed to the article and approved the submitted version.

Funding

This work was partially supported by a grant from the Italian MIUR/PRIN 2017 (2017FJZZRC). BC acknowledges the support from the European Regional Development Fund-POR Campania FESR 2014/2020 (Satin). VS and FM acknowledge the support from University of Napoli "Federico II" (Grant FRA—Line B—2020- MoDiGa).

Conflict of interest

Authors AL and FM were employed by Net4Science srl.

The remaining authors declare that the research was conducted in the absence of any commercial or financial relationships that could be construed as a potential conflict of interest.

Publisher's note

Supplementary material

The Supplementary Material for this article can be found online at: https://www.frontiersin.org/articles/10.3389/fonc.2023.1140730/full#supplementary-material

SUPPLEMENTARY FIGURE 1
(A) The ligand root means square deviation (L-RMSD) plot; **(B)** cluster analysis and **(C)** cluster distribution plot of hLIFR-BAR502 complex after 100ns of MD simulation.

SUPPLEMENTARY FIGURE 2
Different views (frontal, 35° and 90°) of the two representative clusters (cl0 and cl1) of the hLIFR-BAR502 complex after 100ns of MDs. L1, L2 and L3 are highlighted in yellow, blue, and green, respectively. BAR502 and the relevant residues are labelled and coloured.

SUPPLEMENTARY FIGURE 3
Table showing genes modulated by LIF in combination with BAR502 versus LIF resulted by RNA-seq analysis.

SUPPLEMENTARY FIGURE 4
MIA PaCa-2 cells were serum starved and exposed to vehicle or LIF (10 ng/ml) alone or in combination with BAR502 (10 μM) for 24 h. The map shows the pathway main regulated by BAR502 administration. The upregulated genes (Fold Change < –2 or > 2, p value < 0.05) are represented in the map in red and the downregulated genes are in green.

References

1. Rahib L, Smith BD, Aizenberg R, Rosenzweig AB, Fleshman JM, Matrisian LM. Projecting cancer incidence and deaths to 2030: The unexpected burden of thyroid, liver, and pancreas cancers in the united states. *Cancer Res* (2014) 74:2913–21. doi: 10.1158/0008-5472.CAN-14-0155

2. Siegel RL, Miller KD, Jemal A. Cancer statistics, 2020. *CA Cancer J Clin* (2020) 70:7–30. doi: 10.3322/caac.21590

3. De La Cruz MSD, Young AP, Ruffin MT. Diagnosis and management of pancreatic cancer. *Am Fam Phys* (2014) 89:626–32.

4. Páez D, Labonte MJ, Lenz H-J. Pancreatic cancer: medical management (novel chemotherapeutics). *Gastroenterol Clin North Am* (2012) 41:189–209. doi: 10.1016/j.gtc.2011.12.004

5. Yadav D, Lowenfels AB. The epidemiology of pancreatitis and pancreatic cancer. *Gastroenterology* (2013) 144:1252–61. doi: 10.1053/j.gastro.2013.01.068

6. Klein AP, Brune KA, Petersen GM, Goggins M, Tersmette AC, Offerhaus GJA, et al. Prospective risk of pancreatic cancer in familial pancreatic cancer kindreds. *Cancer Res* (2004) 64:2634–8. doi: 10.1158/0008-5472.can-03-3823

7. Zeng S, Pöttler M, Lan B, Grützmann R, Pilarsky C, Yang H. Chemoresistance in pancreatic cancer. *Int J Mol Sci* (2019) 20. doi: 10.3390/ijms20184504

8. Pinho V, Fernandes M, da Costa A, Machado R, Gomes AC. Leukemia inhibitory factor: Recent advances and implications in biotechnology. *Cytokine Growth Factor Rev* (2020) 52:25–33. doi: 10.1016/j.cytogfr.2019.11.005

9. Ma D, Jing X, Shen B, Liu X, Cheng X, Wang B, et al. Leukemia inhibitory factor receptor negatively regulates the metastasis of pancreatic cancer cells *in vitro* and *in vivo*. *Oncol Rep* (2016) 36:827–36. doi: 10.3892/or.2016.4865

10. Viswanadhapalli S, Dileep KV, Zhang KYJ, Nair HB, Vadlamudi RK. Targeting LIF/LIFR signaling in cancer. *Genes Dis* (2022) 9:973–80. doi: 10.1016/j.gendis.2021.04.003

11. Gearing DP, Thut CJ, VandeBos T, Gimpel SD, Delaney PB, King J, et al. Leukemia inhibitory factor receptor is structurally related to the IL-6 signal transducer, gp130. *EMBO J* (1991) 10:2839–48. doi: 10.1002/j.1460-2075.1991.tb07833.x

12. Kamohara H, Ogawa M, Ishiko T, Sakamoto K, Baba H. Leukemia inhibitory factor functions as a growth factor in pancreas carcinoma cells: Involvement of regulation of LIF and its receptor expression. *Int J Oncol* (2007) 30:977–83. doi: 10.3892/ijo.30.4.977

13. Di Giorgio C, Marchianò S, Marino E, Biagioli M, Roselli R, Bordoni M, et al. Next-generation sequencing analysis of gastric cancer identifies the leukemia inhibitory factor receptor as a driving factor in gastric cancer progression and as a predictor of poor prognosis. *Front Oncol* (2022) 12:939969. doi: 10.3389/fonc.2022.939969

14. Wang J, Xie C, Pan S, Liang Y, Han J, Lan Y, et al. N-myc downstream-regulated gene 2 inhibits human cholangiocarcinoma progression and is regulated by leukemia inhibitory factor/MicroRNA-181c negative feedback pathway. *Hepatology* (2016) 64:1606–22. doi: 10.1002/hep.28781

15. Yu H, Yue X, Zhao Y, Li X, Wu L, Zhang C, et al. LIF negatively regulates tumour-suppressor p53 through Stat3/ID1/MDM2 in colorectal cancers. *Nat Commun* (2014) 5:5218. doi: 10.1038/ncomms6218

16. Li X, Yang Q, Yu H, Wu L, Zhao Y, Zhang C, et al. LIF promotes tumorigenesis and metastasis of breast cancer through the AKT-mTOR pathway. *Oncotarget* (2014) 5:788–801. doi: 10.18632/oncotarget.1772

17. Yue X, Zhao Y, Zhang C, Li J, Liu Z, Liu J, et al. Leukemia inhibitory factor promotes EMT through STAT3-dependent miR-21 induction. *Oncotarget* (2016) 7:3777–90. doi: 10.18632/oncotarget.6756

18. Peñuelas S, Anido J, Prieto-Sánchez RM, Folch G, Barba I, Cuartas I, et al. TGF-β increases glioma-initiating cell self-renewal through the induction of LIF in human glioblastoma. *Cancer Cell* (2009) 15:315–27. doi: 10.1016/j.ccr.2009.02.011

19. Liu S-C, Tsang N-M, Chiang W-C, Chang K-P, Hsueh C, Liang Y, et al. Leukemia inhibitory factor promotes nasopharyngeal carcinoma progression and radioresistance. *J Clin Invest* (2013) 123:5269–83. doi: 10.1172/JCI63428

20. Di Giorgio C, Lupia A, Marchianò S, Bordoni M, Bellini R, Massa C, et al. Repositioning mifepristone as a leukaemia inhibitory factor receptor antagonist for the treatment of pancreatic adenocarcinoma. *Cells* (2022) 11. doi: 10.3390/cells11213482

21. Viswanadhapalli S, Luo Y, Sareddy GR, Santhamma B, Zhou M, Li M, et al. EC359: A first-in-Class small-molecule inhibitor for targeting oncogenic LIFR signaling in triple-negative breast cancer. *Mol Cancer Ther* (2019) 18:1341–54. doi: 10.1158/1535-7163.MCT-18-1258

22. Zhang C, Liu J, Wang J, Hu W, Feng Z. The emerging role of leukemia inhibitory factor in cancer and therapy. *Pharmacol Ther* (2021) 221:107754. doi: 10.1016/j.pharmthera.2020.107754

23. Ridlon JM, Harris SC, Bhowmik S, Kang DJ, Hylemon PB. Consequences of bile salt biotransformations by intestinal bacteria. *Gut Microbes* (2016) 7:22–39. doi: 10.1080/19490976.2015.1127483

24. de Aguiar Vallim TQ, Tarling EJ, Edwards PA. Pleiotropic roles of bile acids in metabolism. *Cell Metab* (2013) 17:657–69. doi: 10.1016/j.cmet.2013.03.013

25. Bernstein H, Bernstein C, Payne CM, Dvorakova K, Garewal H. Bile acids as carcinogens in human gastrointestinal cancers. *Mutat Res* (2005) 589:47–65. doi: 10.1016/j.mrrev.2004.08.001

26. Shrader HR, Miller AM, Tomanek-Chalkley A, McCarthy A, Coleman KL, Ear PH, et al. Effect of bacterial contamination in bile on pancreatic cancer cell survival. *Surgery* (2021) 169:617–22. doi: 10.1016/j.surg.2020.09.029

27. Makishima M, Okamoto AY, Repa JJ, Tu H, Learned RM, Luk A, et al. Identification of a nuclear receptor for bile acids. *Sci (80-)* (1999) 284:1362–5. doi: 10.1126/science.284.5418.1362

28. Parks DJ, Blanchard SG, Bledsoe RK, Chandra G, Consler TG, Kliewer SA, et al. Bile acids: natural ligands for an orphan nuclear receptor. *Sci (80-)* (1999) 284:1365–8. doi: 10.1126/science.284.5418.1365

29. Wang H, Chen J, Hollister K, Sowers LC, Forman BM. Endogenous bile acids are ligands for the nuclear receptor FXR/BAR. *Mol Cell* (1999) 3:543–53. doi: 10.1016/s1097-2765(00)80348-2

30. Phelan JP, Reen FJ, Caparros-Martin JA, O'Connor R, O'Gara F. Rethinking the bile acid/gut microbiome axis in cancer. *Oncotarget* (2017) 8:115736–47. doi: 10.18632/oncotarget.22803

31. Kawamata Y, Fujii R, Hosoya M, Harada M, Yoshida H, Miwa M, et al. A G protein-coupled receptor responsive to bile acids. *J Biol Chem* (2003) 278:9435–40. doi: 10.1074/jbc.M209706200

32. Fiorucci S, Carino A, Baldoni M, Santucci L, Costanzi E, Graziosi L, et al. Bile acid signaling in inflammatory bowel diseases. *Dig Dis Sci* (2021) 66:674–93. doi: 10.1007/s10620-020-06715-3

33. Lim S-C, Duong H-Q, Choi JE, Lee T-B, Kang J-H, Oh SH, et al. Lipid raft-dependent death receptor 5 (DR5) expression and activation are critical for ursodeoxycholic acid-induced apoptosis in gastric cancer cells. *Carcinogenesis* (2011) 32:723–31. doi: 10.1093/carcin/bgr038

34. Pyo J-S, Ko YS, Kang G, Kim D-H, Kim WH, Lee BL, et al. Bile acid induces MUC2 expression and inhibits tumor invasion in gastric carcinomas. *J Cancer Res Clin Oncol* (2015) 141:1181–8. doi: 10.1007/s00432-014-1890-1

35. Kim E-K, Cho JH, Kim E, Kim YJ. Ursodeoxycholic acid inhibits the proliferation of colon cancer cells by regulating oxidative stress and cancer stem-like cell growth. *PloS One* (2017) 12:e0181183. doi: 10.1371/journal.pone.0181183

36. Im E, Martinez JD. Ursodeoxycholic acid (UDCA) can inhibit deoxycholic acid (DCA)-induced apoptosis *via* modulation of EGFR/Raf-1/ERK signaling in human colon cancer cells. *J Nutr* (2004) 134:483–6. doi: 10.1093/jn/134.2.483

37. Kim YH, Kim JH, Kim BG, Lee KL, Kim JW, Koh S-J. Tauroursodeoxycholic acid attenuates colitis-associated colon cancer by inhibiting nuclear factor kappaB signaling. *J Gastroenterol Hepatol* (2019) 34:544–51. doi: 10.1111/jgh.14526

38. Vogel SM, Bauer MR, Joerger AC, Wilcken R, Brandt T, Veprintsev DB, et al. Lithocholic acid is an endogenous inhibitor of MDM4 and MDM2. *Proc Natl Acad Sci USA* (2012) 109:16906–10. doi: 10.1073/pnas.1215060109

39. Powell AA, LaRue JM, Batta AK, Martinez JD. Bile acid hydrophobicity is correlated with induction of apoptosis and/or growth arrest in HCT116 cells. *Biochem J* (2001) 356:481–6. doi: 10.1042/0264-6021:3560481

40. Kim YJ, Jeong SH, Kim E-K, Kim EJ, Cho JH. Ursodeoxycholic acid suppresses epithelial-mesenchymal transition and cancer stem cell formation by reducing the levels of peroxiredoxin II and reactive oxygen species in pancreatic cancer cells. *Oncol Rep* (2017) 38:3632–8. doi: 10.3892/or.2017.6045

41. D'Amore C, Di Leva FSS, Sepe V, Renga B, Del Gaudio C, D'Auria MVV, et al. Design, synthesis, and biological evaluation of potent dual agonists of nuclear and membrane bile acid receptors. *J Med Chem* (2014) 57:937–54. doi: 10.1021/jm401873d

42. Carino A, Cipriani S, Marchianò S, Biagioli M, Santorelli C, Donini A, et al. BAR502, a dual FXR and GPBAR1 agonist, promotes browning of white adipose tissue and reverses liver steatosis and fibrosis. *Sci Rep* (2017) 7:42801. doi: 10.1038/srep42801

43. Cipriani S, Renga B, D'Amore C, Simonetti M, De Tursi AAA, Carino A, et al. Impaired itching perception in murine models of cholestasis is supported by dysregulation of GPBAR1 signaling. *PloS One* (2015) 10:e0129866. doi: 10.1371/journal.pone.0129866

44. Lee T-S, Cerutti DS, Mermelstein D, Lin C, LeGrand S, Giese TJ, et al. GPU-Accelerated molecular dynamics and free energy methods in Amber18: Performance enhancements and new features. *J Chem Inf Model* (2018) 58:2043–50. doi: 10.1021/acs.jcim.8b00462

45. Bayly CI, Cieplak P, Cornell W, Kollman PA. A well-behaved electrostatic potential based method using charge restraints for deriving atomic charges: the RESP model. *J Phys Chem* (1993) 97:10269–80. doi: 10.1021/j100142a004

46. Maier JA, Martinez C, Kasavajhala K, Wickstrom L, Hauser KE, Simmerling C. ff14SB: Improving the accuracy of protein side chain and backbone parameters from ff99SB. *J Chem Theory Comput* (2015) 11:3696–713. doi: 10.1021/acs.jctc.5b00255

47. Frisch MJ, Trucks GW, Schlegel HB, Scuseria GE, Robb M a, Cheeseman JR, et al. (2016). G16_C01.

48. Wang J, Wang W, Kollman PA, Case DA. Automatic atom type and bond type perception in molecular mechanical calculations. *J Mol Graph Model* (2006) 25:247–60. doi: 10.1016/j.jmgm.2005.12.005

49. He X, Man VH, Yang W, Lee T-S, Wang J. A fast and high-quality charge model for the next generation general AMBER force field. *J Chem Phys* (2020) 153:114502. doi: 10.1063/5.0019056

50. Jorgensen W, Chandrasekhar J, Madura J, Impey R, Klein M. Comparison of simple potential functions for simulating liquid water. *J Chem Phys* (1983) 79:926–35. doi: 10.1063/1.445869

51. Humphrey W, Dalke A, Schulten K. VMD: Visual molecular dynamics. *J Mol Graph* (1996) 14:33–8. doi: 10.1016/0263-7855(96)00018-5

52. Roe DR, Cheatham TE3rd. PTRAJ and CPPTRAJ: Software for processing and analysis of molecular dynamics trajectory data. *J Chem Theory Comput* (2013) 9:3084–95. doi: 10.1021/ct400341p

53. Genheden S, Ryde U. The MM/PBSA and MM/GBSA methods to estimate ligand-binding affinities. *Expert Opin Drug Discov* (2015) 10:449–61. doi: 10.1517/17460441.2015.1032936

54. Carino A, Biagioli M, Marchianò S, Fiorucci C, Bordoni M, Roselli R, et al. Opposite effects of the FXR agonist obeticholic acid on mafg and Nrf2 mediate the development of acute liver injury in rodent models of cholestasis. *Biochim Biophys Acta Mol Cell Biol Lipids* (2020) 1865:158733. doi: 10.1016/j.bbalip.2020.158733

55. Hunter SA, McIntosh BJ, Shi Y, Sperberg RAP, Funatogawa C, Labanieh L, et al. An engineered ligand trap inhibits leukemia inhibitory factor as pancreatic cancer treatment strategy. *Commun Biol* (2021) 4:452. doi: 10.1038/s42003-021-01928-2

56. Jiang L, Zhang H, Xiao D, Wei H, Chen Y. Farnesoid X receptor (FXR): Structures and ligands. *Comput Struct Biotechnol J* (2021) 19:2148–59. doi: 10.1016/j.csbj.2021.04.029

57. Festa C, Renga B, D'Amore C, Sepe V, Finamore C, De Marino S, et al. Exploitation of cholane scaffold for the discovery of potent and selective farnesoid X receptor (FXR) and G-protein coupled bile acid receptor 1 (GP-BAR1) ligands. *J Med Chem* (2014) 57:8477–95. doi: 10.1021/jm501273r

58. Fiorucci S, Distrutti E, Carino A, Zampella A, Biagioli M. Bile acids and their receptors in metabolic disorders. *Prog Lipid Res* (2021) 82:101094. doi: 10.1016/j.plipres.2021.101094

59. Gradiz R, Silva HC, Carvalho L, Botelho MF, Mota-Pinto A. MIA PaCa-2 and PANC-1 - pancreas ductal adenocarcinoma cell lines with neuroendocrine differentiation and somatostatin receptors. *Sci Rep* (2016) 6:21648. doi: 10.1038/srep21648

60. Shi Y, Gao W, Lytle NK, Huang P, Yuan X, Dann AM, et al. Targeting LIF-mediated paracrine interaction for pancreatic cancer therapy and monitoring. *Nature* (2019) 569:131–5. doi: 10.1038/s41586-019-1130-6

61. Ding Y, Du Y. Clinicopathological significance and prognostic role of chemokine receptor CXCR4 expression in pancreatic ductal adenocarcinoma, a meta-analysis and literature review. *Int J Surg* (2019) 65:32–8. doi: 10.1016/j.ijsu.2019.03.009

62. Echard A, Jollivet F, Martinez O, Lacapère JJ, Rousselet A, Janoueix-Lerosey I, et al. Interaction of a golgi-associated kinesin-like protein with Rab6. *Science* (1998) 279:580–5. doi: 10.1126/science.279.5350.580

63. Sheng Y, Wang W, Hong B, Jiang X, Sun R, Yan Q, et al. Upregulation of KIF20A correlates with poor prognosis in gastric cancer. *Cancer Manag Res* (2018) 10:6205–16. doi: 10.2147/CMAR.S176147

64. Xie F, He C, Gao S, Yang Z, Li L, Qiao L, et al. KIF20A silence inhibits the migration, invasion and proliferation of non-small cell lung cancer and regulates the JNK pathway. *Clin Exp Pharmacol Physiol* (2020) 47:135–42. doi: 10.1111/1440-1681.13183

65. Ma H, Tian T, Liu X, Xia M, Chen C, Mai L, et al. Upregulated circ_0005576 facilitates cervical cancer progression *via* the miR-153/KIF20A axis. *BioMed Pharmacother* (2019) 118:109311. doi: 10.1016/j.biopha.2019.109311

66. Bhutia YD, Hung SW, Krentz M, Patel D, Lovin D, Manoharan R, et al. Differential processing of let-7a precursors influences RRM2 expression and chemosensitivity in pancreatic cancer: role of LIN-28 and SET oncoprotein. *PloS One* (2013) 8:e53436. doi: 10.1371/journal.pone.0053436

67. Stangel D, Erkan M, Buchholz M, Gress T, Michalski C, Raulefs S, et al. Kif20a inhibition reduces migration and invasion of pancreatic cancer cells. *J Surg Res* (2015) 197:91–100. doi: 10.1016/j.jss.2015.03.070

68. Hung SW, Mody HR, Govindarajan R. Overcoming nucleoside analog chemoresistance of pancreatic cancer: a therapeutic challenge. *Cancer Lett* (2012) 320:138–49. doi: 10.1016/j.canlet.2012.03.007

69. Zhang X, Lao M, Xu J, Duan Y, Yang H, Li M, et al. Combination cancer immunotherapy targeting TNFR2 and PD-1/PD-L1 signaling reduces immunosuppressive effects in the microenvironment of pancreatic tumors. *J Immunother Cancer* (2022) 10. doi: 10.1136/jitc-2021-003982

70. Zhou Z, Liu S, Zhang M, Zhou R, Liu J, Chang Y, et al. Overexpression of topoisomerase 2-alpha confers a poor prognosis in pancreatic adenocarcinoma identified by Co-expression analysis. *Dig Dis Sci* (2017) 62:2790–800. doi: 10.1007/s10620-017-4718-4

71. Koppula P, Zhuang L, Gan B. Cystine transporter SLC7A11/xCT in cancer: ferroptosis, nutrient dependency, and cancer therapy. *Protein Cell* (2021) 12:599–620. doi: 10.1007/s13238-020-00789-5

72. Deng J, He M, Chen L, Chen C, Zheng J, Cai Z. The loss of miR-26a-mediated post-transcriptional regulation of cyclin E2 in pancreatic cancer cell proliferation and decreased patient survival. *PloS One* (2013) 8:e76450. doi: 10.1371/journal.pone.0076450

73. Shi X, Xu L, Doycheva DM, Tang J, Yan M, Zhang JH. Sestrin2, as a negative feedback regulator of mTOR, provides neuroprotection by activation AMPK phosphorylation in neonatal hypoxic-ischemic encephalopathy in rat pups. *J Cereb Blood Flow Metab Off J Int Soc Cereb Blood Flow Metab* (2017) 37:1447–60. doi: 10.1177/0271678X16656201

74. Fu H, Ni X, Ni F, Li D, Sun H, Kong H, et al. Study of the mechanism by which curcumin cooperates with Sestrin2 to inhibit the growth of pancreatic cancer. *Gastroenterol Res Pract* (2021) 2021:7362233. doi: 10.1155/2021/7362233

75. Cancello R, Tordjman J, Poitou C, Guilhem G, Bouillot JL, Hugol D, et al. 3. *Diabetes* (2006) 55:1554–61. doi: 10.2337/db06-0133

76. Kellokumpu-Lehtinen P, Talpaz M, Harris D, Van Q, Kurzrock R, Estrov Z. Leukemia-inhibitory factor stimulates breast, kidney and prostate cancer cell proliferation by paracrine and autocrine pathways. *Int J Cancer* (1996) 66:515–9. doi: 10.1002/(SICI)1097-0215(19960516)66:4<515::AID-IJC15>3.0.CO;2-6

77. Bian S-B, Yang Y, Liang W-Q, Zhang K-C, Chen L, Zhang Z-T. Leukemia inhibitory factor promotes gastric cancer cell proliferation, migration, and invasion *via* the LIFR-Hippo-YAP pathway. *Ann N Y Acad Sci* (2021) 1484:74–89. doi: 10.1111/nyas.14466

78. Nakamura M, Takano A, Thang PM, Tsevegjav B, Zhu M, Yokose T, et al. Characterization of KIF20A as a prognostic biomarker and therapeutic target for different subtypes of breast cancer. *Int J Oncol* (2020) 57:277–88. doi: 10.3892/ijo.2020.5060

79. Zhang Q, Di J, Ji Z, Mi A, Li Q, Du X, et al. KIF20A predicts poor survival of patients and promotes colorectal cancer tumor progression through the JAK/STAT3 signaling pathway. *Dis Markers* (2020) 2020:2032679. doi: 10.1155/2020/2032679

80. Saito K, Ohta S, Kawakami Y, Yoshida K, Toda M. Functional analysis of KIF20A, a potential immunotherapeutic target for glioma. *J Neurooncol* (2017) 132:63–74. doi: 10.1007/s11060-016-2360-1

81. Wang L, Meng L, Wang X, Ma G, Chen J. Expression of RRM1 and RRM2 as a novel prognostic marker in advanced non-small cell lung cancer receiving chemotherapy. *Tumour Biol J Int Soc Oncodevelopmental Biol Med* (2014) 35:1899–906. doi: 10.1007/s13277-013-1255-4

82. Ashida R, Nakata B, Shigekawa M, Mizuno N, Sawaki A, Hirakawa K, et al. Gemcitabine sensitivity-related mRNA expression in endoscopic ultrasound-guided fine-needle aspiration biopsy of unresectable pancreatic cancer. *J Exp Clin Cancer Res* (2009) 28:83. doi: 10.1186/1756-9966-28-83

83. Duxbury MS, Ito H, Zinner MJ, Ashley SW, Whang EE. RNA Interference targeting the M2 subunit of ribonucleotide reductase enhances pancreatic adenocarcinoma chemosensitivity to gemcitabine. *Oncogene* (2004) 23:1539–48. doi: 10.1038/sj.onc.1207272

84. Santee SM, Owen-Schaub LB. Human tumor necrosis factor receptor p75/80 (CD120b) gene structure and promoter characterization. *J Biol Chem* (1996) 271:21151–9. doi: 10.1074/jbc.271.35.21151

85. Chen X, Oppenheim JJ. Targeting TNFR2, an immune checkpoint stimulator and oncoprotein, is a promising treatment for cancer. *Sci Signal* (2017) 10. doi: 10.1126/scisignal.aal2328

86. Alam MS, Otsuka S, Wong N, Abbasi A, Gaida MM, Fan Y, et al. TNF plays a crucial role in inflammation by signaling *via* T cell TNFR2. *Proc Natl Acad Sci U.S.A.* (2021) 118. doi: 10.1073/pnas.2109972118

87. Chen X, Bäumel M, Männel DN, Howard OMZ, Oppenheim JJ. Interaction of TNF with TNF receptor type 2 promotes expansion and function of mouse CD4+CD25+ T regulatory cells. *J Immunol* (2007) 179:154–61. doi: 10.4049/jimmunol.179.1.154

88. Govindaraj C, Tan P, Walker P, Wei A, Spencer A, Plebanski M. Reducing TNF receptor 2+ regulatory T cells *via* the combined action of azacitidine and the HDAC inhibitor, panobinostat for clinical benefit in acute myeloid leukemia patients. *Clin Cancer Res an Off J Am Assoc Cancer Res* (2014) 20:724–35. doi: 10.1158/1078-0432.CCR-13-1576

89. Yan F, Du R, Wei F, Zhao H, Yu J, Wang C, et al. Expression of TNFR2 by regulatory T cells in peripheral blood is correlated with clinical pathology of lung cancer patients. *Cancer Immunol Immunother* (2015) 64:1475–85. doi: 10.1007/s00262-015-1751-z

90. Sánchez-Álvarez M, Strippoli R, Donadelli M, Bazhin AV, Cordani M. Sestrins as a therapeutic bridge between ROS and autophagy in cancer. *Cancers (Basel)* (2019) 11. doi: 10.3390/cancers11101415

frontiers | Frontiers in Oncology

TYPE Mini Review
PUBLISHED 16 March 2023
DOI 10.3389/fonc.2023.1138759

OPEN ACCESS

EDITED BY
Jennifer M. Bailey-Lundberg,
University of Texas Health Science Center at Houston, United States

REVIEWED BY
Atul Kumar Ojha,
Indian Institute of Technology Kharagpur, India
Vinod Kumar Yata,
University of South Florida, United States
Julie Guillermet-Guibert,
U1037 Centre de Recherche en Cancérologie de Toulouse (INSERM), France

*CORRESPONDENCE
Erkut H. Borazanci
eborazanci@honorhealth.com

SPECIALTY SECTION
This article was submitted to Gastrointestinal Cancers: Hepato Pancreatic Biliary Cancers, a section of the journal Frontiers in Oncology

RECEIVED 06 January 2023
ACCEPTED 06 March 2023
PUBLISHED 16 March 2023

CITATION
Han MY and Borazanci EH (2023) Malignant ascites in pancreatic cancer: Pathophysiology, diagnosis, molecular characterization, and therapeutic strategies.
Front. Oncol. 13:1138759.
doi: 10.3389/fonc.2023.1138759

Malignant ascites in pancreatic cancer: Pathophysiology, diagnosis, molecular characterization, and therapeutic strategies

Margaret Y. Han[1] and Erkut H. Borazanci[2]*

[1]Department of Biosciences, Rice University, Houston, TX, United States, [2]Department of Oncology, HonorHealth Research Institute, Scottsdale, AZ, United States

Malignant ascites is the accumulation of fluid in the peritoneum as a result of advanced cancer and often signifies the terminal phase of the disease. Management of malignant ascites remains a clinical challenge as symptom palliation is the current standard of cure. Previously, studies examining malignant ascites largely focused on ovarian and gastric cancer. In recent years, there has been a significant increase in research on malignant ascites in pancreatic cancer. Malignant ascites is usually diagnosed based on positive cytology, but cytology is not always diagnostic, indicating the need for novel diagnostic tools and biomarkers. This review aims to summarize the current understanding of malignant ascites in pancreatic cancer and the recent advances in the molecular characterization of malignant ascites fluid from patients with pancreatic cancer including analysis of soluble molecules and extracellular vesicles. Current standard of care treatment options such as paracenteses and diuretics are outlined along with new emerging treatment strategies such as immunotherapy and small-molecule based therapies. New potential investigative directions resulting from these studies are also highlighted.

KEYWORDS

pancreatic cancer, malignant ascites, peritoneal carcinomatosis (PC), metastasis, chemotherapy, paracentesis

Introduction

Pancreatic cancer is a highly lethal disease with a 5-year survival rate of <11% (1). It is currently the third leading cause of cancer death in the United States and is projected to be the second by 2026 after lung cancer (2, 3). Pancreatic ductal adenocarcinoma (PDAC) which accounts for 90% of all pancreatic cancer cases is among the most lethal of all cancers (4). Surgical resection offers the only hope for cure for patients with PDAC but, unfortunately, is only applicable in 10-15% of patients. Prognosis remains very poor with a 5-year survival of < 1% for patients with advanced metastatic disease (5). One main

factor that contributes to the poor prognosis for patients with late stage PDAC is its resistance to chemotherapy and targeted therapies including immunotherapies. The current standard of care therapies such as FOLFIRNOX and gemcitabine plus nab-paclitaxel only extend patient survival by 2-6 months (6–8). One important factor that affects the quality of life and significantly reduces the survival of patients with PDAC is the development of malignant ascites (MA).

Malignant ascites (MA) is defined as the accumulation of fluid in the peritoneal cavity due to cancer that causes troublesome symptoms such as pain, loss of appetite, dyspnea, nausea, and reduced mobility (9). It accounts for approximately 10% of all ascites cases and is prevalent in ovarian, colorectal, pancreatic, gastric, and primary peritoneal cancers (10). Since MA is predominantly associated with ovarian cancer and breast cancer, there is a higher occurrence of MA in women compared to men (11). Around 20% of MA cases have an unknown primary tumor, and 50% of cases present with ascites at initial diagnosis (12). A retrospective study of 209 patients of 17 different cancer types finds that MA is associated with advanced stage or metastatic disease and is a poor prognostic sign with a reported patient survival of less than 6 months upon presentation (11).

While the onset of MA is associated with reduced quality of life and a poor prognosis, there remains no generally accepted evidence-based guidelines for treatment (13). Additionally, there are no preventive measures for MA development due to a lack of clinical predictors. With a wide range of symptoms including abdominal distension, impaired mobility and respiration, and swelling of limbs, MA requires prompt management focusing not only on symptomatic relief but reduction of disease and recurrence. As Saif et al. suggest, individualized treatment is the logical approach to treating patients with MA (13). However, the majority of MA treatments aim towards the palliation of symptoms as there are few effective therapeutic treatments. Thus, new biomarkers and therapeutic targets for more effectively treating patients with MA are urgently needed. This review describes the current state of the characterization and treatment of malignant ascites in PDAC patients while highlighting the recent advances in molecular profiling and novel therapeutics development to guide more effective and individualized treatment of MA beyond simple palliation of symptoms.

Pathophysiology and clinical manifestation of malignant ascites in PDAC

The pathophysiology of malignant ascites in PDAC and other cancers is complex and multifactorial and is yet to be completely understood. Our current understanding of the mechanism of MA formation mainly comes from studies in ovarian and other non-PDAC tumor types. The main physiological factor of MA development is the increased permeability of tumor vessels causing forced production and release of peritoneal fluid (14). Ascites fluid from patients with peritoneal carcinomatosis (PC) has a positive cytology with elevated protein concentration and low (<1.1 g/dL) serum-ascites albumin gradient (SAAG) (15). The elevated protein concentration indicates an alteration in vascular permeability allowing large molecules (i.e., proteins) to accumulate in the intraperitoneal space. This increased permeability has been shown to be caused by marked neovascularization of the parietal peritoneum and glycoprotein production (16). In a study by Garrison and colleagues using a rat breast cancer MA model, infusion of cell-free malignant ascites into the intraperitoneal space resulted in an increase in edema formation in omental vessels, indicating there exists a tumor-induced factor(s) in the fluid that alters vessel permeability and promotes the formation of MA (17). Furthermore, the levels of vascular endothelial growth factor (VEGF) which allows movement of molecules across the vascular endothelium in both normal physiological and pathological disease states were found to be elevated in MA compared to benign ascites and is believed to play an important role in altering vascular permeability and tumor growth (18). One other factor that contributes to the formation of MA is lymphatic obstruction (16). In healthy individuals, lymphatic drainage and differences in oncotic pressure allow for fluid reabsorption. In a mouse MA model for ovarian cancer, obstruction of lymphatic drainage was found to prevent peritoneal fluid absorption and lead to the formation of MA (19). In pancreatic cancer, portal hypertension (PH) induced by portal vein obstruction due to direct tumor invasion and extraluminal compression can also lead to the formation of ascites (20). Although ascites caused by PH can be cytology negative, in many cases they have a positive cytology with evidence of peritoneal carcinomatosis (21). Approximately 23% of ascites cases are associated with PH in pancreatic cancer, which is one of the highest cancer types studied (21). Overall, up to 30% of patients with PDAC develop MA (22).

The clinical manifestation of MA in patients with PDAC is similar to that of patients with other cancer types such as ovarian and gastric cancer. Despite this similarity, overall survival (OS) differs with MA of ovarian origin having better median survival than that of gastrointestinal (GI) origin including pancreatic cancer (11). One reason for this difference is because patients with GI cancers are more likely to have liver metastases which have been associated with significantly poor survival. Frequently reported symptoms in PDAC patients include abdominal distention/discomfort, shortness of breath, weight gain, nausea, and vomiting (23). In a study with 180 PDAC patients who presented/developed ascites, Hicks et al. reported a median overall survival of 1.8 months after ascites development (23). These results are supported by several studies with smaller cohort sizes. For instance, both Zervos et al. (24) and DeWitt et al. (25) reported a median OS of ~ 2 months after ascites development whereas Takahara et al. (22) reported an OS of 47 days regardless of the time of onset. In a case-control study, Baretti et al. confirmed that PDAC patients with ascites had a higher risk of death compared to patients without ascites (OS = 10.2 vs. 15.2 months, $P < 0.001$) (26). Alshuwaykh et al. found that patients with pancreatic cancer with evidence of PC had higher 1 and 5-year mortality rates compared to those without PC (68% vs. 33%, $p = 0.04$ and 57% vs. 17%, $p = 0.02$, respectively) (21).

Diagnosis of MA

In addition to malignancy, a number of other conditions can also cause the formation of ascites including cirrhosis, kidney failure, congestive heart failure, nephrosis, and pancreatitis. To differentiate benign ascites from malignant ascites, cellular and/or molecular analyses of the fluid are necessary as physical exams or radiographic techniques alone are not able to distinguish between the two. As noted above, malignant ascites fluid usually has a positive cytology with elevated protein concentrations and low SAAG (27). However, cytology is not diagnostic in some cases and SAAG can be insensitive and non-specific, which requires additional analyses to accurately diagnose MA in patients with PDAC. In a retrospective analysis of 62 patients with PDAC who presented or developed ascites during the course of their disease and had their ascites fluid analyzed only 36 (58%) had positive cytology and the majority (82%) of the patients had a SAAG ≥ 1 (23). This highlights one of the challenges in managing PDAC patients with ascites as multiple paracentesis may be necessary to confirm the presence of malignancy. To this end, Han et al. reported that mutations identified in tumor DNA isolated from ascites fluid from patients with ovarian cancer agree with those identified in the corresponding primary tumor tissues, which provides a potentially new tool for diagnosing malignant ascites (28). In addition, Li et al. report that combining cytological tests with telomerase activity assay significantly enhances the differential diagnosis between malignant and non-malignant ascites (29). Cytokines such as Interleukin 6 in ascites have also been found to have higher sensitivity and specificity as a diagnostic marker for ovarian cancer (30). These potential biomarkers have yet to be studied in PDAC and their utility in diagnosing MA in patients with PDAC needs future exploration.

Molecular characterization of malignant ascites in PDAC

To improve the outcome of PDAC patients with MA, new biomarkers and therapeutic targets are urgently needed for better diagnosis/monitoring of MA and development of more efficacious therapies. Recently, a number of molecular profiling studies aimed at examining the different contents of MA such as soluble molecules (proteins, DNA, and RNA), extracellular vesicles (EVs), and cells have provided new insights into the MA biology and present new opportunities for the development of new biomarkers and therapies (Figure 1).

Proteomic analysis of ascites from patients with advanced PDAC or patients with liver cirrhosis by Kitamura et al. revealed 18 malignant ascites-specific proteins. The most frequent were CD13, lymphatic vessel endothelial hyaluronan receptor 1, ficolin-3, and V-set and immunoglobulin domain containing 4 (31). Using high-resolution mass spectrometry Kosanam et al. also identified 816 proteins from MA samples of PDAC patients, 20 of which (membrane or extracellular proteins) were further selected as candidate biomarkers that warrant further validation (32). Detecting gene mutations that are commonly found in PDAC tumors in DNA or cells derived from ascites of PDAC patients has also been explored as a method for diagnosing MA. Using targeted next generation sequencing, Bae et al. found KRAS mutations in cells derived from 5 out of 6 pancreatic cancer MA samples, but none was detected in the 3 ascites samples with suspected malignancy by cytology analysis (tumor cells ≤ 2%) (33). Unfortunately, the KRAS mutational status in the primary tumors for those cases were not reported, hence the accuracy or sensitivity of the detection cannot be established. In an extensive KRAS mutation analysis using PCR amplification of DNA samples

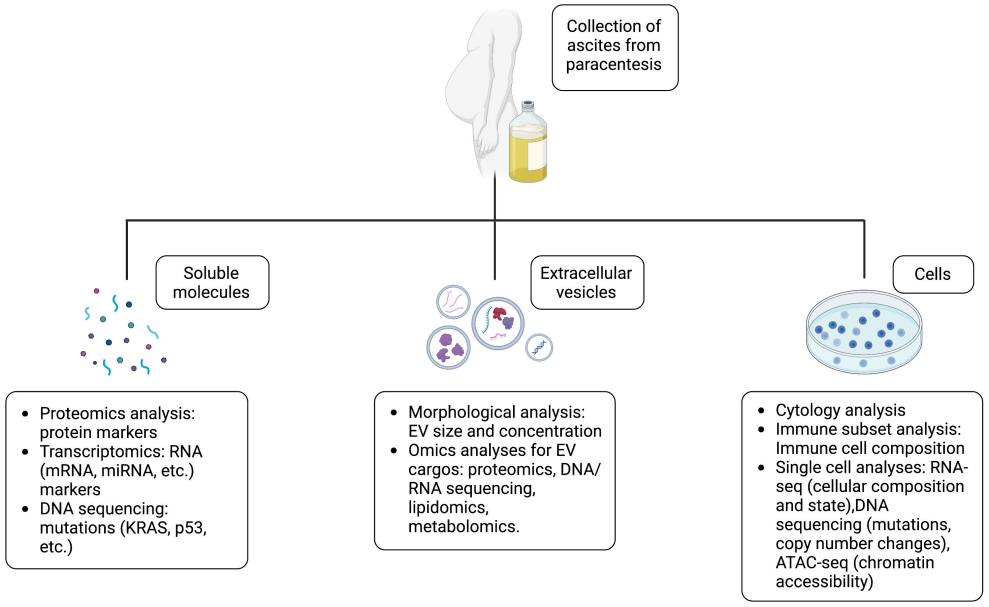

FIGURE 1
Molecular characterization of malignant ascites in PDAC.

isolated from supernatant (cell-free) and cells from ascites fluid as well as primary tumor tissues, Yamashita and colleagues detected KRAS point mutations in 8 out of 9 ascites supernatant samples from patients with pancreatic cancer including 2 cases of negative cytologic diagnosis (34). Direct sequencing also confirmed that the KRAS point mutations detected in the ascites supernatant were identical to those found in ascites cell pellets, microdissected malignant cells from cytologic smears, and primary tumor tissues (34). The proteins and mutations identified in these studies warrant investigation as biomarkers and therapeutic targets in PDAC.

One of the areas that attracted significant attention in the past few years is the characterization of EVs in MA to identify new therapeutic targets and biomarkers. EVs are membrane bound vesicles released into the extracellular space from the cell that contain bioactive molecules such as lipids, proteins, DNA, and RNA. They play important roles in tumor invasion, tumor progression regulation, and neovascularization. Recent studies have shown that EV cargos such as proteins, DNA, and miRNAs can be used as specific markers of PDAC by comparing expression between healthy controls and PDAC patients. For example, higher levels of serum exosomal c-Met and PD-L1 have been correlated with shorter postoperative survival time and thus are possible prognostic factors (35). There have been few studies concerning EVs from ascites fluid of patients with PDAC. Sakaue et al. reported that a higher glycosylation level of CD133 in EVs from ascites could indicate better prognosis for patients with advanced PDAC (36). Proteomic analysis reveals that membrane proteins, glycoproteins, and small GTP binding proteins are enriched in EVs released from PDAC cells and some of them (e.g., CD73) can be detected in EVs derived from MA of PDAC patients (37). Further characterization of EVs in PDAC MA is necessary to explore biomarker and treatment possibilities as done in other cancer types. For example, a phase 1 clinical trial found combining autologous EVs from ascites with granulocyte-macrophage colony stimulating factor to be a possible colorectal cancer treatment (38).

Current treatment options of malignant ascites in PDAC

Current standard of care for malignant ascites in patients with PDAC focuses solely on the palliation of symptoms (Table 1). Common therapies for managing MA include paracenteses and diuretics. While paracentesis is effective in relieving symptoms, it requires repeated treatment which depletes the patients of protein and electrolytes (9). Permanent drains such as the Pluerx and dialysis catheters have been developed to overcome the need of repeated paracentesis. While the permanent drains are an effective alternative to large volume paracentesis, they come with the risk of developing peritonitis, inflammation of the peritoneum due to infection (40). For patients with PDAC, paracentesis provided relief of symptoms in 93% of patients, but only with a mean effect duration of about 10 days (39). Peritoneovenous shunts have also been used to drain MA fluid, but is associated with complications such as shunt occlusion, ascitic leak, and pulmonary edema (57). While not as effective as paracentesis, diuretics such as spironolactone and furosemide have also benefited patients. However, when used in high doses, diuretics can cause systemic blood volume depletion and renal dysfunction (9).

For patients with PC more aggressive therapeutic approaches such as debulking surgery combined with chemotherapy administered at the end of surgery, known as hypothermic intraperitoneal chemotherapy (HIPEC), and pressurized intraperitoneal aerosol chemotherapy (PIPAC) in which diagnostic and staging laparoscopy is combined with an aerosolized drug administered using a high-pressure micro-injection pump have been used in treating MA (Table 1). A study employing laparoscopic HIPEC reported complete resolution of ascites in 94% of the 52 patients with PC (42). A Phase I trial of patients with peritoneal metastases of breast, ovarian, and gastrointestinal cancers including pancreatic cancer given PIPAC using nanoparticle albumin bound paclitaxel (NAB-PTX) demonstrated positive responses in 35% of patients with an overall one-year survival rate of 57% (43). Additionally, Frassini and colleagues compared the benefits of cytoreductive surgery combined with HIPEC, PIPAC, or normothermic intraperitoneal chemotherapy (NIPEC) in a meta-analysis of 212 PDAC patients with or without PC. The authors found that patients treated with HIPEC had a favorable 3-year survival rate of 24% compared to 5.3% and 7.9% for those treated with PIPAC and NIPEC, respectively (44).

There have been a handful of reports on small-molecule-based therapies for malignant ascites in patients with PDAC (Table 1). Shukuya et al. reported a decrease in ascites volume by 30% and an ascites control rate of 60% when patients were given paclitaxel weekly (Direct intravenous infusion for 1 hour) after failure of gemcitabine (45). Fan et al. reported in a retrospective study that treatment with intraperitoneal cisplatin and intravenous gemcitabine combined with regional hypothermia treatment was well tolerated by pancreatic cancer patients with MA with 13 out of 29 patients demonstrating a partial response and an overall survival of 195 days (46). In a Phase I/II clinical trial, Yamada et al. found that adding intraperitoneal paclitaxel to the standard of care intravenous nab-paclitaxel + gemcitabine led to the disappearance of ascites in 12 out of 30 PDAC patients with PC and a median overall survival of 14.5 months (47). Furthermore, patients who underwent conversion surgery did not reach median survival after 30 months follow-up. Adverse side effects observed include grade 3-4 neutropenia in 70% of the patients (47).

Therapeutic antibodies and proteins have also been explored as treatment options for MA. One example is the trifunctional monoclonal antibody catumaxomab administered by intraperitoneal infusions. Catumaxomab binds to epithelial tumor cells *via* the epithelial cell-adhesion molecule (EpCAM) and T-cells *via* CD3. It also activates Fcγ-receptor I-, IIa- and III-positive accessory cells through its functional Fc domain (58). In a randomized Phase II/III study in patients with epithelial cancers including pancreatic cancer, catumaxomab combined with paracentesis was found to lengthen puncture-free survival by 35 days compared to paracentesis alone (46 vs. 11 days, $P < 0.0001$) (48). Patients treated with the antibody also had fewer ascites signs and associated symptoms. Inhibiting the VEGF

TABLE 1 Treatment options and their outcomes for MA in patients with PDAC.

Treatment Type	Treatment	Treatment Outcome	References
Palliative Therapy	Paracentesis	Short term symptom relief, protein and electrolyte depletion	Smith et al. (39)
	Permanent drains (ex. Pleurx, dialysis catheters)	Technically successful, but many complications	Fleming et al. (40)
	Peritoneovenous shunts	Improvement of abdominal fullness, but postoperative complications significantly decreased overall survival	Tamagawa et al. (41)
Chemotherapy	Hypothermic intraperitoneal chemotherapy (HIPEC)	Resolution of ascites, increased overall survival rate	Valle et al. (42)
	Pressurized intraperitoneal aerosol chemotherapy (PIPAC) combined with nab-paclitaxel	Positive palliative responses, increase in overall survival rate	Ceelen et al. (43), Frassini et al. (44)
	Normothermic intraperitoneal chemotherapy (NIPEC)	Positive palliative responses	Frassini et al. (44)
	Paclitaxel	Decrease in ascites volume, increased control of ascites	Shukuya et al. (45)
	i.p. cisplatin + i.v. gemcitabine + regional hypothermia	Partial response in 13 out of 29 patients, OS of 195 days	Fan et al. (46)
	i.p. paclitaxel + i.v. nab-paclitaxel + i.v. gemcitabine	Increased overall survival, peritoneal recurrence in 75% of patients	Yamada et al. (47)
Targeted Therapy	Catumaxomab	Lengthened puncture-free survival by 35 days when combined with paracentesis	Heiss et al. (48)
	Apatnib/gemcitabine	Increased progression-free survival, no longer required paracentesis	Liang et al. (49)
	i.p. bevacizumab	Well tolerated, improved paracentesis-free survival (albeit, not statistically significant when compared to placebo)	Jordan et al. (50)
	NK4	Targets HGFR, suppressed ascites accumulation in an orthotopic mouse model	Tomoika et al. (51)
Immunotherapy	i.p. nivolumab	No longer required paracentesis, almost no cancer cells in ascites samples	Wang et al. (52)
	Concentrated ascites reinfusion therapy (CART)	Improved symptoms and allowed administration of chemotherapy. Increased levels of IL-12 and IFN-γ	Shirakawa et al. (53) Kobori et al. (54)
	NK cells + PD-1 inhibitor	Activation of multiple immune cell types and elimination of cancer cells	Chen et al. (55)
	i.p. oncolytic therapy	Positive ascites control in 8 of 13 patients	Zhang et al. (56)

i.p., intraperitoneal; i.v., intravenous; OS, overall survival; HGFR, hepatocyte growth factor receptor; NK cells, natural killer cells.

pathway may be beneficial in treating MA. In a case report of a 64-year-old PDAC patient given oral apatinib, which targets VEGF receptor 2, combined with intravenous gemcitabine, Liang et al. described that after 1 month of treatment, the patient no longer needed paracenteses and after 10.5 months of treatment, the patient achieved a progression-free survival for 11 months (49). The antiangiogenic antibody, bevacizumab, which targets the angiogenesis factor VEGF, has also been tested for treating MA in patients with pancreatic cancer. In a Phase II study of intraperitoneal bevacizumab for control of MA in gastrointestinal cancers of which the majority (56%) were patients with pancreatic cancer, Jordan et al. found that the treatment was well tolerated but did not result in statistically significant improvement in paracentesis-free survival compared to the placebo control (14.0 vs. 10.5 days, P = 0.16) (50).

In addition, immunotherapies have been investigated as potential treatment options. Wang et al. recently described a case in which a PDAC patient with MA responded to intraperitoneal nivolumab treatment after failed to respond to intraperitoneal paclitaxel. The amount of MA decreased significantly, and paracenteses was no longer needed after 7 doses (20 mg/dose) of intraperitoneal nivolumab with cancer cells barely detectable in the ascites fluid (52). Other immunotherapies such as cell-free and concentrated ascites reinfusion therapy (CART) have also shown promising results as therapy. Shirakawa et al. reported a positive response to CART in a patient with unresectable pancreatic cancer allowing her to have oral intake of chemotherapy (53). Additionally, cytokine expression profiling indicates that interferon-gamma (IFN-γ) and interleukin 12 levels increased in ascites after CART treatment, which may contribute to the growth inhibition of pancreatic cancer cells (54). This points to their potential as biomarkers for assessing clinical efficacy of CART procedures. Other novel immunotherapy regimens have also been investigated. Chen et al. report a case of combined autologous *ex vivo* expanded natural killer (NK) cells and programmed cell death 1 (PD-1) inhibitor therapy in a pancreatic cancer patient with peritoneal metastasis (55). Promising activity was observed with activation of multiple immune cell types and elimination of cancer cells in the ascites after treatment.

Several other novel approaches have also been explored for treating MA in patients with PDAC. Zhang and colleagues tested an oncolytic virotherapy H101 engineered to specifically target cancer

cells with aberrant p53 function in patients with GI cancers (56). Intraperitoneal treatment with H101 was found to induce intraperitoneal immune activation with an increase in both the number of $CD8^+$ cells and PD-1 expression in regulatory T cells in the ascites (56). Of the 13 pancreatic cancer patients who received H101, ascites response (>10% reduction in ascites volume) was observed in 5 patients (38.5%) and ascites control (<10% increase in ascites volume) in 8 patients (61.5%). In addition, NK4, an antagonistic peptide against the hepatocyte growth factor receptor, was found to suppress peritoneal dissemination and ascites accumulation in an orthotopic mouse model for PDAC (51). Given that the therapies described above were all only tested in a small number of patients, further studies are needed to validate their clinical efficacy.

Discussion

MA is an indicator of poor prognosis for patients with PDAC. Positive cytology with low SAAG and increased total protein concentration can be used to diagnose MA, but these methods are not always accurate or sufficiently sensitive. Cell-free ascites DNA analysis has been demonstrated to aid the diagnosis of malignant ascites (34). Current treatments for PDAC patients with ascites focus on palliation with the most common being paracenteses and diuretics. New therapies combining debulking surgery with intraperitoneal chemotherapy such as HIPEC, PIPAC, and NIPEC have shown promising activity in PDAC patients with MA (42, 43).

Biologics including catumaxomab and bevacizumab have demonstrated palliation in gastric and ovarian cancer patients with MA but data on their activity in PDAC patients are sparse. Some successes have also been reported for other therapeutic regimens such as apatinib combined with gemcitabine, intraperitoneal nivolumab, and intraperitoneal oncolytic virotherapy in small studies. Further validation of their clinical utility is needed.

Due to the very limited therapeutic options for treating MA in patients with PDAC, it is imperative to identify new therapeutic targets and biomarkers. Thus, specific analysis of ascites fluid is needed. Some molecular characteristics of ascites recently studied in PDAC including EV cargos are showing some promises. Additional studies focusing on EVs as a potential diagnostic tool and therapeutic target could be very fruitful in bringing about novel approaches for managing MA in patients with PDAC.

In recent years, single cell based genomic tools such as single cell RNA sequencing (scRNA-seq) have been widely used to characterize individual cells in tissues and body fluids such as blood, ascites, and spinal fluids. Several scRNA-seq studies have characterized the cells derived from MA of patients with ovarian, gastric, or colon cancers and revealed a plethora of information on their cellular composition and cell state which could help devise new approaches for the diagnosis and treatment of MA for these cancer types (59–62). For example, scRNA-seq of ascites fluid from gastric cancer revealed dynamic changes of the ascites ecosystem during gastric cancer peritoneal metastasis caused by chemotherapy and immunotherapy providing insight on possible differential treatment strategies (63). Systematic and well-designed single cell-based studies for MA from patients with PDAC are lacking at this point. Similarly, DNA sequencing of MA fluid in PDAC could also reveal differences in mutations between ascites and the primary tumor. Finally, molecular characterization of ascites fluid could also lead to discovery of predictive markers for MA in PDAC and consideration of possible preventive therapies. We believe that such studies could not only significantly help advance our understanding of the biology of MA in PDAC but also lead to new diagnostic markers and therapeutic strategies, potentially making a meaningful impact on the outcome of PDAC patients with MA.

Author contributions

Both authors designed the review. MH prepared the first draft of the manuscript. All authors contributed to the article and approved the submitted version.

Acknowledgments

Figure 1 was created with BioRender.com.

Conflict of interest

The authors declare that the research was conducted in the absence of any commercial or financial relationships that could be construed as a potential conflict of interest.

Publisher's note

References

1. Siegel RL, Miller KD, Fuchs HE, Jemal A. Cancer statistics, 2022. *CA Cancer J Clin* (2022) 72(1):7–33. doi: 10.3322/caac.21708

2. Rahib L, Smith BD, Aizenberg R, Rosenzweig AB, Fleshman JM, Matrisian LM. Projecting cancer incidence and deaths to 2030: the unexpected burden of thyroid,

liver, and pancreas cancers in the united states. *Cancer Res* (2014) 74(11):2913–21. doi: 10.1158/0008-5472.CAN-14-0155

3. Rahib L, Wehner MR, Matrisian LM, Nead KT. Estimated projection of US cancer incidence and death to 2040. *JAMA Netw Open* (2021) 4(4):e214708. doi: 10.1001/jamanetworkopen.2021.4708

4. Hidalgo M. Pancreatic cancer. *N Engl J Med* (2010) 362(17):1605–17. doi: 10.1056/NEJMra0901557

5. Bengtsson A, Andersson R, Ansari D. The actual 5-year survivors of pancreatic ductal adenocarcinoma based on real-world data. *Sci Rep* (2020) 10(1):16425. doi: 10.1038/s41598-020-73525-y

6. Park W, Chawla A, O'Reilly EM. Pancreatic cancer: A review. *JAMA* (2021) 326 (9):851–62. doi: 10.1001/jama.2021.13027

7. Von Hoff DD, Ervin T, Arena FP, Chiorean EG, Infante J, Moore M, et al. Increased survival in pancreatic cancer with nab-paclitaxel plus gemcitabine. *N Engl J Med* (2013) 369(18):1691–703. doi: 10.1056/NEJMoa1304369

8. Conroy T, Desseigne F, Ychou M, Bouche O, Guimbaud R, Becouarn Y, et al. FOLFIRINOX versus gemcitabine for metastatic pancreatic cancer. *N Engl J Med* (2011) 364(19):1817–25. doi: 10.1056/NEJMoa1011923

9. Sangisetty SL, Miner TJ. Malignant ascites: A review of prognostic factors, pathophysiology and therapeutic measures. *World J Gastrointest Surg* (2012) 4 (4):87–95. doi: 10.4240/wjgs.v4.i4.87

10. Runyon BA. Malignancy-related ascites and ascitic fluid "humoral tests of malignancy". *J Clin Gastroenterol* (1994) 18(2):94–8. doi: 10.1097/00004836-199403000-00002

11. Ayantunde AA, Parsons SL. Pattern and prognostic factors in patients with malignant ascites: a retrospective study. *Ann Oncol* (2007) 18(5):945–9. doi: 10.1093/annonc/mdl499

12. Parsons SL, Lang MW, Steele RJ. Malignant ascites: a 2-year review from a teaching hospital. *Eur J Surg Oncol* (1996) 22(3):237–9. doi: 10.1016/S0748-7983(96)80009-6

13. Saif MW, Siddiqui IA, Sohail MA. Management of ascites due to gastrointestinal malignancy. *Ann Saudi Med* (2009) 29(5):369–77. doi: 10.4103/0256-4947.55167

14. Cavazzoni E, Bugiantella W, Graziosi L, Franceschini MS, Donini A. Malignant ascites: pathophysiology and treatment. *Int J Clin Oncol* (2013) 18(1):1–9. doi: 10.1007/s10147-012-0396-6

15. Runyon BA, Hoefs JC, Morgan TR. Ascitic fluid analysis in malignancy-related ascites. *Hepatology* (1988) 8(5):1104–9. doi: 10.1002/hep.1840080521

16. Adam RA, Adam YG. Malignant ascites: past, present, and future. *J Am Coll Surg* (2004) 198(6):999–1011. doi: 10.1016/j.jamcollsurg.2004.01.035

17. Garrison RN, Kaelin LD, Galloway RH, Heuser LS. Malignant ascites. clinical and experimental observations. *Ann Surg* (1986) 203(6):644–51. doi: 10.1097/00000658-198606000-00009

18. Zebrowski BK, Liu W, Ramirez K, Akagi Y, Mills GB, Ellis LM. Markedly elevated levels of vascular endothelial growth factor in malignant ascites. *Ann Surg Oncol* (1999) 6(4):373–8. doi: 10.1007/s10434-999-0373-0

19. Feldman GB, Knapp RC, Order SE, Hellman S. The role of lymphatic obstruction in the formation of ascites in a murine ovarian carcinoma. *Cancer Res* (1972) 32(8):1663–6.

20. Klose J, Ronellenfitsch U, Kleeff J. Management problems in patients with pancreatic cancer from a surgeon's perspective. *Semin Oncol* (2021) 48(1):76–83. doi: 10.1053/j.seminoncol.2021.02.008

21. Alshuwaykh O, Cheung A, Goel A, Kwong A, Dhanasekaran R, Ghaziani TT, et al. Clinical characteristics and outcomes in those with primary extrahepatic malignancy and malignant ascites. *BMC Gastroenterol* (2022) 22(1):410. doi: 10.1186/s12876-022-02487-4

22. Takahara N, Isayama H, Nakai Y, Sasaki T, Saito K, Hamada T, et al. Pancreatic cancer with malignant ascites: clinical features and outcomes. *Pancreas* (2015) 44 (3):380–5. doi: 10.1097/MPA.0000000000000290

23. Hicks AM, Chou J, Capanu M, Lowery MA, Yu KH, O'Reilly EM. Pancreas adenocarcinoma: Ascites, clinical manifestations, and management implications. *Clin Colorectal Cancer.* (2016) 15(4):360–8. doi: 10.1016/j.clcc.2016.04.014

24. Zervos EE, Osborne D, Boe BA, Luzardo G, Goldin SB, Rosemurgy AS. Prognostic significance of new onset ascites in patients with pancreatic cancer. *World J Surg Oncol* (2006) 4:16. doi: 10.1186/1477-7819-4-16

25. DeWitt J, Yu M, Al-Haddad MA, Sherman S, McHenry L, Leblanc JK. Survival in patients with pancreatic cancer after the diagnosis of malignant ascites or liver metastases by EUS-FNA. *Gastrointest Endosc.* (2010) 71(2):260–5. doi: 10.1016/j.gie.2009.08.025

26. Baretti M, Pulluri B, Tsai HL, Blackford AL, Wolfgang CL, Laheru D, et al. The significance of ascites in patients with pancreatic ductal adenocarcinoma: A case-control study. *Pancreas* (2019) 48(4):585–9. doi: 10.1097/MPA.0000000000001262

27. Nagy JA, Herzberg KT, Dvorak JM, Dvorak HF. Pathogenesis of malignant ascites formation: initiating events that lead to fluid accumulation. *Cancer Res* (1993) 53(11):2631–43.

28. Han MR, Lee SH, Park JY, Hong H, Ho JY, Hur SY, et al. Clinical implications of circulating tumor DNA from ascites and serial plasma in ovarian cancer. *Cancer Res Treat* (2020) 52(3):779–88. doi: 10.4143/crt.2019.700

29. Li CP, Huang TS, Chao Y, Chang FY, Whang-Peng J, Lee SD. Advantages of assaying telomerase activity in ascites for diagnosis of digestive tract malignancies. *World J Gastroenterol* (2004) 10(17):2468–71. doi: 10.3748/wjg.v10.i17.2468

30. Amer H, Kartikasari AER, Plebanski M. Elevated interleukin-6 levels in the circulation and peritoneal fluid of patients with ovarian cancer as a potential diagnostic biomarker: A systematic review and meta-analysis. *J Pers Med* (2021) 11(12):1335. doi: 10.3390/jpm11121335

31. Kitamura F, Miyata T, Uemura N, Uchihara T, Imai K, Hayashi H, et al. Proteomic analysis of malignant ascites from patients with pancreatic ductal adenocarcinoma. *Anticancer Res* (2021) 41(6):2895–900. doi: 10.21873/anticanres.15071

32. Kosanam H, Makawita S, Judd B, Newman A, Diamandis EP. Mining the malignant ascites proteome for pancreatic cancer biomarkers. *Proteomics* (2011) 11 (23):4551–8. doi: 10.1002/pmic.201100264

33. Bae GE, Kim SH, Choi MK, Kim JM, Yeo MK. Targeted sequencing of ascites and peritoneal washing fluid of patients with gastrointestinal cancers and their clinical applications and limitations. *Front Oncol* (2021) 11:712754. doi: 10.3389/fonc.2021.712754

34. Yamashita K, Kuba T, Shinoda H, Takahashi E, Okayasu I. Detection of K-ras point mutations in the supernatants of peritoneal and pleural effusions for diagnosis complementary to cytologic examination. *Am J Clin Pathol* (1998) 109(6):704–11. doi: 10.1093/ajcp/109.6.704

35. Lux A, Kahlert C, Grutzmann R, Pilarsky C. C-met and PD-L1 on circulating exosomes as diagnostic and prognostic markers for pancreatic cancer. *Int J Mol Sci* (2019) 20(13):3305. doi: 10.3390/ijms20133305

36. Sakaue T, Koga H, Iwamoto H, Nakamura T, Ikezono Y, Abe M, et al. Glycosylation of ascites-derived exosomal CD133: a potential prognostic biomarker in patients with advanced pancreatic cancer. *Med Mol Morphol.* (2019) 52(4):198–208. doi: 10.1007/s00795-019-00218-5

37. Klein-Scory S, Tehrani MM, Eilert-Micus C, Adamczyk KA, Wojtalewicz N, Schnolzer M, et al. New insights in the composition of extracellular vesicles from pancreatic cancer cells: implications for biomarkers and functions. *Proteome Sci* (2014) 12(1):50. doi: 10.1186/s12953-014-0050-5

38. Dai S, Wei D, Wu Z, Zhou X, Wei X, Huang H, et al. Phase I clinical trial of autologous ascites-derived exosomes combined with GM-CSF for colorectal cancer. *Mol Ther* (2008) 16(4):782–90. doi: 10.1038/mt.2008.1

39. Smith EM, Jayson GC. The current and future management of malignant ascites. *Clin Oncol (R Coll Radiol).* (2003) 15(2):59–72. doi: 10.1053/clon.2002.0135

40. Fleming ND, Alvarez-Secord A, Von Gruenigen V, Miller MJ, Abernethy AP. Indwelling catheters for the management of refractory malignant ascites: a systematic literature overview and retrospective chart review. *J Pain Symptom Manage* (2009) 38 (3):341–9. doi: 10.1016/j.jpainsymman.2008.09.008

41. Tamagawa H, Aoyama T, Inoue H, Fujikawa H, Sawazaki S, Numata M, et al. Therapeutic results of Denver percutaneous peritoneovenous shunt in cancer patients with malignant ascites. *J Cancer Res Ther* (2020) 16(Supplement):S95–S8. doi: 10.4103/jcrt.JCRT_606_18

42. Valle SJ, Alzahrani NA, Liauw W, Sugarbaker PH, Bhatt A, Morris DL. Hyperthermic intraperitoneal chemotherapy (HIPEC) methodology, drugs and bidirectional chemotherapy. *Indian J Surg Oncol* (2016) 7(2):152–9. doi: 10.1007/s13193-016-0498-0

43. Ceelen W, Sandra L, de Sande LV, Graversen M, Mortensen MB, Vermeulen A, et al. Phase I study of intraperitoneal aerosolized nanoparticle albumin based paclitaxel (NAB-PTX) for unresectable peritoneal metastases. *EBioMedicine* (2022) 82:104151. doi: 10.1016/j.ebiom.2022.104151

44. Frassini S, Calabretto F, Granieri S, Fugazzola P, Vigano J, Fazzini N, et al. Intraperitoneal chemotherapy in the management of pancreatic adenocarcinoma: A systematic review and meta-analysis. *Eur J Surg Oncol* (2022) 48(9):1911–21. doi: 10.1016/j.ejso.2022.05.030

45. Shukuya T, Yasui H, Boku N, Onozawa Y, Fukutomi A, Yamazaki K, et al. Weekly paclitaxel after failure of gemcitabine in pancreatic cancer patients with malignant ascites: a retrospective study. *Jpn J Clin Oncol* (2010) 40(12):1135–8. doi: 10.1093/jjco/hyq117

46. Fan YF, Qin Y, Li DG, Kerr D. Retrospective clinical study of advanced pancreatic cancer treated with chemotherapy and abdominal hyperthermia. *J Glob Oncol* (2018) 4:1–4. doi: 10.1200/JGO.2017.009985

47. Yamada S, Fujii T, Yamamoto T, Takami H, Yoshioka I, Yamaki S, et al. Phase I/II study of adding intraperitoneal paclitaxel in patients with pancreatic cancer and peritoneal metastasis. *Br J Surg* (2020) 107(13):1811–7. doi: 10.1002/bjs.11792

48. Heiss MM, Murawa P, Koralewski P, Kutarska E, Kolesnik OO, Ivanchenko VV, et al. The trifunctional antibody catumaxomab for the treatment of malignant ascites due to epithelial cancer: Results of a prospective randomized phase II/III trial. *Int J Cancer.* (2010) 127(9):2209–21. doi: 10.1002/ijc.25423

49. Liang L, Wang L, Zhu P, Xia Y, Qiao Y, Hui K, et al. Apatinib concurrent gemcitabine for controlling malignant ascites in advanced pancreatic cancer patient: A case report. *Med (Baltimore).* (2017) 96(47):e8725. doi: 10.1097/MD.0000000000008725

50. Jordan K, Luetkens T, Gog C, Killing B, Arnold D, Hinke A, et al. Intraperitoneal bevacizumab for control of malignant ascites due to advanced-stage gastrointestinal

cancers: A multicentre double-blind, placebo-controlled phase II study - AIO SUP-0108. *Eur J Cancer.* (2016) 63:127–34. doi: 10.1016/j.ejca.2016.05.004

51. Tomioka D, Maehara N, Kuba K, Mizumoto K, Tanaka M, Matsumoto K, et al. Inhibition of growth, invasion, and metastasis of human pancreatic carcinoma cells by NK4 in an orthotopic mouse model. *Cancer Res* (2001) 61(20):7518–24.

52. Wang ST, Chiu CF, Bai HJ, Bai LY. Intraperitoneal nivolumab in a patient with pancreatic cancer and refractory malignant ascites. *Eur J Cancer.* (2021) 148:48–50. doi: 10.1016/j.ejca.2021.01.045

53. Shirakawa K, Hirahara S, Kubota H, Kuhara Y, Toyota K, Yano R, et al. [A case of unresectable pancreatic cancer with massive cancerous ascites responsive to KM-CART]. *Gan to Kagaku Ryoho.* (2021) 48(1):81–3.

54. Kobori T, Tanaka C, Urashima Y, Takagaki N, Obata T. [IFN-gamma and IL-12 from concentrated ascites in patients with pancreatic cancer exerts growth inhibitory effects against pancreatic cancer cells]. *Yakugaku Zasshi.* (2022) 142(12):1409–17. doi: 10.1248/yakushi.22-00150

55. Chen L, Qian Y, Guo M, Liu Y, Li J, Wu M, et al. Autologous ex vivo expanded NK cells combined with PD-1 inhibitor improved ascitic fluid immune microenvironment of peritoneal metastatic pancreatic cancer: a case study. *Am J Transl Res* (2023) 15(1):316–23.

56. Zhang Y, Qian L, Chen K, Gu S, Wang J, Meng Z, et al. Intraperitoneal oncolytic virotherapy for patients with malignant ascites: Characterization of clinical efficacy and antitumor immune response. *Mol Ther Oncolytics.* (2022) 25:31–42. doi: 10.1016/j.omto.2022.03.003

57. Yarmohammadi H, Getrajdman GI. Symptomatic fluid drainage: Peritoneovenous shunt placement. *Semin Intervent Radiol* (2017) 34(4):343–8. doi: 10.1055/s-0037-1608705

58. Zeidler R, Mysliwietz J, Csanady M, Walz A, Ziegler I, Schmitt B, et al. The fc-region of a new class of intact bispecific antibody mediates activation of accessory cells and NK cells and induces direct phagocytosis of tumour cells. *Br J Cancer.* (2000) 83 (2):261–6. doi: 10.1054/bjoc.2000.1237

59. Wang R, Dang M, Harada K, Han G, Wang F, Pool Pizzi M, et al. Single-cell dissection of intratumoral heterogeneity and lineage diversity in metastatic gastric adenocarcinoma. *Nat Med* (2021) 27(1):141–51. doi: 10.1038/s41591-020-1125-8

60. Eum HH, Kwon M, Ryu D, Jo A, Chung W, Kim N, et al. Tumor-promoting macrophages prevail in malignant ascites of advanced gastric cancer. *Exp Mol Med* (2020) 52(12):1976–88. doi: 10.1038/s12276-020-00538-y

61. Izar B, Tirosh I, Stover EH, Wakiro I, Cuoco MS, Alter I, et al. A single-cell landscape of high-grade serous ovarian cancer. *Nat Med* (2020) 26(8):1271–9. doi: 10.1038/s41591-020-0926-0

62. Poonpanichakul T, Shiao MS, Jiravejchakul N, Matangkasombut P, Sirachainan E, Charoensawan V, et al. Capturing tumour heterogeneity in pre- and post-chemotherapy colorectal cancer ascites-derived cells using single-cell RNA-sequencing. *Biosci Rep* (2021) 41(12):BSR20212093. doi: 10.1042/BSR20212093

63. Huang XZ, Pang MJ, Li JY, Chen HY, Sun JX, Song YX, et al. Single-cell sequencing of ascites fluid illustrates heterogeneity and therapy-induced evolution during gastric cancer peritoneal metastasis. *Nat Commun* (2023) 14(1):822. doi: 10.1038/s41467-023-36310-9

frontiers | Frontiers in Oncology

TYPE Original Research
PUBLISHED 21 September 2023
DOI 10.3389/fonc.2023.1251258

OPEN ACCESS

EDITED BY
Yan-Shen Shan,
National Cheng Kung University Hospital, Taiwan

REVIEWED BY
Irene Hernandez,
Complejo Hospitalario de Navarra, Spain
Li Zhang,
University of Minnesota Twin Cities, United States

*CORRESPONDENCE
Liu Yang
yangliu@hmc.edu.cn
Zhe-Ling Chen
chenzheling@hmc.edu.cn

†These authors have contributed equally to this work

RECEIVED 01 July 2023
ACCEPTED 05 September 2023
PUBLISHED 21 September 2023

CITATION
Lu H-R, Zhu P-F, Deng Y-Y, Chen Z-L and Yang L (2023) Third-line treatment options in metastatic pancreatic cancer patients: a real-world study. *Front. Oncol.* 13:1251258. doi: 10.3389/fonc.2023.1251258

Third-line treatment options in metastatic pancreatic cancer patients: a real-world study

Hong-Rui Lu[1,2†], Peng-Fei Zhu[1,2†], Ya-Ya Deng[2,3], Zhe-Ling Chen[2*] and Liu Yang[1,2*]

[1]Graduate School of Clinical Medicine, Bengbu Medical College, Bengbu, Anhui, China, [2]Cancer Center, Department of Medical Oncology, Zhejiang Provincial People's Hospital, Affiliated People's Hospital, Hangzhou Medical College, Hangzhou, Zhejiang, China, [3]The Qingdao University Medical College, Qingdao, Shandong, China

Background: There are currently no standard therapy regimens for the third-line treatment of metastatic pancreatic cancer (mPC) patients. The aim of the present study was to compare the efficacy and safety of different third-line therapy regimens for mPC in the real-world.

Methods: This study retrospectively analyzed mPC patients admitted to Zhejiang Provincial People's Hospital between June 2013 and January 2023. All patients' diagnoses were pathologically confirmed and their treatment was continued after the second-line therapy failed. The primary study endpoints included median overall survival (mOS), median progression-free survival (mPFS), and disease control rate (DCR).

Results: A total of 72 patients were enrolled in the study. Of these, 36 patients received chemotherapy alone, 16 received chemotherapy combined with targeted therapy or immunotherapy, 14 received chemotherapy-free antitumor therapy, and six received palliative care. The mPFS value for these groups was 4.40 months, 5.20 months, 2.33 months, and 0.80 months, respectively. The mOS value was 6.90 months, 5.90 months, 3.33 months, and 0.80 months, respectively. The DCR was 33.4%, 31.3%, 21.4%, and 0.0%, respectively. Overall, there were significant differences in prognosis between the palliative care group and the other treatment groups (mOS, $P < 0.001$; mPFS $P < 0.001$; DCR, $P < 0.001$). The differences among the mPFS, mOS, and DCR for different antitumor therapy regimens were not statistically significant. Compared to the chemotherapy alone group, the chemotherapy combined with targeted therapy or immunotherapy group experienced more adverse events (100% vs. 75.0%; $P = 0.002$). Chemotherapy combined with targeted therapy or immunotherapy was associated with a higher risk of grade 3/4 hyperaminotransferemia compared to chemotherapy alone (31.3% vs. 0.0%; $P = 0.020$) and chemotherapy-free antitumor therapy (31.3% vs. 0.0%; $P = 0.020$).

Conclusions: Third-line antitumor therapy can prolong the survival time of patients with mPC. Targeted therapy or immunotherapy failed to further improve survival benefits based on chemotherapy results. Patients who underwent the third-line treatment with good physical status and family history of cancer were independent prognostic factors for longer mOS. The sequencing of fluorouracil and gemcitabine in the front-line therapy did not affect third-line mOS.

KEYWORDS

chemotherapy, immunotherapy, pancreatic cancer, targeted therapy, third-line treatment

1 Introduction

Pancreatic cancer (PC) is a highly aggressive tumor. Its five-year survival rate is 5%–10%, and life expectancy at diagnosis is less than 5 months (1). PC is the fourth leading cause of cancer death in the United States and the sixth in China (2, 3). Since PC occurs deep in the abdomen behind the stomach and in front of the spine, it does not cause obvious symptoms in its early stages. About 50% of patients develop metastases at initial diagnosis, which is a major factor in poor outcomes (4). Among all patients receiving first-line chemotherapy for PC, 57% went on to receive second-line therapy and 22% received third-line therapy (5).

Systemic therapy for locally advanced or metastatic disease has been documented in the National Comprehensive Cancer Network guidelines (6). FOLFIRINOX (category 1) and AG (category 1) are listed as the preferred recommended first-line chemotherapy treatments for patients in good physical condition, while gemcitabine monotherapy is recommended for patients in poor physical condition with metastatic PC (mPC) (7, 8). Almost all PC patients progress within a few months during or after first-line chemotherapy (9). Fluoropyrimidine-based regimen is the recommended subsequent treatment option for patients with a good performance status and those previously treated with gemcitabine-based therapy. Gemcitabine-based regimen is advised for patients with a good performance status and those previously treated with fluoropyrimidine-based therapy. Gemcitabine (category 1), capecitabine, and 5-fluoropyrimidine are suggested for patients with a poor performance status (10, 11). Pembrolizumab is used in an advanced disease setting as the first-line and subsequent treatment for PC patients with high microsatellite instability and mismatch repair-deficiency (12). Larotrectinib or entrectinib can be considered for *NTRK* gene fusion-positive diseases (13, 14).

Unfortunately, most patients face the challenges of tumor progression, chemotherapy resistance, and toxic effects after receiving second-line chemotherapy. Chemotherapy remains the standard of care for advanced disease. Research into novel therapies is ongoing and includes immunotherapy, targeted therapy, vaccines, and oncolytic viruses. Although most PC patients have gene mutations, there are few approved targeted therapies. New antitumor drugs for various targets are currently being developed and tested (15). PC is considered to be a 'cold tumor' in immunotherapy due to its typical bone marrow cell infiltration, lack of CD8+ T cells, and low activation markers. Except for 1% of patients with high microsatellite instability, PC is almost completely unsuitable for immunotherapy (16). According to the national guidelines for diagnosis and treatment of PC in China in 2022, continuing chemotherapy for PC patients who failed to respond to second-line chemotherapy is controversial, and there are no clear chemotherapy regimens to recommend (17). However, chemotherapy is still the most common choice for the third-line treatment in PC patients. There are only a handful of third-line chemotherapy drugs available, and many doctors choose to implement chemotherapy re-challenge programs for these patients (18). The efficacy and safety of various third-line treatments in PC patients are still awaiting confirmation, and clinical predictors for third-line treatment option selection are still lacking.

A considerable number of patients still have sufficient physical strength to receive antitumor therapy when the disease progresses to the third-line stage. The present study aimed to compare the efficacy and safety of different third-line therapies for mPC. The efficacy, safety, and relevance of various combinations of third-line antitumor therapies, including chemotherapy, targeted therapy, and immunotherapy, were explored in order to investigate the status of third-line therapy in mPC.

Abbreviations: BMI, Body Mass Index; DCR, Disease control rate; ECOG PS, Eastern Cooperative Oncology Group Performance status; F-based, Fluorouracil based treatment; G-based, Gemcitabine based therapy; MLR, Monocyte to lymphocyte ratio; mOS, Median overall survival; mPC, Metastatic pancreatic cancer; mPFS, Median progression-free survival; NLR, Neutrophil to lymphocyte ratio; PLR, Platelet to lymphocyte ratio.

2 Patients and methods

2.1 Patients

We analyzed 72 patients with mPC who received third-line therapy and were admitted to Zhejiang Provincial People's Hospital

between June 2013 and January 2023. Clinical patient staging was performed according to the American Joint Committee on Cancer guidelines. All procedures were carried out in accordance with the ethical standards of the Committee on Human Experimentation (institutional and national) and the Declaration of Helsinki. The study was approved by the Ethics Committee of Zhejiang Provincial People's Hospital.

2.2 Therapy schedule

The common chemotherapy regimens for third-line treatment are FOLFIRINOX (oxaliplatin 85 mg/m^2, irinotecan 150 mg/m^2, leucovorin 400 mg/m^2, and 5-fluorouracil 2400 mg/m^2 administered every two weeks), FOLFIRI (irinotecan 180 mg/m^2, leucovorin 400 mg/m^2, and 5-fluorouracil 2400 mg/m^2 administered every two weeks), AG (albumin-bound paclitaxel 125 mg/m^2 on days 1 and 8 and gemcitabine 1,000 mg/m^2 on days 1 and 8 administered every three weeks), GS (gemcitabine 1,000 mg/m^2 on days 1 and 8 and S-1 60 mg twice daily on days 1–14 administered every three weeks), CapeOX (oxaliplatin 135 mg/m^2 and capecitabine 1000 mg twice daily on days 1–14 administered every three weeks), GX (gemcitabine 1,000 mg/m^2 on days 1 and 8 and capecitabine 830 mg twice daily on days 1–14 administered every three weeks), AS (albumin-bound paclitaxel 125 mg/m^2 on days 1 and 8 and S-1 60 mg twice daily on days 1–14 administered every three weeks), gemcitabine (gemcitabine 1,000 mg/m^2 on days 1 and 8 administered every three weeks), and S-1 (S-1 60 mg twice daily on days 1–14 administered every three weeks). Pembrolizumab (200 mg administered every three weeks) is a common programmed cell death protein 1 for third-line treatment. Apatinib (500 mg administered every day) is a common targeted drug. Clinicians adjusted the drug dose according to the patient's adverse events (AEs) experienced during therapy.

2.3 Assessment

The tumor response was evaluated based on the revised Response Evaluation Criteria in Solid Tumors (version 1.1) using computed tomography and magnetic resonance imaging every 2–3 treatment cycles. The AEs were evaluated according to the Common Terminology Criteria for Adverse Events (version 5.0).

2.4 Statistical analyses

The median overall survival (mOS) and median progression-free survival (mPFS) rates were the primary endpoints. The disease control rate (DCR) and AEs were the secondary endpoints. All of the statistical analyses were performed using IBM SPSS Statistics software version 26.0 (IBM Corp., Grouponk, NY, NY, USA). Kaplan–Meier method was used to analyze the OS and PFS. Cox proportional regression model was used to analyze the survival and prognosis. Significant factors ($P < 0.1$) identified using univariate Cox regression analysis were included in multivariate Cox regression analysis. T-test was used for AE comparison between groups.

3 Results

3.1 Efficacy and survival analysis of third-line treatment

3.1.1 Clinical factors for patients

Baseline characteristics of mPC patients who received the third-line treatment are shown in Table 1. A total of 72 patients were enrolled in the study, of which 36 received chemotherapy alone, 16 received chemotherapy combined with targeted therapy or immunotherapy, 14 received chemotherapy-free antitumor therapy, and six received palliative treatment. Patient characteristics were not balanced between each group, including the baseline of Eastern Cooperative Oncology Group Performance status (ECOG PS), first-line treatment, and second-line treatment.

3.1.2 Efficacy

The mOS values for the chemotherapy alone, chemotherapy combined with targeted therapy or immunotherapy, chemotherapy-free antitumor therapy, and palliative treatment groups were 6.9 months (95% confidence interval (CI), 0.5–13.9 months), 5.9 months (95% CI, 1.6–10.2 months), 3.3 months (95% CI, 0.2–5.0 months), and 0.8 months (95% CI, 0.1–1.5 months), respectively. The mPFS values were 4.4 months (95% CI, 1.8–7.0 months), 5.2 months (95% CI, 2.7–7.7 months), 2.3 months (95% CI, 0.3–4.6 months), and 0.8 months (95% CI, 0.1–1.5 months), respectively. Kaplan–Meier analysis showed that the mOS and mPFS values in mPC patients who received chemotherapy alone ($P < 0.001$; $P < 0.001$), chemotherapy combined with targeted therapy or immunotherapy ($P < 0.001$; $P < 0.001$), and chemotherapy-free antitumor therapy ($P < 0.001$; $P < 0.001$) were greater than those in patients who received palliative treatment. There was no statistical difference in mOS and mPFS between groups of mPC patients who received antitumor therapy, chemotherapy alone, and chemotherapy combined with targeted therapy or immunotherapy ($P = 0.588$; $P = 0.783$), chemotherapy alone and chemotherapy-free antitumor therapy ($P = 0.061$; $P = 0.189$), chemotherapy combined with targeted therapy or immunotherapy and chemotherapy-free antitumor therapy ($P = 0.265$; $P = 0.154$; Figure 1).

The DCRs for the chemotherapy alone, chemotherapy combined with targeted therapy or immunotherapy, chemotherapy-free antitumor therapy, and palliative treatment groups were 33.4%, 31.3%, 21.4%, and 0.0%, respectively. The DCRs for mPC patients who received chemotherapy alone ($P < 0.001$), chemotherapy combined with targeted therapy or immunotherapy ($P < 0.001$), and chemotherapy-free antitumor therapy ($P < 0.001$) were higher than those for patients who received palliative treatment. There was no statistical difference in DCRs between mPC patients who received antitumor therapy, chemotherapy alone, and chemotherapy combined with targeted therapy or immunotherapy ($P = 0.565$), chemotherapy alone and chemotherapy-free antitumor therapy ($P > 0.999$), chemotherapy combined with targeted therapy or immunotherapy and chemotherapy-free antitumor therapy ($P > 0.999$; Table 2).

10.3389/fonc.2023.1251258

TABLE 1 Patient baseline characteristics of third-line treatment.

Variables	Chemotherapy alone		Chemotherapy combined with targeted or immunotherapy		Chemotherapy-free antitumor therapy		Alleviative treatment		total		p value
	(n=36)		(n=16)		(n=14)		(n=6)		(n=72)		
	No.	%	No.	%	No.	%	No.	%	No.	%	
Sex											0.247
Male	24	66.7	7	43.8	11	78.6	4	66.7	46	63.9	
Female	12	33.3	9	56.2	3	21.4	2	33.3	26	36.1	
Median age (range)	61.75±7.632		62.38±9.959		64.00±10.627		60.00±13.023		62.18±9.135		0.861
BMI											0.830
thin	4	11.1	3	18.8	2	14.3	2	33.3	11	15.3	
healthy	30	83.3	12	75.0	11	78.6	4	66.7	57	79.2	
overweight	1	2.8	1	6.2	1	7.1	0	0.0	3	4.1	
obesity	1	2.8	0	0.0	0	0.0	0	0.0	1	1.4	
ECOG PS											0.030
0-1	26	72.2	8	50.0	5	35.7	0	0.0	39	54.2	
2-5	10	27.8	8	50.0	9	64.3	6	100.0	33	45.8	
First-line treatment											0.030
G-based	24	66.7	10	62.5	3	21.4	4	66.7	41	56.9	
F-based	12	33.3	6	37.5	11	78.6	2	33.3	21	43.1	
First-line PFS (months) (range)	5.75 (2.55-8.32)		3.28 (1.98-7.08)		6.55 (3.25-14.08)		2.90 (1.77-7.87)		5.37 (2.10-8.21)		0.241
Second-line treatment											0.027
F-based	25	69.4	8	50.0	5	35.7	6	100.0	44	61.1	
G-based	11	30.6	6	37.5	8	57.1	0	0.0	25	34.7	
Other	0	0.0	2	12.5	1	7.2	0	0.0	3	4.2	
Second-line PFS (months) (range)	5.03 (2.24-7.83)		4.52 (2.75-7.22)		5.10 (1.63-9.56)		2.52 (0.79-3.99)		4.38 (2.24-7.83)		0.218
First and second line treatment order											0.215
G-based to F-based	17	47.2	7	43.7	3	21.4	4	66.7	31	43.1	
G-based to G-based	6	16.7	1	6.3	1	7.2	0	0.0	8	11.1	
G-based to Other	1	2.7	2	12.4	0	0.0	0	0.0	3	4.2	
F-based to G-based	6	16.7	5	31.3	6	42.9	0	0.0	17	23.6	
F-based to F-based	6	16.7	1	6.3	3	21.4	2	33.3	12	16.7	
F-based to Other	0	0.0	0	0.0	1	7.1	0	0.0	1	1.3	
Sum of first and second line PFS (range)	11.77 (7.17-15.00)		10.70 (6.00-12.28)		14.67 (6.91-27.11)		5.10 (2.95-12.11)		11.00 (6.63-14.80)		0.085
Family history of cancer											0.592
Yes	7	19.4	2	12.5	4	28.6	2	33.3	14	19.4	
No	29	80.6	14	87.5	10	71.4	4	66.7	58	80.6	
Tumor location											0.219

(Continued)

TABLE 1 Continued

Variables	Chemotherapy alone		Chemotherapy combined with targeted or immunotherapy		Chemotherapy-free antitumor therapy		Alleviative treatment		total		p value
	(n=36)		(n=16)		(n=14)		(n=6)		(n=72)		
	No.	%	No.	%	No.	%	No.	%	No.	%	
Head	12	33.3	10	62.5	5	35.7	5	83.3	32	44.4	
Body	0	0.0	0	0.0	1	7.1	0	0.0	1	1.4	
Tail	3	8.3	2	12.5	1	7.1	0	0.0	6	8.4	
Head+body	1	2.8	0	0.0	0	0.0	0	0.0	1	1.4	
Body+tail	20	55.6	4	25.0	7	50.1	1	16.7	32	44.4	
Metastatic type											
Liver	24	66.7	12	75.0	11	78.6	2	33.3	49	68.1	0.238
Peritoneal	22	61.1	8	50.0	7	50.0	2	33.3	39	54.2	0.595
Lung	5	13.9	1	6.3	1	7.1	1	16.7	8	11.1	0.751
Distant lymph node	3	8.3	2	12.5	4	28.6	0	0.0	9	12.5	0.273
Previous surgery											0.158
Yes	20	55.6	4	25.0	6	42.9	4	66.7	34	47.2	
No	16	44.4	12	75.0	8	57.1	2	33.3	38	52.8	
CEA											0.360
Normal	16	44.4	3	18.8	5	35.7	2	33.3	26	36.1	
Abnormal	20	55.6	13	81.2	9	64.3	4	66.7	46	63.9	
CA125											0.090
Normal	21	58.3	6	37.5	3	21.4	2	33.3	32	44.4	
Abnormal	15	41.7	10	62.5	11	78.6	4	66.7	40	55.6	
CA199											>0.999
Normal	7	19.4	3	18.8	3	21.4	1	16.7	14	19.4	
Abnormal	29	80.6	13	81.2	11	78.6	5	83.3	58	80.6	
NLR											0.983
Normal	20	55.6	9	56.3	8	57.1	4	66.7	41	56.9	
Abnormal	16	44.4	7	43.7	6	42.9	2	33.3	31	43.1	
PLR											0.801
Normal	22	61.1	11	68.8	9	64.3	5	83.3	47	65.3	
Abnormal	14	38.9	5	31.2	5	35.7	1	16.7	25	34.7	

BMI, Body Mass Index; ECOG PS, Eastern Cooperative Oncology Group Performance status; G-based, Gemcitabine based therapy; F-based, Fluorouracil based treatment; PFS, Progression-free survival; NLR, Neutrophil to lymphocyte ratio; PLR, Platelet to lymphocyte ratio; MLR, Monocyte to lymphocyte ratio.

3.1.3 Cox proportional hazards regression analysis

Cox proportional hazards models and Kaplan–Meier analysis used for patients undergoing the third-line treatment showed that female patients (Figure 2A), patients with ECOG PS 0–1 (Figure 2B), and those with family history of cancer (Figure 2C) were more likely to respond to the third-line treatment (Supplementary Table 1). Patients with family history of cancer were particularly suitable for the chemotherapy alone regimen (Supplementary Table 2; Figure 2D). There was no independent factor in multivariate Cox proportional hazards models of patients treated with chemotherapy combined with targeted therapy or immunotherapy (Supplementary Table 3) or with chemotherapy-free antitumor therapy (Supplementary Table 4).

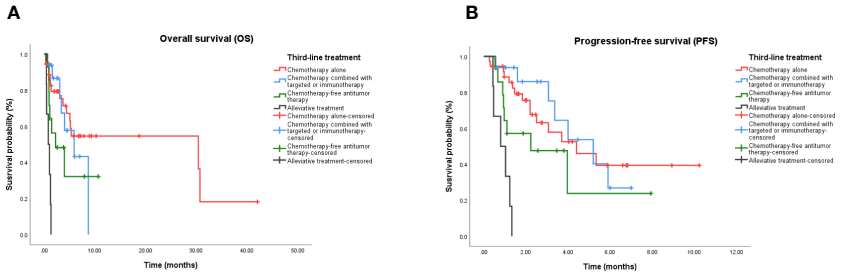

FIGURE 1
Kaplan-Meier curve in patients treated with third-line treatment. **(A)** OS in patients treated with chemotherapy alone, chemotherapy combined with targeted or immunotherapy, chemotherapy-free antitumor therapy, and palliative care. **(B)** PFS in patients treated with chemotherapy alone, chemotherapy combined with targeted or immunotherapy, chemotherapy-free antitumor therapy, and palliative care. OS, Overall survival; PFS, Progression-free survival.

3.1.4 Safety

The AE data for 72 patients are listed in Table 3. Most patients (63, 87.5%) experienced different degrees of AEs, and more than half of patients experienced grade 3/4 AEs (39, 54.2%). Compared to the chemotherapy alone group, chemotherapy combined with targeted therapy or immunotherapy group experienced more AEs (100.0% vs. 75.0%; $P = 0.002$). However, there was no statistical difference between the two groups in grade ¾ AEs (75.0% vs. 47.2%; $P = 0.056$). Compared to the chemotherapy alone (0.0% vs. 31.3%; $P = 0.020$) and chemotherapy-free antitumor therapy (0.0% vs. 31.3%; $P = 0.020$) groups, the chemotherapy combined with targeted therapy or immunotherapy group experienced more grade 3/4 leukopenia.

3.1.5 Dosage and survival

In our study, patients were treated with a complex chemotherapy regimen. Due to adverse reactions and physical conditions, some patients could not undergo adequate chemotherapy during the third-line treatment. Therefore, in order to further analyze the relationship between dosage and survival, we selected the most common chemotherapy regimen, the AG regimen (including combination targeting or immunotherapy regimens), as the study subjects. Among the 72 patients, 12 patients received the AG regimen as third-line treatment. Among them, 5 patients received full-dose chemotherapy, while 7 patients received reduced-dose chemotherapy. The dosage cannot be considered an independent prognostic factor for the survival of AG-treated patients (HR, 0.173; 95% CI,0.016 – 1.903; P = 0.151).

3.2 Subgroup analysis of efficacy and survival analysis in patients who received chemotherapy-based treatment

In the present study, most patients (52, 72.2%) received chemotherapy-based regimens as the third-line treatment. There was no difference in survival time between the chemotherapy alone and chemotherapy combined with targeted therapy or immunotherapy groups. However, the latter had a higher adverse reaction risk. Based on this, the study patients were further stratified according to the chemotherapy regimen to determine the most appropriate treatment intensity for patients receiving third-line therapy.

3.2.1 Clinical factors of patients receiving chemotherapy-based treatment

Baseline characteristics of mPC patients receiving third-line chemotherapy-based treatment are shown in Table 4. Of the 52 patients, 12 received single-agent chemotherapy, 24 received multi-agent chemotherapy, six received single-agent chemotherapy combined with targeted therapy or immunotherapy, and 10

TABLE 2 Rates of response in patients of third-line treatment.

Variables	Chemotherapy alone		Chemotherapy combined with targeted or immunotherapy		Chemotherapy-free antitumor therapy		Alleviative treatment		total		p value
	(n=36)		(n=16)		(n=14)		(n=6)		(n=72)		
	No.	%	No.	%	No.	%	No.	%	No.	%	
Response											
Partial response	1	2.8	1	6.3	1	7.1	0	0.0	3	4.2	
Stable disease	11	30.6	4	25.0	2	14.3	0	0.0	17	23.6	
Progressive disease	24	66.7	11	68.8	11	78.6	6	100.0	52	72.2	
Disease control rate	12	33.4	5	31.3	3	21.4	0	0.0	20	27.8	0.396

10.3389/fonc.2023.1251258

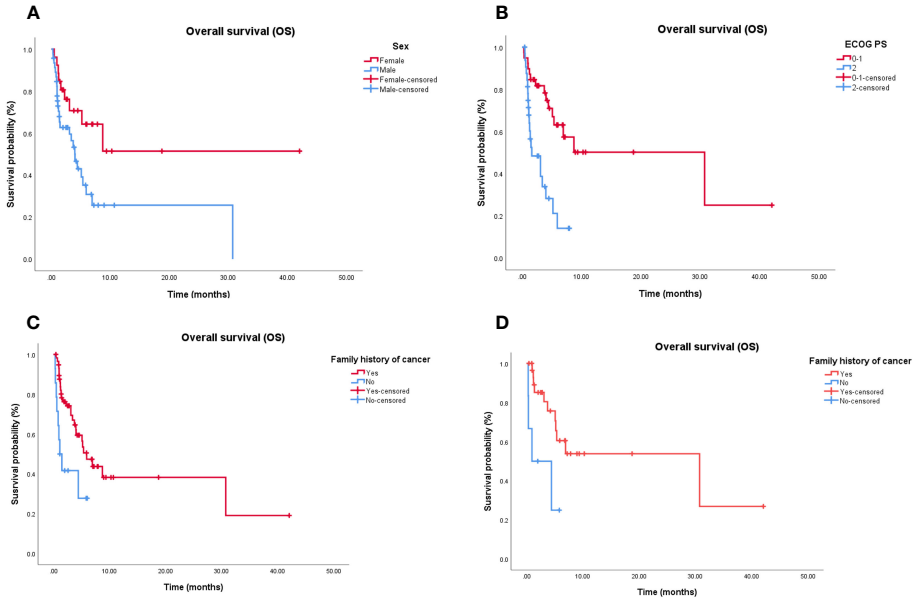

FIGURE 2
Independent significant factors of long-term survival in third-line treatment and chemotherapy alone treatment. **(A)** Women treated with third-line treatment have longer OS than man (P = 0.006). **(B)** Patients treated with third-line treatment, with ECOG PS 0-1 have longer OS than patients with ECOG PS ≥2 (P < 0.001). **(C)** Patients treated with third-line treatment, with family history of cancer have longer OS than patients without family history of cancer (P = 0.035). **(D)** Patients treated with chemotherapy alone, with family history of cancer have longer OS than patients without family history of cancer (P = 0.021). OS, Overall survival; ECOG PS, Eastern Cooperative Oncology Group Performance status.

TABLE 3 Rates of AEs in patients of third-line treatment.

AEs	Chemotherapy alone		Chemotherapy combined with targeted or immunotherapy		Chemotherapy-free antitumor therapy		Alleviative treatment	
	Any grade (%)	Grade 3/4 (%)	Any grade (%)	Grade 3/4 (%)	Any grade (%)	Grade 3/4 (%)	Any grade (%)	Grade 3/4 (%)
Leukopenia	9 (25.0)	0	12 (75.0)	5 (31.3)	2 (14.3)	0	1 (16.7)	0
Thrombocytopenia	4 (11.2)	2 (5.6)	5 (31.2)	3 (18.8)	3 (21.4)	2 (14.3)	0	0
Anemia	13 (36.2)	2 (5.6)	8 (50.0)	2 (12.5)	3 (21.4)	0	2 (33.3)	2 (33.3)
Neutropenia	3 (8.4)	2 (5.6)	3 (18.8)	0	5 (35.7)	3 (21.4)	1 (16.7)	0
Vomiting	7 (19.4)	2 (5.6)	4 (25.0)	2 (12.5)	4 (28.6)	1 (7.1)	1 (16.7)	1 (16.7)
Diarrhea	5 (13.9)	3 (8.3)	2 (12.5)	0	3 (21.4)	2 (14.3)	0	0
Hyperbilirubinemia	10 (27.8)	4 (11.1)	7 (43.7)	3 (18.8)	3 (21.4)	1 (7.1)	0	0
Hyperaminotransferemia	2 (5.6)	0	3 (18.8)	1 (6.3)	1 (7.1)	0	1 (1.4)	0
Hyperalkaline phosphatinemia	10 (27.8)	4 (11.1)	8 (50.0)	4 (25.0)	3 (21.4)	2 (14.3)	3 (50.0)	1 (16.7)
Hypercreatinemia	5 (13.9)	0	4 (25.0)	0	1 (7.1)	0	2 (33.3)	1 (16.7)
Proteinuria	4 (11.1)	0	6 (37.5)	0	3 (11.4)	1 (7.1)	0	0
Hematuria	2 (5.6)	0	3 (18.7)	2 (12.5)	1 (7.1)	0	0	0
Total	27 (75.0)	17 (47.2)	16 (100.0)	12 (75.0)	11 (78.6)	6 (42.9)	5 (83.3)	4 (66.6)

AEs, Adverse Events.

10.3389/fonc.2023.1251258

TABLE 4 Patient baseline characteristics of chemotherapy-based treatment.

Variables	Single-agent chemotherapy		Multi-agent chemotherapy		Single-agent chemotherapy combined with targeted/ immunotherapy		Multi-agent chemotherapy combined with targeted/ immunotherapy		total		p value
	(n=12)		(n=24)		(n=6)		(n=10)		(n=52)		
	No.	%	No.	%	No.	%	No.	%	No.	%	
Sex											0.359
Male	7	58.3	17	70.8	3	50.0	4	40.0	31	59.6	
Female	5	41.7	7	29.2	3	50.0	6	60.0	21	40.4	
Median age (range)	63.00±7.224		61.13±7.903		63.33±5.007		61.80±12.264		61.94±8.321		0.930
BMI											0.490
thin	0	0.0	4	16.7	2	33.3	1	10.0	7	13.5	
healthy	12	100.0	18	75.0	4	66.7	8	80.0	42	80.8	
overweight	0	0.0	1	4.2	0	0.0	1	10.0	2	3.8	
obesity	0	0.0	1	4.2	0	0.0	0	0.0	1	1.9	
ECOG PS											0.111
0-1	6	50.0	20	83.3	1	16.7	7	70.0	29	55.8	
2-5	6	50.0	4	16.7	5	83.3	3	30.0	23	44.2	
First-line treatment											0.532
G-based	9	75.0	15	62.5	5	83.3	5	50.0	34	65.4	
F-based	3	25.0	9	37.5	1	16.7	5	50.0	18	34.6	
First-line PFS (months) (range)	6.30 (4.93-7.71)		5.45 (2.10-8.23)		2.42 (1.56-8.03)		2.22 (1.73-9.24)		5.52 (2.05-7.70)		0.256
Second-line treatment											0.437
F-based	8	66.7	17	70.8	4	66.7	4	40.0	32	61.5	
G-based	4	33.3	7	29.2	1	16.7	5	50.0	17	32.7	
Other	0	0.0	0	0.0	1	16.6	1	10.0	3	5.8	
Second-line PFS (months) (range)	5.97 (2.21-8.21)		3.82 (2.19-5.83)		5.82 (3.08-12.63)		8.23 (1.98-11.41)		4.82 (2.22-8.08)		0.340
First and second line treatment order											0.358
G-based to F-based	6	50	11	45.8	1	16.7	6	60.0	24	46.2	
G-based to G-based	3	25	3	12.5	0	0.0	1	10.0	7	13.5	
G-based to Other	0	0.0	1	4.2	2	33.3	0	0.0	3	5.8	
F-based to G-based	2	16.7	4	16.7	3	50.0	2	20.0	11	21.2	
F-based to F-based	1	8.3	5	20.8	0	0.0	1	10.0	7	13.5	
Sum of first and second line PFS (range)	11.98 (7.16-17.27)		9.37 (5.28-14.14)		7.55 (5.65-20.83)		13.20 (3.91-18.53)		10.62 (6.67-14.73)		0.749
Family history of cancer											0.182
Yes	1	8.3	6	25.0	2	33.3	0	0.0	8	15.7	
No	11	91.7	18	75.0	4	66.7	10	100.0	43	84.3	
Tumor location											0.229

(Continued)

TABLE 4 Continued

Variables	Single-agent chemotherapy		Multi-agent chemotherapy		Single-agent chemotherapy combined with targeted/ immunotherapy		Multi-agent chemotherapy combined with targeted/ immunotherapy		total		p value
	(n=12)		(n=24)		(n=6)		(n=10)		(n=52)		
	No.	%	No.	%	No.	%	No.	%	No.	%	
Head	5	41.7	7	29.1	4	66.7	6	60.0	22	42.3	
Tail	2	16.6	1	4.2	0	0.0	2	20.0	5	9.6	
Head+body	0	0.0	1	4.2	0	0.0	0	0.0	1	1.9	
Body+tail	5	41.7	15	62.5	2	33.3	2	20.0	24	46.2	
Metastatic type											
Liver	8	66.7	16	66.7	3	50.0	9	90.0	36	69.2	0.347
Peritoneal	7	58.3	15	62.5	4	66.7	4	40.0	30	57.7	0.711
Lung	2	16.7	3	12.5	0	0.0	1	10.0	6	11.5	0.930
Distant lymph node	0	0.0	3	12.5	0	0.0	2	20.0	5	9.6	0.375
Previous surgery											0.128
Yes	5	41.7	15	62.5	2	33.3	2	20.0	24	46.2	
No	7	58.3	9	37.5	4	66.7	8	80.0	28	53.8	
CEA											0.073
Normal	3	25.0	13	54.2	2	33.3	1	0.0	18	34.6	
Abnormal	9	75.0	11	45.8	4	66.7	9	100.0	34	65.4	
CA125											0.067
Normal	5	41.7	16	66.7	4	66.7	2	20.0	27	51.9	
Abnormal	7	58.3	8	33.3	2	33.3	8	80.0	25	48.1	
CA199											0.455
Normal	1	8.3	6	25.0	2	33.3	1	10.0	10	19.2	
Abnormal	11	91.7	18	75.0	4	66.7	9	90.0	42	80.8	
NLR											0.420
Normal	9	75.00	11	45.8	3	50.00	6	60.0	29	55.8	
Abnormal	3	25.00	13	54.2	3	50.00	4	40.0	23	44.2	
PLR											0.644
Normal	9	75	13.00	54.2	4	66.7	7	70.0	33	63.5	
Abnormal	3	25	11.00	45.8	2	33.3	3	30.0	19	36.5	

BMI, Body Mass Index; ECOG PS, Eastern Cooperative Oncology Group Performance status; G-based, Gemcitabine based therapy; F-based, Fluorouracil based treatment; PFS, Progression-free survival; NLR, Neutrophil to lymphocyte ratio; PLR, Platelet to lymphocyte ratio; MLR, Monocyte to lymphocyte ratio.

received multi-agent chemotherapy combined with targeted therapy or immunotherapy. The baseline characteristics, including ECOG PS, tumor site, tumor markers, and other factors, were balanced.

3.2.2 Efficacy

The mOS values for the single-agent chemotherapy, multi-agent chemotherapy, single-agent chemotherapy combined with targeted therapy or immunotherapy, and multi-agent chemotherapy combined with targeted therapy or immunotherapy groups were 5.1 months (95% CI, 1.3–10.7 months), 7.9 months (95% CI, 1.3–8.9 months), 7.0 months (95% CI, 0.7–7.5 months), and 6.9 months (95% CI, 2.6–10.2 months), respectively. The mPFS values were 3.1 months (95% CI, 1.0–7.3 months), 6.9 months (95% CI, 1.8–9.2 months), 4.4 months (95% CI, 1.9–6.9 months), and 4.0 months (95% CI, 1.7–5.1 months), respectively. Kaplan–Meier analysis showed that there was no

statistical difference in mOS and mPFS between mPC patients who received chemotherapy-based regimens, single-agent chemotherapy, and multi-agent chemotherapy (P = 0.967; P = 0.991), single-agent chemotherapy and single-agent chemotherapy combined with targeted therapy or immunotherapy (P = 0.951; P = 0.955), multi-agent chemotherapy and multi-agent chemotherapy combined with targeted therapy or immunotherapy (P = 0.809; P = 0.589), single-agent chemotherapy combined with targeted therapy or immunotherapy and multi-agent chemotherapy combined with targeted therapy or immunotherapy (P = 0.583; P = 0.416; Figure 3).

DCRs for the single-agent chemotherapy, multi-agent chemotherapy, single-agent chemotherapy combined with targeted therapy or immunotherapy, and multi-agent chemotherapy combined with targeted therapy or immunotherapy were 50.0%, 25.0%, 33.3%, and 40.0%, respectively. There was no statistical difference in DCRs between the mPC patients who received chemotherapy-based regimens, single-agent chemotherapy, and multi-agent chemotherapy (P = 0.182), single-agent chemotherapy and single-agent chemotherapy combined with targeted therapy or immunotherapy group (P > 0.999), multi-agent chemotherapy and multi-agent chemotherapy combined with targeted therapy or immunotherapy (P = 0.400), single-agent chemotherapy combined with targeted therapy or immunotherapy and multi-agent chemotherapy combined with targeted therapy or immunotherapy (P = 0.400; Table 5).

3.2.3 Cox proportional hazards regression analysis

Cox proportional hazards models and Kaplan–Meier analysis used for patients undergoing chemotherapy-based regimens showed that patients with a normal body mass index (Figure 4A) and family history of cancer (Figure 4B) were more likely to respond to chemotherapy-based regimens (Supplementary Table 5). There was no independent factor in multivariate Cox proportional hazards models of patients treated with multi-agent chemotherapy (Supplementary Table 6). Due to the small sample size, Cox analysis was not applicable to the other three subgroups.

3.2.4 Safety

AEs were assessed in 52 patients (Table 6). Most patients (42, 80.8%) experienced different degrees of AEs, and some patients experienced grade 3/4 AEs (20, 38.5%). Compared to the single-agent chemotherapy group, single-agent chemotherapy combined with targeted therapy or immunotherapy group experienced more AEs (100.0% vs. 66.7%; P = 0.039). However, there was no significant difference between the two groups in grade 3/4 AEs (50.0% vs. 16.7%; P = 0.153). Compared to the multi-agent chemotherapy group, multi-agent chemotherapy combined with targeted therapy or immunotherapy group experienced more AEs (100.0% vs. 75.0%; P = 0.011) and more grade 3/4 leukopenia (30.0% vs. 0.0%; P = 0.037). However, there was no significant difference between the two groups in the total incidence of grade 3/4 AEs (70.0% vs. 33.3%; P = 0.517).

4 Discussion

In this study, the third-line antitumor treatment was demonstrated to benefit patients and prolong their survival time compared to palliative care. Baseline characteristics were analyzed in all patients to identify efficacy predictors. Results showed that female patients, those with ECOG PS 0–1, and patients with family history of cancer were independent prognostic factors for longer OS in a group of mPC patients who received the third-line treatment. In particular, patients with a normal body mass index and family history of cancer were independent prognostic factors for longer OS in a group of mPC patients who received chemotherapy-based treatment. This indicates that not all patients are suitable for third-line antitumor therapy and some screening is still needed. Many retrospective studies have concluded that ECOG PS is an independent prognostic factor associated with treatment efficacy. Most notably, a family history of cancer was an independent factor for longer survival time among different treatment regimes in our study. Existing research studies have reported that family history of *BRCA*-related tumors may correlate with the response to

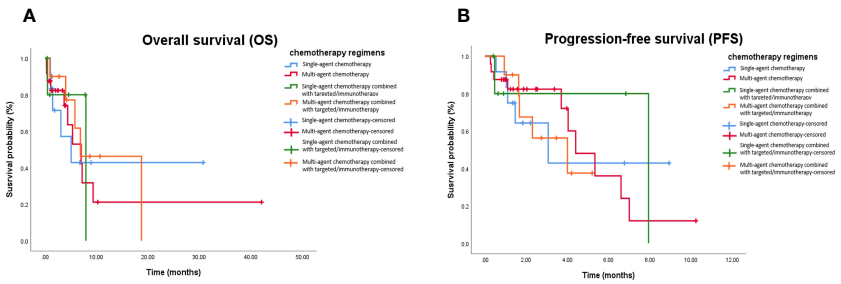

FIGURE 3
Kaplan-Meier curve in patients received chemotherapy-based treatment. **(A)** OS in patients treated with single-agent chemotherapy, multi-agent chemotherapy, single-agent chemotherapy combined with targeted or immunotherapy, and multi-agent chemotherapy combined with targeted or immunotherapy. **(B)** PFS in in patients treated with single-agent chemotherapy, multi-agent chemotherapy, single-agent chemotherapy combined with targeted or immunotherapy, and multi-agent chemotherapy combined with targeted or immunotherapy. OS, Overall survival; PFS, Progression-free survival.

TABLE 5 Rates of response in patients of chemotherapy-based treatment.

Variables	Single-agent chemotherapy		Multi-agent chemotherapy		Single-agent chemotherapy combined with targeted/immunotherapy		Multi-agent chemotherapy combined with targeted/immunotherapy		total		p value
	(n=12)		(n=24)		(n=6)		(n=10)		(n=52)		
	No.	%	No.	%	No.	%	No.	%	No.	%	
Response											
Partial response	0	0.0	2	8.3	1	16.7	0	0.0	3	5.8	
Stable disease	6	50.0	4	16.7	1	16.7	4	40.0	15	28.8	
Progressive disease	6	50.0	18	75.0	4	66.6	6	60.0	34	65.4	
Disease control rate	9	50.0	6	25.0	2	33.3	4	40.0	34	34.6	0.250

chemotherapy and OS in PC, which is similar to the results of our study (19). This may be related to genetic differences and lifestyle changes. Patients with a family history of tumor disease may have some genetic mutations and are more likely to have malignant changes when affected by the external environment compared to those without a family history (20). In addition, it has been suggested that young patients who are aware of their family history may adopt healthy behaviors, such as opportunistic screening, and/or make healthy lifestyle changes, thereby improving their prognosis (21). Surprisingly, female patients were more likely to benefit from third-line treatments for mPC. Patient characteristics were not balanced between each group, including ECOG PS, first-line treatment, and second-line treatment. In order to determine the cause of this imbalance at baseline, a review of the case data revealed that patients with ECOG PS of ≥ 2 had a poor physical performance and were more inclined to choose chemotherapy-free regimens before the third-line treatment, while patients with a better physical performance were more suitable for chemotherapy. Patients receiving palliative treatment with ECOG PS of ≥ 2 at the beginning of the second-line treatment only received fluorouracil single-agent in the second-line treatment. A significant proportion of patients (24, 33.3%) received gemcitabine-based regimen as the first-line treatment and fluorouracil-based regimen as the second-line treatment.

Since our research data and previous studies have shown that third-line antitumor therapy can bring survival benefits to patients, it was necessary to determine whether chemotherapy combined with other treatments can further improve treatment efficacy. With the recent development of novel therapies, such as immunotherapy and targeted therapy, some clinicians have chosen to combine these therapies with chemotherapy or to directly use chemotherapy-free therapies when selecting third-line treatments. This is the first real-world study to compare the efficacy and safety of various third-line treatments for advanced PC. Although there was no statistical difference in P value, Kaplan-Meier analysis showed that the chemotherapy alone (mOS, 6.9 months; 95% CI, 0.5–13.9 months) and chemotherapy combined with targeted therapy or immunotherapy (mOS, 5.9 months; 95% CI, 1.6–10.2 months) groups had a better OS compared to the chemotherapy-free group (mOS, 3.3 months; 95% CI, 0.2–5.0 months). This may be due to the insufficient sample size in the study. This investigation demonstrated for the first time that the combined targeting/immunotherapy based on chemotherapy cannot improve third-line mOS (6.9 months vs. 5.9 months, P = 0.588) compared to chemotherapy alone. This notion has previously been introduced in other studies investigating the first-line treatment. Previous research has revealed that PC promotes an immunosuppressive microenvironment through formation of dense stromal

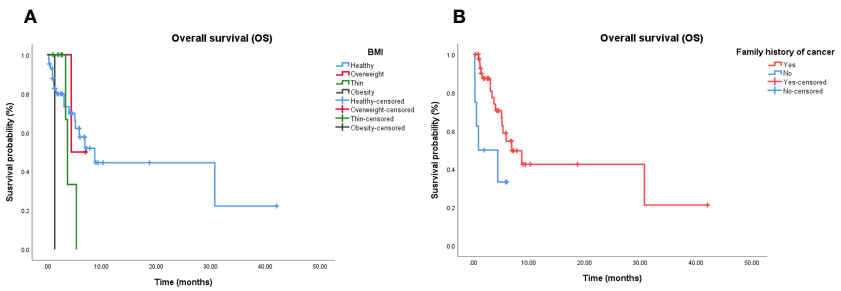

FIGURE 4
Independent significant factors of long-term survival in chemotherapy-based treatment. **(A)** Patients treated with chemotherapy-based treatment, with normal BMI have longer OS than patients with abnormal BMI (P = 0.021). **(B)** Patients treated with chemotherapy-based treatment, with family history of cancer have longer OS than patients without family history of cancer (P = 0.019). BMI, Body Mass Index; OS, Overall survival.

TABLE 6 Rates of AEs in patients of chemotherapy-based treatment.

Events	Single-agent chemotherapy		Multi-agent chemotherapy		Single-agen chemotherapy combined with targeted/immunotherapy		Multi-agent chemotherapy combined with targeted/immunotherapy	
	Any grade (%)	Grade 3/4 (%)	Any grade (%)	Grade 3/4 (%)	Any grade (%)	Grade 3/4 (%)	Any grade (%)	Grade 3/4 (%)
Leukopenia	2 (16.7)	0	4 (16.7)	0	3 (50.0)	1 (16.7)	5 (50.0)	3 (30.0)
Thrombocytopenia	1 (8.3)	0	1 (4.2)	0	0	0	2 (20.0)	0
Anemia	5 (41.7)	0	8 (33.3)	2 (8.3)	3 (50.0)	1 (16.7)	5 (50.0)	1 (10.0)
Neutropenia	1 (8.3)	1 (8.3)	1 (4.2)	0	0	0	3 (30.0)	0
Vomiting	0	0	5 (20.8)	0	1 (16.7)	0	1 (10.0)	0
Diarrhea	0	0	1 (4.2)	0	1 (16.7)	0	0	0
Hyperbilirubinemia	5 (41.7)	0	5 (20.8)	4 (16.7)	3 (50.0)	1 (16.7)	4 (40.0)	2 (20.0)
Hyperaminotransferemia	2 (16.7)	0	0	0	0	0	3 (30.0)	1 (10.0)
Hyperalkaline phosphatinemia	2 (16.7)	1 (8.3)	8 (33.3)	3 (12.5)	2 (33.3)	1 (16.7)	6 (60.0)	3 (30.0)
Hypercreatinemia	2 (16.7)	0	4 (16.7)	0	1 (16.7)	0	4 (40.0)	0
Proteinuria	0	0	4 (16.7)	0	1 (16.7)	0	5 (50.0)	0
Hematuria	1 (8.3)	0	1 (4.2)	0	0	0	1 (10.0)	0
Total	8 (66.7)	2 (16.7)	18 (75.0)	8 (33.3)	6 (100.0)	3 (50.0)	10 (100.0)	7 (70.0)

AEs, Adverse Events.

desmoplasia, and concurrent administration of gemcitabine plus nab-paclitaxel was poised to improve immunotherapy drug access to tumor cells via structural disruption/remodeling of the PC tumor microenvironment (22). Negative results in the CCTG PA.7 trial indicated that it was not sufficient to increase immunotherapy efficacy in the overall patient population. The CCTG PA.7 trial demonstrated no survival benefits from adding durvalumab and tremelimumab to gemcitabine and nab-paclitaxel as the first-line therapy in an unselected population of patients with PC (mOS, 9.8 months vs. 8.8 months, $P = 0.72$). Moreover, the combination of epidermal growth factor receptor inhibitors and chemotherapy failed to achieve the preclinical model estimates. In preclinical models of PC, ibrutinib combined with gemcitabine increased the levels of effector CD8+ T cells and mast cell inhibition, decreased angiogenesis, and reduced desmoplasia in multiple mouse models, resulting in reduced tumor size and increased survival rate (10, 23). In the phase III RESOLVE study, the combination of ibrutinib plus nab-paclitaxel and gemcitabine did not improve survival in patients without any previous cytotoxic chemotherapy for primary PC compared to chemotherapy alone (mOS, 10.8 months vs. 9.7 months, $P = 0.323$) (24). The phase II ACCEPT study demonstrated an mOS of 7.3 months in the afatinib combined with gemcitabine group compared to 7.4 months in the gemcitabine group ($P = 0.80$) (25). This was likely because the addition of targeted therapy to chemotherapy may have mitigated the ability to deliver the complete chemotherapy regimen and the tumor received a lower cumulative dose of all agents compared to patients in the chemotherapy alone group. In the phase II ACCEPT study, AEs were more frequent in the combination therapy group, which was consistent with the present study results showing a significantly higher toxicity burden in the combination group. In our study, we found that chemotherapy combined with targeted therapy was more prone to result in grade 3/4 leukopenia compared to chemotherapy alone. Family history of cancer was an independent mOS predictor for PC patients who received the chemotherapy alone treatment. In addition, the present research also showed that there was no statistical difference in mOS between single- and multi-agent chemotherapy (5.1 months vs. 7.9 months, $P = 0.967$) groups, which was consistent with the randomized phase III NAPOLI-1 trial results (26). The response in the NAPOLI-1 trial was less prominent in patients treated with nanoliposomal irinotecan with fluorouracil/leucovorin compared to fluorouracil/leucovorin as the third-line treatment (mOS, 5.4 months vs. 4.3 months, $P = 0.178$). Therefore, the appropriate use of low-intensity regimen in third-line antitumor therapy can also prolong survival. To our knowledge, no clinical studies have been carried out on third-line antitumor therapy to support this conclusion, which still needs to be confirmed by studies with a larger sample size.

The optimal therapy sequencing remains unknown and is largely defined by physician preference in practice. In our results, the order of gemcitabine- and fluorouracil-based regimens as the first- and second-line treatment pairs was not an independent predictor of third-line treatment OS, which is consistent with what has been reported so far. In the study by Jung et al., first-line palliative chemotherapy regimens and the order of subsequent chemotherapy regimens were not associated with survival outcomes

in third-line treatment patients (27). Advances in systemic chemotherapy over the past decade have been limited, and the mechanism of chemotherapy resistance is still unclear. More trials will be carried out to explore the mechanism of chemotherapy resistance and provide credible data to identify the prognostic factors for chemotherapy rechallenge. According to our results, the order of chemotherapy drug treatment in the process of PC management can be selected according to the patient's physical condition in the first- and second-line treatments. Patients can also receive personalized treatment.

The current study had limitations, as the research was performed at a single institution using retrospective analysis, and the number of patients included in each group was not balanced. First, the retrospective nature of the analysis may result in a potential selection bias such as the increase of survival would be due to the ECOG, and lack of medical records including molecular pathological information and immunohistochemistry may affect independent prognostic factor results. Second, therapeutic drug subgroups could not be analyzed further due to insufficient sample size. Third, the impact of different treatments after disease progression was not estimated in the study, which may affect the OS analysis. Nevertheless, our results are encouraging and support continued use and study of chemotherapy rechallenge to treat patients who fail to respond to the second-line treatment, as well as further optimization of selection of patients who are most likely to benefit.

5 Conclusion

Treatment with chemotherapy-based therapy as the third-line treatment combined with targeted therapy or immunotherapy failed to improve survival benefits and demonstrated higher safety risks. In particular, blood test results should be monitored more closely in patients undergoing multi-agent chemotherapy combined with targeted therapy or immunotherapy to prevent the occurrence of grade 3/4 leukopenia. The treatment order of gemcitabine- and fluorouracil-based regimens in the first- and second-line therapy does not affect third-line OS. Thus, in the first- and second-line therapy, the treatment order of chemotherapy drugs can be selected according to the patient's physical condition. Therefore, patients who tolerate it should be treated mainly with chemotherapy. For patients who cannot tolerate chemotherapy, the use of targeted therapy or immunotherapy represents a survival benefit over supportive therapy. The targeted and immunotherapy drugs included in the present study were mixed, and more clinical trials are needed to explore the feasibility of chemotherapy-free treatment in advanced PC.

Data availability statement

The original contributions presented in the study are included in the article/Supplementary Material. Further inquiries can be directed to the corresponding authors.

Ethics statement

The studies involving humans were approved by the Ethics Committee of Zhejiang Provincial People's Hospital. The studies were conducted in accordance with the local legislation and institutional requirements. The participants provided their written informed consent to participate in this study. Written informed consent was obtained from the individual(s) for the publication of any potentially identifiable images or data included in this article.

Author contributions

H-RL and P-FZ contributed equally to this work. Z-LC, and LY revised the manuscript. All authors wrote and revised the manuscript and issued the final approval for the version to be submitted.

Funding

This study was supported by grants from Zhejiang Provincial Nature Fund Key Project (LZ23H160007), Zhejiang Provincial Medical and Pharmaceutical Health Key Project (WKJ-ZJ-2325) and Spark Program - Oncology Treatment clinical Research Innovation and development project Fund.

Acknowledgments

We thank the patients who participated and clinical staff who assisted. And we also sincerely thank the editors and reviewers for their careful review and valuable opinions that helped to greatly improve the manuscript.

Conflict of interest

The authors declare that the research was conducted in the absence of any commercial or financial relationships that could be construed as a potential conflict of interest.

Publisher's note

Supplementary material

The Supplementary Material for this article can be found online at: https://www.frontiersin.org/articles/10.3389/fonc.2023.1251258/full#supplementary-material

References

1. The Lancet Gastroenterology, H. Pancreatic cancer: a state of emergency? *Lancet Gastroenterol Hepatol* (2021) 6(2):81. doi: 10.1016/S2468-1253(20)30397-6

2. Moore A, Donahue T. Pancreatic cancer. *Jama* (2019) 322(14):1426. doi: 10.1001/jama.2019.14699

3. Zhao C, Gao F, Li Q, Liu Q, Lin X. The distributional characteristic and growing trend of pancreatic cancer in China. *Pancreas* (2019) 48(3):309–14. doi: 10.1097/MPA.0000000000001222

4. Advancing on pancreatic cancer. *Nat Rev Gastroenterol Hepatol* (2021) 18(7):447. doi: 10.1038/s41575-021-00479-5

5. Abrams TA, Meyer G, Meyerhardt AM, Wolpin BM, Schrag D, Fuchs CS. Patterns of chemotherapy use in a U.S.-based cohort of patients with metastatic pancreatic cancer. *Oncologist* (2017) 22(8):925–33. doi: 10.1634/theoncologist.2016-0447

6. Tempero MA, Malafa MP, Al-Hawary M, Behrman SW, Benson AB, Cardin DB, et al. Pancreatic adenocarcinoma, version 2.2021, NCCN clinical practice guidelines in oncology. *J Natl Compr Canc Netw* (2021) 19(4):439–57. doi: 10.6004/jnccn.2021.0017

7. Conroy T, Desseigne F, Ychou M, Bouché O, Guimbaud R, Bécouarn Y, et al. FOLFIRINOX versus gemcitabine for metastatic pancreatic cancer. *N Engl J Med* (2011) 364(19):1817–25. doi: 10.1056/NEJMoa1011923

8. Von Hoff DD, Ervin T, Arena FP, Chiorean EG, Infante J, Moore M, et al. Increased survival in pancreatic cancer with nab-paclitaxel plus gemcitabine. *N Engl J Med* (2013) 369(18):1691–703. doi: 10.1056/NEJMoa1304369

9. Neoptolemos JP, Kleeff J, Michl P, Costello E, Greenhalf D, Palmer DH. Therapeutic developments in pancreatic cancer: current and future perspectives. *Nat Rev Gastroenterol Hepatol* (2018) 15(6):333–48. doi: 10.1038/s41575-018-0005-x

10. Wang-Gillam A, Li C-P, Bodoky G, Dean A, Shan Y-S, Jameson G, et al. Nanoliposomal irinotecan with fluorouracil and folinic acid in metastatic pancreatic cancer after previous gemcitabine-based therapy (NAPOLI-1): a global, randomised, open-label, phase 3 trial. *Lancet* (2016) 387(10018):545–57. doi: 10.1016/S0140-6736(15)00986-1

11. Chiorean EG, Von Hoff DD, Tabernero J, El-Maraghi R, Ma WW, Reni M, et al. Second-line therapy after nab-paclitaxel plus gemcitabine or after gemcitabine for patients with metastatic pancreatic cancer. *Br J Cancer* (2016) 115(2):188–94. doi: 10.1038/bjc.2016.185

12. Marabelle AM, Le DT, Ascierto PA, Di Giacomo AM, De Jesus-Acosta A, Delord J-P, et al. Efficacy of pembrolizumab in patients with noncolorectal high microsatellite instability/mismatch repair-deficient cancer: results from the phase II KEYNOTE-158 study. *J Clin Oncol* (2020) 38(1):1–10. doi: 10.1200/JCO.19.02105

13. Drilon A, Laetsch TW, Kummar S, DuBois SG, Lassen U, Demetri GD, et al. Efficacy of larotrectinib in TRK fusion-positive cancers in adults and children. *N Engl J Med* (2018) 378(8):731–9. doi: 10.1056/NEJMoa1714448

14. Doebele RC, Drilon A, Paz-Ares L, Siena S, Shaw AT, Farago AF, et al. Entrectinib in patients with advanced or metastatic NTRK fusion-positive solid tumours: integrated analysis of three phase 1-2 trials. *Lancet Oncol* (2020) 21(2):271–82. doi: 10.1016/S1470-2045(19)30691-6

15. Luo J. KRAS mutation in pancreatic cancer. *Semin Oncol* (2021) 48(1):10–8. doi: 10.1053/j.seminoncol.2021.02.003

16. Bear AS, Vonderheide RH, O'Hara MH. Challenges and opportunities for pancreatic cancer immunotherapy. *Cancer Cell* (2020) 38(6):788–802. doi: 10.1016/j.ccell.2020.08.004

17. Health Commission Of The People's Republic Of China, N. National guidelines for diagnosis and treatment of pancreatic cancer 2022 in China (English version). *Chin J Cancer Res* (2022) 34(3):238–55. doi: 10.21147/j.issn.1000-9604.2022.03.05

18. Martín AM, Hidalgo M, Alvarez R, Arrazubi V, Martínez-Galán J, Salgado M, et al. From first line to sequential treatment in the management of metastatic pancreatic cancer. *J Cancer* (2018) 9(11):1978–88. doi: 10.7150/jca.23716

19. Goldstein JB, Zhao L, Wang X, Ghelman Y, Overman MJ, Javle MM, et al. Germline DNA sequencing reveals novel mutations predictive of overall survival in a cohort of patients with pancreatic cancer. *Clin Cancer Res* (2020) 26(6):1385–94. doi: 10.1158/1078-0432.CCR-19-0224

20. Ang M, Borg M, O'Callaghan ME. Survival outcomes in men with a positive family history of prostate cancer: a registry based study. *BMC Cancer* (2020) 20(1):894. doi: 10.1186/s12885-020-07174-9

21. Pesola F, Eloranta S, Martling A, Saraste D, Smedby KE. Family history of colorectal cancer and survival: a Swedish population-based study. *J Intern Med* (2020) 287(6):723–33. doi: 10.1111/joim.13036

22. Miyashita T, Tajima H, Makino I, Okazaki M, Yamaguchi T, Ohbatake Y, et al. Neoadjuvant chemotherapy with gemcitabine plus nab-paclitaxel reduces the number of cancer-associated fibroblasts through depletion of pancreatic stroma. *Anticancer Res* (2018) 38(1):337–43. doi: 10.21873/anticanres.12227

23. Soucek L, Buggy JJ, Kortlever R, Adimoolam S, Monclús HA, Allende MTS, et al. Modeling pharmacological inhibition of mast cell degranulation as a therapy for insulinoma. *Neoplasia* (2011) 13(11):1093–100. doi: 10.1593/neo.11980

24. Tempero M, Oh D-Y, Tabernero J, Reni M, Van Cutsem E, Hendifar A, et al. Ibrutinib in combination with nab-paclitaxel and gemcitabine for first-line treatment of patients with metastatic pancreatic adenocarcinoma: phase III RESOLVE study. *Ann Oncol* (2021) 32(5):600–8. doi: 10.1016/j.annonc.2021.01.070

25. Haas M, Waldschmidt DT, Stahl M, Reinacher-Schick A, Freiberg-Richter J, Fischer von Weikersthal L, et al. Afatinib plus gemcitabine versus gemcitabine alone as first-line treatment of metastatic pancreatic cancer: The randomised, open-label phase II ACCEPT study of the Arbeitsgemeinschaft Internistische Onkologie with an integrated analysis of the 'burden of therapy' method. *Eur J Cancer* (2021) 146:95–106. doi: 10.1016/j.ejca.2020.12.029

26. Mercadé TM, Chen L-T, Li C-P, Siveke JT, Cunningham D, Bodoky G, et al. Liposomal irinotecan + 5-FU/LV in metastatic pancreatic cancer: subgroup analyses of patient, tumor, and previous treatment characteristics in the pivotal NAPOLI-1 trial. *Pancreas* (2020) 49(1):62–75. doi: 10.1097/MPA.0000000000001455

27. Chun JW, Woo SM, Lee SH, Choi JH, Park N, Kim JS, et al. A real-world analysis of nanoliposomal-irinotecan with 5-fluorouracil and folinic acid as third- or later-line therapy in patients with metastatic pancreatic adenocarcinoma. *Ther Adv Med Oncol* (2022) 14:17588359221119539. doi: 10.1177/17588359221119539

frontiers | Frontiers in Oncology

TYPE Original Research
PUBLISHED 27 October 2023
DOI 10.3389/fonc.2023.1281545

OPEN ACCESS

EDITED BY
Jennifer M. Bailey-Lundberg,
University of Texas Health Science Center at Houston, United States

REVIEWED BY
Li Zhang,
University of Minnesota Twin Cities, United States
Ying Ma,
Tianjin Medical University Cancer Institute and Hospital, China

*CORRESPONDENCE
Cheng Fang
fangcheng@suda.edu.cn
Mei Ji
jimei_685@163.com

†These authors have contributed equally to this work

RECEIVED 22 August 2023
ACCEPTED 16 October 2023
PUBLISHED 27 October 2023

CITATION
Cheng D, Hu J, Wu X, Wang B, Chen R, Zhao W, Fang C and Ji M (2023) PD-1 blockade combined with gemcitabine plus nab-paclitaxel is superior to chemotherapy alone in the management of unresectable stage III/IV pancreatic cancer: a retrospective real-world study. *Front. Oncol.* 13:1281545. doi: 10.3389/fonc.2023.1281545

PD-1 blockade combined with gemcitabine plus nab-paclitaxel is superior to chemotherapy alone in the management of unresectable stage III/IV pancreatic cancer: a retrospective real-world study

Daoan Cheng†, Jing Hu†, Xiaoyu Wu†, Banglu Wang, Rui Chen, Weiqing Zhao, Cheng Fang* and Mei Ji*

Departments of Oncology, The Third Affiliated Hospital of Soochow University, Changzhou, China

Background: Pancreatic cancer (PC) is widely recognized as one of the most malignant forms of cancer worldwide. Monotherapy with immune checkpoint inhibitors (ICI) has shown limited efficacy in treating this disease. There was controversy surrounding whether combining ICI with chemotherapy provided superior outcomes compared to chemotherapy alone.

Methods: In this study, patients diagnosed with unresectable stage III/IV pancreatic cancer (PC) were classified as receiving programmed cell death protein 1 (PD-1) blockade plus gemcitabine and nab-paclitaxel (AG regimen) (PD-1/chemo, n=27, 50.9%) or chemotherapy alone (chemo, n=26, 49.1%) arm. The primary study endpoints included progression-free survival (PFS) and overall survival (OS), with an additional assessment of treatment-related adverse events graded as three or higher. Chi-square ($\chi 2$) statistics were employed to analyze the clinical differences between the two groups, while Kaplan-Meier curves were used to assess the difference in PFS and OS. Statistical significance was defined as *P*-values less than 0.05 ($P < 0.05$).

Results: The median follow-up duration was 22 months (range 1-28 months). In the PD-1/chemo arm, the median PFS was eight months, whereas it was 3.5 months in the chemo arm (HR=0.459, 95% CI: 0.252-0.846, P=0.002). Furthermore, the median OS was 15 months in the PD-1/chemo arm and eight months in the chemo arm (HR=0.345, 95% CI: 0.183-0.653, P<0.001). Within the PD-1/chemo arm, 15 (55.6%) patients experienced grade 3 treatment-related adverse events, compared to 13 (50.0%) patients in the chemo arm.

Conclusions: PD-1 blockade combined with nab-paclitaxel plus gemcitabine demonstrated superior efficacy to chemotherapy alone for unresectable stage III/IV PC patients. Future studies were warranted to identify immunosensitive patient subgroups within the PC population, ultimately leading to the development of more efficacious therapeutic strategies.

KEYWORDS

pancreatic cancer, PD-1, chemotherapy, immune checkpoint inhibitors, nab-paclitaxel, gemcitabine

1 Introduction

Pancreatic cancer (PC) had the lowest 5-year relative survival rate (OS) among all malignant cancers, with only 11% (1). Pancreatic ductal adenocarcinoma (PDAC), accounting for about 90%, was the leading pathological type (2). Established treatments for unresectable locally advanced or advanced PC include the AG regimen (nab-paclitaxel in combination with gemcitabine) or the FOLFIRINOX regimen (oxaliplatin, irinotecan, fluorouracil, and leucovorin) (3). However, the survival outcomes of patients with PC treated solely with chemotherapy remained suboptimal (4). There was a pressing need for novel treatment modalities to manage locally advanced or metastatic PC that was not amenable to surgical resection.

The emergence of immune checkpoint inhibitors (ICI) therapy has significantly altered the treatment model for several cancers, including lung cancer and malignant melanoma (5). However, except for a small subset of patients (less than 1%) who exhibited microsatellite instability (MSI), ICI monotherapy has shown limited efficacy in PC (6–9). This was attributed to the immunosuppressive tumor microenvironment (TME), little immunogenicity, and low tumor mutation burden (TMB) of PC (2, 10).

Further investigation was needed to apply ICI therapy in PC, and combination therapy represented a promising avenue for exploration. Notably, there were divergent opinions regarding the superiority of ICI plus chemotherapy over standard chemotherapy in PC. Wainberg et al. (11) showed that nivolumab (PD-1 antibody) combined with nab-paclitaxel plus gemcitabine for PC was not superior to nab-paclitaxel plus gemcitabine alone in a phase I trial. Kamath et al. (12) failed to demonstrate superior efficacy of the combination of ipilimumab (CTLA-4 antibody) and gemcitabine for treating advanced PC compared to gemcitabine alone. Similarly, Fu et al. (13) also demonstrated disappointing results in the phase II clinical study, reporting no significant difference in survival benefit between sintilimab (PD-1 antibody) plus the modified FOLFIRINOX arm and modified FOLFIRINOX arm alone among 55 patients with advanced PC. However, Padrón et al. (3) demonstrated that the combination of nivolumab and gemcitabine plus nab-paclitaxel for PC resulted in a higher 1-year OS rate than gemcitabine plus nab-paclitaxel alone (57.7% vs. 35%) in a phase II trial. Gong et al. found that patients with advanced PC who received first-line ICI had longer survival (14). It was necessary to determine whether the addition of ICI to standard chemotherapy conferred superior outcomes compared to chemotherapy alone in PC.

Recently, our center has observed promising responses in patients with PC when combining PD-1 blockade with nab-paclitaxel plus gemcitabine. Therefore, we conducted a retrospective study to investigate whether PD-1 blockade combined with chemotherapy surpasses chemotherapy alone in PC. Within this retrospective study, 53 patients diagnosed with PC were enrolled to receive either PD-1 blockade combined with nab-paclitaxel plus gemcitabine or nab-paclitaxel plus gemcitabine alone. The study assesses whether PD-1 blockade combined with chemotherapy conferred superior efficacy to chemotherapy alone in unresectable stage III/IV PC patients.

2 Methods

2.1 Patients

From January 2020 to January 2023, 53 patients diagnosed with stage III/IV PC were enrolled at the First People's Hospital of Changzhou. The inclusion and exclusion criteria are shown in Figure 1. All patients were diagnosed with primary pancreatic tumors based on histological examinations and immunohistochemical staining of fine needle aspiration biopsy specimens without undergoing surgical resection. Prior to treatment, patients underwent computed tomography (CT), magnetic resonance (MR), or positron emission tomography-CT (PET-CT) imaging, and staging was determined according to the AJCC 8th edition staging system (15). This study was approved by the Ethics Committee of the First People's Hospital of Changzhou. Due to the retrospective nature of the study, informed consent was waived by the Ethics Committee.

2.2 Treatment

All PC patients received first-line PD-1 blockade with or without chemotherapy. Eight patients (29.6%) received

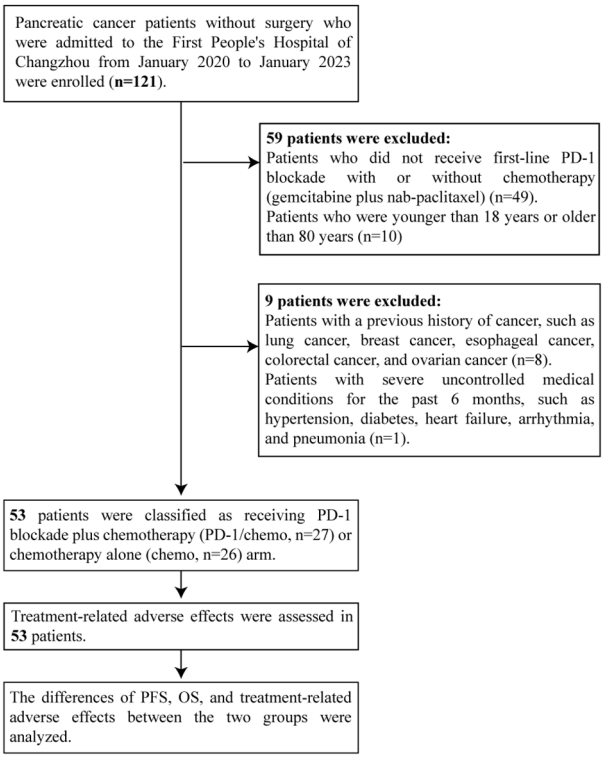

FIGURE 1
Patient flow chart. PD-1: Programmed cell death protein 1; PFS: Progression-free-survival.

sintilimab (200mg, day one every 21 days) in combination with gemcitabine (1000mg/m^2, days 1 and 8 every 21 days) plus nab-paclitaxel (125mg/m^2, days 1 and 8 every 21 days). Two patients (7.4%) received camrelizumab (200mg, day one every 21 days) combined with gemcitabine plus nab-paclitaxel. Sixteen patients (59.3%) received tislelizumab (200mg, day one every 21 days) combined with gemcitabine plus nab-paclitaxel. One patient (3.7%) received pembrolizumab (200mg, day one every 21 days) combined with gemcitabine plus nab-paclitaxel. Twenty-six patients received gemcitabine (1000mg/m^2, days 1 and 8 every 21 days) plus nab-paclitaxel (125mg/m^2, days 1 and 8 every 21 days).

2.3 Data collection and assessment

The patients with PC were classified as receiving PD-1 blockade plus chemotherapy (PD-1/chemo) or chemotherapy alone (chemo) arm. The primary endpoints of the study were progression-free survival (PFS) and overall survival (OS). The PFS was defined as the duration from treatment initiation to either disease progression or death, while OS was defined as the period from treatment initiation to death. The Response Evaluation Criteria in Solid Tumors (RECIST) version 1.1 was employed to assess disease progression (16). The Eastern Cooperative Oncology Group (ECOG) score was evaluated prior to the initiation of treatment in patients. Treatment-related adverse events of grade 3 or higher were also recorded.

2.4 Statistical analysis

Chi-square ($\chi 2$) statistics were utilized to evaluate the characteristic clinical differences between the two groups, while Kaplan-Meier curves were employed to assess the difference in PFS and OS. Median follow-up time was calculated using the reverse Kaplan-Meier method. Statistical significance was defined as P-values less than 0.05 ($P < 0.05$). The statistical software SPSS 25.0 and GraphPad were used for data processing.

3 Results

3.1 Baseline characteristics

Fifty-three patients were enrolled in this study, including 30 males (56.6%) and 23 females (43.4%). The median age of the study patients was 67 years, ranging from 45 to 79 years. All 53 patients (100%) were diagnosed with primary pancreas tumors. TNM stages III and IV distribution among patients with PC before treatment was 45.3% and 54.7%, respectively. The characteristics of the patients were summarized and presented in Table 1.

3.2 PFS and OS

The median follow-up duration was 22 months (range 1-28 months). In the PD-1/chemo arm, the median PFS was eight

10.3389/fonc.2023.1281545

TABLE 1 Clinical characteristics.

Characteristic	Category	All Patients (n=53)	PD-1/chemo (n=27)	chemo (n=26)	*P*
Age (years)	Median (range)	67 (45-79)	64 (55-79)	68 (45-78)	
sex					0.691
	Male	30 (56.6%)	16 (53.3%)	14 (46.7%)	
	Female	23 (43.4%)	11 (47.8%)	12 (52.2%)	
Histology					0.465
Adenocarcinoma		41 (77.4%)	22 (53.7%)	19 (46.3%)	
Unknown		12 (22.6%)	5 (41.7%)	7 (58.3%)	
c-TNM					0.328
	III	24 (45.3%)	14 (58.3%)	10 (41.7%)	
	IV	29 (54.7%)	13 (44.8%)	16 (55.2%)	
Metastic site					
	Liver	25 (47.2%)	10 (40%)	15 (60%)	
	Lung	1 (1.9%)	0 (0.0%)	1 (100%)	
	Bone	2 (3.8%)	0 (0.0%)	2 (100%)	
	Lymph	18 (34.0%)	8 (44.4%)	10 (55.6%)	
	Adrenal glands	3 (5.7%)	2 (66.7%)	1 (33.3%)	
ECOG score					0.497
	0	18 (34.0%)	8 (44.4%)	10 (55.6%)	
	1	35 (66.0%)	19 (54.3%)	16 (45.7%)	
Type of anti-PD-1					
	Sintilimab	8 (29.6%)	8 (100%)	0 (0.0%)	
	Camrelizumab	2 ((7.4%)	2 (100%)	0 (0.0%)	
	Tislelizumab	16 (59.3%)	16 (100%)	0 (0.0%)	
	Pembrolizumab	1 (3.7%)	1 (100%)	0 (0.0%)	

PD-1/chemo, PD-1 blockade plus chemotherapy; chemo, chemotherapy alone; ECOG, Eastern Cooperative Oncology Group.

months, whereas it was 3.5 months in the chemo arm (HR=0.459, 95% CI: 0.252-0.846, *P*=0.002). Furthermore, the median OS was 15 months in the PD-1/chemo arm and 8 months in the chemo arm (HR=0.345, 95% CI: 0.183-0.653, *P*<0.001) (Figure 2). Additionally, Figure 3 showed the CT follow-up outcomes of an individual patient in the PD-1/chemo arm.

3.3 Safety

Within the PD-1/chemo group, 15 patients (55.6%) experienced grade 3 treatment-related adverse events including leukopenia (n=6, 22.2%), neutropenia (n=5, 18.5%), anemia (n=3, 11.1%), thrombocytopenia (n=3, 11.1%), liver dysfunction (n=2, 7.4%), immune-related pneumonia (n=2, 7.4%), and immune-related enteritis (n=1, 3.7%). In the chemo group, 13 patients (50.0%) encountering grade 3 treatment-related adverse events, encompassing leukopenia (n=5, 19.2%), neutropenia (n=6, 23.1%), anemia (n=3, 11.5%), thrombocytopenia (n=5, 19.2%), and liver dysfunction (n=1, 3.8%). Treatment-related adverse events are detailed in Table 2.

4 Discussion

In this retrospective study, the PD-1/chemotherapy arm demonstrated a notable extension in median progression-free survival (PFS) by 4.5 months when compared to the chemotherapy-only arm. Additionally, both arms exhibited similar safety profiles. Notably, the PD-1/chemotherapy combination exhibited a substantial overall survival (OS) benefit, with a 7-month improvement over the chemotherapy-only arm. This suggested that the combination of ICI and chemotherapy might offer superior outcomes compared to the current standard treatment approach of chemotherapy alone for patients with unresectable locally advanced or advanced PC.

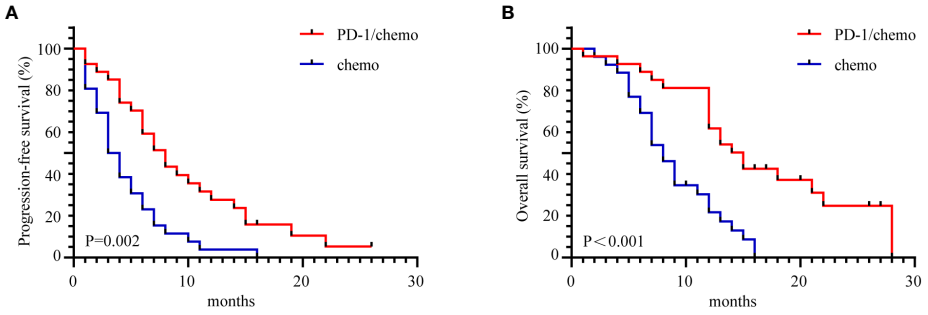

FIGURE 2
The Kaplan-Meier curves demonstrated a significant difference in PFS and OS between the PD-1/chemo arm and the chemo arm. **(A)** PFS of the PD-1/chemo arm was significantly superior to that of the chemo arm. **(B)** OS was significantly better in the PD-1/chemo arm compared to the chemo arm. PFS, Progression-free-survival; OS, overall survival; PD-1/chemo, PD-1 blockade plus chemotherapy; Chemo, Chemotherapy.

The efficacy of ICI monotherapy in PC patients has shown limitations (17, 18), and combination treatment options are being explored. ICI in tandem with chemotherapy has exhibited reliable efficacy in various solid tumors, including lung and breast cancer (19, 20). The superiority of ICI plus chemotherapy over standard chemotherapy for PC remained uncertain. A previous study showed that the median PFS and OS of PC patients treated with gemcitabine plus nab-paclitaxel were 5.5 months and 8.5 months, respectively (21). In a phase I study by Wainberg et al. involving 50 advanced PC patients, the combination of nivolumab with nab-paclitaxel and gemcitabine yielded median PFS and OS were 5.5 and 9.9 months, respectively (11). Therefore, Wainberg et al. (11) concluded that the PD-1 blockade plus chemotherapy was not superior to chemotherapy alone for treating PC. This disparity with our research findings could be attributed to distinct usage of antineoplastic drugs, including dosage and timing. Furthermore, patient heterogeneity may also account for the conflicting results. Importantly, consistent with this study, Padron et al. (3) demonstrated that combining PD-1 blockade with chemotherapy had higher 1-year OS than chemotherapy alone (57.7% vs 35%). And in a phase Ib/II trial of pembrolizumab plus chemotherapy, 12 patients with advanced PC had a median PFS of 9.1 months and OS of 15 months (22). These findings lend further support to the credibility of our research. Based on the available evidence, future studies are needed to identify PC populations susceptible to PD-1 blockade.

Multiple mechanisms contribute to immune resistance in PC (23, 24), and this study provides evidence that nab-paclitaxel and gemcitabine can enhance the immune response in patients with PC. The underlying mechanisms warrant further discussion. The resistance of PC to ICI therapy is mainly attributed to its special TME. ICI therapy relies on immune cells, and the low mutation burden of PC leads to the lack of infiltration of active immune cells in the TME (25). On the other hand, the components of the TME in PC, including tumor-associated macrophages, myeloid-derived suppressor cells, regulatory T cells, and tumor-associated fibroblasts, collectively contribute to immunosuppression (26). Finally, the TME of PC possesses a dense connective tissue stroma (27), which results in low T cell infiltration in the TME (28–30). Nab-paclitaxel or gemcitabine may improve the response of PC to ICI therapy by acting on these resistance pathways. Von Hoff et al. (31) showed that nab-paclitaxel alone or combined with gemcitabine reduced the proliferation of connective tissue stroma in PC. This may increase the infiltration of active immune cells in the TME of PC. However, Wainberg et al. (11) did not observe an increase in the infiltration of $CD8^+$ T cells and $CD4^+$ T cells in the TME of PC treated with nivolumab combined with nab-paclitaxel plus gemcitabine. Given the limited number of samples (11), further investigations are warranted to determine whether paclitaxel or gemcitabine can augment immune cell activation within the TME of PC. On the other hand, the low immunogenicity of PC contributed to the resistance of ICI (17), while chemotherapy had

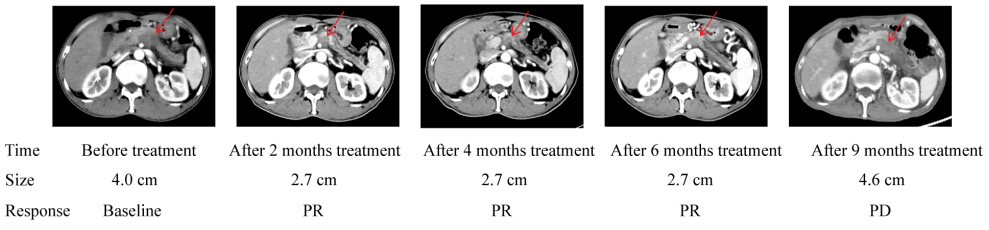

Time	Before treatment	After 2 months treatment	After 4 months treatment	After 6 months treatment	After 9 months treatment
Size	4.0 cm	2.7 cm	2.7 cm	2.7 cm	4.6 cm
Response	Baseline	PR	PR	PR	PD

FIGURE 3
Abdomen CT of the pancreatic cancer patient treated with PD-1/chemo showed a lesion in the pancreatic. The table below shows the response evaluation results according to RECIST 1.1 criteria. PR, Partial response; PD, Progressive disease.

TABLE 2 Treatment-related adverse events.

	Grade, NO. (%)					
	PD-1/chemo arm (n=27)			chemo arm (n=26)		
	Any	1-2	3	Any	1-2	3
TRAEs	22 (81.5)	21 (77.8)	15 (55.6)	21 (80.8)	19 (73.1)	13 (50.0)
Leukopenia	14 (51.9)	8 (29.6)	6 (22.2)	14 (53.8)	9 (34.6)	5 (19.2)
Neutropenia	12 (44.4)	7 (25.9)	5 (18.5)	14 (53.8)	8 (30.8)	6 (23.1)
Anemia	11 (40.7)	8 (29.6)	3 (11.1)	8 (30.8)	5 (19.2)	3 (11.5)
Thrombocytopenia	9 (33.3)	6 (22.2)	3 (11.1)	11 (42.3)	6 (23.1)	5 (19.2)
Liver dysfunction	12 (44.4)	10 (37.0)	2 (7.4)	10 (38.5)	9 (34.6)	1 (3.8)
Kidney dysfunction	3 (11.1)	3 (11.1)	0 (0.0)	1 (3.8)	1 (3.8)	0 (0.0)
Vomit	10 (37.0)	10 (37.0)	0 (0.0)	9 (34.6)	9 (34.6)	0 (0.0)
Immune-related pneumonia	6 (22.2)	4 (14.8)	2 (7.4)	0 (0.0)	0 (0.0)	0 (0.0)
Immune-related rash	6 (22.2)	6 (22.2)	0 (0.0)	0 (0.0)	0 (0.0)	0 (0.0)
Immune-related enteritis	2 (7.4)	1 (3.7)	1 (3.7)	0 (0.0)	0 (0.0)	0 (0.0)

TRAEs, Treatment-related adverse events; PD-1/chemo, programmed cell death protein 1 (PD-1) blockade plus chemotherapy; Chemo, chemotherapy.

the potential to enhance its immunogenicity (32–34). Chemotherapy could enhance ICI efficacy through its ability to increase the release of tumor antigens (35). Further research was necessary to elucidate the mechanism underlying our findings.

5 Limitations and prospects

The limitations inherent in this retrospective study must be acknowledged. Immune biomarkers, such as PD-L1, TMB, and MSI, were not assessed in participants prior to treatment. This limitation impeded our ability to identify a subset of patients with PC who may respond well to PD-1 blockade. The participants in this study were exclusively Chinese, potentially limiting generalizability to other populations.

Immunotherapy for PC remains a critical area of ongoing research with substantial challenges. According to the findings of our study, the combination therapy of PD-1 blockade with nab-paclitaxel and gemcitabine demonstrates the potential for enhancing clinical efficacy in a specific subgroup of patients diagnosed with PC. Future research direction lies in developing novel drug combinations aimed at enhancing the immune response against PC. For example, Rojas et al. (36) have successfully developed a personalized RNA neoantigen vaccine demonstrating the capacity to activate T cells in individuals with PC. Burrack et al. (37) demonstrated that the combination of PD-1 and PD-L1 blockade effectively reinvigorated T cells, resulting in a significant extension of survival in a murine model of PC. This drug combination presents a promising avenue for potential clinical trials. Furthermore, ongoing clinical trials exploring the combination of TIGIT/PD-1 co-blockade and CD40 agonism have exhibited substantial antitumor response in a murine PC model (38).

6 Conclusions

PD-1 blockade combined with nab-paclitaxel plus gemcitabine demonstrated superior efficacy to chemotherapy alone for unresectable stage III/IV PC patients. Subsequent studies should target identification of immunosensitive PC patient subgroups, paving the way for the development of more effective therapeutic strategies.

Data availability statement

The original contributions presented in the study are included in the article/supplementary material. Further inquiries can be directed to the corresponding authors.

Ethics statement

The studies involving humans were approved by Ethics Committee of the First People's Hospital of Changzhou. The studies were conducted in accordance with the local legislation and institutional requirements. Informed consent was waived by Ethics Committee of the First People's Hospital of Changzhou due to retrospective nature of study.

Author contributions

DC: Conceptualization, Formal Analysis, Software, Writing – original draft, Writing – review & editing. JH: Conceptualization, Formal Analysis, Software, Writing – original draft, Writing – review & editing. XW: Conceptualization, Formal Analysis, Software, Writing – original draft, Writing – review & editing. BW: Supervision, Validation, Writing – review & editing. RC: Supervision, Validation,

Writing – review & editing. WZ: Supervision, Validation, Writing – review & editing. CF: Funding acquisition, Supervision, Validation, Writing – review & editing. MJ: Funding acquisition, Supervision, Validation, Writing – review & editing.

Funding

The author(s) declare financial support was received for the research, authorship, and/or publication of this article. This study was supported by the Science and Technology Project for Youth Talent of Changzhou Health Commission (QN201703), Young Talent Development Plan of Changzhou Health Commission (CZQM2020024), Major Science and Technology Project of Changzhou Health Commission (ZD202004, ZD202007), and China Postdoctoral Science Foundation (2020M670064ZX).

Conflict of interest

The authors declare that the research was conducted in the absence of any commercial or financial relationships that could be construed as a potential conflict of interest.

Publisher's note

References

1. Siegel RL, Miller KD, Fuchs HE, Jemal A. Cancer statistics, 2022. *CA Cancer J Clin* (2022) 72(1):7–33. doi: 10.3322/caac.21708

2. Zhu YH, Zheng JH, Jia QY, Duan ZH, Yao HF, Yang J, et al. Immunosuppression, immune escape, and immunotherapy in pancreatic cancer: focused on the tumor microenvironment. *Cell Oncol (Dordr)* (2023) 46(1):17–48. doi: 10.1007/s13402-022-00741-1

3. Padrón LJ, Maurer DM, O'Hara MH, O'Reilly EM, Wolff RA, Wainberg ZA, et al. Sotigalimab and/or nivolumab with chemotherapy in first-line metastatic pancreatic cancer: clinical and immunologic analyses from the randomized phase 2 PRINCE trial. *Nat Med* (2022) 28(6):1167–77. doi: 10.1038/s41591-022-01829-9

4. Christenson ES, Jaffee E, Azad NS. Current and emerging therapies for patients with advanced pancreatic ductal adenocarcinoma: a bright future. *Lancet Oncol* (2020) 21(3):e135–e45. doi: 10.1016/s1470-2045(19)30795-8

5. Sharma P, Siddiqui BA, Anandhan S, Yadav SS, Subudhi SK, Gao J, et al. The next decade of immune checkpoint therapy. *Cancer Discovery* (2021) 11(4):838–57. doi: 10.1158/2159-8290.Cd-20-1680

6. O'Reilly EM, Oh DY, Dhani N, Renouf DJ, Lee MA, Sun W, et al. Durvalumab with or without tremelimumab for patients with metastatic pancreatic ductal adenocarcinoma: A phase 2 randomized clinical trial. *JAMA Oncol* (2019) 5 (10):1431–38. doi: 10.1001/jamaoncol.2019.1588

7. Royal RE, Levy C, Turner K, Mathur A, Hughes M, Kammula US, et al. Phase 2 trial of single agent Ipilimumab (anti-CTLA-4) for locally advanced or metastatic pancreatic adenocarcinoma. *J Immunother* (2010) 33(8):828–33. doi: 10.1097/CJI.0b013e3181eec14c

8. Patnaik A, Kang SP, Rasco D, Papadopoulos KP, Elassaiss-Schaap J, Beeram M, et al. Phase I study of pembrolizumab (MK-3475; anti-PD-1 monoclonal antibody) in patients with advanced solid tumors. *Clin Cancer Res* (2015) 21(19):4286–93. doi: 10.1158/1078-0432.Ccr-14-2607

9. Brahmer JR, Tykodi SS, Chow LQ, Hwu WJ, Topalian SL, Hwu P, et al. Safety and activity of anti-PD-L1 antibody in patients with advanced cancer. *N Engl J Med* (2012) 366(26):2455–65. doi: 10.1056/NEJMoa1200694

10. Lawlor RT, Mattiolo P, Mafficini A, Hong SM, Piredda ML, Taormina SV, et al. Tumor mutational burden as a potential biomarker for immunotherapy in pancreatic cancer: systematic review and still-open questions. *Cancers (Basel)* (2021) 13(13):3119–33. doi: 10.3390/cancers13133119

11. Wainberg ZA, Hochster HS, Kim EJ, George B, Kaylan A, Chiorean EG, et al. Open-label, phase I study of nivolumab combined with nab-paclitaxel plus gemcitabine in advanced pancreatic cancer. *Clin Cancer Res* (2020) 26(18):4814–22. doi: 10.1158/1078-0432.Ccr-20-0099

12. Kamath SD, Kalyan A, Kircher S, Nimeiri H, Fought AJ, Benson A 3rd, et al. Ipilimumab and gemcitabine for advanced pancreatic cancer: A phase Ib study. *Oncologist* (2020) 25(5):e808–e15. doi: 10.1634/theoncologist.2019-0473

13. Fu Q, Chen Y, Huang D, Guo C, Zhang X, Xiao W, et al. Sintilimab plus modified FOLFIRINOX in metastatic or recurrent pancreatic cancer: the randomized phase II CISPD3 trial. *Ann Surg Oncol* (2023) 30(8):5071–80. doi: 10.1245/s10434-023-13383-w

14. Gong X, Zhu Y, Zhang Q, Qiu X, Lu C, Tong F, et al. Efficacy and safety of immune checkpoint inhibitors in advanced pancreatic cancer: A real world study in Chinese cohort. *Hum Vaccin Immunother* (2022) 18(6):2143154–64. doi: 10.1080/21645515.2022.2143154

15. Chun YS, Pawlik TM, Vauthey JN. 8th edition of the AJCC cancer staging manual: pancreas and hepatobiliary cancers. *Ann Surg Oncol* (2018) 25(4):845–47. doi: 10.1245/s10434-017-6025-x

16. Eisenhauer EA, Therasse P, Bogaerts J, Schwartz LH, Sargent D, Ford R, et al. New response evaluation criteria in solid tumours: revised RECIST guideline (version 1.1). *Eur J Cancer* (2009) 45(2):228–47. doi: 10.1016/j.ejca.2008.10.026

17. Wandmacher AM, Letsch A, Sebens S. Challenges and future perspectives of immunotherapy in pancreatic cancer. *Cancers (Basel)* (2021) 13(16):4235–52. doi: 10.3390/cancers13164235

18. Mizugaki H, Yamamoto N, Murakami H, Kenmotsu H, Fujiwara Y, Ishida Y, et al. Phase I dose-finding study of monotherapy with atezolizumab, an engineered immunoglobulin monoclonal antibody targeting PD-L1, in Japanese patients with advanced solid tumors. *Invest New Drugs* (2016) 34(5):596–603. doi: 10.1007/s10637-016-0371-6

19. Gandhi L, Rodriguez-Abreu D, Gadgeel S, Esteban E, Felip E, De Angelis F, et al. Pembrolizumab plus chemotherapy in metastatic non-small-cell lung cancer. *N Engl J Med* (2018) 378(22):2078–92. doi: 10.1056/NEJMoa1801005

20. Schmid P, Adams S, Rugo HS, Schneeweiss A, Barrios CH, Iwata H, et al. Atezolizumab and Nab-paclitaxel in advanced triple-negative breast cancer. *N Engl J Med* (2018) 379(22):2108–21. doi: 10.1056/NEJMoa1809615

21. Von Hoff DD, Ervin T, Arena FP, Chiorean EG, Infante J, Moore M, et al. Increased survival in pancreatic cancer with nab-paclitaxel plus gemcitabine. *N Engl J Med* (2013) 369(18):1691–703. doi: 10.1056/NEJMoa1304369

22. Weiss GJ, Blaydorn L, Beck J, Bornemann-Kolatzki K, Urnovitz H, Schütz E, et al. Phase Ib/II study of gemcitabine, nab-paclitaxel, and pembrolizumab in metastatic pancreatic adenocarcinoma. *Invest New Drugs* (2018) 36(1):96–102. doi: 10.1007/s10637-017-0525-1

23. Sharma P, Hu-Lieskovan S, Wargo JA, Ribas A. Primary, adaptive, and acquired resistance to cancer immunotherapy. *Cell* (2017) 168(4):707–23. doi: 10.1016/j.cell.2017.01.017

24. Bear AS, Vonderheide RH, O'Hara MH. Challenges and opportunities for pancreatic cancer immunotherapy. *Cancer Cell* (2020) 38(6):788–802. doi: 10.1016/j.ccell.2020.08.004

25. Ho WJ, Jaffee EM, Zheng L. The tumour microenvironment in pancreatic cancer - clinical challenges and opportunities. *Nat Rev Clin Oncol* (2020) 17(9):527–40. doi: 10.1038/s41571-020-0363-5

26. Laface C, Memeo R, Maselli FM, Santoro AN, Iaia ML, Ambrogio F, et al. Immunotherapy and pancreatic cancer: A lost challenge? *Life (Basel)* (2023) 13 (7):1482–97. doi: 10.3390/life13071482

27. Hilmi M, Bartholin L, Neuzillet C. Immune therapies in pancreatic ductal adenocarcinoma: Where are we now? *World J Gastroenterol* (2018) 24(20):2137–51. doi: 10.3748/wjg.v24.i20.2137

28. Kanat O, Ertas H. Shattering the castle walls: Anti-stromal therapy for pancreatic cancer. *World J Gastrointest Oncol* (2018) 10(8):202–10. doi: 10.4251/wjgo.v10.i8.202

29. Ene-Obong A, Clear AJ, Watt J, Wang J, Fatah R, Riches JC, et al. Activated pancreatic stellate cells sequester CD8+ T cells to reduce their infiltration of the

juxtatumoral compartment of pancreatic ductal adenocarcinoma. *Gastroenterology* (2013) 145(5):1121–32. doi: 10.1053/j.gastro.2013.07.025

30. Blando J, Sharma A, Higa MG, Zhao H, Vence L, Yadav SS, et al. Comparison of immune infiltrates in melanoma and pancreatic cancer highlights VISTA as a potential target in pancreatic cancer. *Proc Natl Acad Sci U.S.A.* (2019) 116(5):1692–97. doi: 10.1073/pnas.1811067116

31. Von Hoff DD, Ramanathan RK, Borad MJ, Laheru DA, Smith LS, Wood TE, et al. Gemcitabine plus nab-paclitaxel is an active regimen in patients with advanced pancreatic cancer: a phase I/II trial. *J Clin Oncol* (2011) 29(34):4548–54. doi: 10.1200/jco.2011.36.5742

32. Homma Y, Taniguchi K, Nakazawa M, Matsuyama R, Mori R, Takeda K, et al. Changes in the immune cell population and cell proliferation in peripheral blood after gemcitabine-based chemotherapy for pancreatic cancer. *Clin Transl Oncol* (2014) 16 (3):330–5. doi: 10.1007/s12094-013-1079-0

33. Eriksson E, Wenthe J, Irenaeus S, Loskog A, Ullenhag G. Gemcitabine reduces MDSCs, tregs and TGFβ-1 while restoring the teff/treg ratio in patients with pancreatic cancer. *J Transl Med* (2016) 14(1):282–93. doi: 10.1186/s12967-016-1037-z

34. Shibuya KC, Goel VK, Xiong W, Sham JG, Pollack SM, Leahy AM, et al. Pancreatic ductal adenocarcinoma contains an effector and regulatory immune cell infiltrate that is altered by multimodal neoadjuvant treatment. *PloS One* (2014) 9(5): e96565–e77. doi: 10.1371/journal.pone.0096565

35. Reck M, Rodríguez-Abreu D, Robinson AG, Hui R, Csőszi T, Fülöp A, et al. Updated analysis of KEYNOTE-024: pembrolizumab versus platinum-based chemotherapy for advanced non-small-cell lung cancer with PD-L1 tumor proportion score of 50% or greater. *J Clin Oncol* (2019) 37(7):537–46. doi: 10.1200/jco.18.00149

36. Rojas LA, Sethna Z, Soares KC, Olcese C, Pang N, Patterson E, et al. Personalized RNA neoantigen vaccines stimulate T cells in pancreatic cancer. *Nature* (2023) 618 (7963):144–50. doi: 10.1038/s41586-023-06063-y

37. Burrack AL, Spartz EJ, Raynor JF, Wang I, Olson M, Stromnes IM. Combination PD-1 and PD-L1 blockade promotes durable neoantigen-Specific T cell-Mediated immunity in pancreatic ductal adenocarcinoma. *Cell Rep* (2019) 28(8):2140–55.e6. doi: 10.1016/j.celrep.2019.07.059

38. Freed-Pastor WA, Lambert LJ, Ely ZA, Pattada NB, Bhutkar A, Eng G, et al. The CD155/TIGIT axis promotes and maintains immune evasion in neoantigen-expressing pancreatic cancer. *Cancer Cell* (2021) 39(10):1342–60.e14. doi: 10.1016/j.ccell.2021.07.007

frontiers | Frontiers in Oncology

TYPE Systematic Review
PUBLISHED 08 February 2024
DOI 10.3389/fonc.2024.1331706

OPEN ACCESS

EDITED BY
Jennifer M. Bailey-Lundberg,
University of Texas Health Science Center at Houston, United States

REVIEWED BY
Antonella Argentiero,
National Cancer Institute Foundation (IRCCS), Italy
Vinod Kumar Yata,
University of South Florida, United States

*CORRESPONDENCE
Kaifeng Su
kaifeng.su@outlook.com

RECEIVED 01 November 2023
ACCEPTED 22 January 2024
PUBLISHED 08 February 2024

CITATION
Su K, Duan R and Wu Y (2024) Prognostic value of venous thromboembolism in patients with advanced pancreatic cancer: a systematic review and meta-analysis. *Front. Oncol.* 14:1331706. doi: 10.3389/fonc.2024.1331706

Prognostic value of venous thromboembolism in patients with advanced pancreatic cancer: a systematic review and meta-analysis

Kaifeng Su [1]*, Ruifeng Duan [2] and Yang Wu [3]

[1]Medical Faculty of Ludwig-Maximilians-University of Munich, University Hospital of LMU Munich, Munich, Germany, [2]Department of Gastroenterology and Digestive Endoscopy Center, The Second Hospital of Jilin University, Changchun, China, [3]Pancreas Center, The First Affiliated Hospital of Nanjing Medical University, Nanjing, China

Objective: This study aimed to investigate the relationship between the incidence of VTE and the prognosis of patients with advanced pancreatic cancer, as there is currently a lack of systematic research on this topic, despite the prevalence of venous thromboembolism (VTE) in patients with pancreatic cancer.

Methods: Databases including PubMed, Embase, Web of Science, and Cochrane Library were searched until April 9, 2023, to identify studies that explored the relationship between VTE and the prognosis of advanced pancreatic cancer. Duplicate publications, studies without full text or sufficient information for data extraction, animal experiments, reviews, and systematic reviews were excluded. The extracted data were analyzed using STATA 15.1.

Results: The pooled results indicated a significant association between the incidence of VTE and poorer overall survival (HR=1.38, 95% CI: 1.24 - 1.53, $p < 0.001$) and disease-free survival (HR=2.42, 95% CI: 1.94 - 3.04, $p < 0.001$) among patients with advanced pancreatic cancer. Additionally, early VTE showed a significant impact on overall survival (HR=2.03, 95% CI: 1.33 - 3.12, $p = 0.001$), whereas late VTE did not demonstrate a significant association with poor overall survival (HR=1.22, 95% CI: 0.96 - 1.54, $p = 0.099$).

Conclusions: This study found that advanced pancreatic cancer patients with VTE had poorer overall and disease-free survival than those without. Meanwhile, the patients with early VTE had a significantly poorer prognosis, whereas late VTE did not. The findings highlight the importance of timely detection of VTE for patients with advanced pancreatic cancer patients and offer a partial theoretical basis for future clinical endeavors.

Systematic review registration: https://www.crd.york.ac.uk/prospero/display_record.php?ID=CRD42023427043, identifier CRD42023427043.

KEYWORDS

venous thromboembolism, advanced pancreatic cancer, meta-analysis, prognosis, VTE

Introduction

Pancreatic cancer is a deadly disease with dismal prognoses and a rising incidence (1). It has surpassed breast cancer to become the third leading cause of cancer-related death in the United States. Worryingly, it is expected to surpass colorectal cancer and become the primary cause of cancer-related mortality by, 2040, trailing only lung cancer (2). Unfortunately, patients with pancreatic cancer still face bleak prognoses, with an overall survival rate of only 5% across all stages of this disease. Those with localized disease have a slightly higher survival rate of 20%, while patients with distant metastasis experience a survival rate of just 1% to 2% (3). Therefore, identifying prognostic risk factors in advance can enable physicians to implement timely treatment and preventive measures more effectively.

Venous thromboembolism (VTE) is a common complication among cancer patients, It occurs at a four to six-fold higher rate among cancer patients compared to those without cancer, which causes increased morbidity, mortality, and healthcare costs (4, 5). Cancer type and systemic chemotherapy are key risk factors for VTE development in cancer patients and pancreatic cancer is strongly associated with thrombotic problems (6). Multiple studies have demonstrated that advanced tumor stages pose a greater risk for VTE compared to early tumor stages (7–9). In pancreatic cancer patients receiving chemotherapy for advanced disease, the incidence of VTE can reach 40% (10). Notably, Blom et al. (11) recently reported a high incidence of VTE in patients with locally advanced or metastatic pancreatic cancer patients, with a 60-fold increased risk of venous thrombosis compared to the general population and a cumulative risk of nearly 10%. Previous epidemiological investigations have estimated the incidence of VTE in patients with metastatic pancreatic cancer to be as high as 41% (12). As the majority of patients with pancreatic cancer are diagnosed with advanced or metastatic disease, rendering surgery as an impractical curative option (13). Therefore, exploring the relationship between VTE and the prognosis in patients with advanced pancreatic cancer is of paramount importance. However, However, no consensus has been reached on whether VTE influences the prognosis of advanced pancreatic cancer. Some studies have indicated that the incidence of VTE is associated with poor prognosis in patients with pancreatic cancer (14–19), while others have reported no apparent impact caused by VTE on overall survival among patients with advanced pancreatic cancer (20–23).

Given these divergent results, we conducted a systematic literature review and meta-analysis to evaluate the relationship between VTE incidence and survival in patients with advanced pancreatic cancer. We aimed to provide a theoretical foundation for ascertaining and preventing VTE in these patients during their hospitalization.

Methods and materials

This study protocol is registered on PROSPERO (CRD42023427043). We followed the Systematic Reviews and Meta-analyses guidelines.

Literature search and inclusion criteria

We screened studies in PubMed, Embase, Web of Science, and Cochrane Library up to April 9, 2023. The following terms were used for the literature search: ("Pancreatic Neoplasms" [Mesh] OR "Pancreatic Cancer" [Mesh] OR "Pancreatic adenocarcinoma" [Mesh] OR "Pancreatic ductal adenocarcinoma" [Mesh] et al.) AND ("Venous Thrombosis" [Mesh] OR "Venous Thromboembolism" [Mesh] OR "Deep-Vein Thrombosis" [Mesh] et al.). Details of the literature search are presented in Supplementary Table 1.

Inclusion criteria are as follows: I) The studies included in the analysis consisted of both retrospective and prospective cohort studies and case-control studies. II) Participants enrolled in the studies were diagnosed with advanced pancreatic cancer, which included stage III/IV, locally advanced, metastasis, and unresectable cases. III) The exposure cohort consisted of individuals who experienced any type of VTE after the diagnosis of advanced pancreatic cancer, while the compare cohort included participants without VTE after the diagnosis of advanced pancreatic cancer (early VTE was classified as the occurrence before therapy, and late VTE was classified as the occurrence of it after treatment). IV) The primary outcome was overall and disease-free survival among participants.

Exclusion criteria are as follows: I) animal experiments, II) meta-analyses, reviews, conference abstracts and letters, III) randomized controlled studies (it aimed to assess the efficacy of the intervention, hence the lack of data on the prognosis of VTE in pancreatic cancer), IV) cross-sectional studies (its purpose was to evaluate epidemiologic investigations of a specific period. There is no match with our study which requires long term follow up).

Data extraction

Two researchers independently performed the literature search, filtering, and information extraction. In case of uncertainties or disagreements, a third party was consulted before the final decision. The data extraction involved gathering information on authors, publication year, study region, study type, sample size, age, gender, tumor stage, therapy, and outcome measures such as overall survival (OS) and disease-free survival (DFS). For studies providing data on OS and DFS, these two outcomes were expressed as hazard ratio (HR) with 95% confidence interval (CI). For articles presenting survival curves without explicit hazard ratios (HR) and 95% confidence intervals (CI), the Engauge Digitizer software (24) was utilized to extract the HR with 95% CI.

Literature quality assessment

Two researchers independently evaluated the quality of included studies using the Newcastle-Ottawa Scale (NOS) for cohort studies (25). Cohort studies were assessed using the NOS from three perspectives: the selection of study groups, the comparability of the groups, and the ascertainment of either the outcome of interest. A study was awarded up to nine scores, where a

score of no less than seven indicated high quality and a score of less than seven suggested low quality. Any disagreements over the decision on study quality were resolved by discussion with a third reviewer until a consensus was reached.

Statistical analysis

The data extracted from included studies were analyzed using the software STATA version 15.1 (Stata Corporation, College Station, TX, USA). OS and DFS were expressed as HR (95% CI). Heterogeneity across studies was assessed using Cochrane's Q test and the I^2 statistic. P ≥ 0.1 and I^2 ≤ 50% indicated no significant heterogeneity, and then a fixed-effects model would be utilized for data analysis; otherwise, a random-effects model would be employed. Additionally, sensitivity analysis was performed to test the stability of the results, and the publication bias was investigated using Begg's and Egger's tests. A p-value < 0.05 suggested statistical significance.

Results

Literature search

The initial literature search of databases produced 5,889 studies in total. The screening of titles and abstracts excluded 1,366 duplicates and another 4,460 articles. The review of the remaining 63 studies resulted in the removal of 53 studies failing to satisfy the eligibility criteria. Finally, ten studies were determined to be eligible for meta-analysis. The literature screening process is summarized in Figure 1.

Baseline characteristics and quality of the included studies

This meta-analysis targeted ten cohort studies comprising 3,145 patients in total (14–23). The sample sizes in these studies ranged from 170 to 838. Among the ten studies, 1,903 Asian patients (17, 18, 20, 22, 23) and 1,242 European and American patients (14–16, 19, 21) were enrolled. The majority of the patients were middle-aged and elderly individuals diagnosed with advanced pancreatic cancer. Treatment modalities included chemotherapy (14–16, 18–20, 22, 23) or chemoradiotherapy (17, 21). Our research aimed to assess the predictive value of VTE in patients with advanced pancreatic cancer by combining OS and DFS data. Six studies provided the HR with 95% CI directly (14–18, 22), and the rest four only presented survival curves that required independent extraction (19–21, 23). NOS scores for studies were above seven, indicating their quality satisfying the eligibility criteria. Study characteristics are summarized in Table 1.

Overall survival

Ten studies investigated the relationship between VTE and OS, involving 3,145 patients (605 patients with VTE and 2,540 patients without VTE). Since there was no significant heterogeneity across the ten studies (I^2 = 25.4%, p = 0.21), a fixed-effects model was employed to conduct the meta-analysis whose results showed that patients with VTE were significantly associated with poor OS (HR=1.38, 95% CI: 1.24 - 1.53, p < 0.001) (Table 2; Figure 2).

Subgroup analysis

Due to the heterogeneity of the research results, we performed a subgroup analysis based on the timing of the onset of VTE, extraction method, different regions, and types of therapy.

The OS among participants with early or late VTE was compared with that among those without VTE. The analysis results demonstrated that patients with early VTE were significantly associated with poor OS (HR=2.03, 95% CI: 1.33–3.12, p=0.001) (Table 2; Supplementary Figure S1). However, patients with late VTE were not significantly associated with poor OS (HR=1.22, 95% CI: 0.96–1.54, p=0.099) (Table 2; Supplementary Figure S2). The analysis of the HR (95% CI) that studies directly reported showed that patients with VTE were significantly associated with poor OS (HR=1.51, 95% CI: 1.29–1.76, p<0.001). Moreover, the same trend was noted in the analysis of the HR (95% CI) extracted by the software based on survival curves in studies of interest (HR=1.28, 95% CI: 1.10 - 1.48, p=0.001) (Table 2; Supplementary Figures S3, S4). Furthermore, the subgroup analysis based on the study population demonstrated s significant association between VTE and poor OS in both Europe and America (HR=1.55, 95% CI: 1.33–1.81, p < 0.001), as well as in the Asian region (HR=1.24, 95% CI: 1.07–1.43, p=0.005) (Table 2; Supplementary Figures S5, S6). Additionally, the analysis results revealed that VTE was significantly associated with poor OS in patients who underwent chemotherapy (HR=1.37, 95% CI: 1.22–1.53, p < 0.001) or chemoradiotherapy (HR=1.54, 95% CI: 1.05–2.25, p=0.026) (Table 2; Supplementary Figures S7, S8).

Disease-free survival

Among the ten studies, three studies involving 575 patients (122 patients with VTE and 453 patients without VTE) indicated a correlation between VTE and DFS. The meta-analysis of these three studies was performed using a fixed-effects model due to a lower degree of heterogeneous (I^2 = 2.1%, p=0.36). The analysis results showed that patients with VTE were significantly associated with poor DFS (HR=2.42, 95% CI: 1.94 - 3.04, p < 0.001) (Table 2; Figure 3).

Sensitivity analysis

We performed a sensitivity analysis to observe whether a particular article influenced the overall analysis results. Consequently, the results of this meta-analysis turned out to be stable and reliable for the investigation into the relationship between OS and DFS (Figures 4, 5).

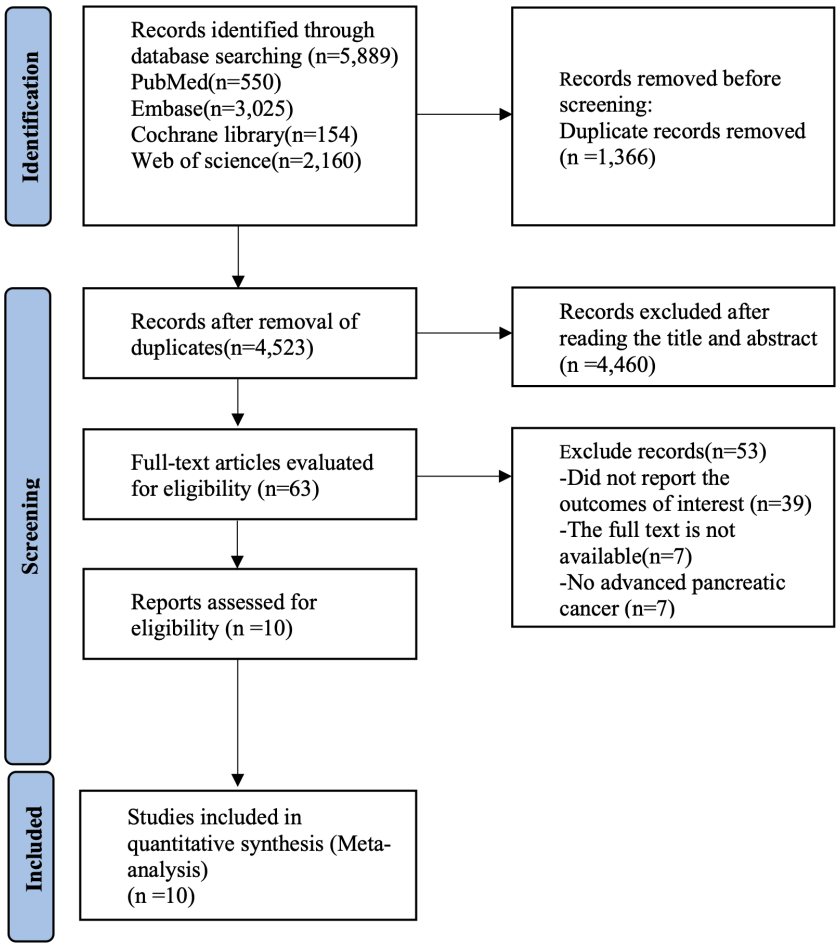

FIGURE 1
Flow diagram for selection of studies.

Publication bias

Egger's and Begg's tests were performed to assess the presence of publication bias across included studies (Figures 6, 7). Begg's test yielded a p-value of 0.107, while the r's test yielded a p-value of 0.041. These results suggested the possibility of publication bias. Therefore, the trim and fill method to was utilized assess the stability of the results. As a result, three articles were filled, and no changes were found in the results ($P < 0.001$) (Figure 8). In this regard, it can be concluded that publication bias did not significantly impact the final analysis results.

A comprehensive summary of the analyses and results can be found in Table 2.

Discussion

In the present systematic review and meta-analysis, we identified a poorer prognosis in patients with advanced pancreatic cancer patients who experienced VTE than those without VTE. Several factors may contribute to this observation.

Biological experiments have demonstrated that pancreatic cancer cells can induce a prothrombotic state by expressing tissue factor or procoagulant extracellular vesicles to hinder physiological inhibitors of coagulation and directly activate platelets to prompt the formation of neutrophil extracellular traps (26–29). In contrast, it has been demonstrated that activation of the hemostatic system promotes the development and progression of pancreatic cancer by enhancing cancer cell proliferation, invasion, metastasis, immune evasion, and chemoresistance (30–32). Therefore, the activation of the hemostatic system may benefit the progression of pancreatic cancer. Moreover, it was reported that a high incidence of VTE was specifically correlated with early metastatic development and the malignant grade of tumors (33). These findings suggest a close relationship between VTE occurrence and the aggressiveness of pancreatic cancer.

Aside from the liver and lung, bone tissue is the most frequent site of hematogenous metastasis (34). The prognosis of patients can be significantly impacted by bone metastases, which can result in bone pain, pathological fractures, spinal cord compression, hypercalcemia, and other unpleasant symptoms (35). Some studies reported the occurrence of bone metastasis in pancreatic

TABLE 1 Baseline Characteristics and Quality Assessment of the Included Studies.

Author	Year	Start Duration	Country	Sample Size	Gender (male/ female)	Age	Tumor Stage	Therapy	Time of VTE	Extraction method	Outcome	NOS Score
Mandala et al. (14)	2007	2001.12 – 2004.12	Italy	227	121/160	63 (38 -82)	locally advanced / metastatic	Chemotherapy	/	HR (95% CI)	OS/PFS	8
Lambert et al. (15)	2016	2001.01 – 2011.05	France	142	87/55	61 (28 -89)	locally advanced / metastatic	Chemotherapy	/	HR (95% CI)	OS	9
Kruger et al. (21)	2017	2002 -	Germany	299	102/70	63 (40 - 83)	locally advanced / metastatic	Chemo and radiotherapy	Before and after therapy	Survival curve	OS	8
Chen et al. (22)	2018	2010 - 2016	Chian	838	497/341	62 (23 -89)	Stage III/IV	Chemotherapy	Within and beyond 1.5 months after therapy	HR (95% CI)	OS	8
Kim et al. (23)	2018	2005.01 – 2015.12	Korea	216	131/85	63 (38 -83)	metastatic	Chemotherapy	Within and beyond 30 days after therapy	Survival curve	OS	8
Yoon et al. (20)	2018	2006.01 – 2012.12	Korea	505	294/211	65 (32 -88)	advanced	Chemotherapy	/	Survival curve	OS	8
Barrau et al. (16)	2021	2010 - 2019	France	174	96/78	67 (60 -75)	locally advanced / metastatic / recurrence after tumor resection	Chemotherapy	Before therapy	HR (95% CI)	OS/PFS	9
Yamai et al. (17)	2022	2017.04 – 2020.03	Japan	174	90/84	63 (45 -79)	unresectable metastatic	Chemo and radiotherapy	After therapy	HR (95% CI)	OS/PFS	9
Jeong et al. (18)	2023	2011.01 – 2020.12	Korea	170	99/71	64 (56 -72)	locally advanced / metastatic	Chemotherapy	After therapy	HR (95% CI)	OS	9
Laderman et al. (19)	2023	2010 - 2016	USA	400	208/192	66 (27-90)	metastatic	Chemotherapy	/	Survival curve	OS	8

"/": not provided in the article.

10.3389/fonc.2024.1331706

TABLE 2 The details of results after analysis.

Subgroups	Independent cohorts	Sample size	I^2	P	HR (95%CI)	P value	Egger	Begg	After Trim and Fill analysis (P)
Overall survival	10	3145	25.40%	0.21	1.38 (1.24 - 1.53)	< 0.001	0.041	0.107	< 0.001
Early VTE	4	1278	75.80%	0.006	2.03 (1.33 - 3.12)	0.001			
Late VTE	5	1531	39.80%	0.156	1.22 (0.96 - 1.54)	0.099			
Extraction method									
HR (95% CI)	6	1725	37%	0.16	1.51 (1.29 - 1.76)	< 0.001			
Survival curve	4	1420	0%	0.629	1.28 (1.10 - 1.48)	0.001			
Region									
Europe and America	5	1242	0%	0.543	1.55 (1.33 - 1.81)	< 0.001			
Asia	5	1903	11%	0.343	1.24 (1.07 - 1.43)	0.005			
Therapy									
Chemotherapy	8	2672	36.70%	0.136	1.37 (1.22 - 1.53)	< 0.001			
Chemo and radiotherapy	2	473	0%	0.422	1.54 (1.05 - 2.25)	0.026			
Disease-free survival	3	575	2.10%	0.36	2.42 (1.94 - 3.04)	< 0.001			

cancer and characterized by unfavorable outcomes. Skeletal metastases represent an underappreciated site of metastasis in patients with pancreatic cancer; however, the incidence of bone metastasis has increased in pancreatic cancer in recent years (36–39). Some patients with cancers were characterized by hypercoagulability and prone to thrombosis, which is the prerequisite for blood metastasis of tumor cells (40). Li et al. (41) studied that bone metastasis is more likely to occur when thrombosis occurs. Patients with bone metastasis were usually accompanied by impaired mobility, raising the incidence of VTE (42). Bone tumors could compress blood arteries, reducing venous blood flow, which increases the risk of vein thrombosis. Therefore, there may be a positive circuit between VTE and bone metastasis, both of which affect the prognosis of patients with pancreatic cancer. The particular mechanism needs to be researched in the future.

In subsequent subgroup analysis, patients were categorized into early and late VTE subgroups based on the timing of the onset of VTE. Interestingly, our findings revealed that only early VTE was associated with reduced patient survival, whereas late VTE did not exhibit the same impact. Generally, cancer cells generate procoagulant activators, such as tissue factor (TF), which trigger the coagulation cascade and contribute to an intrinsic and extrinsic hypercoagulable status, ultimately leading to the development of

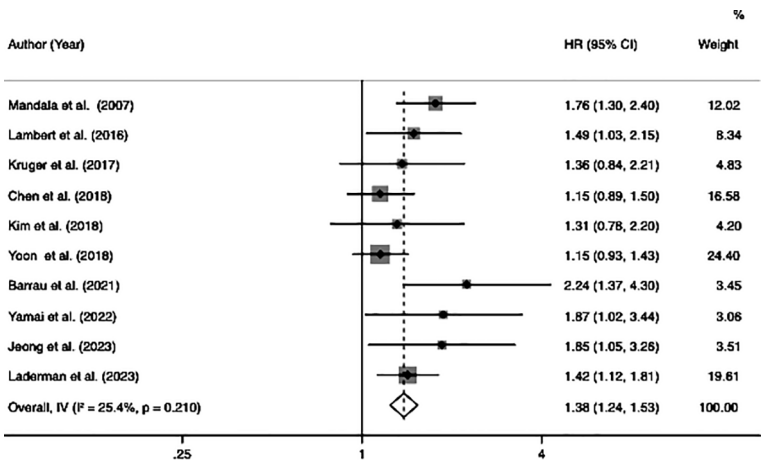

FIGURE 2
Forest plots of 10 studies examining the association between VTE and the overall survival of patients with advanced pancreatic cancer.

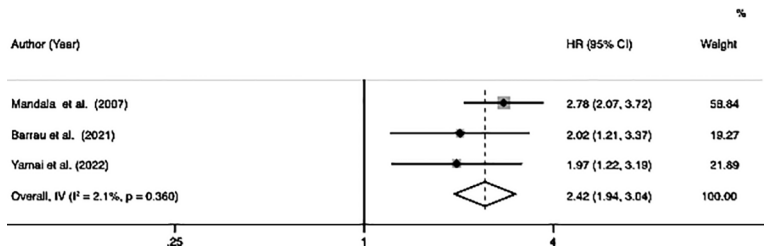

FIGURE 3
Forest plots of 3 studies examining the association between VTE and disease-free survival of patients with advanced pancreatic cancer.

VTE (43). Studies have demonstrated that TF expression occurs early in the neoplastic transformation of pancreatic cancer. This expression is linked to vascular endothelial growth factor (VEGF) expression, enhanced vascular permeability, and increased microvessel density, contributing to heightened mitogenic activity (44). In this regard, we propose that early VTE during cancer diagnosis might indicate an enhanced angiogenic status of the tumor, suggesting biologically aggressive characteristics responsible for a short prognosis. Moreover, it has been found that a hypercoagulable state in the body is correlated with a poor response to chemotherapy (45). Additionally, early VTE detection poses challenges as it often occurs without noticeable symptoms, with two-thirds of patients with early VTE exhibiting asymptomatic VTE, leading to missed therapeutic opportunities (23). Hence, we recommend that VTE screening be conducted even in patients without VTE-related symptoms at the initiation of palliative chemotherapy. Furthermore, the increased mortality observed in patients with early VTE may also be attributed to additional morbidity resulting from VTE itself, interruptions or delays in chemotherapy due to VTE management, or the administration of anticoagulant therapy.

Our data analysis showed that VTE had a significant impact on the OS of patients, whether the data was directly extracted from papers or extracted from the survival curves in articles. This indicates that our results exhibited a reliable and acceptable level of heterogeneity. Furthermore, it was observed that VTE had a detrimental effect on the OS of patients in both Europe and America, as well as in Asia. Despite the common understanding that Asian patients have a lower incidence of VTE compared to Western patients due to genetic, environmental, and lifestyle factors (46, 47), our results highlight the importance of not neglecting the role of VTE in Asian patients, as the effects of VTE did not exhibit significant difference based on region or race.

All patients included in our research received palliative chemotherapy or chemo/radiotherapy. In both of these treatment subgroups, it was observed that VTE had similar effects on patient survival. Chemotherapy exposure is known to independently increase the risk of VTE in patients with pancreatic cancer, and cytotoxic drugs may damage endothelial cells, promote thrombus formation, and alter the expression of coagulation factors, thereby exacerbating the hypercoagulable state associated with tumors (48). Additionally, emerging evidence suggests that radiation could enhance a pro-coagulant response and induce primary hemostasis, potentially leading to thrombosis (33). This raises the question of whether anticoagulant treatment should be considered for patients with advanced pancreatic cancer undergoing palliative therapy. Some researchers propose a preventative strategy to mitigate thrombosis in patients with pancreatic cancer, recommending the use of low molecular weight heparin (LMWH) as a first-line option for primary VTE prevention over several weeks, and several clinical trials have shown that this approach is beneficial for patient survival (44, 49). In fact, some Japanese

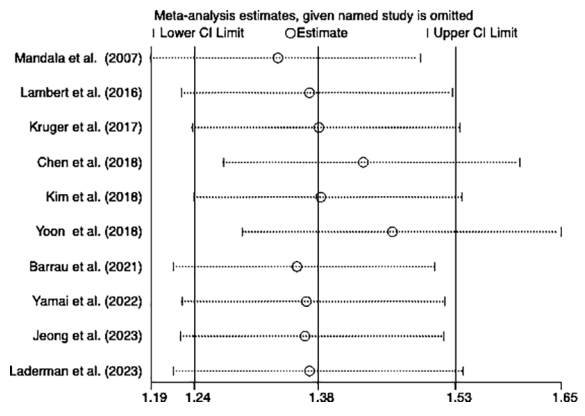

FIGURE 4
Sensitivity on the incidence of VTE and OS of patients.

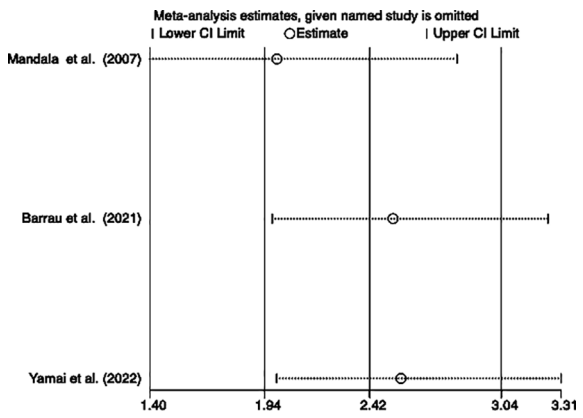

FIGURE 5
Sensitivity on the incidence of VTE and DFS of patients.

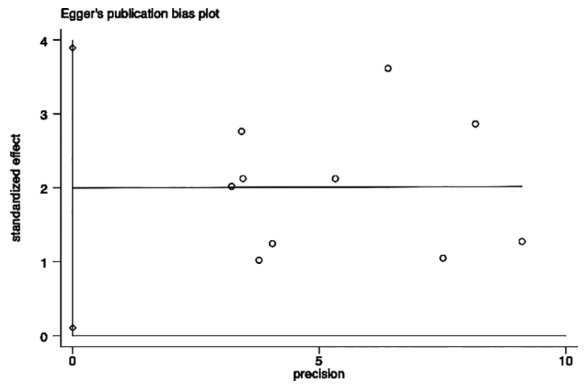

FIGURE 6
Egger test for evaluating the publication bias of this meta-analysis.

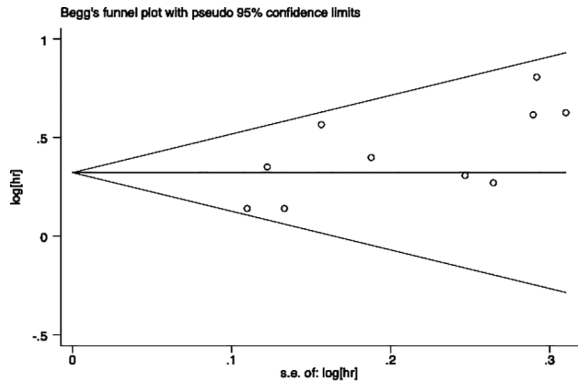

FIGURE 7
Begg test for evaluating the publication bias of this meta-analysis.

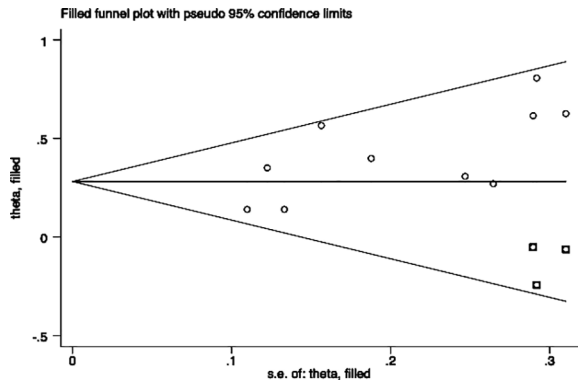

FIGURE 8
Funnel plot after Trim and Fill analysis.

experts have even suggested that patients with pancreatic cancer should receive long-term anticoagulant therapy until the tumor is healed to minimize the risk of VTE recurrence (50). Therefore, further investigation is warranted to determine the optimal details of the future anticoagulant strategy for these patients.

This study has several strengths. Firstly, this is the first study conducted on the effect of VTE on the prognosis of advanced pancreatic cancer. Secondly, all of our included articles were studied over a more extended period, which adds strength of evidence for survival studies. Thirdly, we had all survival analyses, including the survival curves and HR (hazard ratio), and we also conducted subgroup analyses exploring the prognostic impact of VTE under different conditions.

Despite the valuable findings obtained in this research, several limitations should be acknowledged. First, the majority of our data stemmed from retrospective analyses, which inherently introduce the potential for selection bias. Additionally, due to the lack of individual survival data associated with types of VTE and drugs in the original articles, we were unable to specifically classify the types of VTE or the specific palliative treatment drugs. Third, the absence of unified criteria or guidelines to define the timing of early VTE occurrence may have introduced calculation errors, resulting in deviations in the outcomes.

Conclusion

Our analysis collectively demonstrated that VTE predicted a poor prognosis in advanced pancreatic cancer when patients had it. Notably, patients who had early VTE experienced a considerably worse prognosis, but those with late VTE did not in the subgroup analysis. These findings hold partial value for informing further clinical work and reminding clinicians about the crucial role of early VTE detection prior to treatment initiation. it is essential to emphasize the necessity for future multicenter, large-scale, and prospective studies to elucidate the true significance and implications of these findings.

Data availability statement

The original contributions presented in the study are included in the article/Supplementary Material. Further inquiries can be directed to the corresponding author.

Author contributions

KS: Writing – original draft, Writing – review & editing. RD: Writing – review & editing. YW: Writing – review & editing.

Funding

The author(s) declare financial support was received for the research, authorship, and/or publication of this article. We would like to acknowledge the China Scholarship Council (CSC) for supporting the research and work of KS (No., 201908440264).

Conflict of interest

The authors declare that the research was conducted in the absence of any commercial or financial relationships that could be construed as a potential conflict of interest.

Publisher's note

All claims expressed in this article are solely those of the authors and do not necessarily represent those of their affiliated organizations, or those of the publisher, the editors and the reviewers. Any product that may be evaluated in this article, or claim that may be made by its manufacturer, is not guaranteed or endorsed by the publisher.

Supplementary material

The Supplementary Material for this article can be found online at: https://www.frontiersin.org/articles/10.3389/fonc.2024.1331706/full#supplementary-material

References

1. Cai J, Chen H, Lu M, Zhang Y, Lu B, You L, et al. Advances in the epidemiology of pancreatic cancer: Trends, risk factors, screening, and prognosis. *Cancer Lett* (2021) 520:1–11. doi: 10.1016/j.canlet.2021.06.027

2. Halbrook CJ, Lyssiotis CA, Pasca di Magliano M, Maitra A. Pancreatic cancer: Advances and challenges. *Cell* (2023) 186(8):1729–54. doi: 10.1016/j.cell.2023.02.014

3. Chang MC, Wong JM, Chang YT. Screening and early detection of pancreatic cancer in high risk population. *World J Gastroenterol* (2014) 20(9):2358–64. doi: 10.3748/wjg.v20.i9.2358

4. Lyman GH, Culakova E, Poniewierski MS, Kuderer NM. Morbidity, mortality and costs associated with venous thromboembolism in hospitalized patients with cancer. *Thromb Res* (2018) 164 Suppl 1:S112–S8. doi: 10.1016/j.thromres.2018.01.028

5. Heit JA, Silverstein MD, Mohr DN, Petterson TM, O'Fallon WM, Melton LJ 3rd. Risk factors for deep vein thrombosis and pulmonary embolism: A population-based case-control study. *Arch Intern Med* (2000) 160(6):809–15. doi: 10.1001/archinte.160.6.809

6. Khorana AA, Dalal M, Lin J, Connolly GC. Incidence and predictors of venous thromboembolism (Vte) among ambulatory high-risk cancer patients undergoing chemotherapy in the United States. *Cancer* (2013) 119(3):648–55. doi: 10.1002/cncr.27772

7. Cronin-Fenton DP, Sondergaard F, Pedersen LA, Fryzek JP, Cetin K, Acquavella J, et al. Hospitalisation for venous thromboembolism in cancer patients and the general population: A population-based cohort study in Denmark, 1997-2006. *Br J Cancer* (2010) 103(7):947–53. doi: 10.1038/sj.bjc.6605883

8. Gade IL, Braekkan SK, Naess IA, Hansen JB, Cannegieter SC, Overvad K, et al. The impact of initial cancer stage on the incidence of venous thromboembolism: The Scandinavian thrombosis and cancer (Stac) cohort. *J Thromb Haemost* (2017) 15(8):1567–75. doi: 10.1111/jth.13752

9. Timp JF, Braekkan SK, Versteeg HH, Cannegieter SC. Epidemiology of cancer-associated venous thrombosis. *Blood* (2013) 122(10):1712–23. doi: 10.1182/blood-2013-04-460121

10. Boone BA, Zenati MS, Rieser C, Hamad A, Al-Abbas A, Zureikat AH, et al. Risk of venous thromboembolism for patients with pancreatic ductal adenocarcinoma undergoing preoperative chemotherapy followed by surgical resection. *Ann Surg Oncol* (2019) 26(5):1503–11. doi: 10.1245/s10434-018-07148-z

11. Blom JW, Osanto S, Rosendaal FR. High risk of venous thrombosis in patients with pancreatic cancer: A cohort study of 202 patients. *Eur J Cancer* (2006) 42(3):410–4. doi: 10.1016/j.ejca.2005.09.013

12. Kruger S, Haas M, Burkl C, Goehring P, Kleespies A, Roeder F, et al. Incidence, outcome and risk stratification tools for venous thromboembolism in advanced pancreatic cancer - a retrospective cohort study. *Thromb Res* (2017) 157:9–15. doi: 10.1016/j.thromres.2017.06.021

13. Frere C, Bournet B, Benzidia I, Jamelot M, Debourdeau P, Hij A, et al. Venous thromboembolism and pancreatic cancer. *J Med Vasc* (2018) 43(4):246–54. doi: 10.1016/j.jdmv.2018.05.003

14. Mandala M, Reni M, Cascinu S, Barni S, Floriani I, Cereda S, et al. Venous thromboembolism predicts poor prognosis in irresectable pancreatic cancer patients. *Ann Oncol* (2007) 18(10):1660–5. doi: 10.1093/annonc/mdm284

15. Lambert M, Ploquin A, Declerck L, Duhamel A, Makhloufi S, Turpin A, et al. Deep vein thrombosis: An independent poor prognosis factor of advanced pancreatic adenocarcinoma. *Anticancer Res* (2016) 36(10):5527–30. doi: 10.21873/anticanres.11135

16. Barrau M, Maoui K, Le Roy B, Roblin X, Mismetti P, Phelip JM, et al. Early venous thromboembolism is a strong prognostic factor in patients with advanced pancreatic ductal adenocarcinoma. *J Cancer Res Clin Oncol* (2021) 147(11):3447–54. doi: 10.1007/s00432-021-03590-x

17. Yamai T, Ikezawa K, Hiraga E, Kawamoto Y, Hirao T, Higashi S, et al. Early detection of venous thromboembolism after the initiation of chemotherapy predicts a poor prognosis in patients with unresectable metastatic pancreatic cancer who underwent first-line chemotherapy with gemcitabine plus nab-paclitaxel. *PloS One* (2022) 17(3):e0264653. doi: 10.1371/journal.pone.0264653

18. Jeong HT, Bae JH, Kim HG, Han J. Venous thromboembolism in patients with advanced pancreatic cancer receiving palliative chemotherapy: Incidence and effect on prognosis. *Korean J Gastroenterol* (2023) 81(3):109–20. doi: 10.4166/kjg.2022.137

19. Laderman L, Sreekrishnanilayam K, Pandey RK, Handorf E, Blumenreich A, Sorice KA, et al. Venous thromboembolism in metastatic pancreatic cancer. *Eur J Haematol* (2023) 110(6):706–14. doi: 10.1111/ejh.13955

20. Yoon SY, Lee M-Y, Yoon J, Kim HJ, Kim K-H, Kim SH, et al. The incidence of venous thromboembolism is not lowin Korean patients with advanced pancreatic cancer. *Blood Res* (2018) 53(3):227–32. doi: 10.5045/br.2018.53.3.227

21. Kruger S, Haas M, Burkl C, Goehring P, Kleespies A, Roeder F, et al. Incidence, outcome and risk stratification tools for venous thromboembolism in advanced pancreatic cancer – a retrospective cohort study. *Thromb Res* (2017) 157:9–15. doi: 10.1016/j.thromres.2017.06.021

22. Chen J-S, Hung C-Y, Chang H, Liu C-T, Chen Y-Y, Lu C-H, et al. Venous thromboembolism in asian patients with pancreatic cancer following palliative chemotherapy: Low incidence but a negative prognosticator for those with early onset. *Cancers* (2018) 10(12):501. doi: 10.3390/cancers10120501

23. Kim JS, Kang EJ, Kim DS, Choi YJ, Lee SY, Kim HJ, et al. Early venous thromboembolism at the beginning of palliative chemotherapy is a poor prognostic factor in patients with metastatic pancreatic cancer: A retrospective study. *BMC Cancer* (2018) 18(1):1260. doi: 10.1186/s12885-018-5154-3

24. Tierney JF, Stewart LA, Ghersi D, Burdett S, Sydes MR. Practical methods for incorporating summary time-to-event data into meta-analysis. *Trials* (2007) 8:16. doi: 10.1186/1745-6215-8-16

25. Cook DA, Reed DA. Appraising the quality of medical education research methods: The medical education research study quality instrument and the newcastle-ottawa scale-education. *Acad Med* (2015) 90(8):1067–76. doi: 10.1097/ACM.0000000000000786

26. Moik F, Prager G, Thaler J, Posch F, Wiedemann S, Schramm T, et al. Hemostatic biomarkers and venous thromboembolism are associated with mortality and response to chemotherapy in patients with pancreatic cancer. *Arterioscler Thromb Vasc Biol* (2021) 41(11):2837–47. doi: 10.1161/ATVBAHA.121.316463

27. Campello E, Ilich A, Simioni P, Key NS. The relationship between pancreatic cancer and hypercoagulability: A comprehensive review on epidemiological and biological issues. *Br J Cancer* (2019) 121(5):359–71. doi: 10.1038/s41416-019-0510-x

28. Hisada Y, Ay C, Auriemma AC, Cooley BC, Mackman N. Human pancreatic tumors grown in mice release tissue factor-positive microvesicles that increase venous clot size. *J Thromb Haemost* (2017) 15(11):2208–17. doi: 10.1111/jth.13809

29. Hisada Y, Grover SP, Maqsood A, Houston R, Ay C, Noubouossie DF, et al. Neutrophils and neutrophil extracellular traps enhance venous thrombosis in mice bearing human pancreatic tumors. *Haematologica* (2020) 105(1):218–25. doi: 10.3324/haematol.2019.217083

30. Ruf W, Disse J, Carneiro-Lobo TC, Yokota N, Schaffner F. Tissue factor and cell signalling in cancer progression and thrombosis. *J Thromb Haemost* (2011) 9 Suppl 1 (Suppl 1):306–15. doi: 10.1111/j.1538-7836.2011.04318.x

31. Queiroz KC, Shi K, Duitman J, Aberson HL, Wilmink JW, van Noesel CJ, et al. Protease-activated receptor-1 drives pancreatic cancer progression and chemoresistance. *Int J Cancer* (2014) 135(10):2294–304. doi: 10.1002/ijc.28726

32. Schweickert PG, Yang Y, White EE, Cresswell GM, Elzey BD, Ratliff TL, et al. Thrombin-par1 signaling in pancreatic cancer promotes an immunosuppressive microenvironment. *J Thromb Haemost* (2021) 19(1):161–72. doi: 10.1111/jth.15115

33. Hamza MS, Mousa SA. Cancer-associated thrombosis: risk factors, molecular mechanisms, future management. *Clin Appl Thromb Hemost* (2020) 26:1076029620954282. doi: 10.1177/1076029620954282

34. Taniguchi Y, Tamiya A, Nakahama K, Naoki Y, Kanazu M, Omachi N, et al. Impact of metastatic status on the prognosis of egfr mutation-positive non-small cell lung cancer patients treated with first-generation egfr-tyrosine kinase inhibitors. *Oncol Lett* (2017) 14(6):7589–96. doi: 10.3892/ol.2017.7125

35. Kuchuk M, Kuchuk I, Sabri E, Hutton B, Clemons M, Wheatley-Price P. The incidence and clinical impact of bone metastases in non-small cell lung cancer. *Lung Cancer* (2015) 89(2):197–202. doi: 10.1016/j.lungcan.2015.04.007

36. Iguchi H, Yasuda M, Matsuo T, Sumii T, Funakoshi A. [Clinical features and management of pancreatic cancer with bone metastases]. *Nihon Shokakibyo Gakkai Zasshi* (2004) 101(8):872–8.

37. Borad MJ, Saadati H, Lakshmipathy A, Campbell E, Hopper P, Jameson G, et al. Skeletal metastases in pancreatic cancer: A retrospective study and review of the literature. *Yale J Biol Med* (2009) 82(1):1–6.

38. Argentiero A, Calabrese A, Solimando AG, Notaristefano A, Panarelli MMG, Brunetti O. Bone metastasis as primary presentation of pancreatic ductal adenocarcinoma: A case report and literature review. *Clin Case Rep* (2019) 7(10):1972–6. doi: 10.1002/ccr3.2412

39. Saif MW, Galanina N, Ravage-Mass L, Kaley K, Cornfeld D, Lamb L, et al. Bone metastasis as the only metastatic site in a patient with pancreatic cancer following distal pancreatectomy. *Case Rep Med* (2010) 2010:634975. doi: 10.1155/2010/634975

40. Tang C, Liao Z, Hess K, Chance WW, Zhuang Y, Jensen G, et al. Prognosis and predictors of site of first metastasis after definitive radiation therapy for non-small cell lung cancer. *Acta Oncol* (2016) 55(8):1022–8. doi: 10.3109/0284186X.2016.1154602

41. Li Y, Xu C, Yu Q. Risk factor analysis of bone metastasis in patients with non-small cell lung cancer. *Am J Transl Res* (2022) 14(9):6696–702.

42. Macedo F, Ladeira K, Pinho F, Saraiva N, Bonito N, Pinto L, et al. Bone metastases: an overview. *Oncol Rev* (2017) 11(1):321. doi: 10.4081/oncol.2017.321

43. Rickles FR, Patierno S, Fernandez PM. Tissue factor, thrombin, and cancer. *Chest* (2003) 124(3 Suppl):58S–68S. doi: 10.1378/chest.124.3_suppl.58s

44. Ansari D, Ansari D, Andersson R, Andren-Sandberg A. Pancreatic cancer and thromboembolic disease, 150 years after trousseau. *Hepatobiliary Surg Nutr* (2015) 4 (5):325–35. doi: 10.3978/j.issn.2304-3881.2015.06.08

45. Tomimaru Y, Yano M, Takachi K, Kishi K, Miyashiro I, Ohue M, et al. Correlation between pretherapeutic D-dimer levels and response to neoadjuvant chemotherapy in patients with advanced esophageal cancer. *Dis Esophagus* (2008) 21 (4):281–7. doi: 10.1111/j.1442-2050.2007.00758.x

46. Klatsky AL, Baer D. What protects asians from venous thromboembolism? *Am J Med* (2004) 116(7):493–5. doi: 10.1016/j.amjmed.2004.01.005

47. Steffen LM, Folsom AR, Cushman M, Jacobs DR Jr., Rosamond WD. Greater fish, fruit, and vegetable intakes are related to lower incidence of venous thromboembolism: The longitudinal investigation of thromboembolism etiology. *Circulation* (2007) 115(2):188–95. doi: 10.1161/CIRCULATIONAHA.106.641688

48. Dallos MC, Eisenberger AB, Bates SE. Prevention of venous thromboembolism in pancreatic cancer: Breaking down a complex clinical dilemma. *Oncologist* (2020) 25 (2):132–9. doi: 10.1634/theoncologist.2019-0264

49. Sarantis P, Karamouzis MV. The impact of thromboprophylaxis with lmwhs on the survival of patients with pancreatic cancer. *Thromb Res* (2022) 213 Suppl 1:S120–S6. doi: 10.1016/j.thromres.2022.02.004

50. Suzuki T, Hori R, Takeuchi K, Yamamura R, Katoh H, Noji Y, et al. Venous thromboembolism in Japanese patients with pancreatic cancer. *Clin Appl Thromb Hemost* (2021) 27:10760296211051766. doi: 10.1177/10760296211051766

frontiers | Frontiers in Oncology

TYPE Review
PUBLISHED 21 February 2024
DOI 10.3389/fonc.2024.1345810

OPEN ACCESS

EDITED BY
Jennifer M. Bailey-Lundberg,
University of Texas Health Science Center at Houston, United States

REVIEWED BY
Antonella Argentiero,
National Cancer Institute Foundation (IRCCS), Italy
Vinod Kumar Yata,
University of South Florida, United States

*CORRESPONDENCE
Yue Wang
wangyue1@cancerhosp-ln-cmu.com
Yang Liu
yangliu5490@163.com

†These authors share first authorship

RECEIVED 28 November 2023
ACCEPTED 29 January 2024
PUBLISHED 21 February 2024

CITATION
Zhao G, Chen X, Zhu M, Liu Y and Wang Y (2024) Exploring the application and future outlook of Artificial intelligence in pancreatic cancer.
Front. Oncol. 14:1345810.
doi: 10.3389/fonc.2024.1345810

Exploring the application and future outlook of Artificial intelligence in pancreatic cancer

Guohua Zhao[1†], Xi Chen[1,2†], Mengying Zhu[1,2], Yang Liu[3*] and Yue Wang[1*]

[1]Department of General Surgery, Cancer Hospital of China Medical University, Liaoning Cancer Hospital & Institute, Liaoning, China, [2]Department of Clinical integration of traditional Chinese and Western medicine, Liaoning University of Traditional Chinese Medicine, Liaoning, China, [3]Department of Ophthalmology, First Hospital of China Medical University, Liaoning, China

Pancreatic cancer, an exceptionally malignant tumor of the digestive system, presents a challenge due to its lack of typical early symptoms and highly invasive nature. The majority of pancreatic cancer patients are diagnosed when curative surgical resection is no longer possible, resulting in a poor overall prognosis. In recent years, the rapid progress of Artificial intelligence (AI) in the medical field has led to the extensive utilization of machine learning and deep learning as the prevailing approaches. Various models based on AI technology have been employed in the early screening, diagnosis, treatment, and prognostic prediction of pancreatic cancer patients. Furthermore, the development and application of three-dimensional visualization and augmented reality navigation techniques have also found their way into pancreatic cancer surgery. This article provides a concise summary of the current state of AI technology in pancreatic cancer and offers a promising outlook for its future applications.

KEYWORDS

pancreatic cancer, Artificial intelligence, early screening, personalized treatment, management

1 Introduction

Pancreatic carcinoma represents a prevalent malignancy of the digestive system, characterized by elusive prodromal symptoms, heightened invasiveness, and an elevated propensity for postoperative metastasis and relapse. As delineated by the International Agency for Research on Cancer, pancreatic cancer assumes the fourteenth position amidst the 36 most prevalent malignant neoplasms in terms of incidence, and ranks seventh in mortality rates (1). An additional epidemiological analysis revealed a staggering 60,430 newly diagnosed cases of pancreatic cancer, resulting in 48,220 fatalities within the United States during the year 2021 (2). Projections suggest that by 2030, pancreatic cancer could ascend to become the second leading cause of cancer-related mortality in the United States (3). The sentence is clear and properly structured. The current diagnostic paradigm for

pancreatic cancer primarily hinges upon imaging modalities such as CT and MRI, supplemented by the judicious use of PET-CT for comprehensive assessment when warranted. Notably, endoscopic ultrasonography (EUS) and EUS-guided fine needle biopsy assume pivotal roles in the diagnosis and staging of pancreatic cancer, albeit their diagnostic precision is subject to multifarious technical considerations. While radical surgery remains the cornerstone of pancreatic carcinoma management (4), neoadjuvant therapy has emerged as a burgeoning area of investigation (5). However, the absence of a standardized framework for assessing its efficacy poses a significant challenge. Furthermore, the prognosis following pancreatic cancer resection remains fraught with a substantial risk of tumor recurrence, thereby necessitating vigilant surveillance through regular follow-up regimens.

The term "Artificial intelligence (AI)" was first coined in 1956, with a focus on using machines to imitate human learning and cognitive abilities. Machine learning, a practical application of AI, employs diverse algorithms such as decision trees, random forests, artificial neural networks, support vector machines, logistic regression, Bayesian methods, K-nearest neighbors, among others. One such method, deep learning, is classified under the category of artificial neural networks (6) and has exhibited exceptional performance in image processing, notably through convolutional neural networks. By accurately and objectively identifying characteristic values of images based on standardized decision-making protocols, deep learning can comprehensively analyze statistical relationships between these values and associated outcomes. AI-based radiomics can thus achieve precise diagnosis of pancreatic cancer, while deep learning can establish early high-risk prediction models for pancreatic cancer and postoperative recurrence risk prediction models, facilitating early screening and assisting in the management of complications after pancreatic cancer surgery.

2 AI-assisted early screening and risk prediction of pancreatic cancer

By harnessing foundational data encompassing precancerous lesions, population-level health parameters, and a spectrum of biological markers pertinent to pancreatic cancer, AI holds promise in constructing predictive models to gauge the propensity for pancreatic cancer incidence, thereby enabling early detection and intervention. Intraductal papillary mucinous neoplasm (IPMN) serves as a precursor lesion in the development of pancreatic cancer (7). To explore IPMN, a study (8) curated an extensive compendium of 3,970 endoscopic ultrasound (EUS) images sourced from histopathologically validated IPMN patients, serving as inputs for sophisticated deep learning algorithms. Introducing the concept of the AI value, a continuous variable spanning 0 to 1, as well as the AI malignancy probability, denoting the mean AI value per patient, the researchers discerned markedly elevated average AI values in malignant IPMN vis-à-vis benign instances (0.808 vs. 0.104, $P<0.01$). Importantly, the model showcased commendable predictive prowess, exemplified by an impressive area under the curve (AUC) of 0.98 for the receiver operating characteristic curve of AI malignancy probability, thus validating its potential in prognosticating the transformation of IPMN into malignant tumors. Notably, the AI-based diagnosis exhibited superior sensitivity, specificity, and accuracy (95.7%, 92.6%, and 94.0% respectively) compared to physicians' diagnostic accuracy (56.0%).

Constituting a reservoir of cumulative healthcare data, longitudinal electronic health records have emerged as a pivotal asset for researchers endeavoring to construct predictive models targeting medical prognostication. Recent investigations spearheaded (9–11) have honed in on the development of predictive frameworks tailored to unearthing high-risk subcohorts vulnerable to pancreatic cancer within the diabetic patient cohort. Particularly salient is the work (9), that derived a prognostic schema from a cohort of newly diagnosed diabetes patients, synthesizing key determinants encompassing age at diabetes onset, body mass index, and glycemic fluctuations. This intricately woven algorithm furnished predictive scores adept at forecasting the incipient trajectory toward pancreatic neoplasms within a triennial window. Notably, patients scoring 3 or above evinced a diagnostic sensitivity and specificity of 80% for pancreatic carcinoma (AUC=0.87), marking a 4.4-fold escalation in pancreatic cancer incidence vis-à-vis their diabetic counterparts. Meanwhile, another study (10) leveraged both logistic regression and artificial neural network methodologies to craft predictive architectures pertinent to type 2 diabetes patients in Taiwan, marshaling parameters inclusive of age, antidiabetic pharmaceutical usage, and comorbid ailments as prospective risk determinants for pancreatic cancer. Intriguingly, the logistic regression model emerged as the more discerning performer, boasting an AUC of 0.727. In a similar vein, Blyuss et al. (12) developed a novel pancreatic cancer patient risk scoring system (PancRisk) predicated on urinary biomarkers. The team measured three urine biomarkers (LYVE1, REC1B, TFF1) in 199 pancreatic ductal adenocarcinoma patients and 180 healthy individuals and applied machine learning algorithms to analyze and compare the datasets. The resulting logistic regression model demonstrated remarkable diagnostic power with an AUC of 0.94. When combined with the established tumor marker CA19-9, the model achieved a diagnostic specificity and sensitivity of 96%.

3 AI-assisted diagnosis of pancreatic cancer

Diagnosing pancreatic cancer is a multifaceted process that typically involves clinical manifestations, high-risk factors, serum tumor markers, and imaging techniques such as endoscopic ultrasound (EUS). However, imaging examination remains the most crucial approach for clinical diagnosis of pancreatic cancer, with contrast-enhanced CT and MRI being the standard options (13). In recent years, deep learning models have emerged as a promising tool to aid pancreatic cancer diagnosis. Zhejiang

University, for example, developed a deep learning model trained on 319 patients' abdominal contrast-enhanced CT images that could provide pancreatic tumor diagnosis suggestions based on original abdominal CT images without preprocessing. Impressively, this model achieved an AUC of 0.871 and an F1 score of 88.5%, with an average diagnostic accuracy of 82.7% for all tumor types. Moreover, the model demonstrated exceptional accuracy in distinguishing IPMN and pancreatic ductal adenocarcinoma, reaching 100% and 87.6%, respectively (14). Additionally, a study from China (15) developed a convolutional neural network model trained on 7245 CT images from 222 pathologically confirmed pancreatic cancer patients and 190 normal pancreatic patients. The model was trained to differentiate between two categories (with or without pancreatic cancer) and three categories (no cancer, tumor in the body/tail of the pancreas, tumor in the head/neck of the pancreas), demonstrating remarkable accuracy in diagnosing plain scan images (95.47%) with high sensitivity (91.58%) and specificity (98.27%). Notably, the three-category model proved particularly adept at diagnosing tumors in the head/neck of the pancreas using arterial phase images.

Endoscopic ultrasound (EUS) is an indispensable tool for diagnosing pancreatic tumors and chronic pancreatitis (13). With the advent of AI, EUS images' diagnostic efficiency has been remarkably improved. To address the challenge of distinguishing autoimmune pancreatitis (AIP) from pancreatic ductal adenocarcinoma, chronic pancreatitis, and normal pancreas, Marya et al. (16) developed a convolutional neural network model based on EUS images. The model was trained using static images and videos from EUS examinations of patients. Impressively, the model achieved high sensitivity and specificity rates for differentiating AIP from pancreatic ductal adenocarcinoma (90% and 93%, respectively), normal pancreas (99% and 98%, respectively), and chronic pancreatitis (94% and 71%, respectively). Moreover, another research (17) implemented age grouping into the AI model trained on EUS images and conducted stratified analysis by dividing patients into three age groups (<40 years old, 40-60 years old, and >60 years old). The results showed that the grouped model outperformed the ungrouped one in terms of classification accuracy, sensitivity, and specificity, with rates ranging from 88.5% to 94.1%. Notably, the study highlights the importance of age grouping in enhancing the diagnostic efficiency of AI models for EUS images.

Additionally, substantial strides have been made in AI-driven research concerning tissue pathology slices and tumor biology markers. Notably, unsupervised learning methodologies have demonstrated efficacy in the identification of specific tumor markers linked to pancreatic cancer (18), offering a novel approach to screening potential markers with clinical relevance. Furthermore, the pursuit of developing a sophisticated model capable of precisely identifying and autonomously segmenting pancreatic tumors stands as a critical frontier in medical research, holding great promise for advancing diagnostic capabilities and refining treatment modalities for pancreatic malignancies. These developments underscore the transformative potential of AI in reshaping the landscape of pancreatic cancer research and clinical practice.

4 Application of AI in the surgical treatment of pancreatic cancer

At present, radical resection surgery represents the cornerstone of curative strategies for pancreatic cancer. A seminal report published in 2006 chronicled a remarkable series of 1,000 consecutive pancreatico-duodenectomies performed by an esteemed surgeon at Johns Hopkins Hospital between 1969 and 2003 (19). Over this period, the frequency of these surgeries exhibited a steady rise, with only three cases documented prior to 1980. Remarkably, the median operating time decreased from 8.8 hours in the 1970s to 5.5 hours in the 2000s, yielding a strikingly low mortality rate of merely 1% within 30 days or during hospitalization. Akin to these findings, an extensive analysis encompassing 2,050 operations conducted at Massachusetts General Hospital between 1941 and 2011 further underscored the progressive improvements achieved in surgical management (20). Nevertheless, the advent and application of neoadjuvant therapy hold immense promise in broadening the population eligible for radical resection surgery and fostering improved prognoses. Notably, AI has emerged as a potent tool in the realm of neoadjuvant therapy for pancreatic cancer. A study from Netherlands conducted an insightful investigation to assess the efficacy of neoadjuvant therapy, employing histological examinations of surgical specimens following neoadjuvant chemotherapy (21). By employing digital processing techniques on HE-stained sections from 64 pancreatic cancer patients, they meticulously delineated three distinct categories (tumor, normal duct, and residual epithelium), effectively training a tumor segmentation model with an average F1 score of 0.86. Similarly, another study from USA utilized machine learning approaches to compare enhanced CT images before and after neoadjuvant therapy, successfully identifying and extracting treatment-related image features, culminating in the establishment of a prediction model boasting an impressive AUC of 0.94 (22). These seminal studies unequivocally affirm the feasibility of harnessing AI to evaluate the outcomes of neoadjuvant therapy in pancreatic cancer. By objectively assessing the response to neoadjuvant therapy, AI holds immense potential in guiding the selection of optimal neoadjuvant therapy regimens, thereby optimizing surgical interventions. Furthermore, researchers have made noteworthy strides in leveraging deep neural networks to precisely locate and even track pancreatic tumors without relying on internal markers (23). Additionally, they have pioneered automated segmentation methods for accurately delineating organ-threatening contours, providing invaluable guidance for radiotherapy planning (24). Deep learning techniques have also emerged as a valuable asset in the treatment planning of stereotactic radiotherapy for pancreatic cancer, enabling accurate predictions of radiation dose distribution (25).

AI has emerged as a potent tool in the field of surgery, particularly in the domain of three-dimensional reconstruction and visualization. A study form China published a seminal study demonstrating the high accuracy, sensitivity, and specificity of three-dimensional reconstruction in assessing pancreatic cancer (26). Collaborating with this team in 2019, we harnessed three-dimensional visualization technology to observe the location, size, and adjacency to surrounding organs of pancreatic head tumors prior to pancreaticoduodenectomy, optimizing surgical plans and

effectively reducing surgical time, intraoperative blood loss, and postoperative recovery time for patients (27). In a similar vein, a study from Japan used three-dimensional reconstruction before surgery to precisely determine the size and position of the main pancreatic duct and select the best anastomosis technique (28). Augmented reality navigation technology represents a promising surgical navigation technique that merges three-dimensional virtual images with real-time intraoperative conditions. Okamoto et al. conducted a rigorous evaluation of five patients who underwent augmented reality navigation-assisted pancreatic resection surgery, revealing strong agreement between the positions of various organs in surface-stained images and their actual positions (29). Additionally, Volonte et al. applied augmented reality navigation technology to laparoscopic distal pancreatectomy, projecting nodules in the tail of the pancreas onto the patient's body, enhancing anatomical understanding and localization for physicians (30). Moreover, Tang et al. even employed augmented reality software on smartphones to overlay reconstructed three-dimensional images onto the surgical area displayed on the phone screen, providing intermittent navigation assistance that helped identify the boundaries of pancreatic head cancer invasion and facilitate the removal of relevant blood vessels, ultimately achieving R0 resection for all surgical patients (31). The integration of AI into surgical practice holds great promise in improving patient outcomes through precise and personalized surgical interventions.

5 AI-assisted prediction and management of postoperative complications in pancreatic cancer patients

Pancreatic cancer surgery is often burdened by postoperative complications, including postoperative pancreatic fistula, bile fistula, postoperative bleeding, abdominal infection, and delayed gastric emptying (32, 33). The most common complication is pancreatic fistula, which can lead to serious complications such as abdominal infection and life-threatening bleeding. However, the current risk scoring system for pancreatic fistula only considers four factors, which has significant limitations (34). To address this issue, scholars in Korea developed an AI-driven postoperative pancreatic fistula risk prediction platform using random forest and neural network algorithms to analyze 38 variables from 1,769 patients who underwent pancreaticoduodenectomy (PD) from 2007 to 2016 (35). By combining neural networks with recursive feature elimination, the platform achieved a maximum AUC of 0.74, ultimately identifying 16 risk factors for postoperative pancreatic fistula, including pancreatic duct diameter, body mass index, preoperative serum albumin, lipase level, and age, among others. In addition, Skawran et al. used a gradient boosting tree model based on MRI radiomics to predict postoperative pancreatic fistula after PD, achieving a high AUC of 0.90 (36). Furthermore, Zhang et al. developed a predictive model for postoperative ICU admission with an AUC of 0.8 by employing a support vector machine model to analyze clinical features of patients with pancreatic ductal adenocarcinoma, revealing bilirubin, CA19-9, and preoperative albumin as associated factors for postoperative bleeding in patients (37). The use of AI in predicting postoperative complications in pancreatic cancer surgery holds great potential in improving patient outcomes and facilitating targeted treatment strategies.

6 AI prediction of prognosis in pancreatic cancer patients

The relationship between patient survival and recurrence in pancreatic cancer is of utmost importance, necessitating the identification of relevant factors contributing to recurrence. Lee et al. conducted a meticulous analysis using multicenter registry data to evaluate the probability of postoperative recurrence and ascertain its major prognostic factors in pancreatic cancer (38). By employing random forest and Cox proportional hazards models, disease-free survival was predicted in a large cohort of 4,846 patients. Remarkably, tumor size, tumor grade, TNM stage, T stage, and lymphovascular invasion emerged as key prognostic factors for postoperative disease-free survival based on their variable importance. The Cox model exhibited a higher mean C-index (0.7738) compared to the random forest model (0.6805), indicating its superior predictive ability. Additionally, Tong et al. (39) conducted a study involving 221 patients with unresectable pancreatic cancer, collecting data on 32 clinical parameters. They developed three artificial neural network models based on different sets of basic features (3, 7, and 32) to predict the 8-month survival rate of patients. Impressively, all three artificial neural network models exhibited favorable performance, surpassing the corresponding logistic regression models in terms of AUC values (0.811 vs. 0.680, 0.844 vs. 0.722, 0.921 vs. 0.849, all $P < 0.05$). These findings emphasize the potential of artificial neural networks in accurately predicting the survival rate of patients with unresectable pancreatic cancer.

7 Summary and outlook

In recent years, the rapid evolution of deep learning and AI has engendered burgeoning interest in their potential implications in the realm of pancreatic cancer. The application of AI technology has exhibited substantial promise in the realms of early screening, diagnosis, surgical interventions, and prognostic evaluations for pancreatic cancer, equipping clinicians with more precise and expeditious decision-making tools, consequently ameliorating treatment outcomes and enhancing patients' survival rates (40). Nevertheless, notwithstanding the manifold affirmative prospects for the integration of AI in the domain of pancreatic cancer, certain constraints are inevitably encountered. Firstly, the interpretability conundrum of deep learning models utilized in pancreatic cancer screening, diagnosis, surgery, and prognostication

frequently lacks transparency, impeding comprehension and engendering skepticism. Consequently, dedicated research endeavors are imperative to heighten interpretability and foster a more transparent decision-making process. Secondly, the generalization capacity of models across heterogeneous datasets is a significant concern. While deep learning models for pancreatic cancer developed on single-center datasets may demonstrate disparate accuracies when transposed to alternative medical facilities, enhancing generalization capacity assumes paramount importance in ensuring consistent performance across diverse clinical settings (41). Moreover, the limited sample size inherent in rare disease models such as pancreatic cancer poses a formidable obstacle to effective training and validation, culminating in erratic performance. Innovative methodologies including cross-center collaboration and synthetic sample generation warrant exploration to surmount this challenge and bolster reliability (42). Finally, the normative intricacies surrounding the utilization of AI in pancreatic cancer diagnosis and treatment necessitate the establishment of ethical benchmarks and standards to safeguard patient confidentiality and data integrity. Research initiatives should be concentrated on formulating pertinent protocols and mechanisms for data dissemination, while upholding the sanctity of patient rights and privacy (43). In conclusion, despite the hurdles associated with interpretability, generalization, sample size, and ethical considerations, the potential dividends of deep learning and AI in pancreatic cancer research are profound. Future pursuits should revolve around the amalgamation of multi-omics data analysis to devise personalized treatment regimens tailored to individual patients, ultimately augmenting therapeutic efficacy and survival rates (44, 45). Synergistic collaborations between clinicians and researchers are indispensable in effectuating the seamless integration of these technologies into clinical practice.

Author contributions

GZ: Investigation, Writing – review & editing. XC: Writing – original draft. MZ: Investigation, Validation, Writing – review & editing. YL: Investigation, Writing – review & editing. YW: Conceptualization, Writing – review & editing.

Funding

The author(s) declare financial support was received for the research, authorship, and/or publication of this article. Natural Science Cultivation Foundation of China of Liaoning Cancer Hospital [grant number 2021-ZLLH-18].

Conflict of interest

The authors declare that the research was conducted in the absence of any commercial or financial relationships that could be construed as a potential conflict of interest.

Publisher's note

References

1. Sung H, Ferlay J, Siegel RL, Laversanne M, Soerjomataram I, Jemal A, et al. Global Cancer Statistics 2020: GLOBOCAN estimates of incidence and mortality worldwide for 36 cancers in 185 countries. *CA Cancer J Clin* (2021) 71(3):209–49. doi: 10.3322/caac.21660

2. Siegel RL, Miller KD, Fuchs HE, Jemal A. Cancer statistics, 2021. *CA Cancer J Clin* (2021) 71(1):7–33. doi: 10.3322/caac.21654

3. Rahib L, Smith BD, Aizenberg R, Rosenzweig AB, Fleshman JM, Matrisian LM, et al. Projecting cancer incidence and deaths to 2030: the unexpected burden of thyroid, liver, and pancreas cancers in the United States. *Cancer Res* (2014) 74(11):2913–21. doi: 10.1158/0008-5472.CAN-14-0155

4. Mollberg N, Rahbari NN, Koch M, Hartwig W, Hoeger Y, Büchler MW, et al. Arterial resection during pancreatectomy for pancreatic cancer: a systematic review and meta-analysis. *Ann Surgery* (2011) 254(6):882–93. doi: 10.1097/SLA.0b013e31823ac299

5. Heinemann V, Haas M, Boeck S. Neoadjuvant treatment of borderline resectable and non-resectable pancreatic cancer. *Ann Oncol* (2013) 24(10):2484–92. doi: 10.1093/annonc/mdt239

6. LeCun Y, Bengio Y, Hinton G. Deep learning. *Nature* (2015) 521(7553):436–44. doi: 10.1038/nature14539

7. Campbell NM, Katz SS, Escalon JG, Do RK, et al. Imaging patterns of intraductal papillary mucinous neoplasms of the pancreas: an illustrated discussion of the International Consensus Guidelines for the Management of IPMN. *Abdominal Imaging* (2015) 40(3):663–77. doi: 10.1007/s00261-014-0236-4

8. Kuwahara T, Hara K, Mizuno N, Okuno N, Matsumoto S, Obata M, et al. Usefulness of deep learning analysis for the diagnosis of Malignancy in intraductal papillary mucinous neoplasms of the pancreas. *Clin Transl Gastroenterol* (2019) 10(5):1–8. doi: 10.14309/ctg.0000000000000045

9. Sharma A, Kandlakunta H, Nagpal S, Feng Z, Hoos W, Petersen GM, et al. Model to determine risk of pancreatic cancer in patients with new-onset diabetes. *Gastroenterology* (2018) 155(3):730–9. doi: 10.1053/j.gastro.2018.05.023

10. Hsieh MH, Sun LM, Lin CL, Hsieh MJ, Hsu CY, Kao CH, et al. Development of a prediction model for pancreatic cancer in patients with type 2 diabetes using Logistic regression and artificial neural network models. *Cancer Manag Res* (2018) 10:6317–24. doi: 10.2147/CMAR.S180791

11. Baecker A, Kim S, Risch HA, Nuckols TK, Wu BU, Hendifar AE, et al. Do changes in health reveal the possibility of undiagnosed pancreatic cancer? Development of a risk-prediction model based on health care claims data. *PloS One* (2019) 14(6):e0218580. doi: 10.1371/journal.pone.0218580

12. Blyuss O, Zaikin A, Cherepanova V, Munblit D, Kiseleva EM, Prytomanova OM, et al. Development of PancRISK, a urine biomarker-based risk score for stratified screening of pancreatic cancer patients. *Br J Cancer* (2020) 122(5):692–6. doi: 10.1038/s41416-019-0694-0

13. Verheijen T, Bachet JB, Van Cutsem E, Rougier P. Pancreatic adenocarcinoma: ESMO-ESDO Clinical Practice Guidelines for diagnosis, treatment and follow-up. *Ann Oncol* (2012) 23:vii33–40. doi: 10.1093/annonc/mds224

14. Si K, Xue Y, Yu X, Zhu X, Li Q, Gong W, et al. Fully end-to-end deep learning-based diagnosis of pancreatic tumors. *Theranostics* (2021) 11(4):1982–90. doi: 10.7150/thno.52508

15. Ma H, Liu ZX, Zhang J, Wu FT, Xu CF, Shen Z, et al. Construction of a convolutional neural network classifier developed by computed tomography images for pancreatic cancer diagnosis. *World J Gastroenterol* (2020) 26(34):5156–68. doi: 10.3748/wjg.v26.i34.5156

16. Marya NB, Powers PD, Chari ST, Gleeson FC, Leggett CL, Abu Dayyeh BK, et al. Utilisation of AI for the development of an EUS-convolutional neural network model trained to enhance the diagnosis of autoimmune pancreatitis. *Gut* (2021) 70(7):1335–44. doi: 10.1136/gutjnl-2020-322821

17. Ozkan M, Cakiroglu M, Kocaman O, Kurt M, Yilmaz B, Can G, et al. Age-based computer-aided diagnosis approach for pancreatic cancer on endoscopic ultrasound images. *Endosc Ultrasound* (2016) 5(2):101–7. doi: 10.4103/2303-9027.180473

18. Ryan DP, Hong TS, Bardeesy N. Pancreatic adenocarcinoma. *New Engl J Med* (2014) 371(11):1039–49. doi: 10.1056/NEJMra1404198

19. Are C, Dhir M, Ravipati L. History of pancreaticoduodenectomy: early misconceptions, initial milestones and the pioneers. *HPB* (2011) 13(6):377–84. doi: 10.1111/j.1477-2574.2011.00305.x

20. Fernández-del Castillo C, Morales-Oyarvide V, McGrath D, Wargo JA, Ferrone CR, Thayer SP, et al. Evolution of the Whipple procedure at the Massachusetts General Hospital. *Surgery* (2021) 152(3 Suppl 1):S56–63. doi: 10.1016/j.surg.2012.05.022

21. Janssen BV, Theijse R, van Roessel S, de Ruiter R, Berkel A, Huiskens J, et al. AI-based segmentation of residual tumor in histopathology of pancreatic cancer after neoadjuvant treatment. *Cancers (Basel)* (2021) 13(20):5089. doi: 10.3390/cancers13205089

22. Nasief H, Zheng C, Schott D, Hall W, Tsai S, Erickson B, et al. A machine learning based delta-radiomics process for early prediction of treatment response of pancreatic cancer. *NPJ Precis Oncol* (2019) 3:25. doi: 10.1038/s41698-019-0096-z

23. Trebeschi S, van Griethuysen JJM, Lambregts DMJ, Lahaye MJ, Parmar C, Bakers FCH, et al. Deep learning for fully-automated localization and segmentation of rectal cancer on multiparametric MR. *Sci Rep* (2017) 7(1):5301. doi: 10.1038/s41598-017-05728-9

24. Han X, Hong J, Reyngold M, Crane C, Cuaron J, Hajj C, et al. Deep-learning-based image registration and automatic segmentation of organs-at-risk in cone-beam CT scans from high-dose radiation treatment of pancreatic cancer. *Med Phys* (2021) 48 (6):3084–95. doi: 10.1002/mp.14906

25. Osman AFI, Tamam NM. Attention-aware 3D U-Net convolutional neural network for knowledge-based planning 3D dose distribution prediction of head-and-neck cancer. *J Appl Clin Med Phys* (2022) 23(7):e13630. doi: 10.1002/acm2.13630

26. Fang CH, Zhu W, Wang H, Xiang N, Fan Y, Yang J, et al. A new approach for evaluating the resectability of pancreatic and periampullary neoplasms. *Pancreatology* (2012) 12(4):364–71. doi: 10.1016/j.pan.2012.05.006

27. Yang J, Fang CH, Fan YF, Xiang N, Liu J, Zhu W, et al. To assess the benefits of medical image three-dimensional visualization system assisted pancreaticoduodenectomy for patients with hepatic artery variance. *Int J Med Robot* (2014) 10(4):410–7. doi: 10.1002/rcs.1590

28. Miyamoto R, Oshiro Y, Nakayama K, Kohno K, Hashimoto S, Fukunaga K, et al. Three-dimensional simulation of pancreatic surgery showing the size and location of the main pancreatic duct. *Surg Today* (2017) 47(3):357–64. doi: 10.1007/s00595-016-1377-6

29. Okamoto T, Onda S, Yasuda J, Yanaga K, Suzuki N, Hattori A, et al. Navigation surgery using an augmented reality for pancreatectomy. *Dig Surg* (2015) 32(2):117–23. doi: 10.1159/000371860

30. Volonte F, Pugin E, Bucher P, Sugimoto M, Ratib O, Morel P, et al. Augmented reality and image overlay navigation with OsiriX in laparoscopic and robotic surgery: not only a matter of fashion. *Hepatobiliary Pancreat Dis Int* (2011) 18(4):506–9. doi: 10.1007/s00534-011-0385-6

31. Tang R, Yang W, Hou Y, Yu L, Wu G, Tong X, et al. Augmented reality-assisted pancreaticoduodenectomy with superior mesenteric vein resection and reconstruction. *Gastroenterol Res Pract* (2021) 2021:9621323. doi: 10.1155/2021/9621323

32. Pulvirenti A, Ramera M, Bassi C. Modifications in the International Study Group for Pancreatic Surgery (ISGPS) definition of postoperative pancreatic fistula. *Transl Gastroenterol Hepatol* (2017) 2:107. doi: 10.21037/tgh.2017.11.14

33. Bassi C, Marchegiani G, Dervenis C, Sarr M, Abu Hilal M, Adham M, et al. International Study Group on Pancreatic Surgery (ISGPS). The 2016 update of the International Study Group (ISGPS) definition and grading of postoperative pancreatic fistula: 11 Years After. *Surgery* (2017) 161(3):584–91.

34. Callery MP, Pratt WB, Kent TS, Müller PC, Kuemmerli C, Linecker M, et al. A prospectively validated clinical risk score accurately predicts pancreatic fistula after pancreatoduodenectomy. *J Am Coll Surg* (2013) 216(1):1–14. doi: 10.1016/j.jamcollsurg.2012.09.002

35. HanI W, Cho K, Ryu Y, Shin SH, Heo JS, Choi DW, et al. Risk prediction platform for pancreatic fistula after pancreatoduodenectomy using AI. *World J Gastroenterol* (2020) 26(30):4453–64. doi: 10.3748/wjg.v26.i30.4453

36. Skawran SM, Kambakamba P, Baessler B, von Spiczak J, Kupka M, Müller PC, et al. Can magnetic resonance imaging radiomics of the pancreas predict postoperative pancreatic fistula? *Eur J Radiol* (2021) 140:109733. doi: 10.1016/j.ejrad.2021.109733

37. Zhang Y, Zhu S, Yuan Z, Li Q, Ding R, Bao X, et al. Risk factors and socio-economic burden in pancreatic ductal adenocarcinoma operation: a machine learning-based analysis. *BMC Cancer* (2020) 20(1):1161. doi: 10.1186/s12885-020-07626-2

38. Lee KS, Jang JY, Yu YD, Heo JS, Han HS, Yoon YS, et al. Usefulness of AI for predicting recurrence following surgery for pancreatic cancer: Retrospective cohort study. *Int J Surg* (2021) 93:106050. doi: 10.1016/j.ijsu.2021.106050

39. Tong Z, Liu Y, Ma H, Zhang J, Lin B, Bao X, et al. Development, validation and comparison of artificial neural network models and logistic regression models predicting survival of unresectable pancreatic cancer. *Front Bioeng Biotechnol* (2020) 8:196. doi: 10.3389/fbioe.2020.00196

40. Shin HC, Roth HR, Gao M, Lu L, Xu Z, Nogues I, et al. Deep convolutional neural networks for computer-aided detection: CNN architectures, dataset characteristics and transfer learning. *IEEE Trans Med Imaging* (2016) 35(5):1285–98. doi: 10.1109/TMI.2016.2528162

41. Gulshan V, Peng L, Coram M, Stumpe MC, Wu D, Narayanaswamy A, et al. Development and validation of a deep learning algorithm for detection of diabetic retinopathy in retinal fundus photographs. *JAMA* (2016) 316(22):2402–10. doi: 10.1001/jama.2016.17216

42. Rajkomar A, Oren E, Chen K, Dai AM, Hajaj N, Hardt M, et al. Scalable and accurate deep learning with electronic health records. *NPJ Digit Med* (2018) 1:18. doi: 10.1038/s41746-018-0029-1

43. Jiang F, Jiang Y, Zhi H, Dong Y, Li H, Ma S, et al. AI in healthcare: past, present and future. *Stroke Vasc Neurol* (2017) 2(4):230–43. doi: 10.1136/svn-2017-000101

44. Deng L, Yu D. Deep learning: methods and applications. *Foundations Trends Signal Processing* (2014) 7(3-4):1–199. doi: 10.1561/9781601988157

45. Kim P, Che J, Cho YK. SLAM-driven robotic mapping and registration of 3D point clouds. *Automation Construction* (2018) 89:38–48. doi: 10.1016/j.autcon.2018.01.009

frontiers | Frontiers in Oncology

TYPE Mini Review
PUBLISHED 04 March 2024
DOI 10.3389/fonc.2024.1362247

OPEN ACCESS

EDITED BY
Yinan Zhang,
Nanjing University of Chinese Medicine, China

REVIEWED BY
Jingjing Zhuang,
Shandong University, China
Xiaoman Li,
Nanjing University of Chinese Medicine, China

*CORRESPONDENCE
Yanna Cao
Yanna.Cao@uth.tmc.edu
Tien C. Ko
Tien.C.Ko@uth.tmc.edu

RECEIVED 28 December 2023
ACCEPTED 15 February 2024
PUBLISHED 04 March 2024

CITATION
Tindall RR, Bailey-Lundberg JM, Cao Y and Ko TC (2024) The TGF-β superfamily as potential therapeutic targets in pancreatic cancer.
Front. Oncol. 14:1362247.
doi: 10.3389/fonc.2024.1362247

The TGF-β superfamily as potential therapeutic targets in pancreatic cancer

Rachel R. Tindall[1], Jennifer M. Bailey-Lundberg[2], Yanna Cao[1*] and Tien C. Ko[1*]

[1]McGovern Medical School, Department of Surgery, The University of Texas Health Science Center at Houston, Houston, TX, United States, [2]McGovern Medical School, Department of Anesthesiology, Critical Care, and Pain Medicine, The University of Texas Health Science Center at Houston, Houston, TX, United States

The transforming growth factor (TGF)-β superfamily has important physiologic roles and is dysregulated in many pathologic processes, including pancreatic cancer. Pancreatic cancer is one of the most lethal cancer diagnoses, and current therapies are largely ineffective due to tumor resistance and late-stage diagnosis with poor prognosis. Recent efforts are focused on the potential of immunotherapies in improving therapeutic results for patients with pancreatic cancer, among which TGF-β has been identified as a promising target. This review focuses on the role of TGF-β in the diseased pancreas and pancreatic cancer. It also aims to summarize the current status of therapies targeting the TGF-β superfamily and postulate potential future directions in targeting the TGF-β signaling pathways.

KEYWORDS

TGF-β, acute pancreatitis, chronic pancreatitis, pancreatic ductal adenocarcinoma, pancreatic stellate cells

1 Introduction

Cytokines mediate the body's natural response to injury at a systemic level (1). These cytokines can be subcategorized into the transforming growth factor (TGF)-β superfamily, interleukins, interferons, chemokines, and the tumor necrosis factor (TNF) superfamily (2–5). The TGF-β superfamily, one of the major groups, was first described as a family of growth factors released by fibroblasts that stimulated cell growth (6). In 1981, further investigation into these growth factors led to the purification of TGF-β, the first named member of the TGF-β superfamily (7, 8). While studying the purification techniques of this protein, isoforms of TGF-β were discovered, which were called TGF-β1, TGF-β2, and TGF-β3 (9–11). The role of these proteins was further elucidated with the discovery of other members, including the bone morphogenic proteins (BMP)s (12). Currently, 33 proteins are recognized in this superfamily, with subtypes including TGF-βs, BMPs, growth differentiation factors (GDF)s, inhibins, and activins (Table 1) (13–16). This mini-review focuses on the role of the TGF-β superfamily in

10.3389/fonc.2024.1362247

TABLE 1 Members of the TGF-β superfamily.

Subfamily	Ligand name	Associated gene	Other name	Receptors		R-Smad
				Type I	Type 2	
Transforming Growth Factor (TGF)-β	TGF-β1	*TGFB1*		TGFBRI, ALK-5	TGFBRII	Smad2/3
	TGF-β2	*TGFB2*		TGFBRI, ALK-5	TGFBRII	Smad2/3
	TGF-β3	*TGFB3*		TGFBRI, ALK-5	TGFBRII	Smad2/3
Bone Morphogenic Protein (BMP)	BMP-2	*BMP2*		BMPRIA, BMPRIB	BMPRII, ActRII, ActRIIB	Smad1/5/8
	BMP-3	*BMP3*		ALK-4	BMPRII, ActRII, ActRIIB	Smad2/3
	BMP-4	*BMP4*		BMPRIA, BMPRIB	BMPRII, ActRII, ActRIIB	Smad1/5/8
	BMP-5	*BMP5*		BMPRIA, BMPRIB, ALK-2	BMPRII, ActRII, ActRIIB	Smad1/5/8
	BMP-6	*BMP6*	Vgr1	BMPRIA, BMPRIB, ALK-2	BMPRII, ActRII, ActRIIB	Smad1/5/8
	BMP-7	*BMP7*		BMPRIA, BMPRIB, ALK-2	BMPRII, ActRII, ActRIIB	Smad1/5/8
	BMP-8A	*BMP8A*		BMPRIA, BMPRIB, ALK-2	BMPRII, ActRII, ActRIIB	Smad1/5/8
	BMP-8B	*BMP8B*		BMPRIA, BMPRIB, ALK-2	BMPRII, ActRII, ActRIIB	Smad1/5/8
	BMP-9	*GDF2*	GDF-2	ALK-1, ALK-2	BMPRII, ActRII, ActRIIB	Smad1/5/8
	BMP-10	*BMP10*		ALK-1, ALK-2	BMPRII, ActRII, ActRIIB	Smad1/5/8
Growth Differentiation Factor (GDF)	GDF-1	*GDF1*		ALK-7	BMPRII, ActRII, ActRIIB	Smad2/3
	GDF-3	*GDF3*	Vgr2	ALK-7	BMPRII, ActRII, ActRIIB	Smad2/3
	GDF-5	*GDF5*	BMP-14	BMPRIB	BMPRII, ActRII, ActRIIB	Smad1/5/8
	GDF-6	*GDF6*	BMP-13	BMPRIB	BMPRII, ActRII, ActRIIB	Smad1/5/8
	GDF-7	*GDF7*	BMP-12	BMPRIB	BMPRII, ActRII, ActRIIB	Smad1/5/8
	GDF-8	*MSTN*	myostatin	none	ActRIIB	Smad2/3
	GDF-9	*GDF9*		ALK-5	BMPRII, ActRII, ActRIIB	Smad2/3
	GDF-9B	*BMP15*	BMP-15	ALK-5	BMPRII, ActRII, ActRIIB	Smad2/3
	GDF-10	*GDF10*	BMP-3B	ALK-4	BMPRII, ActRII, ActRIIB	Smad2/3
	GDF-11	*GDF11*	BMP-11	ALK-4, ALK-5	ActRIIB	Smad2/3
	GDF-15	*GDF15*	MIC-1	unknown	unknown	unknown
Nodal	Nodal	*Nodal*	BMP-16	ALK-7	BMPRII, ActRII, ActRIIB	Smad2/3
Inhibin	Inhibin A	*INHA, INHBA*		none	ActRII, ActRIIB	none

(Continued)

TABLE 1 Continued

Subfamily	Ligand name	Associated gene	Other name	Receptors		R-Smad
				Type I	Type 2	
	Inhibin B	*INHA, INHBB*		none	ActRII, ActRIIB	none
Activin	Activin A	*INHBA*		ALK-4, ALK-7	ActRII, ActRIIB	Smad2/3
	Activin B	*INHBB*		ALK-4, ALK-7	ActRII, ActRIIB	Smad2/3
	Activin AB	*INHBA, INHBB*		ALK-4, ALK-7	ActRII, ActRIIB	Smad2/3
Lefty	Lefty A	*LEFTY2*		none	ActRII, ActRIIB	none
	Lefty B	*LEFTY1*		none	ActRII, ActRIIB	none
Anti-Mullerian Hormone	AMH	*AMH*	Mullerian-inhibiting substance	BMPRIA, BMPRIB, ALK-2	AMHRII	Smad1/5/8

Adapted from (13–16).
TGFBRI, Type I TGF-β receptor; TGFBRII, Type II TGF-β receptor; BMPRIA, Type IA BMP receptor; BMPRIB, Type IB BMP receptor; ActRII, Type II Activin receptor; ActRIIB, Type IIB Activin receptor.

pancreatic diseases, including pancreatic ductal adenocarcinoma (PDAC), and the current therapeutics targeting these pathways.

1.1 Physiologic role of TGF-β superfamily

TGF-β is produced in a latent form. Activation of the latent form is initiated by regulatory T cells with a transmembrane protein, glycoprotein A repetitions predominant (GARP), which binds and cleaves pro-TGF-β to produce latent TGF-β. The latent form is activated by integrins (Figure 1A) (17, 18). BMPs, GDFs, and Lefty A and B are produced and processed similarly, with inactive precursors being cleaved and activated by proteases (Table 1) (19–21). The activins and inhibins are composed of common subunits and are formed by cleavage of dimerized subunits; inhibins are αβ heterodimers, and activins are ββ homodimers (Table 1) (16). The TGF-β superfamily is essential in physiologic functions, including tissue development and differentiation, regulation of immunologic

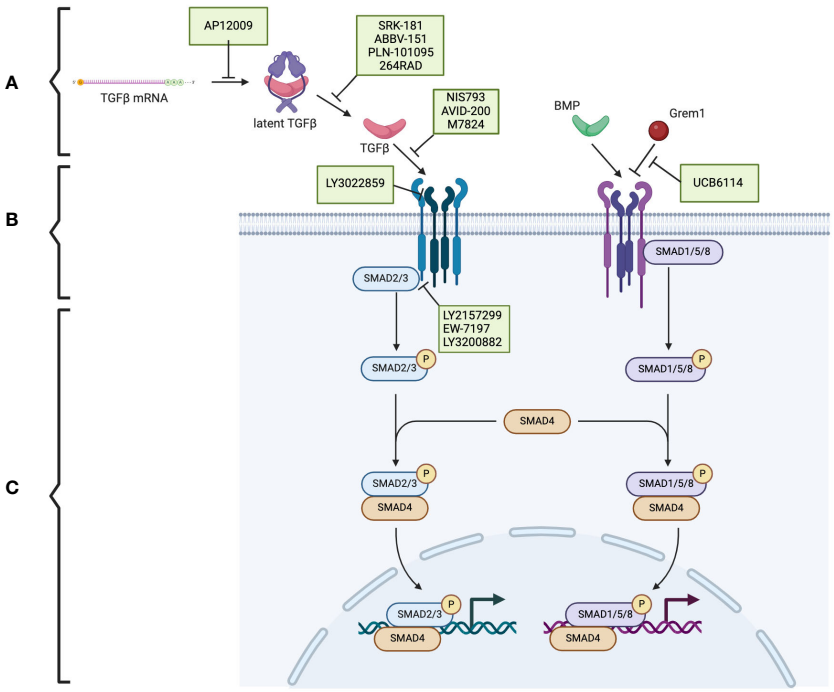

FIGURE 1
The TGF-β superfamily signaling pathway and the potential therapeutic targets in pancreatic cancer. **(A)** The TGF-β superfamily members. **(B)** TGF-β receptors and the phosphorylation/activation of the intracellular mediators of SMAD2/3 and SMAD1/5/8. **(C)** Downstream of the phosphorylated SMAD2/3 and SMAD1/5/8. Therapeutics (indicated in green boxes) targeting specific steps in the TGF-β superfamily signaling pathway are currently under investigation. Created using BioRender.com.

responses, and tissue healing (13). These members activate physiologic activities through canonical and non-canonical signaling (22). Canonical signaling occurs through the SMAD pathway, where receptor-activated (R) SMAD1/5/8 and SMAD2/3 are phosphorylated by receptors following ligand binding (Figure 1B). These phosphorylated SMADs then complex with SMAD4 and translocate to the nucleus to regulate the expression of the target genes (Figure 1C) (13). Non-canonical pathways can be activated upon the ligand binding to the receptors, such as Erk, involved in epithelial-mesenchymal transition (EMT), and JNK/p38, involved in EMT and apoptosis (23).

These signaling pathways play an essential role in proliferation and in controlling the growth of specific cell types, including epithelial cells, endothelial cells, immune cells, and neuronal cells, through growth inhibition and induction of apoptosis (24). BMPs are specifically involved in developing and maintaining skeletal tissues and are regulated extracellularly by antagonists, including Noggin, Chordin, and Gremlin1 (Grem1) (Figure 1A) (14). Additionally, activin A is a critical mesoderm-inducing factor (25), and GDFs are primarily involved in developmental processes (26). Inhibins antagonize activin signaling, and lefty inhibits phosphorylation of SMAD2 and subsequently regulates downstream signaling (Table 1) (16, 27).

TGF-β also plays a role in immunoregulation by inhibiting T-lymphocyte proliferation and promoting T-cell differentiation (28–30). Additionally, these proteins play an essential role in fibroblast activation and are involved in routine wound healing; TGF-β1 is secreted by the platelets forming the hemostatic plug and is a chemoattractant for monocytes and fibroblasts essential to tissue repair (31–34).

1.2 Pathologic role of TGF-β superfamily

In addition to the essential role of TGF-β in physiologic mechanisms, aberrantly increased TGF-β has been shown to contribute to excess fibrosis (35). Administration of exogenous TGF-β leads to fibrosis in subcutaneous tissues, lung parenchyma, and hepatic tissue (36–38). Furthermore, dysregulation of the TGF-β signaling pathway contributes to carcinogenesis (39). For example, tumor cells have been shown to evade the growth regulation of TGF-β through mutations in the TGF-β receptors and SMAD family (40, 41).

PDAC is currently the third leading cause of cancer-related death (42). Poor outcomes can be attributed to both late diagnosis and a fibrotic tumor microenvironment that surrounds the cancer cells, creating a chemo-resistant barrier. Further understanding of the role of the TGF-β superfamily may elucidate potential targets for novel therapies that could improve patient outcomes.

2 Role of TGF-β superfamily in pancreatic disease

TGF-β activity is paradoxical in pancreatic diseases, promoting or suppressing disease progression. The TGF-β superfamily modulates acute pancreatitis (AP) by regulating inflammation and apoptosis through canonical or non-canonical signaling. The TGF-β superfamily also plays distinct roles in the progression of chronic pancreatitis (CP) and PDAC through effects on pancreatic stellate cells (PSCs) and the extracellular matrix (ECM) production.

2.1 Acute pancreatitis

AP results from injury to the pancreatic acinar cells, leading to premature activation of pancreatic enzymes and causing pancreatic autodigestion and tissue inflammation (43). Apoptosis and suppression of proliferation have been reported to limit the inflammatory cascade in response to the insult in AP (44). TGF-β is released by various cells at the site of injury and induces apoptosis and suppress the proliferation of pancreatic acinar cells (45). However, this was contradicted by a study showing the induction of apoptosis upon suppressing the TGF-β signaling pathway in pancreatic epithelial cells (46). Additionally, our group has demonstrated that BMP signaling is upregulated in AP and causes dysregulation of autophagic processes. Administration of a BMP antagonist Noggin *in vivo* in a mouse model attenuated AP inflammation, suggesting a proinflammatory role of BMP signaling in AP (47).

In addition to involvement with apoptosis, TGF-β mediates the inflammatory response in AP through T-cell activation. Specifically, TGF-β induces the differentiation of both Th9 and Th17 cells, which are proinflammatory (48, 49). Th17 cells are known to secrete IL-17, associated with increased inflammatory markers and severity of AP (50).

2.2 Chronic pancreatitis

CP results from repeated injury to the pancreas from recurrent bouts of AP, which leads to the replacement of normal pancreatic tissue with fibrotic scarring (51). This is primarily facilitated by the activation of PSCs, which secrete growth factors and chemokines such as TGF-β and produce excess ECM (52). The TGF-β secreted by activated PSCs is directly related to the characteristic fibrosis of CP (53). This fibrosis results from increased ECM production by PSCs (54) and inhibition of matrix metalloproteinases, which are involved in ECM degradation (55). Our group has shown that BMPs oppose the fibrogenic function of TGF-β on PSCs in CP by activating the SMAD1/5/8 pathway, which inhibits SMAD2 (56, 57).

Other modulators of TGF-β superfamily pathways are also involved in CP pathophysiology. Our group has shown that Grem1, an endogenous BMP antagonist, is pro-fibrogenic in a CP mouse model (58). Additionally, SMAD7, a known inhibitory SMAD, suppressed TGF-β signaling and modulated CP fibrosis through decreased ECM deposition and decreased inflammatory cell response in an *in vivo* mouse model (59).

2.3 Pancreatic ductal adenocarcinoma

The TGF-β superfamily plays dual roles in PDAC, promoting tumorigenesis in some capacities while acting as an inhibitor in others (60). In the early stages of PDAC, TGF-β has been shown to

suppress tumor progression by promoting apoptosis and regulation of the cell cycle and promoting the stroma's development by activating PSCs and increasing stromal production (61). Additionally, BMP2 expression is increased in pancreatic cancer and has variable mitogenic effects on pancreatic cancer cell lines, with a greater capacity to stimulate growth in cell lines with SMAD mutations (62). BMP signaling has also been shown to play a role in EMT through canonical BMP signaling, mediated by Grem1 inhibitory feedback, resulting in a maintenance of heterogeneity (63). Our group has also shown that activated fibroblasts express Grem1 and that increased expression is associated with a more severe tumor stage (64).

3 Genetic alterations in PDAC

PDAC is associated with several common mutations in oncogenes and tumor suppressor genes, including mutations in *KRAS, TP53, CDKN2A*, and *SMAD4.* These mutations can affect TGF-β signaling pathways at various points, including the intracellular signaling molecules and receptors (65).

3.1 *SMAD4* mutation

SMAD4 mutations are common in PDAC and are identified in approximately 60% of cases (66). Interestingly, an isolated *SMAD4* mutation does not independently cause cancer; it must be paired with another mutation, such as *KRAS* (67). SMAD4 is part of the intracellular signaling pathway that complexes with activated and phosphorylated SMAD2/3 and SMAD1/5/8 in response to TGF-β and BMP binding their respective receptors (68). Mutation of *SMAD4* results in loss of the tumor suppressor function of canonical TGF-β signaling (69). Loss of *SMAD4* results in decreased T-cell recruitment and a suppressed immune response (70). Additionally, knockout of *Smad4* in a PDAC mouse model has increased tumor sensitivity to host immune control and induced DNA damage (71).

3.2 Receptor mutations

Mutations in TGF-β receptors have been identified as disruptions of TGF-β signaling pathways that result in the loss of TGF-β suppressive effects. Studies have shown that mutations in *TGFBR1*, which encodes TGF-β type I receptor (TGFBRI), occur in approximately 1% of cases, and mutations in *TGFBR2*, which encodes TGF-β Type II receptor (TGFBRII), appear in approximately 4% of patients (72). Type III TGF-β receptor mutations also occur and result in increased EMT-associated increased motility and invasiveness (73).

Disruption in the expression of other receptors has also been reported. Deletion of *ACVR1B*, which encodes the ALK-4 receptor for activin A, is associated with a more aggressive cancer phenotype (74). Interestingly, mutations in *BMPRI* are described in patients with hereditary juvenile polyposis. *BMPRI* and *BMPRII* mRNA levels are upregulated in pancreatic cancers, and cells with higher levels have been shown to have more significant metastatic potential (75, 76).

3.3 Other mutations

KRAS is frequently mutated in human carcinomas and approximately 85% of PDAC cases (77). *KRAS* mutations are often detectable early in disease progression (78). *GREM1* is upregulated in hereditary mixed polyposis syndrome, where duplications of the gene result in increased antagonism of BMP signaling (79). Similar mutations are observed in sporadic intestinal polyps (80). However, mutations in *GREM1* have not been reported in cases of PDAC.

4 Therapeutic potential of targeting the TGF-β superfamily

Management options for pancreatic cancer depend primarily on the stage of the cancer when it is diagnosed. Distant metastasis, retroperitoneal invasion, and invasion of the mesenteric root are contraindications to surgical resection. Chemotherapy is the standard of care for metastatic pancreatic cancer. Gemcitabine was considered the first line for a couple of decades following a randomized control trial showing more favorable outcomes than fluorouracil. However, survival for patients treated with gemcitabine was still dismal, with a median survival of 5.65 months (81). This regimen has been improved following the PRODIGE and MPACT studies, which evaluated FOLFIRINOX and albumin-bound paclitaxel plus gemcitabine, showing significant improvement in survival time compared to gemcitabine alone (82, 83). Despite these improved regimens, outcomes remain poor, leading to a focus on the potential of other treatment modalities, including immunotherapy.

Interestingly, chemotherapy has been shown to alter the tumor microenvironment through reprogramming and increased synthesis of chemokines, including TGF-β (84). Thus, TGF-β appears to be involved in the resistance to chemotherapy. Inhibiting TGF-β has become a focus of therapeutic intervention and shows promising results in treating PDAC.

4.1 Inhibition of TGF-β signaling

Because of the complexity of the TGF-β signaling pathway, numerous potential targets are under investigation (Figure 1). Therapeutic strategies include antisense oligonucleotides, neutralizing antibodies, ligand traps, and small molecule kinase inhibitors. Many of these therapies are being investigated in several cancers, including pancreatic cancer.

4.1.1 Antisense oligonucleotides

Trabedersen (AP12009), specific for *TGFB2* mRNA, reduced *TGFB2* expression in human pancreatic cancer cell lines, resulted

in decreased proliferation and migration, and reversed immunosuppressive effects (Figure 1A) (85). A phase 2 clinical study showed a good safety profile, with the only identified adverse effect being transient thrombocytopenia and a mean survival of 13.4 months for 61 patients with pancreatic cancer (86). Further clinical trials have yet to be published.

4.1.2 Neutralizing antibodies

In preclinical studies, SRK-181, which specifically targets latent TGF-β1, countered TGF-β-mediated resistance to cancer checkpoint blockade therapy (Figure 1A) (87). It is currently under investigation in the DRAGON trial (NCT04291079), a phase 1 clinical trial investigating it as a monotherapy or in combination with anti-PD-L1 in patients with solid tumors, including pancreatic tumors, which has shown no dose-limiting toxicity and adverse effects limited to fatigue, anorexia, and nausea. One patient with pancreatic cancer who was treated with SRK-181 as a monotherapy showed stable disease (88).

Livmoniplimab (ABBV-151) targets GARP-TGF-β1 and prevents the release of active TGF-β1 (Figure 1A). It is currently under investigation in a phase 1 trial (NCT03821935), investigating it as a single agent or combined with Budigalimab in patients with locally advanced or metastatic solid tumors. This clinical trial is still in the recruiting phase, and preliminary results are not yet available (89).

PLN-101095 targets integrin αvβ8 and αvβ1 and prevents activation of TGF-β (Figure 1A). It has shown enhanced response to standard chemotherapy regimens in preclinical studies (90) and is currently in a phase 1 clinical trial (91). Additionally, 264RAD inhibits integrin αvβ6 and has shown promising results in preclinical trials (92); however, further clinical trials have not been pursued.

NIS793 binds and neutralizes active TGF-β with high affinity and has been shown to decrease fibroblasts and enhance tumor cell chemosensitivity (Figure 1B) (93). In a phase 1b trial (NCT02947165), 120 patients, of which ten had pancreatic cancer, were treated with NIS793 as a monotherapy or in combination with spartalizumab. Partial response was observed in 2.5% of patients, and stable disease was observed in 24.2% of patients. While no dose-limiting toxicity was observed, nearly half experienced an adverse event, most commonly rash (94). A phase 2 trial (NCT04390763) and phase 3 trial (NCT04935359) are ongoing to evaluate the drug's effect in patients with metastatic pancreatic ductal adenocarcinoma.

LY3022859 targets the type II TGF-β receptor and inhibits signaling activation (Figure 1B). A phase 1 trial (NCT01646203) was discontinued due to patients developing uncontrollable cytokine release syndrome (95).

4.1.3 Ligand traps

AVID-200 is explicitly designed to resemble the receptor ectodomain for TGF-β1 and TGF-β3 and has been shown to enhance the efficacy of immune checkpoint inhibitors in preclinical trials (Figure 1B) (96, 97). It recently underwent a phase 1 clinical trial (NCT03834662) for solid tumors, including PDAC (98).

Activated T-cells present PD-1 on the surface, which can be exploited by tumor cells expressing PD-L1. PD-L1 binding to PD-1 inactivates the T-cells and prevents the T-cell-regulated destruction of the tumor cells (99). Thus, the PD-1 signaling pathway has been identified as a promising target for cancer immunotherapy (100). Specific interest has arisen in dual inhibition of the PD-1 and TGF-β signaling pathways, which is hypothesized to enhance the anti-tumor activity (101). Bintrafusp alfa (M7824) is a bifunctional fusion protein with a type II TGF-β receptor fused to an antibody against PD-L1 (Figure 1B) (102), which has undergone a phase 1 clinical trial (NCT02517398) that included five patients with pancreatic cancer. Three patients had a response of stable disease, one of partial response, and one of progressive disease (103).

4.1.4 Small molecule kinase inhibitors

Galunisertib (LY2157299) is an oral drug that inhibits the type I TGF-β receptor kinase and down-regulates the phosphorylation of SMAD2 (Figure 1B) (104). In phase 1 and 2 clinical trials, a combination of galunisertib and gemcitabine resulted in an improved survival time of 8.9 months compared to 7.1 months in patients treated with just galunisertib with minimal increase in toxicity in patients with locally advanced or metastatic pancreatic adenocarcinoma (105).

Vactosertib (EW-7197), a type I TGF-β receptor inhibitor, has been shown to augment gemcitabine and decrease the expression of ECM components, improving the sensitivity of pancreatic cancer cells to gemcitabine (Figure 1B) (106). It also has synergistic effects when combined with T1-44, an inhibitor of PRMT5 methyltransferase (107). It has been investigated in a phase 1b clinical trial in combination with FOLFOX in sixteen patients with pancreatic ductal adenocarcinoma; three patients had a partial response, and five had stable disease (108).

LY3200882, an oral type I TGF-β receptor inhibitor, was investigated in a phase 1 clinical trial (Figure 1B). LY3200882 was used in combination with gemcitabine and nab-paclitaxel in twelve patients with pancreatic cancer. Six of the twelve patients had partial responses, and all but one demonstrated decreased tumor size (109).

4.2 Other targets

In addition to TGF-β, other members of the TGF-β superfamily are promising targets for cancer therapeutics. Interestingly, ginisortamab (UCB6114), an antibody that neutralizes Grem1 and blocks its antagonistic effects on BMP signaling, has been shown to restore BMP signaling pathways in human colorectal cancer cell lines and fibroblasts (Figure 1B) (110). It is currently being evaluated by a phase 1/2 clinical trial (NCT04393298) in advanced solid tumors, including pancreatic adenocarcinomas.

GDF-15 has also been identified as a potential target. While the exact signaling pathway has yet to be elucidated, recent studies have identified a unique GDF-15 receptor glial cell-derived neurotrophic factor family receptor α-like (GFRAL) and have shown that GDF-15 inhibits leukocyte integrin activation and T cell migration, which is reversed with neutralization of GDF-15 (111, 112). Visugromab

(CTL-002), a neutralizing antibody of GDF-15, is currently under evaluation in phase 2a of the GDFATHER trial (NCT04725474) and is showing promising results in combination with nivolumab in advanced non-small cell lung cancer and urothelial cancer.

5 Discussion

TGF-β and associated proteins undoubtedly play a role in the development of pancreatic disease and disease progression from AP to CP to PDAC. However, the heterogeneous nature of pancreatic tissue and the dynamic role of the TGF-β superfamily and associated signaling pathways result in nuanced implications for therapeutics that target these pathways.

Systemic therapies such as chemotherapy have been the standard of care for patients with pancreatic cancer following trials such as PRODIGE 4/ACCORD 11 and MPACT; however, outcomes remain very poor with short survival times (83, 113). This has led to an interest in targeted therapies such as immunotherapy, which modulate a patient's immune system response. Such therapies have survival benefits in several types of solid tumors, including upper gastrointestinal tumors and colorectal cancers (114, 115). However, similar benefits from these immunotherapies have not been seen in pancreatic cancer, mainly because pancreatic tumors are immunologically cold due to the unique immunosuppressive tumor microenvironment with limited immune cells (116). Thus, current strategies seek to target components of the microenvironment that contribute to this immunosuppression to improve the responsiveness of tumors to immunotherapy (117). Subsequently, TGF-β signaling pathways became targets of interest, given the role of TGF-β in immunosuppression and ECM production.

Several therapeutics that target TGF-β and associated pathway molecules are currently under investigation in early clinical trials for solid tumors, including pancreatic tumors. These targets include modulating the TGF-β signaling pathway directly and targeting other proteins in the superfamily, such as Grem1, which inhibits BMP signaling. Additionally, antagonism of BMP has been suggested as a potential target to block and reduce pancreatic cancer invasiveness (118). However, due to the context-dependent manner of BMP signaling, the efficacy of such therapeutics varies greatly, and further investigation into the subtleties of BMP signaling in both oncogenic and tumor-suppressive functions is warranted (119).

Because the TGF-β superfamily has heterogenous roles in pancreatic tumor development, the effectiveness of these therapies has yet to be fully elucidated. TGF-β signaling pathways are involved in immunosuppression and ECM production, but TGF-β pathways also regulate cell cycle progression. Regardless, data from the recent clinical trials suggest hopeful results. Side effect profiles were essentially minimal, but the potential adverse effects of TGF-β targeting drugs when delivered systemically should be a point of investigation in future studies, as blockage of the signaling pathways has previously been shown to have contradictory effects depending on cell type (120). Targeted drug delivery to the pancreatic tumor microenvironment may help mitigate such effects.

Ultimately, definitive management of pancreatic disease will likely require a multifaceted treatment plan due to the heterogeneous nature of the disease processes. TGF-β has been shown to augment the microenvironment, which likely contributes to the characteristic resistance and poor outcomes of PDAC. Inhibition of these signaling pathways shows promising results in boosting the effects of traditional therapeutics. Pairing modulators of TGF-β signaling pathways with conventional systemic treatments such as chemotherapy and other immune modulators such as PD-1 inhibitors will address the mechanisms of resistance that have contributed to the poor outcomes of pancreatic cancer and allow for a more comprehensive treatment regimen.

Author contributions

RT: Conceptualization, Validation, Writing – original draft, Writing – review & editing, Funding acquisition, Investigation, Visualization. JB-L: Conceptualization, Writing – review & editing, Funding acquisition, Investigation, Visualization. YC: Conceptualization, Supervision, Validation, Writing – review & editing, Investigation, Project administration, Visualization. TK: Conceptualization, Supervision, Writing – review & editing, Funding acquisition, Investigation, Project administration.

Funding

The author(s) declare financial support was received for the research, authorship, and/or publication of this article. This study was partially supported by the NIH R21 AA027014 and Jack H Mayfield M.D. Distinguished Professorship in Surgery (TK), Dean's fund for Summer Research Program at UTHealth MMS (RT). JB-L is supported by NIH R01 CA277161.

Acknowledgments

Figure 1 was created with BioRender.com.

Conflict of interest

The authors declare that the research was conducted in the absence of any commercial or financial relationships that could be construed as a potential conflict of interest.

The author(s) declared that they were an editorial board member of Frontiers, at the time of submission. This had no impact on the peer review process and the final decision.

Publisher's note

References

1. Rochman Y, Spolski R, Leonard WJ. New insights into the regulation of T cells by gamma(c) family cytokines. *Nat Rev Immunol*. (2009) 9:480–90. doi: 10.1038/nri2580

2. Dinarello CA. Interleukin-1 in the pathogenesis and treatment of inflammatory diseases. *Blood*. (2011) 117:3720–32. doi: 10.1182/blood-2010-07-273417

3. Boehm U, Klamp T, Groot M, Howard JC. Cellular responses to interferon-gamma. *Annu Rev Immunol*. (1997) 15:749–95. doi: 10.1146/annurev.immunol.15.1.749

4. Zlotnik A, Yoshie O. Chemokines: a new classification system and their role in immunity. *Immunity*. (2000) 12:121–7. doi: 10.1016/S1074-7613(00)80165-X

5. Wallach D, Varfolomeev EE, Malinin NL, Goltsev YV, Kovalenko AV, Boldin MP. Tumor necrosis factor receptor and Fas signaling mechanisms. *Annu Rev Immunol*. (1999) 17:331–67. doi: 10.1146/annurev.immunol.17.1.331

6. de Larco JE, Todaro GJ. Growth factors from murine sarcoma virus-transformed cells. *Proc Natl Acad Sci U S A*. (1978) 75:4001–5. doi: 10.1073/pnas.75.8.4001

7. Moses HL, Branum EL, Proper JA, Robinson RA. Transforming growth factor production by chemically transformed cells. *Cancer Res*. (1981) 41:2842–8.

8. Roberts AB, Anzano MA, Lamb LC, Smith JM, Sporn MB. New class of transforming growth factors potentiated by epidermal growth factor: isolation from non-neoplastic tissues. *Proc Natl Acad Sci U S A*. (1981) 78:5339–43. doi: 10.1073/pnas.78.9.5339

9. Cheifetz S, Weatherbee JA, Tsang ML, Anderson JK, Mole JE, Lucas R, et al. The transforming growth factor-beta system, a complex pattern of cross-reactive ligands and receptors. *Cell*. (1987) 48:409–15. doi: 10.1016/0092-8674(87)90192-9

10. Derynck R, Lindquist PB, Lee A, Wen D, Tamm J, Graycar JL, et al. A new type of transforming growth factor-beta, TGF-beta 3. *EMBO J*. (1988) 7:3737–43. doi: 10.1002/embj.1988.7.issue-12

11. ten Dijke P, Hansen P, Iwata KK, Pieler C, Foulkes JG. Identification of another member of the transforming growth factor type beta gene family. *Proc Natl Acad Sci U S A*. (1988) 85:4715–9. doi: 10.1073/pnas.85.13.4715

12. Wozney JM, Rosen V, Celeste AJ, Mitsock LM, Whitters MJ, Kriz RW, et al. Novel regulators of bone formation: molecular clones and activities. *Science*. (1988) 242:1528–34. doi: 10.1126/science.3201241

13. Morikawa M, Derynck R, Miyazono K. TGF-beta and the TGF-beta family: context-dependent roles in cell and tissue physiology. *Cold Spring Harb Perspect Biol*. (2016) 8. doi: 10.1101/cshperspect.a021873

14. Katagiri T, Watabe T. Bone morphogenetic proteins. *Cold Spring Harb Perspect Biol*. (2016) 8. doi: 10.1101/cshperspect.a021899

15. Low EL, Baker AH, Bradshaw AC. TGFbeta, smooth muscle cells and coronary artery disease: a review. *Cell Signal*. (2019) 53:90–101. doi: 10.1016/j.cellsig.2018.09.004

16. Namwanje M, Brown CW. Activins and inhibins: roles in development, physiology, and disease. *Cold Spring Harb Perspect Biol*. (2016) 8. doi: 10.1101/cshperspect.a021881

17. Lienart S, Merceron R, Vanderaa C, Lambert F, Colau D, Stockis J, et al. Structural basis of latent TGF-beta1 presentation and activation by GARP on human regulatory T cells. *Science*. (2018) 362:952–6. doi: 10.1126/science.aau2909

18. Wipff PJ, Hinz B. Integrins and the activation of latent transforming growth factor beta1 - an intimate relationship. *Eur J Cell Biol*. (2008) 87:601–15. doi: 10.1016/j.ejcb.2008.01.012

19. Nelsen SM, Christian JL. Site-specific cleavage of BMP4 by furin, PC6, and PC7. *J Biol Chem*. (2009) 284:27157–66. doi: 10.1074/jbc.M109.028506

20. Bauskin AR, Brown DA, Junankar S, Rasiah KK, Eggleton S, Hunter M, et al. The propeptide mediates formation of stromal stores of PROMIC-1: role in determining prostate cancer outcome. *Cancer Res*. (2005) 65:2330–6. doi: 10.1158/0008-5472.CAN-04-3827

21. Ulloa L, Creemers JW, Roy S, Liu S, Mason J, Tabibzadeh S. Lefty proteins exhibit unique processing and activate the MAPK pathway. *J Biol Chem*. (2001) 276:21387–96. doi: 10.1074/jbc.M006933200

22. Kubiczkova L, Sedlarikova L, Hajek R, Sevcikova S. TGF-beta - an excellent servant but a bad master. *J Transl Med*. (2012) 10:183. doi: 10.1186/1479-5876-10-183

23. Zhang YE. Non-Smad pathways in TGF-beta signaling. *Cell Res*. (2009) 19:128–39. doi: 10.1038/cr.2008.328

24. Siegel PM, Massague J. Cytostatic and apoptotic actions of TGF-beta in homeostasis and cancer. *Nat Rev Cancer*. (2003) 3:807–21. doi: 10.1038/nrc1208

25. Asashima M, Nakano H, Shimada K, Kinoshita K, Ishii K, Shibai H, et al. Mesodermal induction in early amphibian embryos by activin A (erythroid differentiation factor). *Rouxs Arch Dev Biol*. (1990) 198:330–5. doi: 10.1007/BF00383771

26. Wischhusen J, Melero I, Fridman WH. Growth/differentiation factor-15 (GDF-15): from biomarker to novel targetable immune checkpoint. *Front Immunol*. (2020) 11:951. doi: 10.3389/fimmu.2020.00951

27. Ulloa L, Tabibzadeh S. Lefty inhibits receptor-regulated Smad phosphorylation induced by the activated transforming growth factor-beta receptor. *J Biol Chem*. (2001) 276:21397–404. doi: 10.1074/jbc.M010783200

28. Kehrl JH, Wakefield LM, Roberts AB, Jakowlew S, Alvarez-Mon M, Derynck R, et al. Production of transforming growth factor beta by human T lymphocytes and its potential role in the regulation of T cell growth. *J Exp Med*. (1986) 163:1037–50. doi: 10.1084/jem.163.5.1037

29. Chen W, Jin W, Hardegen N, Lei KJ, Li L, Marinos N, et al. Conversion of peripheral CD4+CD25- naive T cells to CD4+CD25+ regulatory T cells by TGF-beta induction of transcription factor Foxp3. *J Exp Med*. (2003) 198:1875–86. doi: 10.1084/jem.20030152

30. Liu Y, Zhang P, Li J, Kulkarni AB, Perruche S, Chen W. A critical function for TGF-beta signaling in the development of natural CD4+CD25+Foxp3+ regulatory T cells. *Nat Immunol*. (2008) 9:632–40. doi: 10.1038/ni.1607

31. Assoian RK, Komoriya A, Meyers CA, Miller DM, Sporn MB. Transforming growth factor-beta in human platelets. Identification of a major storage site, purification, and characterization. *J Biol Chem*. (1983) 258:7155–60. doi: 10.1016/S0021-9258(18)32345-7

32. Wahl SM, Hunt DA, Wakefield LM, McCartney-Francis N, Wahl LM, Roberts AB, et al. Transforming growth factor type beta induces monocyte chemotaxis and growth factor production. *Proc Natl Acad Sci U S A*. (1987) 84:5788–92. doi: 10.1073/pnas.84.16.5788

33. Postlethwaite AE, Keski-Oja J, Moses HL, Kang AH. Stimulation of the chemotactic migration of human fibroblasts by transforming growth factor beta. *J Exp Med*. (1987) 165:251–6. doi: 10.1084/jem.165.1.251

34. Lodyga M, Hinz B. TGF-beta1 - A truly transforming growth factor in fibrosis and immunity. *Semin Cell Dev Biol*. (2020) 101:123–39. doi: 10.1016/j.semcdb.2019.12.010

35. Peng D, Fu M, Wang M, Wei Y, Wei X. Targeting TGF-beta signal transduction for fibrosis and cancer therapy. *Mol Cancer*. (2022) 21:104. doi: 10.1186/s12943-022-01569-x

36. Roberts AB, Sporn MB, Assoian RK, Smith JM, Roche NS, Wakefield LM, et al. Transforming growth factor type beta: rapid induction of fibrosis and angiogenesis *in vivo* and stimulation of collagen formation *in vitro*. *Proc Natl Acad Sci U S A*. (1986) 83:4167–71. doi: 10.1073/pnas.83.12.4167

37. Sime PJ, Xing Z, Graham FL, Csaky KG, Gauldie J. Adenovector-mediated gene transfer of active transforming growth factor-beta1 induces prolonged severe fibrosis in rat lung. *J Clin Invest*. (1997) 100:768–76. doi: 10.1172/JCI119590

38. Dooley S, ten Dijke P. TGF-beta in progression of liver disease. *Cell Tissue Res*. (2012) 347:245–56. doi: 10.1007/s00441-011-1246-y

39. Korkut A, Zaidi S, Kanchi RS, Rao S, Gough NR, Schultz A, et al. A pan-cancer analysis reveals high-frequency genetic alterations in mediators of signaling by the TGF-beta superfamily. *Cell Syst*. (2018) 7:422–37.e7. doi: 10.1016/j.cels.2018.08.010

40. Bharathy S, Xie W, Yingling JM, Reiss M. Cancer-associated transforming growth factor beta type II receptor gene mutant causes activation of bone morphogenic protein-Smads and invasive phenotype. *Cancer Res*. (2008) 68:1656–66. doi: 10.1158/0008-5472.CAN-07-5089

41. Shi Y, Hata A, Lo RS, Massague J, Pavletich NP. A structural basis for mutational inactivation of the tumour suppressor Smad4. *Nature*. (1997) 388:87–93. doi: 10.1038/40431

42. Siegel RL, Miller KD, Fuchs HE, Jemal A. Cancer statistics, 2021. *CA Cancer J Clin*. (2021) 71:7–33. doi: 10.3322/caac.21654

43. Bhatia M, Wong FL, Cao Y, Lau HY, Huang J, Puneet P, et al. Pathophysiology of acute pancreatitis. *Pancreatology*. (2005) 5:132–44. doi: 10.1159/000085265

44. Bhatia M. Apoptosis of pancreatic acinar cells in acute pancreatitis: is it good or bad? *J Cell Mol Med*. (2004) 8:402–9. doi: 10.1111/j.1582-4934.2004.tb00330.x

45. Tachibana I, Imoto M, Adjei PN, Gores GJ, Subramaniam M, Spelsberg TC, et al. Overexpression of the TGFbeta-regulated zinc finger encoding gene, TIEG, induces apoptosis in pancreatic epithelial cells. *J Clin Invest*. (1997) 99:2365–74. doi: 10.1172/JCI119418

46. Liu X, Yu M, Chen Y, Zhang J. Galunisertib (LY2157299), a transforming growth factor-beta receptor I kinase inhibitor, attenuates acute pancreatitis in rats. *Braz J Med Biol Res*. (2016) 49:e5388. doi: 10.1590/1414-431X20165388

47. Cao Y, Yang W, Tyler MA, Gao X, Duan C, Kim SO, et al. Noggin attenuates cerulein-induced acute pancreatitis and impaired autophagy. *Pancreas*. (2013) 42:301–7. doi: 10.1097/MPA.0b013e31825b9f2c

48. Travis MA, Sheppard D. TGF-beta activation and function in immunity. *Annu Rev Immunol*. (2014) 32:51–82. doi: 10.1146/annurev-immunol-032713-120257

49. Jabeen R, Kaplan MH. The symphony of the ninth: the development and function of Th9 cells. *Curr Opin Immunol*. (2012) 24:303–7. doi: 10.1016/j.coi.2012.02.001

50. Jia R, Tang M, Qiu L, Sun R, Cheng L, Ma X, et al. Increased interleukin-23/17 axis and C-reactive protein are associated with severity of acute pancreatitis in patients. *Pancreas*. (2015) 44:321–5. doi: 10.1097/MPA.0000000000000284

51. Witt H, Apte MV, Keim V, Wilson JS. Chronic pancreatitis: challenges and advances in pathogenesis, genetics, diagnosis, and therapy. *Gastroenterology*. (2007) 132:1557–73. doi: 10.1053/j.gastro.2007.03.001

52. Apte MV, Pirola RC, Wilson JS. Pancreatic stellate cells: a starring role in normal and diseased pancreas. *Front Physiol*. (2012) 3:344. doi: 10.3389/fphys.2012.00344

53. Yoo BM, Yeo M, Oh TY, Choi JH, Kim WW, Kim JH, et al. Amelioration of pancreatic fibrosis in mice with defective TGF-beta signaling. *Pancreas*. (2005) 30:e71–9. doi: 10.1097/01.mpa.0000157388.54016.0a

54. Vogelmann R, Ruf D, Wagner M, Adler G, Menke A. Effects of fibrogenic mediators on the development of pancreatic fibrosis in a TGF-beta1 transgenic mouse model. *Am J Physiol Gastrointest Liver Physiol*. (2001) 280:G164–72. doi: 10.1152/ajpgi.2001.280.1.G164

55. Shek FW, Benyon RC, Walker FM, McCrudden PR, Pender SL, Williams EJ, et al. Expression of transforming growth factor-beta 1 by pancreatic stellate cells and its implications for matrix secretion and turnover in chronic pancreatitis. *Am J Pathol*. (2002) 160:1787–98. doi: 10.1016/S0002-9440(10)61125-X

56. Gao X, Cao Y, Yang W, Duan C, Aronson JF, Rastellini C, et al. BMP2 inhibits TGF-beta-induced pancreatic stellate cell activation and extracellular matrix formation. *Am J Physiol Gastrointest Liver Physiol*. (2013) 304:G804–13. doi: 10.1152/ajpgi.00306.2012

57. Gao X, Cao Y, Staloch DA, Gonzales MA, Aronson JF, Chao C, et al. Bone morphogenetic protein signaling protects against cerulein-induced pancreatic fibrosis. *PLoS One*. (2014) 9:e89114. doi: 10.1371/journal.pone.0089114

58. Staloch D, Gao X, Liu K, Xu M, Feng X, Aronson JF, et al. Gremlin is a key pro-fibrogenic factor in chronic pancreatitis. *J Mol Med (Berl)*. (2015) 93:1085–93. doi: 10.1007/s00109-015-1308-9

59. Li X, Nania S, Fejzibegovic N, Moro CF, Klopp-Schulze L, Verbeke C, et al. Cerulein-induced pancreatic fibrosis is modulated by Smad7, the major negative regulator of transforming growth factor-beta signaling. *Biochim Biophys Acta*. (2016) 1862:1839–46. doi: 10.1016/j.bbadis.2016.06.017

60. Akhurst RJ, Derynck R. TGF-beta signaling in cancer–a double-edged sword. *Trends Cell Biol*. (2001) 11:S44–51. doi: 10.1016/s0962-8924(01)02130-4

61. Principe DR, Timbers KE, Atia LG, Koch RM, Rana A. TGFbeta signaling in the pancreatic tumor microenvironment. *Cancers (Basel)*. (2021) 13:5086. doi: 10.3390/cancers13205086

62. Kleeff J, Maruyama H, Ishiwata T, Sawhney H, Friess H, Buchler MW, et al. Bone morphogenetic protein 2 exerts diverse effects on cell growth *in vitro* and is expressed in human pancreatic cancer *in vivo*. *Gastroenterology*. (1999) 116:1202–16. doi: 10.1016/s0016-5085(99)70024-7

63. Lan L, Evan T, Li H, Hussain A, Ruiz EJ, Zaw Thin M, et al. GREM1 is required to maintain cellular heterogeneity in pancreatic cancer. *Nature*. (2022) 607:163–8. doi: 10.1038/s41586-022-04888-7

64. Davis JM, Cheng B, Drake MM, Yu Q, Yang B, Li J, et al. Pancreatic stromal Gremlin 1 expression during pancreatic tumorigenesis. *Genes Dis*. (2022) 9:108–15. doi: 10.1016/j.gendis.2020.05.001

65. Maitra A, Hruban RH. Pancreatic cancer. *Annu Rev Pathol*. (2008) 3:157–88. doi: 10.1146/annurev.pathmechdis.3.121806.154305

66. Hahn SA, Schutte M, Hoque AT, Moskaluk CA, da Costa LT, Rozenblum E, et al. DPC4, a candidate tumor suppressor gene at human chromosome 18q21.1. *Science*. (1996) 271:350–3. doi: 10.1126/science.271.5247.350

67. Leung L, Radulovich N, Zhu CQ, Wang D, To C, Ibrahimov E, et al. Loss of canonical Smad4 signaling promotes KRAS driven Malignant transformation of human pancreatic duct epithelial cells and metastasis. *PloS One*. (2013) 8:e84366. doi: 10.1371/journal.pone.0084366

68. Attisano L, Wrana JL. Signal transduction by the TGF-beta superfamily. *Science*. (2002) 296:1646–7. doi: 10.1126/science.1071809

69. Levy L, Hill CS. Smad4 dependency defines two classes of transforming growth factor beta (TGF-beta) target genes and distinguishes TGF-beta-induced epithelial-mesenchymal transition from its antiproliferative and migratory responses. *Mol Cell Biol*. (2005) 25:8108–25. doi: 10.1128/MCB.25.18.8108-8125.2005

70. Principe DR, Underwood PW, Kumar S, Timbers KE, Koch RM, Trevino JG, et al. Loss of SMAD4 is associated with poor tumor immunogenicity and reduced PD-L1 expression in pancreatic cancer. *Front Oncol*. (2022) 12:806963. doi: 10.3389/fonc.2022.806963

71. Xiong W, He W, Wang T, He S, Xu F, Wang Z, et al. Smad4 deficiency promotes pancreatic cancer immunogenicity by activating the cancer-autonomous DNA-sensing signaling axis. *Adv Sci (Weinh)*. (2022) 9:e2103029. doi: 10.1002/advs.202103029

72. Goggins M, Shekher M, Turnacioglu K, Yeo CJ, Hruban RH, Kern SE. Genetic alterations of the transforming growth factor beta receptor genes in pancreatic and biliary adenocarcinomas. *Cancer Res*. (1998) 58:5329–32.

73. Gordon KJ, Dong M, Chislock EM, Fields TA, Blobe GC. Loss of type III transforming growth factor beta receptor expression increases motility and invasiveness associated with epithelial to mesenchymal transition during pancreatic cancer progression. *Carcinogenesis*. (2008) 29:252–62. doi: 10.1093/carcin/bgm249

74. Togashi Y, Sakamoto H, Hayashi H, Terashima M, de Velasco MA, Fujita Y, et al. Homozygous deletion of the activin A receptor, type IB gene is associated with an aggressive cancer phenotype in pancreatic cancer. *Mol Cancer*. (2014) 13:126. doi: 10.1186/1476-4598-13-126

75. Zhou XP, Woodford-Richens K, Lehtonen R, Kurose K, Aldred M, Hampel H, et al. Germline mutations in BMPR1A/ALK3 cause a subset of cases of juvenile polyposis syndrome and of Cowden and Bannayan-Riley-Ruvalcaba syndromes. *Am J Hum Genet*. (2001) 69:704–11. doi: 10.1086/323703

76. Zhang L, Zhou W, Velculescu VE, Kern SE, Hruban RH, Hamilton SR, et al. Gene expression profiles in normal and cancer cells. *Science*. (1997) 276:1268–72. doi: 10.1126/science.276.5316.1268

77. Cox AD, Fesik SW, Kimmelman AC, Luo J, Der CJ. Drugging the undruggable RAS: Mission possible? *Nat Rev Drug Discovery*. (2014) 13:828–51. doi: 10.1038/nrd4389

78. Lohr M, Kloppel G, Maisonneuve P, Lowenfels AB, Luttges J. Frequency of K-ras mutations in pancreatic intraductal neoplasias associated with pancreatic ductal adenocarcinoma and chronic pancreatitis: a meta-analysis. *Neoplasia*. (2005) 7:17–23. doi: 10.1593/neo.04445

79. Jaeger E, Leedham S, Lewis A, Segditsas S, Becker M, Cuadrado PR, et al. Hereditary mixed polyposis syndrome is caused by a 40-kb upstream duplication that leads to increased and ectopic expression of the BMP antagonist GREM1. *Nat Genet*. (2012) 44:699–703. doi: 10.1038/ng.2263

80. Davis H, Irshad S, Bansal M, Rafferty H, Boitsova T, Bardella C, et al. Aberrant epithelial GREM1 expression initiates colonic tumorigenesis from cells outside the stem cell niche. *Nat Med*. (2015) 21:62–70. doi: 10.1038/nm.3750

81. Burris HA, Moore MJ, Andersen J, Green MR, Rothenberg ML, Modiano MR, et al. Improvements in survival and clinical benefit with gemcitabine as first-line therapy for patients with advanced pancreas cancer: a randomized trial. *J Clin Oncol*. (1997) 15:2403–13. doi: 10.1200/JCO.1997.15.6.2403

82. Conroy T, Desseigne F, Ychou M, Bouche O, Guimbaud R, Becouarn Y, et al. FOLFIRINOX versus gemcitabine for metastatic pancreatic cancer. *N Engl J Med*. (2011) 364:1817–25. doi: 10.1056/NEJMoa1011923

83. Von Hoff DD, Ervin T, Arena FP, Chiorean EG, Infante J, Moore M, et al. Increased survival in pancreatic cancer with nab-paclitaxel plus gemcitabine. *N Engl J Med*. (2013) 369:1691–703. doi: 10.1056/NEJMoa1304369

84. Principe DR, Narbutis M, Kumar S, Park A, Viswakarma N, Dorman MJ, et al. Long-term gemcitabine treatment reshapes the pancreatic tumor microenvironment and sensitizes murine carcinoma to combination immunotherapy. *Cancer Res*. (2020) 80:3101–15. doi: 10.1158/0008-5472.CAN-19-2959

85. Schlingensiepen KH, Jaschinski F, Lang SA, Moser C, Geissler EK, Schlitt HJ, et al. Transforming growth factor-beta 2 gene silencing with trabedersen (AP 12009) in pancreatic cancer. *Cancer Sci*. (2011) 102:1193–200. doi: 10.1111/j.1349-7006.2011.01917.x

86. Oettle H, Seufferlein T, Luger T, Schmid RM, v. Wichert G, Endlicher E, et al. Final results of a phase I/II study in patients with pancreatic cancer, Malignant melanoma, and colorectal carcinoma with trabedersen. *J Clin Oncol*. (2012) 30:4034–4. doi: 10.1200/jco.2012.30.15_suppl.4034

87. Martin CJ, Datta A, Littlefield C, Kalra A, Chapron C, Wawersik S, et al. Selective inhibition of TGFbeta1 activation overcomes primary resistance to checkpoint blockade therapy by altering tumor immune landscape. *Sci Transl Med*. (2020) 12:eaay8456. doi: 10.1126/scitranslmed.aay8456

88. Yap T, Gainor J, McKean M, Johnson M, Bockornv B, Barve M, et al. 780 SRK-181, a latent TGFβ1 inhibitor: safety, efficacy, and biomarker results from the dose escalation portion of a phase I trial (DRAGON trial) in patients with advanced solid tumors. *J ImmunoTherapy Cancer*. (2022) 10:A812–2. doi: 10.1136/jitc-2022-SITC2022.0780

89. Powderly J, Spira A, Kondo S, Doi T, Luke JJ, Rasco D, et al. Model informed dosing regimen and phase I results of the anti-PD-1 antibody budigalimab (ABBV-181). *Clin Transl Sci*. (2021) 14:277–87. doi: 10.1111/cts.12855

90. Fajardo DC, Moore CL, Porazinski S, McLean B, Borbilas E, Australian Pancreatic, et al. 1467 Selective targeting of integrins αVβ8 and αVβ1 within the dynamic ecosystem of pancreatic cancer to improve the overall anti-tumor response. *J ImmunoTherapy Cancer*. (2023) 11:A1631–1. doi: 10.1136/jitc-2023-SITC2023.1467

91. Daud A, Barnes CN, Owen S, Turner SM, Sznol M, Lefebvre EA, et al. 714 Phase 1a trial of PLN-101095, an integrin αvβ8 and αvβ1 inhibitor, as monotherapy and in combination with pembrolizumab, in treatment-resistant patients with advanced or metastatic solid tumors. *J ImmunoTherapy Cancer*. (2023) 11:A809–9. doi: 10.1136/jitc-2023-SITC2023.0714

92. Reader CS, Vallath S, Steele CW, Haider S, Brentnall A, Desai A, et al. The integrin alphavbeta6 drives pancreatic cancer through diverse mechanisms and represents an effective target for therapy. *J Pathol*. (2019) 249:332–42. doi: 10.1002/path.5320

93. Qiang L, Hoffman MT, Ali LR, Castillo JI, Kageler L, Temesgen A, et al. Transforming growth factor-beta blockade in pancreatic cancer enhances sensitivity to combination chemotherapy. *Gastroenterology*. (2023) 165:874–90.e10. doi: 10.1053/j.gastro.2023.05.038

94. Bauer TM, Santoro A, Lin CC, Garrido-Laguna I, Joerger M, Greil R, et al. Phase I/Ib, open-label, multicenter, dose-escalation study of the anti-TGF-β monoclonal antibody, NIS793, in combination with spartalizumab in adult patients with advanced tumors. *J ImmunoTherapy Cancer*. (2023) 11:e007353. doi: 10.1136/jitc-2023-007353

95. Tolcher AW, Berlin JD, Cosaert J, Kauh J, Chan E, Piha-Paul SA, et al. A phase 1 study of anti-TGFbeta receptor type-II monoclonal antibody LY3022859 in patients with advanced solid tumors. *Cancer Chemother Pharmacol*. (2017) 79:673–80. doi: 10.1007/s00280-017-3245-5

96. O'Connor-McCourt MD, Tremblay G, Lenferink A, Sulea T, Zwaagstra J, Koropatnick J. Abstract 1759: AVID200, a highly potent TGF-beta trap, exhibits optimal isoform selectivity for enhancing anti-tumor T-cell activity, without promoting metastasis or cardiotoxicity. *Cancer Res.* (2018) 78:1759–9. doi: 10.1158/1538-7445.Am2018-1759

97. Tremblay G, Gruosso T, Denis J-F, Figueredo R, Koropatnick J, O'Connor-McCourt M. Abstract 6710: AVID200, a first-in-class selective TGF-beta 1 and -beta 3 inhibitor, sensitizes tumors to immune checkpoint blockade therapies. *Cancer Res.* (2020) 80:6710–0. doi: 10.1158/1538-7445.Am2020-6710

98. Yap TA, Lakhani NJ, Araujo DV, Ahnert JR, Chandana SR, Sharma M, et al. AVID200, first-in-class TGF-beta 1 and 3 selective and potent inhibitor: Safety and biomarker results of a phase I monotherapy dose-escalation study in patients with advanced solid tumors. *J Clin Oncol.* (2020) 38:3587–7. doi: 10.1200/JCO.2020.38.15_suppl.3587

99. Juneja VR, McGuire KA, Manguso RT, LaFleur MW, Collins N, Haining WN, et al. PD-L1 on tumor cells is sufficient for immune evasion in immunogenic tumors and inhibits CD8 T cell cytotoxicity. *J Exp Med.* (2017) 214:895–904. doi: 10.1084/jem.20160801

100. Iwai Y, Hamanishi J, Chamoto K, Honjo T. Cancer immunotherapies targeting the PD-1 signaling pathway. *J BioMed Sci.* (2017) 24:26. doi: 10.1186/s12929-017-0329-9

101. Gulley JL, Schlom J, Barcellos-Hoff MH, Wang XJ, Seoane J, Audhuy F, et al. Dual inhibition of TGF-beta and PD-L1: a novel approach to cancer treatment. *Mol Oncol.* (2022) 16:2117–34. doi: 10.1002/1878-0261.13146

102. Knudson KM, Hicks KC, Luo X, Chen JQ, Schlom J, Gameiro SR. M7824, a novel bifunctional anti-PD-L1/TGFbeta Trap fusion protein, promotes anti-tumor efficacy as monotherapy and in combination with vaccine. *Oncoimmunology.* (2018) 7:e1426519. doi: 10.1080/2162402X.2018.1426519

103. Strauss J, Heery CR, Schlom J, Madan RA, Cao L, Kang Z, et al. Phase I trial of M7824 (MSB0011359C), a bifunctional fusion protein targeting PD-L1 and TGFbeta, in advanced solid tumors. *Clin Cancer Res.* (2018) 24:1287–95. doi: 10.1158/1078-0432.CCR-17-2653

104. Herbertz S, Sawyer JS, Stauber AJ, Gueorguieva I, Driscoll KE, Estrem ST, et al. Clinical development of galunisertib (LY2157299 monohydrate), a small molecule inhibitor of transforming growth factor-beta signaling pathway. *Drug Des Devel Ther.* (2015) 9:4479–99. doi: 10.2147/DDDT.S86621

105. Melisi D, Garcia-Carbonero R, Macarulla T, Pezet D, Deplanque G, Fuchs M, et al. Galunisertib plus gemcitabine vs. gemcitabine for first-line treatment of patients with unresectable pancreatic cancer. *Br J Cancer.* (2018) 119:1208–14. doi: 10.1038/s41416-018-0246-z

106. Lee JE, Lee P, Yoon YC, Han BS, Ko S, Park MS, et al. Vactosertib, TGF-beta receptor I inhibitor, augments the sensitization of the anti-cancer activity of gemcitabine in pancreatic cancer. *BioMed Pharmacother.* (2023) 162:114716. doi: 10.1016/j.biopha.2023.114716

107. Hong E, Barczak W, Park S, Heo JS, Ooshima A, Munro S, et al. Combination treatment of T1-44, a PRMT5 inhibitor with Vactosertib, an inhibitor of TGF-beta signaling, inhibits invasion and prolongs survival in a mouse model of pancreatic tumors. *Cell Death Dis.* (2023) 14:93. doi: 10.1038/s41419-023-05630-5

108. Kim ST, Hong JY, Park YS, Kim S-J, Park JO. Phase 1b study of vactosertib in combination with oxaliplatin with 5FU/LV (FOLFOX) in patients with metastatic pancreatic cancer who have failed first-line gemcitabine/nab-paclitaxel. *J Clin Oncol.* (2022) 40:e16299–9. doi: 10.1200/JCO.2022.40.16_suppl.e16299

109. Yap TA, Vieito M, Baldini C, Sepulveda-Sanchez JM, Kondo S, Simonelli M, et al. First-in-human phase I study of a next-generation, oral, TGFbeta receptor 1 inhibitor, LY3200882, in patients with advanced cancer. *Clin Cancer Res.* (2021) 27:6666–76. doi: 10.1158/1078-0432.CCR-21-1504

110. Davies GCG, Dedi N, Jones PS, Kevorkian L, McMillan D, Ottone C, et al. Discovery of ginisortamab, a potent and novel anti-gremlin-1 antibody in clinical development for the treatment of cancer. *MAbs.* (2023) 15:2289681. doi: 10.1080/19420862.2023.2289681

111. Haake M, Haack B, Schafer T, Harter PN, Mattavelli G, Eiring P, et al. Tumor-derived GDF-15 blocks LFA-1 dependent T cell recruitment and suppresses responses to anti-PD-1 treatment. *Nat Commun.* (2023) 14:4253. doi: 10.1038/s41467-023-39817-3

112. Yang L, Chang CC, Sun Z, Madsen D, Zhu H, Padkjaer SB, et al. GFRAL is the receptor for GDF15 and is required for the anti-obesity effects of the ligand. *Nat Med.* (2017) 23:1158–66. doi: 10.1038/nm.4394

113. Gourgou-Bourgade S, Bascoul-Mollevi C, Desseigne F, Ychou M, Bouche O, Guimbaud R, et al. Impact of FOLFIRINOX compared with gemcitabine on quality of life in patients with metastatic pancreatic cancer: results from the PRODIGE 4/ACCORD 11 randomized trial. *J Clin Oncol.* (2013) 31:23–9. doi: 10.1200/JCO.2012.44.4869

114. Kelly RJ, Ajani JA, Kuzdzal J, Zander T, Van Cutsem E, Piessen G, et al. Adjuvant nivolumab in resected esophageal or gastroesophageal junction cancer. *N Engl J Med.* (2021) 384:1191–203. doi: 10.1056/NEJMoa2032125

115. André T, Shiu KK, Kim TW, Jensen BV, Jensen LH, Punt C, et al. Pembrolizumab in microsatellite-instability-high advanced colorectal cancer. *N Engl J Med.* (2020) 383:2207–18. doi: 10.1056/NEJMoa2017699

116. Ullman NA, Burchard PR, Dunne RF, Linehan DC. Immunologic strategies in pancreatic cancer: making cold tumors hot. *J Clin Oncol.* (2022) 40:2789–805. doi: 10.1200/JCO.21.02616

117. Zabransky DJ, Yarchoan M, Jaffee EM. Strategies for heating up cold tumors to boost immunotherapies. *Annu Rev Cancer Biol.* (2023) 7:149–70. doi: 10.1146/annurev-cancerbio-061421-040258

118. Gordon KJ, Kirkbride KC, How T, Blobe GC. Bone morphogenetic proteins induce pancreatic cancer cell invasiveness through a Smad1-dependent mechanism that involves matrix metalloproteinase-2. *Carcinogenesis.* (2009) 30:238–48. doi: 10.1093/carcin/bgn274

119. Ehata S, Yokoyama Y, Takahashi K, Miyazono K. Bi-directional roles of bone morphogenetic proteins in cancer: another molecular Jekyll and Hyde? *Pathol Int.* (2013) 63:287–96. doi: 10.1111/pin.12067

120. Kong P, Shinde AV, Su Y, Russo I, Chen B, Saxena A, et al. Opposing actions of fibroblast and cardiomyocyte smad3 signaling in the infarcted myocardium. *Circulation.* (2018) 137:707–24. doi: 10.1161/circulationaha.117.029622

frontiers | Frontiers in Oncology

TYPE Review
PUBLISHED 06 March 2024
DOI 10.3389/fonc.2024.1371421

OPEN ACCESS

EDITED BY
Kathleen E. DelGiorno,
Vanderbilt University, United States

REVIEWED BY
Elva Morretta,
Università degli Studi di Salerno, Italy
Mukulika Bose,
University of Texas MD Anderson Cancer Center, United States

*CORRESPONDENCE
Yingjie Jia
1614236405@qq.com

†These authors have contributed equally to this work

RECEIVED 16 January 2024
ACCEPTED 23 February 2024
PUBLISHED 06 March 2024

CITATION
Xu Q, Jia C, Ou Y, Zeng C and Jia Y (2024) Dark horse target Claudin18.2 opens new battlefield for pancreatic cancer.
Front. Oncol. 14:1371421.
doi: 10.3389/fonc.2024.1371421

Dark horse target Claudin18.2 opens new battlefield for pancreatic cancer

Qian Xu[1,2†], Caiyan Jia[1,2†], Yan Ou[1,2†], Chuanxiu Zeng[1,2] and Yingjie Jia[1,2*]

[1]Department of Oncology, First Teaching Hospital of Tianjin University of Traditional Chinese Medicine, Tianjin, China, [2]Department of Oncology, National Clinical Research Center for Chinese Medicine Acupuncture and Moxibustion, Tianjin, China

Pancreatic cancer is one of the deadliest malignant tumors, which is a serious threat to human health and life, and it is expected that pancreatic cancer may be the second leading cause of cancer death in developed countries by 2030. Claudin18.2 is a tight junction protein expressed in normal gastric mucosal tissues, which is involved in the formation of tight junctions between cells and affects the permeability of paracellular cells. Claudin18.2 is highly expressed in pancreatic cancer and is associated with the initiation, progression, metastasis and prognosis of cancer, so it is considered a potential therapeutic target. Up to now, a number of clinical trials for Claudin18.2 are underway, including solid tumors such as pancreatic cancers and gastric cancers, and the results of these trials have not yet been officially announced. This manuscript briefly describes the Claudia protein, the dual roles of Cluadin18 in cancers, and summarizes the ongoing clinical trials targeting Claudin18.2 with a view to integrating the research progress of Claudin18.2 targeted therapy. In addition, this manuscript introduces the clinical research progress of Claudin18.2 positive pancreatic cancer, including monoclonal antibodies, bispecific antibodies, antibody-drug conjugates, CAR-T cell therapy, and hope to provide feasible ideas for the clinical treatment of Claudin18.2 positive pancreatic cancer.

KEYWORDS

pancreatic cancer, Claudin18.2, targeted therapy, immunotherapy, trials

1 Introduction

Claudins are important proteins in normal tissue tight junctions (TJ), which are related to the formation of epithelial and epidermal tight junction proteins (1), and were first discovered and named by researchers Mikio Furuse and Shoichiro Tsukita of Kyoto University in Japan in 1998. The name “Claudin” originated from the Latin word “claudere (to close)” (2). Three main functions of Claudins are intracellular signaling, fence, and barrier. While the function of fence divides the apical and basolateral domains and controls substance mobility in the plasma membrane, the function of barrier is the capacity to

control the paracellular permeation of ions, water, immune cells, and macromolecules, selectively (3–5). Claudins include at least 27 family members, 4 transmembrane structural domains, and 2 extracellular loops (Schematic diagram of Claudins protein structure, Figure 1), which allow the Claudins proteins to effectively sustain the polarity of epithelial and endothelial cells, thereby effectively regulating paracellular permeability and conductance (6). Claudin18 is one of the Claudins (CLDN) proteins family, which has two different isoforms, Claudin18.1 and Claudin18.2, due to the optional exons 1a and 1b (7). Claudin18.2 is the highly targeted marker protein with tissue-specific expression. The expression of Claudin18.2 in normal tissues is restricted to differentiated gastric mucosal epithelial cells, which results that it is masked and is mostly untouched by intravenous antibodies. However, if the tissues are cancerous, changes in cell polarity expose the epitope of Claudin18.2 to the cell surface and increase the expression (8). Claudin18.2 is expressed in many tumors, including gastric cancer, pancreatic cancer, esophageal cancer, ovarian cancer, etc. (8–11). In a study of 414 cancer patients with immunohistochemistry (IHC) analysis to assess Claudin18.2 expression in different tumor types, a total of 4.1% (N=17) of subjects were Claudin18.2 positive, including pancreatic cancer (16.7%, 1/6), gastric cancer (14.1%, 12/85), colorectal cancer (0.9%, 2/203), biliary tract cancer (6.3%, 1/16), and genitourinary/miscellaneous (2.2%, 1/46) (12). The expression of Claudin18.2 is not only in the primary tumor, but also in metastases. In one study, pancreatic ductal adenocarcinoma (PDAC), which is the most common kind of pancreatic cancers, showed 59.2% (103/174) Claudin18.2 expression, of which 54.6% were strongly expressed (N=95). In the lymphatic metastasis, 69.4% (N=34) expressed Claudin18.2 with strong staining. Whereas the number of tumor cells in the samples expressing Claudin 18.2 was positively linked with the staining intensity (RS = 0.871, p<0.001). The results are similar in liver metastasis samples. 65.7% of samples (N=23) expressed Claudin18.2 and all positive samples showed 2+ or higher staining intensity (13). Jiang H et al. finds that the expression of Claudin18.2 in the metastatic lesions is in line with the expression in the primary cancer tissues (14). And the expression of Claudin18.2 was more obvious in the disease progression. Samples from lymph nodes and liver metastases showed expression that was either identical to or higher than that in the original lesion, and the high expression of Claudin18.2 were related to the poor prognostic factors of positive lymph nodes (15). The longer median progression-free survival (mPFS) is related to the lower Claudin18.2 expression level in gastric cancer (p = 0.047) (16). Researchers also revealed that claudin18 expression correlates with poor survival in patients with CRC. And the prognosis of patients with positive claudin18 expression was significantly poorer than in negative cases (P= 0.0106) (17). While Jun et al. found that in patients with Claudin18 expression, OS was longer than those without Claudin18 expression (5-year survival rate, 90.5% vs. 64.8%) (18). Another study also found that patients with high expression levels of claudin18 have longer survival time than those with low claudin18 expression (19). Overexpression of Claudin18.2 may activate related signaling pathways, like SPAK-p38 MAPK signaling pathway, epidermal growth factor receptor (EGFR)/ extracellular signal-regulated kinase (ERK) signaling et al., which leads to tumor cell proliferation (20–22). Another study on human pancreatic cancer cells showed Claudin18 is predominantly controlled at the transcriptional level by specific protein kinase C signaling pathways and modified by DNA methylation (23). At present, the exact mechanism that Claudin18.2 impacts on distant metastasis and tumor lymph node metastasis is unclear, and it is possible that its unusual expression changes the structure and function of tight junctions between cells. The studies have also found that different expressions of Claudin have been shown to be

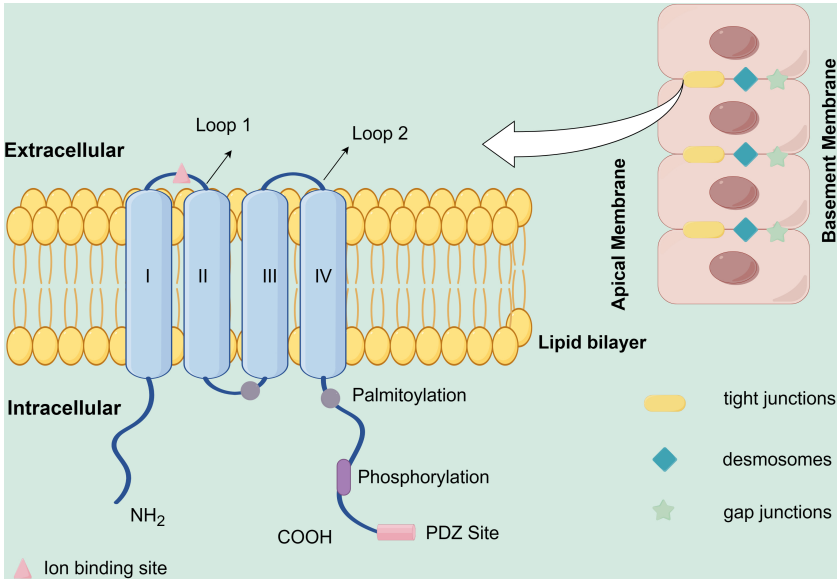

FIGURE 1
Schematic diagram of Claudins protein structure. (By Figdraw).

significant in the prognosis of cancer. For example, claudin-1 is associated with colon cancer prognosis (24), claudin-18 is related to gastric cancer (GC) prognosis (25), and claudin-10 is relevant to hepatocellular carcinoma prognosis (26). In summary, Claudin18.2 protein is involved in the migration, differentiation, and proliferation of tumor cells. And because of its specific expression it may be used as the target of precise attack on tumors, so the value of Claudin18.2 in the diagnosis, treatment and prognosis of tumors should be further explored.

2 The double-edged sword role of Claudin18 in cancers

There are many antigens with dual roles in tumor microenvironment, for example, TGF-β, desmosomes, HMGB1 (a nuclear DNA-binding protein) and cancer testis antigens etc. (27–30). Claudin18 also has different effects in tumors, acting as a tumor suppressant in gastric and lung cancers, but playing a promoting role in other gastrointestinal tumors, such as pancreatic cancer, colorectal cancer, and esophageal cancer (31). At present, only a few articles have elucidated the mechanism of action of Claudin18 in different tumors, which needs further summary.

2.1 Inhibition of tumors

Oshima et al. found that the Ki-67 index was inversely correlated with the level of Claudin18 in the front of gastric cancer invasion, and the loss of Claudin18 was also shown to be associated with the proliferation and invasion of GC cells in subsequent cell experiments (32). Helicobacter pylori infection in mice attenuated the expression of Claudin18 in the early stage of GC development, leading to rapid tumor development, which may be related to the involvement of Claudin18 in the regulation of cytokines, Wnt and Notch signaling pathways (33). Zhou et al. found that Claudin18 can inversely regulate the activity of Yes-associated protein (YAP), thereby promoting cell proliferation and tumorigenesis (34). Claudin18.1 can inhibit yes-associated protein/tafazzin (Yap/Taz) and insulin-like growth factor 1 receptor (IGF-1R) signaling pathway, resulting in AKT inhibition (35, 36). It proved that Claudins is an important signaling center involved in cell proliferation and tumorigenesis. In Claudin18-deficient mice, the frequency of lung adenocarcinoma also increased accordingly (37).

2.2 Promotion of tumors

The cancer-promoting effects of Claudin18 are mostly manifested in its ectopically activated cancers. For bile duct carcinoma cells, the overactivation of EGFR leads to the activation of the downstream Ras/Raf/MEK/ERK cascade, which induces the expression of Claudin18, and the expression of Claudin18 can further induce ERK1/2 phosphorylation, forming a positive feedback loop, and playing a role in promoting cancer (21). In the normal esophageal squamous epithelium, Claudin18 is not expressed, but the expression of Claudin18 in the columnar epithelium of Barrett's esophagus is doubled, and Claudin18 can reduce the permeability of tightly junction H^+ ions, prevent its attack and destroy the esophageal squamous epithelium, thereby promoting tumorigenesis (38). Claudin18.2 is mainly regulated by the hypomethylation gene sequence CpG island promoter and the transcription factor cAMP-response element blinding protein (CREB) in its genetic coding sequence (8), and its overexpression may be related to signaling pathways, like PKC pathway, ERK/MAPK pathway, and HER2/HER3 pathway, which promote the proliferation of tumor cells (31, 39, 40). In addition, the high expression of Claudin18.2 can regulate cell polarity, disrupt the tight junctions of tumor cells, change the adhesion and plasticity of tumor cells, increase their ability to metastasize and infiltration, and increase the degree of malignancy of tumors (41).

3 Current research of Claudin18.2

At present, there are no products targeting Claudin18.2 on the market, but research on various types of drugs targeting Claudin18.2 is in full swing, of which the indications are mostly focusing on Claudin18.2 positive gastric cancer and pancreatic cancer. Immunotherapy for solid tumor targeting Claudin18.2 includes monoclonal antibody, bispecific antibody, antibody-drug conjugate (ADC), and CAR-T cell. For example, the first targeted development drug, Zolbetuximab (IMAB362), is an IgG1 monoclonal antibody that specifically links structurally chimeric to Clauidn18.2 on the surface of tumor cells. It causes antibody-dependent cellular cytotoxicity (ADCC), complement-dependent cytotoxicity (CDC), apoptosis and inhibits cell proliferation. Its powerful capacity to eradicate cancer cells and regulate illness has been effectively confirmed by preclinical research (42). CMG901, monoclonal antibody + monomethyl auristatin E (MMAE) drug conjugates, can efficiently target tumor cells by anti-Claudin18.2 antibodies and trigger endocytosis, which allows the small molecule toxin MMAE to enter tumor cells to provide antitumor effects (14). Here, we list the latest clinical trials in Claudin18.2-targeted agents developed in ClinicalTrials.gov (Table 1) for further research.

4 Application of Claudin18.2 in pancreatic cancer

Pancreatic cancer (PC) is one of the deadliest tumors, which seriously threatens human health. Given that pancreatic cancer has no special clinical manifestations and its unique anatomical location, it is considered to be a "silent killer". In 2020, there were more than 490,000 new cases and more than 460,000 deaths worldwide. Pancreatic cancer kills almost as many people as it does, and the highest incidence rates are found in Europe and Northern America (26). With the lowest 5-year survival rate of any cancer type (10%), PC is also expected to become the second leading cause of cancer-

TABLE 1 Latest clinical trials in Claudin18.2-targeted agents in ClinicalTrials.gov.

Agent	Type of Agents	NCT Number	Indications	Status	Phase	References
CMG901	ADC	NCT04805307	Advanced Solid Tumor, Gastric Cancer, Gastroesophageal Junction Adenocarcinoma, Pancreatic Cancer	Recruiting	I	(43)
SYSA1801	ADC	NCT05009966	Advanced Solid Tumor, Gastric Cancer, Gastroesophageal Junction Cancer, Pancreatic Cancer	Recruiting	I	
LM-302	ADC	NCT05161390	Advanced Solid Tumor	Recruiting	I/II	
LM-302	ADC	NCT05994001	Biliary Tract Cancer	Recruiting	I/II	
LM302	ADC	NCT05934331	Gastric Cancer, Pancreatic Cancer	Recruiting	II	
LM-302	ADC	NCT05001516	Advanced Solid Tumor	Active, not recruiting	I	
EO-3021	ADC	NCT05980416	Pancreas Neoplasm, Stomach Neoplasm, Gastrointestinal Neoplasms, Digestive System Neoplasm, Neoplasms by Site, Neoplasms	Recruiting	I	
SKB315 for injection	ADC	NCT05367635	Advanced Solid Tumors	Recruiting	I	
RC118-ADC	ADC	NCT05205850	Advanced Solid Tumor	Recruiting	I/II	
RC118	ADC	NCT06038396	Advanced Solid Tumor	Recruiting	I/II	
TORL-2-307-ADC	ADC	NCT05156866	Advanced Solid Tumor, Gastric Cancer, Pancreas Cancer, Gastroesophageal Junction Adenocarcinoma	Recruiting	I	
AMG-910	Bispecific antibodies	NCT04260191	Gastric and Gastroesophageal Junction Adenocarcinoma	Completed	I	(44)
Q-1802	Bispecific antibodies	NCT04856150	Advanced Solid Tumors	Recruiting	I	
SG1906	Bispecific antibodies	NCT05857332	Locally Advanced Unresectable or Metastatic Solid Tumors	Recruiting	I	
QLS31905	Bispecific antibodies	NCT06041035	Solid Tumor	Not yet recruiting	I/II	
AZD5863	Bispecific Antibodies	NCT06005493	Gastric Cancer, Gastro-esophageal Junction Cancer, Pancreatic Ductal Adenocarcinoma, Esophageal Adenocarcinoma	Recruiting	I/II	
QLS31905	Bispecific antibodies	NCT05278832	Advanced Solid Tumors	Recruiting	I	
PM1032 injection	Bispecific antibodies	NCT05839106	Advanced Tumor	Recruiting	I/II	(45)
ASP2138	Bispecific antibodies	NCT05365581	Gastric Adenocarcinoma, Gastroesophageal Junction (GEJ) Adenocarcinoma, Pancreatic Adenocarcinoma	Recruiting	I	
IBI389	Bispecific antibodies	NCT05164458	Advanced Solid Tumors	Recruiting	I	
CAR-CLD18 T Cells	CAR-T	NCT03159819	Advanced Gastric Adenocarcinoma, Pancreatic Adenocarcinoma	Unknown	Not Applicable	(46)
Engineered CAR-T Cells	CAR-T	NCT03198052	Lung Cancer, Cancer	Recruiting	I	
CAR-CLDN18.2 T Cells	CAR-T	NCT03874897	Advanced Solid Tumor	Recruiting	I	(47)
CT041	CAR-T	NCT04581473	Gastric Adenocarcinoma, Pancreatic Cancer, Gastroesophageal Junction Adenocarcinoma	Recruiting	I/II	(48)

(Continued)

TABLE 1 Continued

Agent	Type of Agents	NCT Number	Indications	Status	Phase	References
CT041	CAR-T	NCT04404595	Gastric Cancer, Pancreatic Cancer	Recruiting	I/II	(49)
CT041	CAR-T	NCT05911217	Pancreatic Cancer	Recruiting	I	
LCAR-C18S	CAR-T	NCT04467853	Advanced solid Tumors	Terminated	I	
LY011	CAR-T	NCT04966143	Pancreatic Cancer	Recruiting	I	
LY011	CAR-T	NCT04977193	Advanced Gastric Adenocarcinoma	Recruiting	I	
TAC01-CLDN18.2	CAR-T	NCT05862324	Metastatic Solid Tumor	Recruiting	I/II	
IBI345	CAR-T	NCT05199519	Solid Tumors	Completed	I	
Claudin18.2 CAR-T cells	CAR-T	NCT05620732	Advanced Pancreatic Carcinoma, Advanced Gastric Carcinoma	Recruiting	Not Applicable	
Claudin 18.2 CAR-T	CAR-T	NCT05472857	Gastric Cancer, Pancreatic Cancer, Advanced Ovarian Carcinoma, Gastroesophageal Junction Adenocarcinoma	Recruiting	I	
RD07 Cell Injection	CAR-T	NCT05284968	Solid Tumor	Not yet recruiting	I	
LB1908	CAR-T	NCT05539430	Gastric Cancer, Gastroesophageal-junction Cancer, Esophageal Cancer, Pancreatic Cancer	Recruiting	I	
XKDCT086	CAR-T	NCT05952375	Gastric Cancer	Recruiting	Not Applicable	
HEC-016	CAR-T	NCT05277987	Advanced Gastric/Esophagogastric Junction Adenocarcinoma, Pancreatic Cancer	Recruiting	I	
AZD6422	CAR-T	NCT05981235	Gastrointestinal Tumors	Not yet recruiting	I	
KD-496	CAR-T	NCT05583201	Gastric Cancer, Pancreatic Cancer, Solid Tumor	Recruiting	I	
Dual-targeting CLDN18.2 and PD-L1 CAR-T cells	CAR-T	NCT06084286	Advanced Solid Tumor	Not yet recruiting	I	
CT048	CAR-T	NCT05393986	Gastric Adenocarcinoma, Pancreatic Cancer, Gastroesophageal Junction Adenocarcinoma, Advanced Solid Tumors	Recruiting	I	
IMC002 injection	CAR-T	NCT05946226	Advanced Digestive System Tumor	Recruiting	I	
IMC008	CAR-T	NCT05837299	Advanced Solid Tumor	Recruiting	I	
Zolbetuximab (IMAB362)	Monoclonal antibodies	NCT03504397	Locally Advanced Unresectable or Metastatic Gastric or Gastroesophageal Junction (GEJ) Adenocarcinoma	Active, not recruiting	III	
Zolbetuximab (IMAB362)	Monoclonal antibodies	NCT03505320	Metastatic or Locally Advanced Unresectable Gastric or Gastroesophageal Junction (GEJ) Adenocarcinoma	Recruiting	II	
Zolbetuximab (IMAB362)	Monoclonal antibodies	NCT03653507	Locally Advanced Unresectable or Metastatic Gastric or Gastroesophageal Junction (GEJ) Adenocarcinoma	Active, not recruiting	III	
Zolbetuximab (IMAB362)	Monoclonal antibodies	NCT03816163	Pancreatic Cancer, Metastatic Pancreatic Cancer, Metastatic Pancreatic Adenocarcinoma	Recruiting	II	(50)
Zolbetuximab (IMAB363)	Monoclonal antibodies	NCT01630083	Adenocarcinoma of the Gastroesophageal Junction, Adenocarcinoma of Esophagus, Gastric Adenocarcinoma	Completed	II	

(Continued)

TABLE 1 Continued

Agent	Type of Agents	NCT Number	Indications	Status	Phase	References
Zolbetuximab	Monoclonal antibodies	NCT06048081	Locally Advanced Unresectable Gastroesophageal Junction (GEJ) Adenocarcinoma Cancer, Locally Advanced Unresectable Gastric Adenocarcinoma Cancer, Metastatic Gastric Adenocarcinoma Cancer, Metastatic Gastroesophageal Junction (GEJ) Adenocarcinoma	Available		
AB011	Monoclonal antibodies	NCT04400383	Solid Tumors, Gastric Cancer, Pancreatic Adenocarcinoma	Active, not recruiting	I	(51)
TST001	Monoclonal antibodies	NCT04495296	Advanced Cancer	Recruiting	I/II	
TST001	Monoclonal antibodies	NCT04396821	Advanced Cancer, Gastric Cancer, Gastroesophageal-junction Cancer, Pancreatic Cancer	Recruiting	I/II	
TST001	Monoclonal antibodies	NCT05190575	Biliary Tract Neoplasms	Completed	II	
TST001	Monoclonal antibodies	NCT06093425	Gastric Cancer, Gastroesophageal-junction Cancer, Advanced Cancer	Not yet recruiting	III	
ASKB589	Monoclonal antibodies	NCT04632108	Malignant Solid Tumor	Recruiting	I/II	
89Zr-NY005	Monoclonal antibodies	NCT04989010	Solid Tumor	Unknown	Not Applicable	
ZL-1211	Monoclonal antibodies	NCT05065710	Advanced Solid Tumors	Recruiting	I/II	
IMAB362	Monoclonal antibodies	NCT01671774	Gastric Adenocarcinoma, Adenocarcinoma of the Gastroesophageal Junction, Adenocarcinoma of Esophagus	Completed	I	
SPX-101	Monoclonal antibodies	NCT05231733	Solid Tumor	Not yet recruiting	I	
TORL-2-307-MAB	Monoclonal antibodies	NCT05159440	Advanced Solid Tumor, Gastric Cancer, Pancreas Cancer, Gastroesophageal Junction Adenocarcinoma	Recruiting	I	
M108	Monoclonal antibodies	NCT04894825	Advanced Unresectable Solid Tumors	Recruiting	I	
NBL-015	Monoclonal antibodies	NCT05153096	Advanced Solid Tumors	Not yet recruiting	I	
MIL93	Monoclonal antibodies	NCT04671875	Advanced Malignancies	Recruiting	I	

related mortality in the United States by 2030 (52, 53). As the population grows, the aging process accelerates and the westernized lifestyles become more prevalent, in the coming years the incidence of pancreatic cancer is likely to continue to rise. Currently, surgery treatment is the only promising method for pancreatic cancer, usually followed by postoperative adjuvant radiotherapy and chemotherapy, and the survival rate of five year in patients is only 30% (54). Exocrine cell tumors account for 95% of pancreatic cancer cases, and the most common of these is PDAC. However, PDAC is characterized by early invasive metastases, with more than 50% of patients presenting with distant metastases, only 15%-20% of patients with PDAC can perform the surgery and most surgical patients also experience metastases within four years (55, 56). At present, the survival status of pancreatic cancer patients is not optimistic, and the treatment choices are limited. The median overall survival (mOS) of patients with advanced pancreatic cancer is only 11.1 months (41), so there is an imperative need to find new targets and new therapies to bring new hope to patients. In both pancreatic adenocarcinoma and its metastases, claudin18.2 is heavily expressed. Patients who have high expression of claudin18 live longer than individuals without this target (57). So, at present, the research on claudin18 monoclonal antibodies, bispecific antibodies, antibody-drug conjugates, and CAR-T cell therapy are in full swing, which may offer fresh ideas to the treatment of pancreatic cancer.

4.1 Monoclonal antibodies – the potential of Claudin18.2 is emerging

4.1.1 Zolbetuximab (IMAB362)

Zolbetuximab (IMAB362) is one of monoclonal antibody drugs targeting Claudin 18.2. It can trigger ADCC and CDC by specifically connecting to Claudin18.2 on the surface of tumor cells, which may result in tumor cell lysis and death. The extent of cytotoxic effects induced by Zolbetuximab was found to be related to the expression of Claudin18.2 on the surface of cells (58). The study (NCT03816163) to evaluate the safety and effectiveness of the combination of Nab-Paclitaxel and Gemcitabine (Nab-P + GEM) with Zolbetuximab (IMAB362) as the first-line therapy for patients with metastatic pancreatic adenocarcinoma who are also Claudin18.2 positive is ongoing (50). The study is predicted to include 369 pancreatic cancer patients with high expression of Claudin18.2 (IHC staining intensity ≥75%). In order to assess the safety and tolerability of Zolbetuximab + GN, the trial involved a safety lead-in that enrolled 3-12 patients. And after 28 days, dose-limiting toxicities (DLTs) will be evaluated. About 357 patients will be assigned 2:1 randomly to receive either GN alone on Days 1, 8, and 15 of each cycle or Zolbetuximab Q2W on Days 1 and 15 plus GN on Days 1, 8, and 15 of each cycle, according to the recommended phase 2 dosage (RP2D), which was confirmed during the safety lead-in period. Liver metastases and ECOG performance status will be used to determine the randomization process. Patients will have the baseline MRI or CT every eight weeks until the beginning of another systemic anticancer treatment, or until the period that investigators assessed the disease progression, whichever occurs first. The main goals are to ascertain the safety and tolerability of Zolbetuximab + GN, and whether the treatment with Zolbetuximab + GN compared to GN alone improves overall survival (OS). Progression-free survival (PFS), objective response rate (ORR), disease control rate (DCR), pharmacokinetics, duration of response (DOR), and health-related quality of life are secondary endpoints. We are now looking forward to the final results of this experiment. Up to now, Zolbetuximab (IMAB362) has been approved for the first-line treatment for metastatic pancreatic cancer in China, and is expected to become the first marketed Claudin18.2 monoclonal antibody in the world.

4.1.2 TST001

TST001 is a monoclonal antibody targeting Claudin18.2 that was developed globally following IMAB362. Compared to IMAB362, TST001 exhibits better affinity and Fc fragment receptor (FcR) binding activity because of its enhanced natural killer cell-mediated ADCC and fewer fucose content (59). Preclinical studies found that TST001 shows strong anti-tumor abilities in tumor models, with moderate to high levels of Claudin18.2 expression and synergistic anti-cancer effects with immune checkpoint inhibitors (ICIs) (60). The study has found that the combination of TST001 (Osemitamab) and atezolizumab has better anti-tumor activity than the single agent (61). There is an ongoing trial (NCT04396821) about TST001 to study the safety and tolerability in advanced or metastatic solid tumors. In cohort C of the trial, subjects with previously untreated, locally advanced, unresectable, or metastatic pancreatic adenocarcinoma will be enrolled. These participants will be given TST001 at a dose of 2 mg/kg or 4 mg/kg Q2W together with albumin-bound paclitaxel AND gemcitabine. The key observational indicators comprise the frequency and severity of adverse events, maximum tolerated dosage, safety and tolerability. And the secondary observational indicators include immunogenicity, PFS, ORR, DOR et al. We are awaiting the latest research progress.

4.1.3 AB011

A humanized recombinant monoclonal antibody injection against Claudin18.2 is known as AB011. which is the first monoclonal antibody against Claudin18.2 independently developed in China and the first humanized monoclonal antibody against this target in the world. Currently, AB011 is in the phase I clinical trial (NCT04400383) for the treatment of Claudin18.2 positive solid tumors (pancreatic adenocarcinoma, gastric cancer, and solid tumors). The study is consisted of two phases: the first phase is a single treatment and the second phase is a combination therapy. From Aug 2020 to Aug 2021, in Part 1, 14 patients in the dose-escalation stage were given AB011 at different dosage and 21 patients in the dose-expansion stage (11 at 30 mg/kg, 10 at 20 mg/kg). 77.1% have had at least two lines of treatment before. Twelve subjects (12/46, 46.2%) of GC/gastroesophageal junction (GEJ) adenocarcinoma had three or more metastatic organs, of which fifteen (56.7%) had peritoneal metastases. Six out of nine (66.7%) pancreatic cancer subjects had two or more metastatic organs. Eight patients (3 in 20 mg/kg, 5 in 30 mg/kg) suffered treatment-related adverse events (TRAEs) of grade 3, with grade 1-2 accounting for the majority of TRAEs. One case of DLT (grade 3 dyspnea) was reported in the 30 mg/kg group. Twelve patients achieved disease control out of the twenty patients with evaluable disease and at least one tumor assessment, and one GC without target lesions was shown to be complete response (CR) (51). There are some other monoclonal antibodies against Claudin18.2 that are being studied, like ASKB589 (NCT04632108), M108 (NCT04894825), MIL93 (NCT04671875), NBL-015 (NCT05153096), ZL-1211 (NCT05065710).

4.2 Bispecific antibodies – Claudin 18.2 is a strong combination

Two distinct epitopes on the same or different antigens are bound by bispecific antibodies. Bispecific antibodies exert activity that exceeds that of beyond natural antibodies due to the dual specificity of soluble or cell surface antigens, which may present additional therapeutic application potential (62). Currently, bispecific antibodies that have entered clinical trials include: Claudin18.2/CD3 (NCT04260191) (44), Claudin18.2/4-1BB (NCT05839106) (45), Claudin18.2/PD-L1 (NCT04856150) et al. These bispecific antibodies have stronger specificity and lower off-target toxicity than some monoclonal antibodies, and have more

therapeutic potential for gastric and pancreatic cancers. AZD5863 is a bispecific antibody which targets Claudin18.2 and CD3 T cells. The safety, pharmacokinetics, pharmacodynamics, and effectiveness of AZD5863 in adult patients who have advanced or metastatic solid tumors are being investigated in the trial (NCT06005493). In this experiment, the AZD5863 will be infused in two different forms, intravenous and subcutaneous, to observe the number of adverse reactions and ORR. Clinical studies of other bispecific antibodies are ongoing, for example, IBI389 (NCT05164458), QLS31905 (NCT05278832), SG1906 (NCT05857332) et al.

4.3 Antibody-drug conjugates – Claudin 18.2 is getting better

4.3.1 CMG901

The most common form of antibody-drug conjugates (ADC) is monoclonal antibodies (mAbs) linked to cytotoxic medicines via chemical linkers by covalent bonds. Because of the benefits of strong killing power and high specificity targeting ability, it removes cancer cells effectively, making it a hotspot in the production of anticancer medications (63). CMG901 is the first ADC drug for Claudin18.2 in the world, which has shown strong anti-cancer efficacy through CDC, ADCC, and MMAE-mediated cytotoxicity with bystander killing. The phase I trial (NCT04805307) in patients who have advanced solid tumors is ongoing. As of August 4, 2022, CMG901 had been administered to 27 participants (14 patients with pancreatic cancer and 13 patients with gastric/GEJ cancer) at doses of 3.4 mg/kg. The median line of prior systemic treatment was 2, with the range of 1 to 5. 3/27 (11.1%) of the patients experienced grade 3 adverse events (AEs) as a result of the medicine. There were no documented grade 4 or 5 AEs linked to the drug. MTD wasn't accomplished. The ORR and DCR in patients with gastric/GEJ cancer who were positive for Claudin18.2 were 75.0% and 100%, respectively. In the 2.6, 3.0, and 3.4 mg/kg Q3W dosage groups, ORR was 100%. The mOS and mPFS had not yet been reached. Patients exhibited little exposure to unconjugated MMAE systemically, according to the data. The results will be reported on an ongoing basis (43).

4.3.2 LM-302

LM-302 can specifically target Claudin18.2-positive tumor cells and enter tumor cells through endocytosis, releasing small molecule toxins, thus exerting anti-tumor effects. Preclinical studies of LM-302 (TPX-4589) have shown favorable safety profile and activity *in vitro* and *in vivo*, including good tumor suppression and decreasing tumor size in tumor models with high- or low-expression of Claudin18.2 (64). The Food and Drug Administration (FDA) has declared the medicine as the orphan drug (ODD) in 2021 for pancreatic cancer, gastric cancer and gastric junction cancer. Currently, experiments on LM-302 are underway, like NCT05161390, NCT05994001, NCT05934331, NCT05001516.

4.3.3 EO-3021/SYSA1801

A monoclonal antibody specific to the Claudin18.2 target and an MMAE payload site-specifically attached by cleavable linkers make up EO-3021/SYSA1801. The trial found that EO-3021 exhibits antitumor activity by inducing tumor regression with the single dosage in the models of gastric cancers, pancreatic cancers, and lung cancers with low, medium, and high Claudin18.2 expression (65). SYSA1801 is being assessed in patients with advanced solid tumors who are Claudin18.2 positive for the safety, anticancer efficacy, tolerability, and pharmacokinetics in the phase 1 trial (NCT05009966).

4.4 CAR-T cell – there is a breakthrough targeting Claudin18.2

4.4.1 CT041

Artificial receptor molecule made by genetic engineering technology, CAR can direct lymphocytes, most often T cells, to identify and destroy cells that express particular target antigens. Regardless of the major histocompatibility complex (MHC) receptor, the CAR connects to the target antigens that presented on the cell surface, leading to strong T cell activity and powerful anti-tumor effect (66). As the first CAR-T cell drug targeting Claudin18.2 in the world, CT041 appeared in 2019, and its remarkable efficacy shows good prospects for the treatment of digestive system tumors. Twelve patients-seven with gastric cancer and five with pancreatic cancer-were offered with CAR-positive T cell infusions in the open-label, single-arm, phase I study (NCT03159819). The results were found that among the 11 evaluable individuals one had CR who had a gastric adenocarcinoma, three had partial response (PR) (two gastric and one pancreatic adenocarcinoma), five had stable disease (SD), and two had progressive disease (PD). There was a 33.3% ORR, with a 130 days mPFS. This suggests that patients with advanced gastric cancer and pancreatic cancer may benefit from CAR- Claudin18.2 T cells (46). Qi C et al. reported two cases (NCT04581473 and NCT03874897) of CT041 in patients who had failed standard therapy with Claudin18.2 positive metastatic pancreatic cancer (48). After lymphocyte depletion, CAR-T cells were injected in the example 1, where the expression of Claudin18.2 was 2+, 70%. On day 1, there was grade 1 cytokine release syndrome (CRS) appeared, which was handled successfully by tocilizumab. PR was reached with a significant reduction in lung metastases, based on RECIST v1.1. There was a rise in $CD8^+$ T cells and Treg cells and a decrease in $CD4^+$ T cells and B cells. The IHC in the example 2 for

Claudin18.2 was 3+, 60%. After that, Claudin18.2 CAR-T cells were given. The patient had grade 2 CRS, which was treated by tocilizumab. In addition, CR was attained in the lung metastatic target lesions. From peripheral blood, similar results that there were rises in both $CD8^+$ T cells and Treg cells. Furthermore, decreasing transforming growth factor-β1 (TGF-β1) and increasing interleukin-8 (IL-8) were also reported. Until the final follow-up on July 18, 2023, the tumor was remained under control. In the interim results of a phase I trial (NCT03874897), the total of 37 patients with metastatic gastrointestinal tumors (five patients with pancreatic cancer) were included to receive CT041 infusion. For all patients, the ORR was 48.6% (95% confidence interval (CI); 31.9, 65.6) and the DCR was 73.0% (95% CI; 55.9, 86.2). The mPFS was 3.7 months (95% CI; 2.6, 5.4), and the OS rate was 80.1% (95% CI; 62.5, 90.0) at 6 months. In pancreatic cancer and other cancers group (n=9), 2 had PR, 4 had SD. The ORR and DCR were 22.2% (95% CI; 2.8,60.0) and 66.7% (95% CI; 29.9,92.5), respectively. The mPFS was 2.6 months (95% CI; 1.8,3.5) (47). In the single-arm, open-label, phase Ib study (NCT04404595), at the end of February 15, 2022, eleven participators (5 had gastric cancer and 6 had pancreatic cancer) were treated with CT041 at the dose between 2.5 and 4×10^8 cells. Two patients with pancreatic cancer were in stable disease with reduced tumor size, and there were also 3 patients with pancreatic cancer who progressed on the disease. The ORR was 37.5% (3/8) in patients (49). There are also experiments (NCT05911217) on CT041 that are in progress. The studies above have demonstrated that CT041, a Claudin18.2-targeted CAR-T cell drug, has good anti-tumor activity in advanced gastrointestinal tumors, including pancreatic cancer, and is safe and reliable.

4.4.2 Other CAR-T drugs

LY011 is one of the third generation of CAR-T cell products against Claudin18.2. Currently, two phase I trials (NCT04977193, NCT04966143) are being conducted in patients with Claudin18.2 positive pancreatic cancer and advanced gastric cancer, and as of now the results have not been officially reported. In addition, LB1908 (NCT05539430), HEC-016 (NCT05277987), KD-496 (NCT05583201), and CT048 (NCT05393986) have entered clinical trials for the treatment of pancreatic cancer, gastric cancer, and other solid tumors to verify their safety, tolerability and efficacy. The results of these clinical studies are awaiting.

More and more evidence suggest that pancreatic cancer has the firm barrier, deep invasion of immunosuppressive cells, and deficiency of effector T cells in the suppressive tumor microenvironment, which is considered as the major factor in chemotherapy resistance, immunotherapy insensitivity, and recurrence and metastasis (67). Therefore, in order to improve the anti-tumor effect of Claudin18.2-targeted CAR-T cell in the pancreatic cancer, a feasible strategy may be to remodel the immune microenvironment. This also means that there is still room for further advancement and promotion of the clinical use of Claudin18.2 targets. In addition, the combination of other immunomodulators, targeted tumor angiogenesis drugs, or improvement of CAR-T cells may also provide more effective treatments for pancreatic cancer patients.

5 Summary and outlook

In summary, Claudin18.2 is expected to become a “dark horse” target due to its high selectivity for pancreatic cancer in the future, and its targeted drugs include monoclonal antibodies, bispecific antibodies, ADC, CAR-T and other mainstream directions. And a number of ongoing clinical trials are also expected to offer more choices for patients who have Claudin18.2 positive pancreatic cancer. At present, the research and development of medicine which target Claudin18.2 is mostly based on IHC, but there are differences in the detection antibodies used by different institutions and the patient populations included, resulting in differences in the positive rate of Claudin18.2. Therefore, accurate diagnosis and multi-dimensional screening methods are essential for the detection of Claudin18.2-positive patients, while screening for beneficiary populations is also a key issue in accurately defining Claudin18.2-positive patients. But overall, targeted Claudin18.2 therapy has a “bright future”.

Author contributions

QX: Writing – original draft, Writing – review & editing. CJ: Writing – original draft, Writing – review & editing. YO: Writing – original draft, Writing – review & editing. CZ: Visualization, Writing – review & editing. YJ: Validation, Writing – review & editing.

Funding

The author(s) declare that no financial support was received for the research, authorship, and/or publication of this article.

Acknowledgments

Thanks to Figdraw for the drawing support.

Conflict of interest

The authors declare that the research was conducted in the absence of any commercial or financial relationships that could be construed as a potential conflict of interest.

Publisher’s note

References

1. Niimi T, Nagashima K, Ward JM, Minoo P, Zimonjic DB, Popescu NC, et al. claudin-18, a novel downstream target gene for the T/EBP/NKX2.1 homeodomain transcription factor, encodes lung- and stomach-specific isoforms through alternative splicing. *Mol Cell Biol*. (2001) 21:7380–90. doi: 10.1128/MCB.21.21.7380-7390.2001

2. Furuse M, Fujita K, Hiiragi T, Fujimoto K, Tsukita S. Claudin-1 and -2: novel integral membrane proteins localizing at tight junctions with no sequence similarity to occludin. *J Cell Biol*. (1998) 141:1539–50. doi: 10.1083/jcb.141.7.1539

3. Zihni C, Mills C, Matter K, Balda MS. Tight junctions: from simple barriers to multifunctional molecular gates. *Nat Rev Mol Cell Biol*. (2016) 17:564–80. doi: 10.1038/nrm.2016.80

4. Tsukita S, Furuse M, Itoh M. Multifunctional strands in tight junctions. *Nat Rev Mol Cell Biol*. (2001) 2:285–93. doi: 10.1038/35067088

5. Zeisel MB, Dhawan P, Baumert TF. Tight junction proteins in gastrointestinal and liver disease. *Gut*. (2019) 68:547–61. doi: 10.1136/gutjnl-2018-316906

6. Brunner J, Ragupathy S, Borchard G. Target specific tight junction modulators. *Adv Drug Delivery Rev*. (2021) 171:266–88. doi: 10.1016/j.addr.2021.02.008

7. Türeci O, Koslowski M, Helftenbein G, Castle J, Rohde C, Dhaene K, et al. Claudin-18 gene structure, regulation, and expression is evolutionary conserved in mammals. *Gene*. (2011) 481:83–92. doi: 10.1016/j.gene.2011.04.007

8. Sahin U, Koslowski M, Dhaene K, Usener D, Brandenburg G, Seitz G, et al. Claudin-18 splice variant 2 is a pan-cancer target suitable for therapeutic antibody development. *Clin Cancer Res*. (2008) 14:7624–34. doi: 10.1158/1078-0432.CCR-08-1547

9. Lee JH, Kim KS, Kim TJ, Hong SP, Song SY, Chung JB, et al. Immunohistochemical analysis of claudin expression in pancreatic cystic tumors. *Oncol Rep*. (2011) 25:971–8. doi: 10.3892/or.2011.1132

10. Singh P, Toom S, Huang Y. Anti-claudin 18.2 antibody as new targeted therapy for advanced gastric cancer. *J Hematol Oncol*. (2017) 10:105. doi: 10.1186/s13045-017-0473-4

11. Hong JY, An JY, Lee J, Park SH, Park JO, Park YS, et al. Claudin 18.2 expression in various tumor types and its role as a potential target in advanced gastric cancer. *Transl Cancer Res*. (2020) 9:3367–74. doi: 10.21037/tcr-19-1876

12. Wöll S, Schlitter AM, Dhaene K, Roller M, Esposito I, Sahin U, et al. Claudin 18.2 is a target for IMAB362 antibody in pancreatic neoplasms. *Int J Cancer*. (2014) 134:731–9. doi: 10.1002/ijc.28400

13. Jiang H, Shi Z, Wang P, Wang C, Yang L, Du G, et al. Claudin18.2-specific chimeric antigen receptor engineered T cells for the treatment of gastric cancer. *J Natl Cancer Inst*. (2019) 111:409–18. doi: 10.1093/jnci/djy134

14. Wang C, Wu N, Pei B, Ma X, Yang W. Claudin and pancreatic cancer. *Front Oncol*. (2023) 13:1136227. doi: 10.3389/fonc.2023.1136227

15. Cao W, Xing H, Li Y, Tian W, Song Y, Jiang Z, et al. Claudin18.2 is a novel molecular biomarker for tumor-targeted immunotherapy. *biomark Res*. (2022) 10:38. doi: 10.1186/s40364-022-00385-1

16. Xu B, Chen F, Zhang X, Wang Z, Che K, Wu N, et al. Antigen-specific T cell immunotherapy targeting claudin18.2 in gastric cancer. *Cancers (Basel)*. (2022) 14:2758. doi: 10.3390/cancers14112758

17. Matsuda M, Sentani K, Noguchi T, Hinoi T, Okajima M, Matsusaki K, et al. Immunohistochemical analysis of colorectal cancer with gastric phenotype: claudin-18 is associated with poor prognosis. *Pathol Int*. (2010) 60:673–80. doi: 10.1111/j.1440-1827.2010.02587.x

18. Jun KH, Kim JH, Jung JH, Choi HJ, Chin HM. Expression of claudin-7 and loss of claudin-18 correlate with poor prognosis in gastric cancer. *Int J Surg*. (2014) 12:156–62. doi: 10.1016/j.ijsu.2013.11.022

19. Karanjawala ZE, Illei PB, Ashfaq R, Infante JR, Murphy K, Pandey A, et al. New markers of pancreatic cancer identified through differential gene expression analyses: claudin 18 and annexin A8. *Am J Surg Pathol*. (2008) 32:188–96. doi: 10.1097/PAS.0b013e31815701f3

20. Shen CH, Lin JY, Lu CY, Yang SS, Peng CK, Huang KL. SPAK-p38 MAPK signal pathway modulates claudin-18 and barrier function of alveolar epithelium after hyperoxic exposure. *BMC Pulm Med*. (2021) 21:58. doi: 10.1186/s12890-021-01408-7

21. Takasawa K, Takasawa A, Osanai M, Aoyama T, Ono Y, Kono T, et al. Claudin-18 coupled with EGFR/ERK signaling contributes to the Malignant potentials of bile duct cancer. *Cancer Lett*. (2017) 403:66–73. doi: 10.1016/j.canlet.2017.05.033

22. Resnick MB, Konkin T, Routhier J, Sabo E, Pricolo VE. Claudin-1 is a strong prognostic indicator in stage II colonic cancer: a tissue microarray study. *Mod Pathol*. (2005) 18:511–8. doi: 10.1038/modpathol.3800301

23. Ito T, Kojima T, Yamaguchi H, Kyuno D, Kimura Y, Imamura M, et al. Transcriptional regulation of claudin-18 via specific protein kinase C signaling pathways and modification of DNA methylation in human pancreatic cancer cells. *J Cell Biochem*. (2011) 112:1761–72. doi: 10.1002/jcb.23095

24. Sanada Y, Oue N, Mitani Y, Yoshida K, Nakayama H, Yasui W. Down-regulation of the claudin-18 gene, identified through serial analysis of gene expression data analysis, in gastric cancer with an intestinal phenotype. *J Pathol*. (2006) 208:633–42. doi: 10.1002/path.1922

25. Cheung ST, Leung KL, Ip YC, Chen X, Fong DY, Ng IO, et al. Claudin-10 expression level is associated with recurrence of primary hepatocellular carcinoma. *Clin Cancer Res*. (2005) 11:551–6. doi: 10.1158/1078-0432.551.11.2

26. Sung H, Ferlay J, Siegel RL, Laversanne M, Soerjomataram I, Jemal A, et al. Global cancer statistics 2020: GLOBOCAN estimates of incidence and mortality worldwide for 36 cancers in 185 countries. *CA Cancer J Clin*. (2021) 71:209–49. doi: 10.3322/caac.21660

27. Liu YQ, Zou HY, Xie JJ, Fang WK. Paradoxical roles of desmosomal components in head and neck cancer. *Biomolecules*. (2021) 11:914. doi: 10.3390/biom11060914

28. Zhang Z, Auyeung KK, Sze SC, Zhang S, Yung KK, Ko JK. The dual roles of calycosin in growth inhibition and metastatic progression during pancreatic cancer development: A "TGF-β paradox". *Phytomedicine*. (2020) 68:153177. doi: 10.1016/j.phymed.2020.153177

29. Cebrián MJ, Bauden M, Andersson R, Holdenrieder S, Ansari D. Paradoxical role of HMGB1 in pancreatic cancer: tumor suppressor or tumor promoter? *Anticancer Res*. (2016) 36:4381–9. doi: 10.21873/anticanres.10981

30. Bose M. Preferentially expressed antigen in melanoma is a multifaceted cancer testis antigen with diverse roles as a biomarker and therapeutic target. *Int J Transl Med*. (2023) 3:334–59. doi: 10.3390/ijtm3030024

31. Chen J, Xu Z, Hu C, Zhang S, Zi M, Yuan L, et al. Targeting CLDN18.2 in cancers of the gastrointestinal tract: New drugs and new indications. *Front Oncol*. (2023) 13:1132319. doi: 10.3389/fonc.2023.1132319

32. Oshima T, Shan J, Okugawa T, Chen X, Hori K, Tomita T, et al. Down-regulation of claudin-18 is associated with the proliferative and invasive potential of gastric cancer at the invasive front. *PloS One*. (2013) 8:e74757. doi: 10.1371/journal.pone.0074757

33. Hagen SJ, Ang LH, Zheng Y, Karahan SN, Wu J, Wang YE, et al. Loss of tight junction protein claudin 18 promotes progressive neoplasia development in mouse stomach. *Gastroenterology*. (2018) 155:1852–67. doi: 10.1053/j.gastro.2018.08.041

34. Zhou B, Flodby P, Luo J, Castillo DR, Liu Y, Yu FX, et al. Claudin-18-mediated YAP activity regulates lung stem and progenitor cell homeostasis and tumorigenesis. *J Clin Invest*. (2018) 128:970–84. doi: 10.1172/JCI90429

35. Shimobaba S, Taga S, Akizuki R, Hichino A, Endo S, Matsunaga T, et al. Claudin-18 inhibits cell proliferation and motility mediated by inhibition of phosphorylation of PDK1 and Akt in human lung adenocarcinoma A549 cells. *Biochim Biophys Acta*. (2016) 1863:1170–8. doi: 10.1016/j.bbamcr.2016.02.015

36. Luo J, Chimge NO, Zhou B, Flodby P, Castaldi A, Firth AL, et al. CLDN18.1 attenuates Malignancy and related signaling pathways of lung adenocarcinoma in vivo and in *vitro*. *Int J Cancer*. (2018) 143:3169–80. doi: 10.1002/ijc.31734

37. Kotton DN. Claudin-18: unexpected regulator of lung alveolar epithelial cell proliferation. *J Clin Invest*. (2018) 128:903–5. doi: 10.1172/JCI99799

38. Jovov B, Van Itallie CM, Shaheen NJ, Carson JL, Gambling TM, Anderson JM, et al. Claudin-18: a dominant tight junction protein in Barrett's esophagus and likely contributor to its acid resistance. *Am J Physiol Gastrointest Liver Physiol*. (2007) 293:G1106–13. doi: 10.1152/ajpgi.00158.2007

39. Yano K, Imaeda T, Niimi T. Transcriptional activation of the human claudin-18 gene promoter through two AP-1 motifs in PMA-stimulated MKN45 gastric cancer cells. *Am J Physiol Gastrointest Liver Physiol*. (2008) 294:G336–43. doi: 10.1152/ajpgi.00328.2007

40. Tanaka M, Shibahara J, Fukushima N, Shinozaki A, Umeda M, Ishikawa S, et al. Claudin-18 is an early-stage marker of pancreatic carcinogenesis. *J Histochem Cytochem*. (2011) 59:942–52. doi: 10.1369/0022155411420569

41. Kyuno D, Takasawa A, Takasawa K, Ono Y, Aoyama T, Magara K, et al. Claudin-18.2 as a therapeutic target in cancers: cumulative findings from basic research and clinical trials. *Tissue Barriers*. (2022) 10:1967080. doi: 10.1080/21688370.2021.1967080

42. Zhang J, Dong R, Shen L. Evaluation and reflection on claudin 18.2 targeting therapy in advanced gastric cancer. *Chin J Cancer Res*. (2020) 32:263–70. doi: 10.21147/j.issn.1000-9604.2020.02.13

43. Xu RH, Wei X, Zhang D, Qiu M, Zhang Y, Zhao H, et al. A phase 1a dose-escalation, multicenter trial of anti-claudin 18.2 antibody drug conjugate CMG901 in patients with resistant/refractory solid tumors. *J Clin Oncol*. (2023) 41:352. doi: 10.1200/JCO.2023.41.4_suppl.352

44. Zhu G, Foletti D, Liu X, Ding S, Melton Witt J, Hasa-Moreno A, et al. Targeting CLDN18.2 by CD3 bispecific and ADC modalities for the treatments of gastric and pancreatic cancer. *Sci Rep*. (2019) 9:8420. doi: 10.1038/s41598-019-44874-0

45. Gao J, Wang Z, Jiang W, Zhang Y, Meng Z, Niu Y, et al. CLDN18.2 and 4-1BB bispecific antibody givastomig exerts antitumor activity through CLDN18.2-expressing tumor-directed T-cell activation. *J Immunother Cancer*. (2023) 11:e006704. doi: 10.1136/jitc-2023-006704

46. Zhan X, Wang B, Li Z, Li J, Wang H, Chen L, et al. Phase I trial of Claudin 18.2-specific chimeric antigen receptor T cells for advanced gastric and pancreatic adenocarcinoma. *J Clin Oncol*. (2019) 37:2509. doi: 10.1200/JCO.2019.37.15_suppl.2509

47. Qi C, Gong J, Li J, Liu D, Qin Y, Ge S, et al. Claudin18.2-specific CAR T cells in gastrointestinal cancers: phase 1 trial interim results. *Nat Med*. (2022) 28:1189–98. doi: 10.1038/s41591-022-01800-8

48. Qi C, Xie T, Zhou J, Wang X, Gong J, Zhang X, et al. CT041 CAR T cell therapy for Claudin18.2-positive metastatic pancreatic cancer. *J Hematol Oncol*. (2023) 16:102. doi: 10.1186/s13045-023-01491-9

49. Botta GP, Becerra CR, Jin Z, Kim DW, Zhao D, Lenz H-J. Multicenter phase Ib trial in the U.S. @ of salvage CT041 CLDN18.2-specific chimeric antigen receptor T-cell therapy for patients with advanced gastric and pancreatic adenocarcinoma. *J Clin Oncol*. (2022) 40:2538. doi: 10.1200/JCO.2022.40.16_suppl.2538

50. Park W, O'Reilly EM, Furuse J, Li CP, Oh DY, Garcia-Carbonero R, et al. Zolbetuximab plus gemcitabine and nab-paclitaxel (GN) in first-line treatment of claudin 18.2-positive metastatic pancreatic cancer (mPC): Phase 2, open-label, randomized study. *J Clin Oncol*. (2023) 41(4):782. doi: 10.1200/JCO.2023.41.4_suppl.TPS782

51. Li J, Pan H, Liu T, Xu N, Zhang Y, Qin Y, et al. A multicenter, phase 1 study of AB011, a recombinant humanized anti-CLDN18.2 monoclonal antibody, as monotherapy and combined with capecitabine and oxaliplatin (CAPOX) in patients with advanced solid tumors. *J Clin Oncol*. (2023) 41:391. doi: 10.1200/JCO.2023.41.4_suppl.391

52. Siegel RL, Miller KD, Fuchs HE, Jemal A. Cancer statistics, 2021. *CA Cancer J Clin*. (2021) 71:7–33. doi: 10.3322/caac.21654

53. Rahib L, Smith BD, Aizenberg R, Rosenzweig AB, Fleshman JM, Matrisian LM. Projecting cancer incidence and deaths to 2030: the unexpected burden of thyroid, liver, and pancreas cancers in the United States. *Cancer Res*. (2014) 74:2913–21. doi: 10.1158/0008-5472.CAN-14-0155

54. Zhu H, Li T, Du Y, Li M. Pancreatic cancer: challenges and opportunities. *BMC Med*. (2018) 16:214. doi: 10.1186/s12916-018-1215-3

55. Li D, Xie K, Wolff R, Abbruzzese JL. Pancreatic cancer. *Lancet*. (2004) 363:1049–57. doi: 10.1016/S0140-6736(04)15841-8

56. Grossberg AJ, Chu LC, Deig CR, Fishman EK, Hwang WL, Maitra A, et al. Multidisciplinary standards of care and recent progress in pancreatic ductal adenocarcinoma. *CA Cancer J Clin*. (2020) 70:375–403. doi: 10.3322/caac.21626

57. Conroy T, Desseigne F, Ychou M, Bouché O, Guimbaud R, Bécouarn Y, et al. FOLFIRINOX versus gemcitabine for metastatic pancreatic cancer. *N Engl J Med*. (2011) 364:1817–25. doi: 10.1056/NEJMoa1011923

58. Türeci Ö, Mitnacht-Kraus R, Wöll S, Yamada T, Sahin U. Characterization of zolbetuximab in pancreatic cancer models. *Oncoimmunology*. (2018) 8:e1523096. doi: 10.1080/2162402X.2018.1523096

59. Chen Y, Hou X, Li D, Ding J, Liu J, Wang Z, et al. Development of a CLDN18.2-targeting immuno-PET probe for non-invasive imaging in gastrointestinal tumors. *J Pharm Anal*. (2023) 13:367–75. doi: 10.1016/j.jpha.2023.02.011

60. Gabrail NY, Tolcher A, Alese OB, Cecchini M, Manish P, Park H, et al. A phase I clinical trial to evaluate the safety, tolerability, and pharmacokinetics of TST001 in patients with locally advanced or metastatic solid tumors. *J Clin Oncol* (2022) 40(4):375. doi: 10.1200/JCO.2022.40.4_suppl.TPS375

61. Qian X, Teng F, Guo H, Yao X, Shi L, Wu Y, et al. 1560P Osemitamab (TST001): An ADCC enhanced humanized anti-CLDN18.2 mab, demonstrated improved efficacy in combination with anti-PD-L1/PD-1 mab and oxaliplatin/5-FU in preclinical tumor models. *Ann Oncol*. (2023) 34:S873. doi: 10.1016/j.annonc.2023.09.1472

62. Brinkmann U, Kontermann RE. Bispecific antibodies. *Science*. (2021) 372:916–7. doi: 10.1126/science.abg1209

63. Fu Z, Li S, Han S, Shi C, Zhang Y. Antibody drug conjugate: the "biological missile" for targeted cancer therapy. *Signal Transduct Target Ther*. (2022) 7:93. doi: 10.1038/s41392-022-00947-7

64. Huang W, Li Y, Liu Z, Rodon L, Correia S, Li R. Preclinical activity for TPX-4589 (LM-302), an antibody-drug conjugate targeting tight junction protein CLDN18.2 in solid tumors. *Eur J Cancer*. (2022) 174:S41–2. doi: 10.1016/S0959-8049(22)00911-X

65. Dan M, Hui X, Wang Y, Yuan C, O'Hare T, Jansen VM, et al. Therapeutic potential of EO-3021/SYSA1801, a Claudin18.2 antibody-drug conjugate, for the treatment of CLDN18.2-expressing cancers. *Cancer Res*. (2023) 83:6300. doi: 10.1158/1538-7445.AM2023-6300

66. Sadelain M, Brentjens R, Rivière I. The basic principles of chimeric antigen receptor design. *Cancer Discovery*. (2013) 3:388–98. doi: 10.1158/2159-8290.CD-12-0548

67. Zhang H, Ye L, Yu X, Jin K, Wu W. Neoadjuvant therapy alters the immune microenvironment in pancreatic cancer. *Front Immunol*. (2022) 13:956984. doi: 10.3389/fimmu.2022.956984

Frontiers in Oncology

Advances knowledge of carcinogenesis and tumor progression for better treatment and management

The third most-cited oncology journal, which highlights research in carcinogenesis and tumor progression, bridging the gap between basic research and applications to imrpove diagnosis, therapeutics and management strategies.

Discover the latest Research Topics

See more →

Frontiers

Avenue du Tribunal-Fédéral 34
1005 Lausanne, Switzerland
frontiersin.org

Contact us

+41 (0)21 510 17 00
frontiersin.org/about/contact